From the Institut für Experimentelle Tumorforschung

(Director: Prof. Dr. rer. nat. Susanne Sebens)

at the University Medical Center Schleswig-Holstein, Campus Kiel

at Kiel University

Diabetes mellitus as risk factor for pancreatic cancer: Impact of hyperglycaemia on the phenotype of macrophages and their influence on pancreatic ductal epithelial cells

Dissertation

to acquire the doctoral degree (Dr. med.)

at the Faculty of Medicine

at Kiel University

presented by

Lilli Luise Otto

from Heidelberg

Kiel 2020

1st Reviewer:	Prof. Dr. rer. nat. Susanne Sebens, Institut für Experimentelle Tumorforschung
2 nd Reviewer:	Prof. Dr. Dr. Janka Held-Feindt, Klinik für Neurochirurgie

Date of oral examination: 14.07.2021

Approved for printing, Kiel, 10.05.2021

Signed.: Prof. Dr. rer. nat. Susanne Sebens

(Chairperson of the Examination Committe

Content

List of figures

List of abbreviations

(v/v)	**V**olume/**v**olume percent
(w/v)	**W**eight/**v**olume percent
°C	Degree Celsius
α-SMA	alpha-**S**mooth **M**uscle **A**ctin
µ	**M**i**c**ro
ABCG2	**A**TP-**B**inding **C**assette super-family **G** member **2**
AKT	Protein Kinase B
ALDH	**Al**dehyde **d**e**h**ydrogenase
ANOVA	**An**alysis **o**f **va**riance
APS	**A**mmonium **p**er**s**ulfate
Arg-1	**Arg**inase-**1**
AT	***A**ustria*
BPE	**B**ovine **p**ituitary **e**xtract
BSA	**B**ovine **s**erum **a**lbumin
CCL	**C-**C **C**hemokine **L**igand
CCR	**C-**C **C**hemokine **R**eceptor
CD	**C**luster of **D**ifferentiation
cDNA	**C**omplementary **d**eoxyribo**n**ucleic **a**cid
CFA	**C**olony **f**ormation **a**ssay
CH	Switzerland
CO_2	**C**arbon **di**hydroxide
CSC	**C**ancer **s**tem **c**ell
Ctrl	**c**on**tr**o**l**
ctrl siRNA	**C**on**tr**o**l siRNA**
CXCR4	**C**-**X**-C **C**hemokine **R**eceptor type **4**
ddH_2O	**D**ouble **d**estilled **water**
DE	**Germany**
DMSO	**Dim**ethyl **s**ulf**o**xide
dNTP	**D**eoxy**n**ucleotide **t**ri**p**hosphate
DNA	**D**eoxyribo**n**ucleic **a**cid
DTT	**Di**thio**t**hreitol
ECM	**E**xtra**c**ellular **m**atrix
EDTA	**E**thylen**d**iamine**t**etraacetic **a**cid
EGF	**E**pidermal **G**rowth **F**actor
ELISA	**E**nzyme-**l**inked **I**mmuno**s**orbent **A**ssay
EMT	**E**pithelial **M**esenchymal **T**ransition
et al.	And others (Latin: ***et al**ii)*
FACS	**F**luorescence **a**ctivated **c**ell **s**orting
FCS	**F**etal **C**alf **S**erum
FGF	**F**ibrocyte **G**rowth **F**actor
g	**g**ram

GAPDH	**G**lycerin**a**ldehyd-3-**P**hosphat-**D**e**h**ydrogenase
Glc	**Glu**cose
GM-CSF	**G**ranulocyte **m**acrophage-**c**olony **s**timulating **f**actor
h	**h**our
HIF-1α	**H**ypoxia-**i**nducible **f**actor-**1α**
HLA-DR	**H**uman **l**eucocyte **a**ntigen **DR**
HPDE	**H**uman **p**ancreatic **d**uctal **e**pithelium
HPV	**H**uman **P**apilloma **V**irus
HRP	**H**orse**r**adish **p**eroxidase
HSP	**H**eat **s**hock **p**rotein
IgG	**I**mmuno**g**lobulin **G**
IGF	**I**nsulin-like **g**rowth **f**actor
IFNγ	**I**nter**f**ero**n**-**γ**
IL	**I**nter**l**eukin
IL-6	**I**nterleukin-**6**
IL-8	**I**nterleukin-**8**
IL-10	**I**nterleukin-**10**
IL-1ra	**IL-1**-**r**eceptor **a**ntagonist
iNOS	**I**nducible **NO s**ynthase
IPMN	**I**ntraductal **P**apillary **M**ucinous **N**eoplasm
KCl	Potassium chloride
kDA	**K**ilo **Da**lton
kras	V-Ki-ras2 **K**irsten **ra**t **s**arcoma viral oncogene homolog
l	**L**iter
LPS	**L**ipo**p**oly**s**accharides
LRS	**L**euco**r**eduction **s**ystem chamber
m	**M**eter
MΦ	**M**acrophage
M1- MΦ	**M1**-polarised **MΦ**
M2- MΦ	**M2**-polarised **MΦ**
mA	**M**illi**A**mpere
MACS	**M**agnetic **a**ctivated **c**ell **s**orting
MAPK	**M**itogen-**a**ctivated **P**rotein **K**inase
M-CSF	**M**acrophage-**c**olony **s**timulating **f**actor
MCN	**M**ucinous **C**ystic **N**eoplasms
miRNA	**mi**cro**RNA**
ml	**M**illi**l**iter
mM	**M**illi **m**olar
MMP	**M**atrix **M**etalloproteinases
mRNA	**M**essenger **RNA**
NaCl	Sodium chloride
NF-κB	**N**uclear **F**actor-**kappaB**

nm	**n**ano**m**eter
n/s	**N**ot **s**pecified
Oct-4	**Oc**tamer-binding **t**ranscription factor **4**
P16/CDKN2A	**c**yclin-**d**ependent **k**inase **in**hibitor **2A**
PanIN	**Pan**creatic **I**ntraepithelial **N**eoplasia
PBMC	**P**eripheral **b**lood **m**ononuclear **c**ell
PBS	**P**hosphate **b**uffered **s**aline
PBS-T	**PBS**-**T**ween
PDAC	**P**ancreatic **d**uctal **a**deno**c**arcinoma
PDEC	**P**ancreatic **d**uctal **e**pithelial **c**ell
Pen/Strep	**Pen**icillin **strep**tomycin
PFA	**P**ara**f**orm**a**ldehyde
p-p65	**P**hosphorylated-**p65**
PSC	**P**ancreatic **s**tellate **c**ells
PVDF	**P**oly**v**inylid**enf**luorid
qRT-PCR	**Q**uantitative **r**eal**t**ime- **p**olymerase **c**hain **r**eaction
RNA	**R**ibo**n**ucleic **a**cid
RNI	**R**eactive **n**itrogen **i**ntermediates
ROS	**R**eactive **o**xygen **s**pecies
RPMI	**R**oswell **P**ark **m**emorial **i**nstitute
RT	**R**oom **t**emperature
rpm	**r**ounds **p**er **m**inute
SDS	**S**odium **d**odecyl **s**ulfate
SDS-PAGE	**SDS**-**p**olyacryl**a**mide **g**el **e**lectrophoresis
SEM	**S**tandard **e**rror of **m**ean
siRNA	**S**mall **i**nterfering **RNA**
SMAD4	**SMAD** family member **4**
STAT 3	**S**ignal **T**ransducer and **A**ctivator of **T**ranscription **3**
T2DM	**T**ype **II** **d**iabetes **m**ellitus
TAM	**T**umour **a**ssociated **m**acrophages
TBS	**T**ris **b**ase **s**odium chloride
TBS-T	**TBS-T**ween
TEMED	**Te**tra**m**ethyl**e**thylene**d**iamine
TGF-β1	**T**ansforming **G**rowth **F**actor -**b**eta **1**
TGF-βRII	**TGF-β-r**eceptor-**II**
Th1	**T**-**h**elper cells type **1**
Th2	**T**-**h**elper cells type **2**
TLR2	**T**oll-**l**ike **r**eceptor **2**
TNF-α	**T**umor **n**ecrosis **f**actor-**alpha**
TP53	**T**umour **p**rotein **53**
t-p65	**T**otal-**p65**
UKSH	***U**niversitäts **K**linik **S**chleswig **H**olstein*
US	**U**nited **S**ates

VCAM-1	**V**ascular **C**ell **A**dhesion **M**olecule-**1**
VEGF	**V**ascular **E**ndothelial **G**rowth **F**actor
Zeb1	**Z**inc finger **E**-**b**ox binding protein **1**

1 Introduction

1.1 Pancreatic ductal adenocarcinoma

Malignant transformations of the pancreas are classified by the histological origin of the neoplastic cells. The most frequent one is the pancreatic ductal adenocarcinoma (PDAC) representing 90% of all pancreatic neoplasms (Pelosi et al., 2017). Pancreatic neuroendocrine tumours are the second most common form, accounting for 5%, and all tumour subgroups deriving from acinar pancreatic cells (pancreatoblastom, solid-pseudopapillary neoplasm and pancreatic acinar cell carcinoma) make out less than 5% of pancreatic neoplasms (Pelosi et al., 2017).

1.1.1 Epidemiology

With less than 4%, the PDAC represents a small share in newly detected cancers but is among the few tumour entities with increasing incidence and mortality (Rahib et al., 2014; Q. Zhang et al., 2016). Due to demographic changes and the general adoption of a tumour-promoting lifestyle, an annual increase of 1.3% on average is estimated in the incidence of PDAC (Rahib et al., 2014). In Germany, more than 18.370 new PDAC cases were diagnosed in 2016 (9.180 in men, 9.190 in women) and a total of 19.900 new diagnoses are expected for 2020 (10.200 in men and 9.700 in women)(Kaatsch and Spix, 2019). Currently ranked fourth in cancer related deaths, it is predicted that PDAC will be the second most lethal neoplasia in the United States (US) by the year of 2030 (**Figure 1**) (Rahib et al., 2014). One reason for this development is the lack of specific early symptoms, impeding the introduction of standardised screening methods which has considerably contributed to the decline of cancer-induced deaths in other tumour entities (Rahib et al., 2014; Malvezzi et al., 2018). 80% of all PDAC patients are first diagnosed in late stages of tumourigenesis, leaving palliative treatment as only option and leading to an overall 5-year survival rate of less than 10% (Q. Zhang et al., 2016; Pelosi et al., 2017; Siegel et al., 2018). The only curative therapeutic approach is the chirurgical resection which is eligible for less than 20% of the patients as it requires a localised tumour mass (Groot et al., 2018). And even after successful resection, the 5-year survival rate is no more than 17-23% as most of the patients develop local recurrence or metastasis causing their death within 18 to 23 months following surgery (Ferrone et al., 2013; Groot et al., 2018).

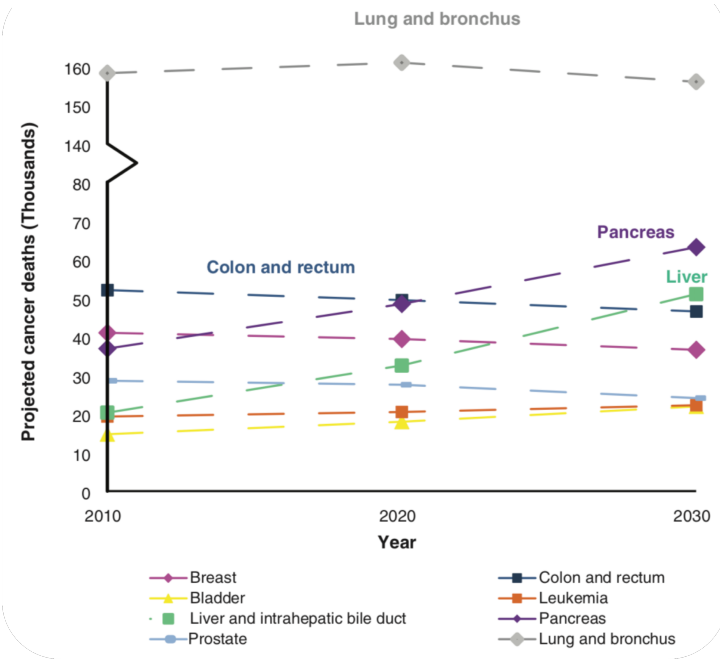

Figure 1: Projection of cancer related deaths up to the year of 2030 of the eight most deadliest cancer entities. PDAC is estimated to be the second most lethal neoplasia by the year of 2030 in Western countries. Figure modified according to (Rahib et al., 2014).

1.1.2 Pathology

The pancreas can be divided into an endocrine and an exocrine part. Tumours originating from the endocrine cells are less frequent than tumours arising from exocrine cells (Fesinmeyer et al., 2005). The latter represent 95% of all pancreatic neoplasms, among which the PDAC is the most frequent entity making up 90% of the cases (Han and von Hoff, 2014). It originates from the pancreatic ductal epithelial cells (PDEC) and is characterised by a much poorer prognosis than the endocrine and also than other exocrine tumours (Fesinmeyer et al., 2005). This is mainly due to its lack of early symptoms impeding timely diagnosis and due to its low therapeutic response (Fesinmeyer et al., 2005; Halfdanarson et al., 2009).

It has long been understood that PDAC develops via precursor lesions, stepwise gaining malignant potential and metastatic capacity (Hezel et al., 2006). Most importance is attributed to the Pancreatic Intraepithelial Neoplasia (PanIN) which are the most common precursor lesions, albeit not the only ones. Cystic lesions such as Intraductal Papillary Mucinous Neoplasms (IPMN) and mucinous cystic neoplasms (MCN) have also been reported as early precancerous stages in the development of PDAC (Koorstra et al., 2008; Basturk et al., 2015; Pelosi et al., 2017).

By definition, PanIN are lesions in small pancreatic ducts (Koorstra et al., 2008). They are classified into three groups according to their histological and cytological appearance and the grade of dysplasia (**Figure 2**). PanIN-1, further divided into PanIN-1a and PanIN-1b, are low-grade, PanIN-2 intermediate and PanIN-3 high-grade lesions. Whereas low-grade PanIN are characterised by columnar cells with mucin production (1a) or papillary architecture (1b), PanIN-2 are marked by cell crowding, nuclear abnormalities and the loss of cell polarity. High-grade lesions show enhanced nuclear atypia, a high mitosis rate and a pronounced architectural disorder with cells budding into the ductal lumen. They differ from carcinoma by still representing a non-invasive lesion with intact basement membrane (Hruban et al., 2000; Distler et al., 2014; Pelosi et al., 2017). PanIN-3 are also referred to as *carcinoma in situ*.

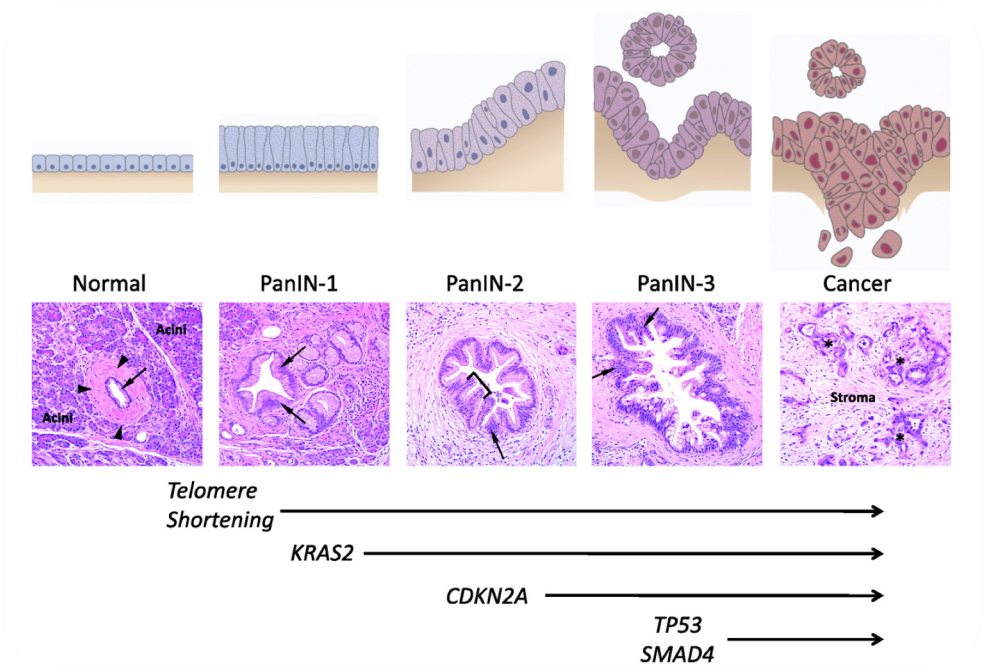

Figure 2: PDAC development. Schematic depiction (top) and corresponding histological images (middle) of healthy pancreatic ductal epithelium developing to PDAC via precursor lesions with stepwise increasing dysplasia. PDAC initiation is accompanied by genetic and epigenetic alterations; the most frequent ones are shown in the lower panel. Modified according to (Hezel et al., 2006; Iacobuzio-Donahue, 2012).

The multistep PanIN progression towards PDAC is accompanied by the accumulation of genetic alterations. Jones *et al.* revealed an average of 63 genomic alterations in PDAC, mainly manifested in form of point mutations (Jones et al., 2008). Telomerase shortening, an early event observed in 90% of PanIN-1 lesions, causes chromosomal instability and predisposes pancreatic lesions to accumulate mutational alterations (van Heek et al., 2002; Maitra et al., 2006).

The most common mutation found in 90% of all PDAC is the activation of the oncogene *kras* (Kanda et al., 2012). The point mutational activation of the GTPase causes permanent signalling via several signalling pathways involved in cell proliferation, differentiation, apoptosis and migration (Spaargaren et al., 1995). As this alteration is already detectable in many early precancerous lesions (in 36% of all PanIN-1a and 44% of all PanIN-1b), it is assumed to be an important contributor not only to the progression but also to the initiation of PDAC (Löhr et al., 2005).

Further frequent mutations are found in other oncogenes and tumour suppressor genes such as *P16/CDKN2A*, *TP53* and *SMAD4* (found in 90%, 70%, 55% of all PDAC respectively) (Pelosi et al., 2017). Together with mutational activation of *kras* these are commonly referred to as the four driver mutations of PDAC (Korc, 2010; Pelosi et al., 2017). Whereas the inactivation of P16/CDKN21 is already detectable in PanIN-2 stages, the loss of function of P53 and SMAD4 is a later event in tumourigenesis correlated to PanIN-3 stages (Distler et al., 2014).

Epigenetic alterations also play a meaningful role in PDAC progression. Especially abnormally methylated CpG islands, which can lead to the inactivation of certain tumour suppressor genes and metabolic pathways, are of importance (Koorstra et al., 2008). Similar to telomerase shortening, hypermethylation is already

detectable in early PanIN lesions and shows an increase in prevalence throughout cancer progression. To name one example, P16/CDKN21 is not only silenced through genetic alterations (as described above) but also by hypermethylation of its promotor region in 15-20% of PDACs (Hruban et al., 2008).

1.1.3 Risk factors

With an average age at manifestation timepoint of 75 years in women and 72 years in men, PDAC is a disease of elderly people, age featuring as one risk factor (Krebs in Deutschland für 2013/2014, 2017).

Whereas only 5 to 10% of all PDAC involve a hereditary component, the main proportion of cases is associated to lifestyle and environment attributable risk factors (Raimondi et al., 2009). Tobacco consumption is shown to increase the risk of PDAC development in an intensity and cumulative dose dependent manner, showing an up to 2.2-fold higher risk in smokers than non-smokers. 20 to 35% of all PDAC cases are caused by smoking, and even after cessation the risk of PDAC takes 15 to 20 years to adapt back to the one of the non-smoking population (Becker et al., 2014).

Alcohol consumption alone turned out to be not that closely related to PDAC as had long been thought. Meta-analyses could show that the consumption of three drinks per day leads to a 1.22 to 1.36-fold elevated risk for PDAC (Becker et al., 2014; Rahman et al., 2015). Alcohol in combination with smoking, however, significantly increases the risk of PDAC (Rahman et al., 2015). Furthermore, sincere alcohol abuse is correlated with pancreatitis which, in its chronic form, is also considered as a risk factor of PDAC with a 13.3-fold relative risk (Becker et al., 2014).

Additionally, obesity is linked to an increased probability of PDAC development. A study of the year 2003 could show that a body mass index (BMI) higher than 40 is associated with a relative risk of 1.49 and 2.76 for men and women, respectively, assigned to the obesity-induced inflammatory tissue (Calle et al., 2003). Moreover, a high fat diet has been connected to enhanced *kras* activation and increased tumour formation (Philip et al., 2013).

Similarly, a meta-analysis could show that with every 0.56 mmol/L increase in fasting blood glucose, PDAC risk is elevated by 14% (Liao et al., 2015), thereby identifying type II diabetes mellitus (T2DM) as a further risk factor. Cohort studies stated a 2-fold higher probability for diabetic patients to develop PDAC compared to the non-diabetic population (Becker et al., 2014). However, no correlation between the duration of diabetic illness and risk magnitude was identified, and in 39% of the cases diabetes and PDAC where even diagnosed simultaneously (Hassan et al., 2007). Hence, diabetes is discussed as both consequence and risk factor of PDAC. Molecular mechanisms linking T2DM and PDAC will be discussed in detail in the following section.

Dietary changes have led to increased incidence of obesity and T2DM worldwide. It is therefore estimated that metabolic diseases associated with impaired glucose tolerance will become important risk factors for PDAC in the future (Malik et al., 2010; Matrisian et al., 2012).

1.1.4 Type II diabetes mellitus, obesity and PDAC

T2DM and obesity are considered two important risk factors of PDAC development, even though the underlying molecular interactions are not fully understood. As they share several pathological characteristics, their individual impacts on PDAC intersect and are not to be clearly distinguished (Chang and Yang, 2016). T2DM, which is also referred to as "non-insulin dependent diabetes", represents the most common form of diabetic diseases with 90 to 95% of all cases (Chang and Yang, 2016). It is characterised by an insulin resistance with compensatory elevated insulin levels leading to hyperglycaemia. Obesity is characterised by chronical low-grade inflammation and correlated to the acquisition of an impaired insulin metabolism and the occurrence of T2DM (Wellen and Hotamisligil, 2015). The fact that 86% of diabetic patients are overweight or obese (Daousi et al., 2006), underlines the close link between these two diseases.

As insulin can inhibit the production of insulin-like growth factor (IGF) binding protein in the liver, excess in insulin induces elevated levels of active IGF-1. Consequently, downstream signalling of insulin and IGF-1 (e.g. via the mitogen-activated protein kinase (MAPK) or protein kinase B (AKT)) is promoted, causing proliferation, invasion and decreased apoptosis as well as enhanced expression of angiogenesis mediators (Pollak, 2009). These pathways are often dysregulated in PDAC (Li and Mao, 2015), suggesting an involvement of insulin/IGF-1 signalling in PDAC development. This is encouraged by findings of Duan *et al.* who demonstrated diminished PDAC risk via the reduction of insulin and IGF-1 by metformin treatment (Duan et al., 2017). Similar results were also obtained in *in vivo* experiments: metformin administration was shown to inhibit the growth of Panc1 xenografts in nude mice (Kisfalvi et al., 2013).

A further link between T2DM, obesity and PDAC is inflammation. Both diabetic and obese tissues are characterised by chronic low-grade inflammation. Pro-inflammatory cytokines such as Interleukin - 6 (IL-6) and Tumour necrosis factor-alpha (TNF-α), transcriptional factors such as Nuclear Factor kappa-light-chain-enhancer of activated B-cells (NF-κB) and Signal Transducer and Activator of Transcription 3 (STAT3) as well as adipokines promote tumour growth, migration and invasiveness through interaction with tumour-promoting immune cells (Scholz et al., 2003; Sciacca et al., 2013; Chang and Yang, 2016). In line with this, Braune *et al.* recently demonstrated that IL-6 stimulates macrophages in adipose tissue and promotes their local proliferation (Braune et al., 2017). Moreover, inflammation-induced abundant reactive oxygen species (ROS) production damages cellular components and also contributes to malignant progression (D. Li, 2012; Wellen and Hotamisligil, 2015).

In a KrasG12D mouse model, obesity provoked ample inflammatory signs characterised by a high number of infiltrating cells (especially macrophages), an elevated level of inflammatory cytokines and enhanced stromal fibrosis. These reactions resulted in an accelerated formation of PDAC precursor lesions (Dawson et al., 2014). The group of Lanza-Jacobi demonstrated that calorie restriction in LSL-KrasG12D; Pdc-1/Cre mice attenuates PDAC progression by reduction of cell proliferation, IGF-1 levels and expression of the glucose transporter Glut1 among others (Lanza-Jacoby et al., 2013).

In a diabetic mouse model, persistent exposure to hyperglycaemia and inflammatory microenvironment also led to accelerated tumour growth. Therapeutic intervention inhibiting inflammatory signalling not only decreased the tumour volume in diabetic mice but also led to prolonged survival (Wang et al., 2016).

Furthermore, both metabolic disorders encourage a remodelling of the pancreatic microenvironment (Mohapatra et al., 2015; Yang et al., 2016). High glucose and insulin levels activate pancreatic stellate cells which adopt a proliferative myofibroblast phenotype and produce a bulk of extracellular matrix (ECM) proteins and cytokines. This subsequently leads to pronounced fibrosis and desmoplasia and promotes PDAC development (Yang et al., 2016).

It is evident that a better understanding of the molecular interaction linking T2DM, obesity and PDAC is of great importance for developing screening methods for detection of high-risk patients and improved therapeutic options. And as these metabolic disorders can be positively influenced by the adoption of a healthier lifestyle, it also seems important to sensitise the population for the magnitude of the two risk factors.

1.1.5 Inflammatory microenvironment in PDAC

PDAC progression is characterised by a gradually increasing desmoplastic stroma. First signs of tissue remodelling and inflammatory infiltration are already detectable in precursor lesions (Rasheed et al., 2012). Whereas desmoplasia is counted among the hallmarks of cancer in various cancer entities (Hanahan and Weinberg, 2011), the extent to which it is present in PDAC is unique: up to 90% of the entire tumour mass can be made up by dense stroma (Erkan et al., 2012). Within this vast compartment a complex interplay takes place between fibroblasts, pancreatic stellate cells (PSC), immune cells, ECM proteins such as collagens I and III and fibronectin, blood vessels, hyaluronic acids and various secreted soluble mediators; this interplay impacts on tumour progression (Rasheed et al., 2012). An advanced degree of desmoplastic reaction has been shown to correlate with poorer clinical outcome (Erkan et al., 2008).

The major contributors to the desmoplastic reaction are PSC (Pandol et al., 2009; Rasheed et al., 2012). In healthy tissue they are present in a quiescent state, characterised by a slow proliferation rate and low production of ECM proteins and cytokines (Masamune and Shimosegawa, 2009). In PanIN- and PDAC-associated stroma, however, they are activated and switch into a myofibroblastic state with an amplified secretion rate (Masamune and Shimosegawa, 2009; Pandol et al., 2009). In particular, elevated levels of Transforming Growth Factor-β1 (TGF-β1), Fibrocyte Growth Factor (FGF) and Epidermal Growth Factor (EGF) have been shown to impact on tumour progression (Masamune and Shimosegawa, 2009; Merika et al., 2012). Moreover, increased secretion of Matrix Metalloproteinases (MMP) has been described in the context of PSC activation. MMP are able to break down basement membranes, thereby facilitating the metastatic spreading of cancer cells (Bergers et al., 2000; Phillips et al., 2003).

Besides PSC, infiltrating immune cells including mast and plasma cells, macrophages and leucocytes contribute to the desmoplastic reaction (Pandol et al., 2009). Especially, tumour-associated macrophages (TAM) are of importance (Grivennikov et al., 2011). They encourage tumour initiation by producing ROS and reactive nitrogen intermediates (RNI), leading to DNA damage and paving the way for tumour promoting mutations (**Figure 3**). Besides this, macrophages can also promote ROS accumulation inside PDEC themselves via pro-inflammatory cytokine-mediated signalling (Grivennikov et al., 2011).

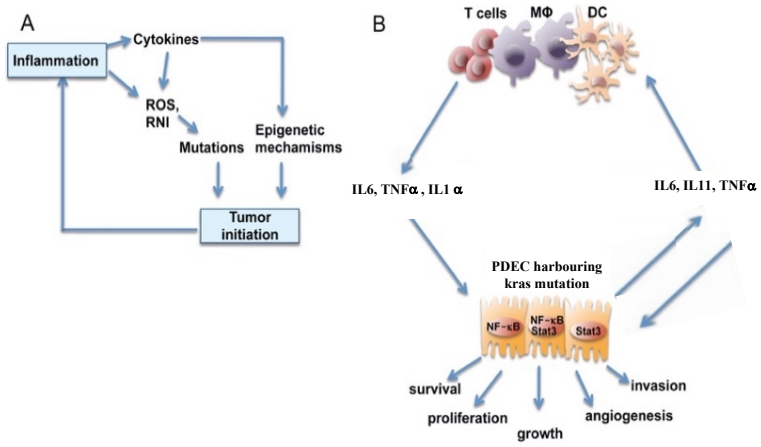

Figure 3: Impact of an inflammatory microenvironment on PDAC progression. A) Inflammatory cells produce ROS and RNI leading to mutational alterations in PDEC. Additionally, immune cell derived pro-inflammatory cytokines stimulate PDEC to produce ROS and RNI themselves and initiate epigenetic mechanisms resulting in tumour initiation. B) *Kras* mutated PDEC produce cytokines which activate inflammatory signalling cascades via NF-κB and STAT3 promoting cell survival, proliferation, growth, angiogenesis and invasion. Moreover, immune cells are attracted and stimulated to secrete IL-6 and TNF-α which further enforces STAT3 and NF-κB activation in PDEC. Tumour progression is promoted. Modified according to (Grivennikov et al., 2011).

Additionally, mutated *kras* plays an important role in the inflammatory microenvironment of PDAC (Gukovsky et al., 2013). *Kras*-dependent secretion of inflammatory cytokines activates STAT3 and NF-κB in an autocrine manner and simultaneously attracts immune cells which activate STAT3 or NF-κB in a paracrine manner by secreting IL-6 or TNF-α and IL-1, respectively. These self-amplifying signals promote cell survival, proliferation and invasiveness of PDEC (Lesina et al., 2011; Gukovsky et al., 2013). IL-6 seems to play an especially important role: elevated IL-6-serum levels in PDAC patients have been correlated with enhanced tumour growth and poorer prognosis (Scholz et al., 2003; Ebrahimi et al., 2004). Similarly, deficiency of its downstream effector STAT 3 diminishes PanIN formation (Scholz et al., 2003; Lesina et al., 2011).

Further possible mechanisms by which inflammatory cells promote tumour progression are the generation of an immunosuppressive microenvironment through secretion of IL-8, IL-10 and TGF-β1 (Kleeff et al., 2007; Rasheed et al., 2012), regulation of angiogenesis via the Vascular Endothelial Growth Factor (VEGF) and immune surveillance (Pandol et al., 2009).

Moreover, enhanced desmoplasia has been shown to promote chemoresistance in PDAC in several studies (Müerköster et al., 2004, 2008, Miyamoto et al., 2004).

1.2 Macrophages

1.2.1 Origin, polarisation and function

Macrophages are myeloid innate immune cells occurring throughout the body tissue and are endowed with a wide range of functions. The phagocytes are involved in tissue protection and regeneration, in the defence

against pathogens, in inflammatory processes and in the promotion of tumour cell proliferation and dissemination (Shi and Pamer, 2009; Sica et al., 2015). Since their first description by Ilya Metchnikoff there were several theories concerning their origin leading up to the current understanding that the majority of macrophages are tissue resident ones, formed prenatally and characterised by longevity and the capacity of self-renewal (Yona et al., 2013; Epelman et al., 2015). Additional macrophages can differentiate from monocytes in the form of a constant replenishment during homeostasis or in an enhanced form to back up local macrophages during inflammation (Varol et al., 2015). Monocytes derive from the bone marrow and are released into the bloodstream allowing them to circulate throughout the whole body (Serbina et al., 2008). They can express a broad range of chemokine receptors such as CCR1, CCR2, CXCR2 and CX3CR1 (Serbina et al., 2008). In case of tissue damage or inflammation, monocytes are attracted to the site by chemoattractants such as CCL2 and infiltrate into the tissue. Their further differentiation is strongly dependent on the stimuli they receive from the local microenvironment (Geissmann et al., 2010; Sica et al., 2015). A dichotomic classification of M1- and M2-macrophages has been established, considering the expressed cytokine profile and manner of activation (**Figure 4**). M1-macrophages are also referred to as classically activated macrophages and are induced by either lipopolysaccharides (LPS), Interferon-γ (IFNγ) expressed by T-helper cells type 1 (Th1) or the Granulocyte macrophage - colony stimulation factor (GM-CSF) (Sica et al., 2015). They are characterised by a pro-inflammatory profile with enhanced secretion of IL-1β, IL-6, IL-12 and TNF-α and the possibility to attract further immune cells via chemokines such as CCL9 and CCL10 (Rőszer, 2015). Moreover, high expression levels of CD11c are a marker of classical macrophage activation (Torres-Castro et al., 2016). Due to an amplified expression of the human leucocyte antigen DR (HLA-DR), classically activated macrophages have a great capacity to present antigens. Through high expression levels of Toll-like receptor 2 (TLR2) and inducible NO synthase (iNOS) as well as an increased production of ROS and reactive nitrogen species (RNS), they are capable to react in a bactericidal manner upon invasion of pathogens (Tan et al., 2016; Mills et al., 2016). Given these pro-inflammatory characteristics M1-macrophages are often classified as tumour suppressive cells (Mantovani et al., 2006).
M2-macrophages on the other hand are induced by IL-4 and IL-13 expressed by T-helper cells type 2 (Th2) or by Macrophage-colony stimulating factor (M-CSF) (Martinez and Gordon, 2014). This is also referred to as alternative activation. They are characterised by the secretion of the anti-inflammatory cytokines IL-10 and IL-1-receptor antagonist (IL-1ra), secretion of the growth factors TGF-β, VEGF, EGF and FGF, which are correlated to angiogenesis, tissue remodelling and wound healing (Rőszer, 2015). CCL17, CCL18 and CCL22 are chemokines indicating M2-activation (Rőszer, 2015). Furthermore, M2-macrophages are known to express high levels of the mannose receptor CD206, the scavenger receptors CD163 and CD204 and Arginase-1 (Arg-1) (Sica et al., 2006; Torres-Castro et al., 2016). In the tumour context, alternatively activated macrophages are said to possess a tumour promoting effect (Mantovani et al., 2006).

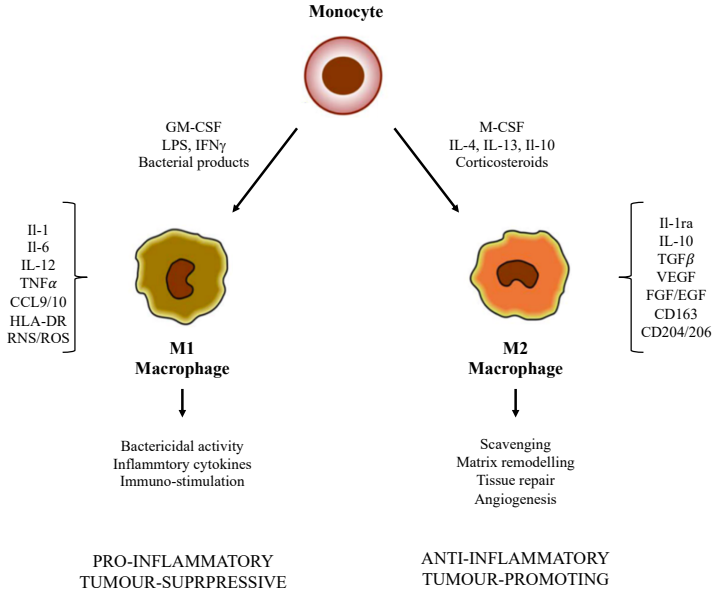

Figure 4: Differentiation into M1- and M2-polarised macrophages is dependent of the received stimuli from the microenvironment. Schematic overview of macrophages' polarisation and their distinct surface markers, soluble factors and main functions. Figure modified according to (Sica et al., 2006).

Even though the differentiation between M1- and M2-macrophages is well established in the literature and is a useful tool in *in vitro* experiments, it is not that easily transferrable into *in vivo* situation. Recent work has shown that macrophages cannot always be categorised into one of these two extremes as they often express a mixed phenotype (Helm et al., 2014a). Furthermore, they can even exhibit a certain plasticity, showing more pro- or anti-inflammatory characteristics depending on the local microenvironment they are exposed to (Helm et al., 2014a; Martinez and Gordon, 2014).

1.2.2 Macrophages, hyperglycaemia and obesity

M1- and M2-polarised macrophages differ in their primary metabolic pathways. Whereas the pro-inflammatory macrophages predominantly rely on glycolysis to meet their energetical needs, anti-inflammatory macrophages metabolise fatty acids via oxidative phosphorylation (Vats et al., 2006). In line with this, *in vitro* and *in vivo* experiments have shown that LPS-triggered M1-polarisation of macrophages leads to metabolic reprogramming with consecutive enhanced glycolysis (Blagih and Jones, 2012; Haschemi et al., 2012).

However, several other studies promote the idea that it is the glucose metabolism that shapes the phenotype of macrophages. The group around Freemerman could show that macrophages in inflammatory tissues express enhanced levels of Glut-1 transporters. The resulting pronounced glucose uptake into the cells leads to a metabolic switch towards glycolysis with resulting lactate and ROS accumulation and enhanced pro-inflammatory phenotype of macrophages (Freemerman et al., 2014).

High glucose levels also alter the cytokine expression profile of macrophages promoting a pro-inflammatory M1-associated phenotype. Enhanced levels of TNF-α, IL-1β, IL-6, IL-8 and IL-12 among others were detected in both *in vitro* (Haidet et al., 2012; Cheng et al., 2015) and *in vivo* (Pan et al., 2012) studies upon

exposure to hyperglycaemia. These transcriptional upregulations were partially dependent of NF-κB activation (Pan et al., 2012; Cheng et al., 2015). Similarly, increased levels of CD11c and iNOS and decreased levels of Arg-1 and IL-10 also imply a polarisation towards an M1-phenotype in a hyperglycaemic microenvironment (Torres-Castro et al., 2016). Furthermore, high CD11c expression on macrophages could be correlated with higher BMI, insulin resistance and excess triglycerides in hyperglycaemic patients, highlighting the close correlation between obesity, hyperglycaemia and inflammatory processes (Torres-Castro et al., 2016). This is in line with previous findings that the adipose tissue of lean individuals predominantly comprises M2-macrophages, whereas there is a shift towards M1-macrophages with weight onset (Johnson et al., 2012; Castoldi et al., 2016). Within the adipose of obese, a complex crosstalk between adipocytes and macrophages with abundant secretion of chemokines and cytokines adopts a self-enhancing character recruiting further macrophages and adipocytes and promotes inflammation and insulin resistance (Xu et al., 2003; Weisberg et al., 2003) (**Figure 5**).

Additionally, hypoxia is a common feature of adipose tissue and an initiator of M1-polarisation. Besides leading to increased Glut-1 expression, levels of pro-inflammatory cytokines are enhanced upon exposure to hypoxic conditions (Fujisaka et al., 2013).

There is evidence that the reciprocal influence between hyperglycaemia, obesity and macrophages adopts a crucial role within diseases and inflammatory processes. As the incidence of metabolic disorders such as T2DM and obesity rise in an alarming pace, an integral grasp of the intertwined signalling cascades is of great importance for potential therapeutic targeting. One such possible target is the intervention into metabolic pathways of macrophages thereby disabling their repolarisation and acquaintance of a pro-inflammatory character.

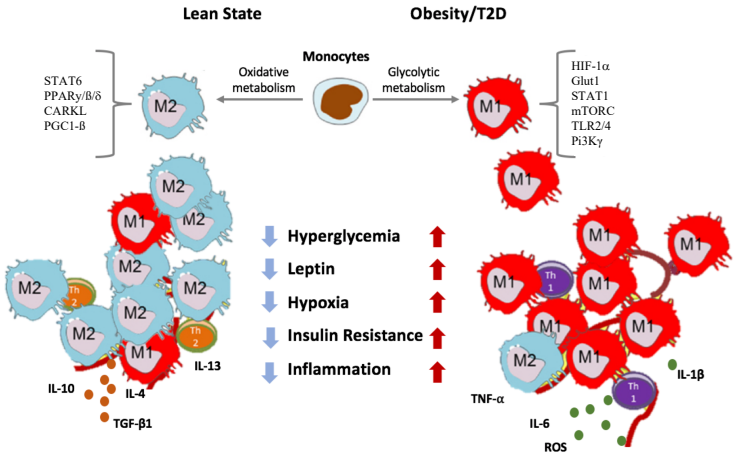

Figure 5: **Schematic illustration of macrophage polarisation in healthy state (lean) and metabolic disorder (obesity/T2DM).** In lean state (left), M2-polarised macrophages form the predominant immune cell population in fat tissue. They rely on STAT6- and PPARγ,β,δ-dependent oxidative phosphorylation to meet their energetical needs. This is facilitated by PGC-1ß and CARKL. M2-macrophages secrete anti-inflammatory cytokines and growth factors such as IL-10 and TGF-β1. In the state of metabolic disorder (e.g. Obesity or T2DM), macrophages adopt a pro-inflammatory M1-related phenotype with secretion of TNF-α, IL-1β, IL-6 and others (right). They primarily metabolise glucose via hypoxia-inducible factor-1α (HIF-1α)-dependent glycolysis. For this, further intracellular molecules such as TLR2/4, STAT1, Glut-1, mTORC1 need to be activated. Downstream targets of TLRs such as JNK, ERK, IκB, IKKβ, and Pi3Kγ are intertwined in the signalling cascade promoting insulin resistance. Figure modified according to (Plundrich, 2017; Castoldi et al., 2016).

1.2.3 Macrophages in PDAC

As described in section 1.1.5, the composition of the tumour micromilieu does not only have an important role in regard to PDAC progression but is also of prognostic value. As TAM are one of the main immune cell populations within the desmoplastic stroma and macrophage accumulation is also described for other tumour entities besides PDAC, their role in tumour promotion has been analysed in various studies in the recent years (Noy and Pollard, 2014). Zhu *et al.* recently showed that TAM derive from tissue resident macrophages (embryonic origin) as well as from circulating monocytes (Zhu et al., 2017). Despite slightly differing functionalities and key points of attack, all TAM promote tumour growth by enhanced cytokine secretion and angiogenesis, immune evasion mechanisms and cytotoxic activities (Sica et al., 2015).

The majority of TAM in PDAC are positive for both cell surface markers CD163 and CD204, which classifies them as M2-polarised macrophages according to the dichotomic model (Nielsen et al., 2016). Several studies have shown that the number of M2-macrophages present within the pancreatic stroma is closely correlated to the prognosis of PDAC patients (Ino et al., 2013; Protti and De Monte, 2013). Kurahara *et al.* were able to link poorer survival of PDAC patients with abundant M2-polarised macrophages to enhanced lymph node metastasis. One possible explanation for this is that the increased VEGF production of M2-macrophages leads to enhanced formation of peritumoural lymph vessels (Kurahara et al., 2011, 2013). Further pro-tumourigenic factors excreted by TAM are IL-6, IL-10, TNF-α and VEGF (Mantovani et al., 2006; Hermano et al., 2014). As described in section 1.1.5, IL-6 promotes tumour progression via STAT3 signalling (Lesina et al., 2011). In low concentrations corresponding to those of TAM secretion, TNF-α predominantly promotes cancer cell growth and angiogenesis similar to VEGF (Sica et al., 2015).

Moreover, macrophages in PDAC tissue are characterised by higher CCL18 levels than in healthy pancreatic tissue. Meng *et al.* stated a CCL18-dependent upregulation of the transcriptional factor Snail in PDEC, indicating progression via Epithelial Mesenchymal Transition (EMT) (Meng et al., 2015). Macrophages' contribution to PDAC progression was further corroborated through the finding, that CCL18 promotes an NF-κB-dependent increase of Vascular Cell Adhesion Molecule-1 (VCAM-1), which encourages proliferation, colony formation and mobility of PDEC. Additionally, VCAM-1 promotes a metabolic shift in PDEC towards enhanced glycolysis leading to lactate accumulation, which activates and polarises TAM towards M2-macrophages in a positive feedback loop (Meng et al., 2015; Ye et al., 2018).

There are several other pathways also associating macrophages to PDAC progression. The macrophage kinase PI3Kg has been shown to initiate crucial signalling cascades for the promotion of an immunosuppressive micromilieu allowing immune evasion and tumour cell growth (Kaneda et al., 2016a; Kaneda et al., 2016b). Its signalling cascades via AKT/mTOR diminish NF-κB-dependent transcription of pro-inflammatory cytokines and simultaneously promotes the transcription of immunosuppressive factors such as Arg-1 (Kaneda et al., 2016a).

However, TAM do not exclusively exhibit characteristics concomitant with anti-inflammatory M2-macrophages but also M1-attributed ones. Pro-inflammatory features such as an ample secretion of IL-1β, IL-6, TNF-α, CCL2 and expression of HLA-DR, among others, are also detectable in TAM and contribute to their PDAC promoting effect (Helm et al., 2014b; Hermano et al., 2014). Likewise, isolated TAM and *in*

vitro generated M1- and M2-macrophages were shown to promote EMT in benign and malignant PDEC, independently of their phenotype (Helm et al., 2014a).

1.3 Malignant progression

The capacity of local invasion and metastasis of tumour cells are comprised among the hallmarks of cancer by Hanahan and Weinberg (Hanahan and Weinberg, 2011). Over 90% of all cancer patients die as a consequence of advanced metastatic disease and not of the primary tumour itself, underlining the significance of malignant progression (Gupta and Massagué, 2006).

The invasion-metastasis cascade is a well described phenomenon composed of a complex course of events. These include local invasion into the surrounding tissue, intravasation into the nearby blood-vessels, adherence in distant organ tissue with successive extravasation, formation of micrometastasis and proliferation (Gupta and Massagué, 2006).

In PDAC, metastatic spreading is a common and early event in tumourigenesis (Rhim et al., 2012; Gaianigo et al., 2017). Therefore, the understanding of the mechanisms orchestrating malignant progression is of great importance towards improved therapeutic targeting. It is possible that primary and secondary tumour lesions possess differing resistance mechanisms towards chemotherapy and call for an adapted therapeutic approach for effective targeting (Gaianigo et al., 2017).

1.3.1 Epithelial-Mesenchymal-Transition

A prerequisite for malignant progression is the ability of cells to overcome the intrinsic epithelial barrier in order to leave the primary context (Thiery et al., 2009). For this, changes in cell morphology and functionality are necessary and underlie a complex program summarised as EMT (Kalluri and Weinberg, 2009). It comprises the loss of epithelial markers and subsequent dissolution of cell-cell-contacts, the loss of cellular polarisation and the gain in mesenchymal characteristics including enhanced motility (Valastyan and Weinberg, 2011). Physiological forms of EMT are undergone during embryonic development: implantation, gastrulation and neural crest development in all vertebrates rely on this process (Thiery et al., 2009). Similarly, wound healing and tissue regeneration are dependent on EMT (Thiery et al., 2009). Pathological forms of EMT are associated with organ fibrosis and cancer progression (Kalluri and Weinberg, 2009; Thiery et al., 2009).

A key-step in the process of EMT is the reduction of E-Cadherin, an adhesion molecule contributing to the maintenance of stable cell-cell-contacts via adherens- and tight-junctions (Peri et al., 1998). Its expression levels have been shown to be inversely correlated with patient survival in various cancer entities (Yang et al., 2014; Li et al., 2017; Radulović and Kruślin, 2018). The downregulation of the epithelial marker is closely linked to the upregulation and enhanced activity of EMT-inducing transcription factors such as Slug, Snail and Zeb1, which repress E-Cadherin expression through binding to its promotor (Peinado et al., 2007; Weinberg, 2008). Simultaneously, the transcription of other epithelial markers such as Occludin and Claudin is also repressed, whereas it is induced in the case of mesenchymal markers such as Vimentin and alpha-Smooth Muscle Actin (α-SMA) (Peinado et al., 2007). There are several other known points of interaction

for EMT regulation. For example, Snail can induce Zeb1 expression, thereby intensifying and prolonging its repressive effect on epithelial genes (Guaita et al., 2002). Additionally, an interplay of microRNA (miRNA) and EMT-inducing transcriptional factors has been identified. Members of the miRNA-200 family which are promotors of epithelial differentiation are repressed by Zeb1 (Korpal et al., 2008; Wellner et al., 2009).

Furthermore, the tumour microenvironment plays a crucial role in malignant progression. TAM, cancer myofibroblasts and other cells of the desmoplastic stroma produce pro-inflammatory cytokines and growth factors such as IL-1β, IL-6, TNF-α and TGF-β1, which are strong EMT inducers (Xu et al., 2009; Jing et al., 2011; Leibovich-Rivkin et al., 2013). Their effect is predominantly exerted via ROS- and NF-κB-dependent signalling (Rhyu et al., 2005; Karin, 2006). Among these pro-inflammatory factors, TGF-β1 is referred to as one of the most potent EMT inducers (Jing et al., 2011). Through both SMAD-dependent and -independent (e.g. p38/JNK/MAPK or PI3k/AKT/mTOR) signalling pathways, it influences the transcription factors Snail, Slug and Zeb1 (Xu et al., 2009). Additionally, its impact on the EMT program can be amplified by autocrine TGF-β1 production (Kalluri and Weinberg, 2009). Moreover, TGF-β1 is intertwined with the induction of the adhesion molecule L1CAM. Upon exposure to myofibroblasts, L1CAM expression in PDEC is upregulated in a TGF-β- and Slug-dependent manner, leading to a more mesenchymal and motile phenotype (Geismann et al., 2009).

Several other stress associated factors are known to play a pivotal role in the acquisition of metastatic potential. T2DM-related hyperglycaemic conditions were shown to foster EMT progression in PDAC (Zhou et al., 2010; Rahn et al., 2018) and other tumour entities such as breast cancer (Samuel et al., 2018) and colorectal cancer (Wu et al., 2018). The underlying mechanisms are multifold but are all closely linked to inflammatory signalling cascades (Wang et al., 2016; Li et al., 2016). Similarly, hypoxia induces EMT through HIF-1α and ROS accumulation and increases in TGF-β1-levels (Jing et al., 2011).

1.4 Cancer stemness

1.4.1 Stem cells

Stem cells are a small cell population within the tissue of mammals and can be divided into two groups according to their origin (Herreros-Villanueva et al., 2014). Embryonic stem cells derive from the inner cell mass of a blastocyst and are pluripotent, which implies that they can differentiate into all cell types (Donovan and Gearhart, 2001). Multipotent adult stem cells can be found in various tissues throughout the body and are of great importance for the maintenance of homeostasis and in the context of wound healing (Alison et al., 2002).

Adult stem cells are characterised by their ability to undergo both symmetric and asymmetric cell division, giving them the unique capacity of self-renewal (**Figure 6**). Symmetric cell division implies that one stem cell gives rise to two identical daughter stem cells, allowing the maintenance and regulation of their cell number. By asymmetric cell division, one stem cell gives rise to one daughter stem cell and one progenitor cell which can subsequently differentiate into a functional tissue cell. Controlled asymmetric cell division is

essential for growth, tissue remodelling and wound healing (Fulawka et al., 2014; Batlle and Clevers, 2017). Whereas stem cells are long-living and possess an intermittent division rate with a slow cell cycle, their progenies are short-living but highly proliferative (Morrison and Kimble, 2006; Fulawka et al., 2014).

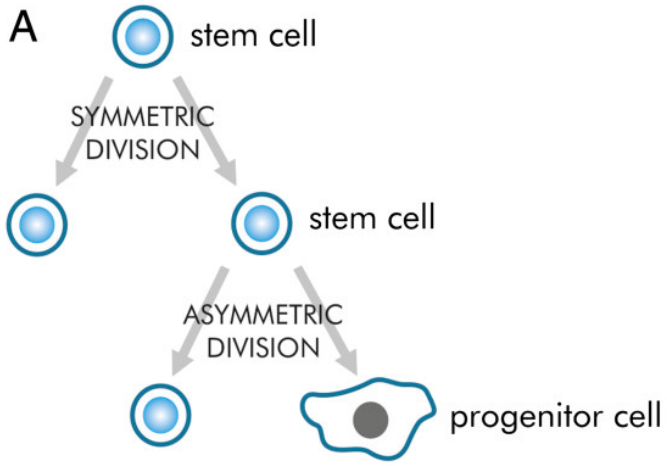

Figure 6: **Schematic overview of stem cell division.** Stem cells can divide in a symmetric manner giving rise to two identical daughter stem cells or in an asymmetric manner giving rise to one daughter stem cell and one progenitor cell capable of differentiation to various specialised tissue cells. An equilibrium of both forms of cell division is of importance for the maintenance of tissue homeostasis. Figure modified from (Fulawka et al., 2014).

As tumour growth is a continuous process showing an astonishing resistance towards multiple external factors such as low oxygen and nutrient levels or chemotherapeutics, it has assumed that the tumour tissue comprises some cells with similar characteristics to adult stem cells (Batlle and Clevers, 2017). Leukaemia was the first cancer entity in which a small subset of distinct cancer cells with enhanced stemness properties was detected and proven to be of significance for tumour initiation and growth (Bonnet and Dick, 1997). Since then, cancer stem cells (CSC) have also been identified in a multitude of solid tumour entities, such as breast, brain and colorectal cancer and PDAC (Al-Hajj et al., 2003; Singh et al., 2004; Li et al., 2007; Ricci-Vitiani et al., 2007) and are linked to tumour heterogeneity, malignant progression and chemoresistance besides tumour initiation and growth (Valle et al., 2018).

1.4.2 Cancer stem cells

CSC are attributed the capacity of self-renewal and the ability to give rise to differentiated tumour cells. They represent a very small proportion (less than 5%) of the tumour mass but are crucial contributors to tumour development (Reya et al., 2001; Li et al., 2007). Whereas the bulk of differentiated tumour cells shows very limited proliferation, CSC have a dominant proliferative potential. These observations led to a new model of cancer initiation.

The concept of clonal evaluation assuming that all cells within a tumour mass have malignant potential with high proliferative rates had been the prevailing notion for a long time (Nowell, 1976; Sugihara and Saya, 2013). It postulates that genomic instability and subsequent clonal selection results in a heterogeneous tumour tissue (**Figure 7** A). With the increased awareness of CSC, the cancer stemness model was proposed (Shackleton et al., 2009; Sugihara and Saya, 2013). It attributes tumour heterogeneity to the presence of CSC in multiple stages of differentiation (stem cells, progenitor, mature cells) (**Figure 7** B). The current

interpretation suggests a combined model which considers that CSC are also subject to genomic instability, giving rise to clonal variants of stem cells and subsequently leading to clonal variants of progenitor cells (**Figure 7** C) (Fulawka et al., 2014). It has been reported that CSC-properties can be lost and gained in a context dependent manner, which additionally contributes to the vast heterogenicity and plasticity attributed to CSC (Fulawka et al., 2014).

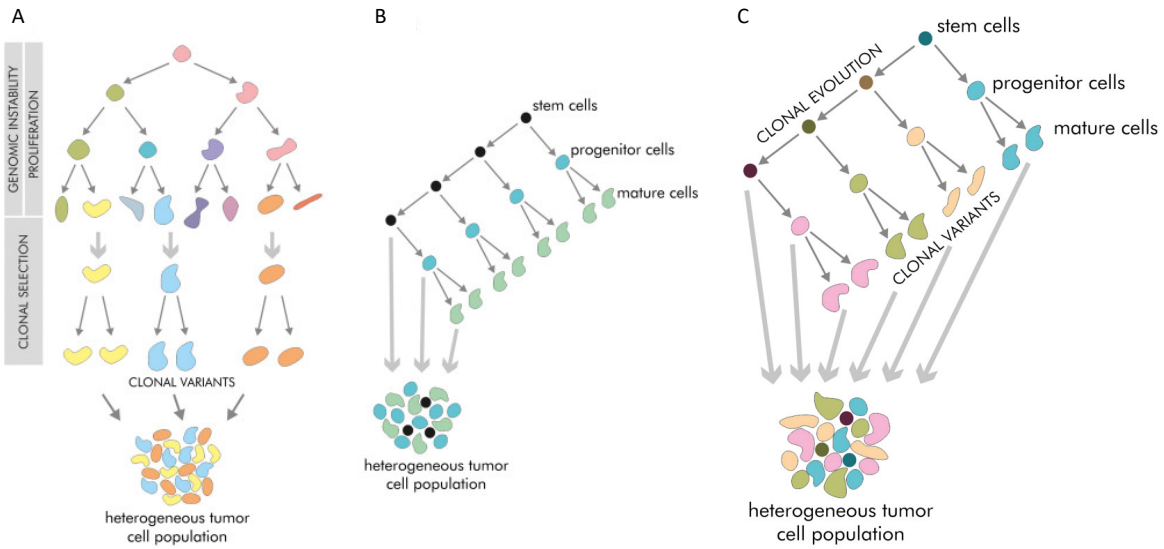

Figure 7: Overview of tumour progression models. A) The clonal evolution model assumes that heterogeneity in tumour tissue is caused by genomic and epigenetic instability and subsequent clonal selection. B) the CSC model defines a small subset of cells within the tumour - CSC - as sole cancer initiators. Tumour heterogeneity is attributed to cells in differing stages of maturation. C) In the combined model, CSC undergo clonal evolution and hence give rise to clonal variance of progenitor and mature cells. Modified after (Fulawka et al., 2014).

Many studies have been dedicated to the identification of CSC markers. Due to the heterogeneity of CSC, markers can not only vary between differing tumour entities but also within one entity. Still, a wide panel of markers has been established. In PDAC, cell surface markers such as CXCR4, CD44, CD24, CD133, ATP-Binding Cassette super-family G member 2 (ABCG2), cytoplasmic proteins such as Nestin and aldehyde dehydrogenase (ALDH) and the transcriptional factors Oct-4, Sox2 and Nanog serve as CSC markers (Silva et al., 2009; Matsuda et al., 2011; Fulawka et al., 2014; Herreros-Villanueva et al., 2014; Xia, 2014).

A functional assessment of stemness features *in vitro* is the performance of colony formation assays (CFA). These assays are based on the self-renewal capacity of CSC to generate colonies from single cells (Franken et al., 2006; Han et al., 2014). Based on the morphological differences, colonies are categorised as holo-, mero- and paraclones: holoclones are characterised by small, densely packed cells with very distinct borders and comprise the highest amount of CSC of all colony types. Paraclones are characterised by widely spread cells with fragmented borders and consist of differentiated cells. Meroclones are an intermediate type, best to distinguish from holoclones through smaller number of CSC (Tan et al., 2011). Contrary to the other two colony forms, holoclones were shown to possess the capacity of long-term self-renewal *in vitro* and to express higher amounts of CSC-related cell surface markers (Tan et al., 2011). Furthermore, holoclones were the only clones able to initiate tumour growth in a mouse model (Tan et al., 2011; Beaver et al., 2014). Therefore, increased levels of holoclones implicate enhanced stemness characteristics.

Besides being strongly associated with tumour initiation and progression, CSC are of crucial importance in tumour metastasis and responsiveness to chemotherapeutic treatment (Batlle and Clevers, 2017; Valle et al., 2018). A pronounced resistance towards multiple chemotherapeutics of CSC compared to non-CSC has been observed in PDAC (Hermann et al., 2007; Pozza et al., 2015), explaining the frequent recurrence of cancer after chemotherapeutic treatment. Classic chemotherapeutics may target the main (proliferating) tumour cell population in an effective manner but miss out on (quiescent, rarely dividing) CSC which can subsequently re-establish tumour growth (Fulawka et al., 2014; Aponte and Caicedo, 2017; Batlle and Clevers, 2017; Valle et al., 2018).

Furthermore, Hermann *et al.* could detect a distinct subpopulation of CSC at the invasive front of PDAC which were characterised by high CD133 and CXCR4 expression levels (Hermann et al., 2007). Depletion of these proteins led to reduced metastasis by sustained tumourigenic potential in a mouse model. Similar results were obtained in PDAC patients: high CXCR4 expression levels were correlated with high migratory potential of tumour cells and advanced metastatic disease in (Wehler et al., 2006; Krieg et al., 2015; Zhang et al., 2018).

Several other studies aimed to elucidate the contribution of the microenvironment to the acquisition of CSC-related properties. Just like somatic stem cells, CSC reside in cellular niches where they are subject to abundant signals (Plaks et al., 2015; Batlle and Clevers, 2017). A complex crosstalk between tumour microenvironment and CSC establishes a favourable milieu for maintenance and enhancement of features linked to stemness with subsequent tumour promotion (Ye et al., 2014; Plaks et al., 2015). Especially, inflammatory cells within the niche have been reported to be of great importance. In hepatocellular carcinoma, TAM-derived IL-6 was linked to CSC expansion *in vitro* and *in vivo* (Wan et al., 2015). In PDAC, blocking TAM infiltration decreases the number of CSC, enables metastasis and ameliorates the responsiveness towards chemotherapeutics (Mitchem et al., 2014), underlining the direct contribution of TAM to the promotion of CSC features. Additionally, CSC are able to recruit TAM towards the tumour site and to modulate their phenotype, establishing a positive feedback loop resulting in reinforced tumour progression and stemness-associated characteristics (Sainz et al., 2014).

Besides an inflammatory microenvironment, a hyperglycaemic one has also been revealed as potential modulator of CSC-properties. In lung adenocarcinoma cells, high glucose levels increase the fraction of cells exhibiting stem cell features (Liu et al., 2014). Moreover, the facilitative glucose transporter Glut-1 plays a crucial role for the maintenance of CSC in PDAC and other tumour entities. Inhibition of the transporter abolished self-renewal capacity and tumour initiation (Shibuya et al., 2014). PDEC exposed to hyperglycaemia were altered in a TGF-β1-signalling dependent manner. Besides amplified stemness features a mesenchymal phenotype could also be demonstrated (Rahn et al., 2018). Similarly, Zhao *et al.* attributed enhanced glycolysis and ROS accumulation to the maintenance of both EMT- and stemness-associated properties in PDEC (Zhao et al., 2017). These findings support a link between acquisition of CSC features and EMT, which has been first describes by Mani *et al.* (Mani et al., 2009).

1.4.3 EMT and plasticity of CSC

As stemness is correlated to cell heterogeneity, plasticity and the capacity of metastatic spreading very much alike to EMT and both are regulated by similar pathways, it was hypothesised that these two phenomena might be closely linked. Indeed, Mani *et al.* were the first to show that breast cancer cells that undergo the process of EMT simultaneously acquire CSC features. And also conversely, cultured CSC and CSC extracted from breast cancer were proven to exhibit a mesenchymal phenotype (Mani et al., 2009). Similarly, IL-6-induced EMT amplified CSC-characteristics in breast cancer cells (Xie et al., 2012). In the meantime, a connection between EMT and CSC has also been established in PDAC. Su *et al.* demonstrated a TGF-β1/SMAD-pathway dependent link between expression levels of the stemness marker Nestin and EMT. Whereas overexpression of Nestin results in a more mesenchymal phenotype, Nestin knockdown leads to amplified epithelial characteristics with reduced tumour growth and migratory capacity (Su et al., 2013). Furthermore, it has been revealed that the EMT-inducer Zeb1 silences stemness-inhibiting members of the miRNA-200 thereby fostering mesenchymal, migratory CSC (Burk et al., 2008; Wellner et al., 2009). The above-mentioned findings provide evidence of the close interconnection between the acquisition of stemness-associated features and EMT. However, the underlying molecular mechanisms have not been fully elucidated and require further research.

1.5 Aim of the study

A link between PDAC and metabolic disorders is long established. Whereas it is acknowledged that metabolic disorders such as obesity and T2DM are associated with hyperglycaemia and chronic low-grade inflammation in the surrounding tissue, the underlying molecular mechanisms by which this might promote PDAC initiation and progression largely remain obscure.

Within the inflammatory stroma of PDAC, macrophages are attributed great importance as they already accumulate in early lesions and present the main immune cell population of the tumour stroma. They were shown to possess the ability of EMT induction, thus facilitating the malignant progression of PDEC (Helm et al., 2014a). Moreover, hyperglycaemia was identified as an additional promotor of EMT- and CSC-associated characteristics in PDEC (Rahn et al., 2018). Previous studies could show that hyperglycaemia also influences the phenotype of macrophages, imposing the question whether an interplay of high glucose concentrations and macrophages further promotes malignancy-associated alterations in PDEC.

As short-term exposure to high glucose levels and macrophages predominantly led to EMT-associated alterations in PDEC (Plundrich, 2017), it was hypothesised that a prolonged subjection to these T2DM-related surroundings might intensify the effects and also impact on their CSC-associated characteristics.

Therefore, the aim of the current study was to analyse the long-term impact of hyperglycaemia itself and in interplay with macrophages on PDEC in regard to EMT and the acquisition of stemness features. Furthermore, macrophages were to be characterised in regard to their inflammatory cytokine profile after coculture with PDEC under normo- and hyperglycaemic conditions to gain a more explicit insight into their contribution to the malignancy-associated alterations in PDEC associated to malignancy.

2 Materials

2.1 Devices

Device	Manufacturer
Centrifuges	
Avanti™ J-20 XP Centrifuge	Beckmann Coulter GmbH, Krefeld, DE
Heraus Biofuge pico	Thermo Scientific, Schwerte, DE
Heraeus Fresco 17	Thermo Scientific, Schwerte, DE
Heraeus Multifufe X1	Thermo Scientific, Schwerte, DE
Heraeus Pico 17	Thermo Scientific, Schwerte, DE
JE-5.0 Elutriator	Beckmann Coulter GmbH, Krefeld, DE
Rotina 420 R	Hettrich, Tuttlingen, DE
Sprout mini-centrifuge	Heathrow Scientific, Vermion Hills, US
Incubators	
BBD 6220 CO_2 Incubator	Thermo Scientific, Schwerte, DE
Gyro Twister 3D shaker	Labnet, Woodbridge, US
QBA1 Table Incubator	Grant, Cambridge, UK
Stuart SRT9 Roll mixer	Bibby Scientific Ltd., Stone, UK
WNB 7-45 Water bath	Memmert, Schwabach, DE
WTC ED-53 Incubator	Bindner, Tuttlingen, DE
Measuring devices	
Fusion SL Detection System	Vilber Lourmat, Eberhardzell, DE
FACScaliburTM Flow Cytometer	Beckton Dickinson, Heidelberg, DE
Infinite® 200 PRO, Microplate- Reader	Tecan, Crailsheim, DE
Light Cycler 480 II	Roche, Basel, CH
NanoQuant Plate	Tecan, Crailsheim, DE
Neubauer counting chamber	Marienfeld, Lauda-Koenigshofen, DE
pH 7110 pH-Meter	ionLab, Weilheim, DE
Microscopes	
AE2000	Motic, Wetzlar, DE
Evos XL Core Cell Imaging System	AMG, Bothell, US
Lionheart FX	Biotec, Bad Friedrichshall, DE
Other devices	
ARPEGE 110 nitrogen tank	AirLiquide, Paris, FR
CS-300V Powersupply	Cleaver Scientific, West Sussex, UK
Freezer (-20 °C)	Liebherr, Ochsenhausen, DE

HERAFreeze Basic Freezer (-80 °C)	Thermo Scientific, Schwerte, DE
Laboport vacuum pump	KNF Neuberger GmbH, Freiburg, DE
MACS Multistand	Milteny Biotec GmbH, Bergisch Gladbach, DE
MACS Quatro Magnet	Milteny Biotec GmbH, Bergisch Gladbach, DE
MILLI-Q Reafent Water System	Merck Millipore, Billerica, US
MR Hei-Mix S Magnetic Stirrer	Heidoph Instruments, Schwabach, DE
OmniPAGE VS10D Gel chamber	Cleaver scientific, West Sussex, UK
Refrigerator (4 °C)	Liebherr, Ochsenhausen, DE
SD20 Semi Dry Maxi Transfer Chamber	Cleaver scientific, West Sussex, UK
Sonicator Sonoplus	Bandelin, Berlin, DE
Vortex Genius 3	IKA-Werke, Staufen, DE
Sterile benches	
HERA Safe	Thermo Scientific, Schwerte, DE
HERA Safe KS	Thermo Scientific, Schwerte, DE
Scales	
Precisa BJ 2100D	Precisa Gravimetrics AG, Dietikon, CH
Precisa XB120A	Precisa Gravimetrics AG, Dietikon, CH
Pipettes	
Finnpipette F1 0.2 – 2 µl	Thermo Scientific, Schwerte, DE
Finnpipette F1 1 – 10 µl	Thermo Scientific, Schwerte, DE
Finnpipette F1 2 – 20 µl	Thermo Scientific, Schwerte, DE
Finnpipette F1 20 – 200 µl	Thermo Scientific, Schwerte, DE
Finnpipette F1 100 – 1000 µl	Thermo Scientific, Schwerte, DE
Finnpipette F2 30 – 300 µl, multichannel pipette	Thermo Scientific, Schwerte, DE
Macro Pipette Controlle	Thermo Scientific, Schwerte, DE
Pipetboy-acu	Integra-Biosciences, Fernwald, DE

2.2 Consumables

Consumables	Manufacturer
0.1–10 µl, 10–200 µl, 100-1000 µl pipette tips	Sarstedt, Nümbrecht, DE
1.25 ml, 5.0 ml Ritips	Ritter, Schwabmuenchen, DE
0.5 ml, 1.5 ml, 2 ml Safe Seal tubes	Sarstedt, Nümbrecht, DE
15 ml, 50 ml tubes	Sarstedt, Nümbrecht, DE

5 ml, 10 ml, 25 ml serological pipettes	Sarstedt, Nümbrecht, DE
6-/ 12-/ 96-Well flat-bottom plates	Sarstedt, Nümbrecht, DE
25 cm^2 cell culture flasks	Sarstedt, Nümbrecht, DE
75 cm^2 cell culture flasks	Sarstedt, Nümbrecht, DE
96-well PCR plate, white	Roche, Basel, CH
Cell Scraper 25 cm	Sarstedt, Nümbrecht, DE
Coverslips Thermanox Plastic, 15 mm	Nunc Brand Products, Rochester, New York, US
CryoPure tube 1.0 ml white	Sarstedt, Nümbrecht, D
FACS-tube	Sterilin, Lodon, UK
Feather Disposable scalpel	PFM medical, Cologne, DE
MACS-LD columns	Milteny Biotec GmbH, Bergisch Gladbach, DE
Micro-Touch Nitril gloves	Ansell GmbH, München, DE
Parafilm M	Brand, Wertheim, DE
Pasteur pipettes ISO 7712, 230 mm	Glaswarenfabrik Karl Hecht GmbH&CoKG, Sondheim/Röhn, DE
Pre-Separation filter, 30 µm	Milteny Biotec GmbH, Bergisch Gladbach, DE
Syringe, 20 ml	Becton Dickinson, Heidelberg, DE
Sterile filter Minisart	Sartorius Stedin Biotech, Göttingen, DE
Transfer pipettes 3.5 ml	Sarstedt, Nümbrecht, DE
Whatman-3MM filter paper	FE Healthcare, Buckinghamshire, UK
Westran Polyvinylidenfluorid (PVDF) membrane 0.45 µm	Th. Geyer GmbH, Renningen, DE

2.3 Chemicals and Reagents

Chemicals	**Manufacturer**
2-Mercaptoethanol	Sigma-Aldrich, München, DE
6-Aminocaproic acid	Sigma-Aldrich, München, DE
Accutase solution	EMD Millipore Corporation, Temecula, California, US
Acetic acid 10 %	Carl Roth GmbH, Karlsruhe, DE
AEC substrate-Chromogen	Dako Diagnostika, Hamburg, DE
Ammonium persulfat (APS)	Merck Millipore, Darmstadt, DE
Bovine serum albumin (BSA), FractionV	Biomol, Hamburg, DE
Bromphenol blue	Merck Millipore, Darmstadt, DE

CD11b-Microbeads	Milteny Biotec GmbH, Bergisch Gladbach, DE
Citric acid	Carl Roth GmbH, Karlsruhe, DE
Dimethyl sulfoxide (DMSO)	Chemsolute, Th. Geyer, Renningen, DE
Sodium phosphate dibasic dihydrate (Na_2HPO_4 x 2 H_2O)	Carl Roth GmbH, Karlsruhe, DE
Dithiothreitol (DTT)	Sigma-Aldrich, München, DE
EGF, human recombinant	Life Technologies, Darmstadt, DE
EpCam-Microbeads	Milteny Biotec GmbH, Bergisch Gladbach, DE
Ethanol 99 %, denaturated	Chemsolute, Th. Geyer, Renningen, DE
Ethanol absolute, puriss.	Chemsolute, Th. Geyer, Renningen, DE
GM-CSF, human recombinant	BioLegend, Fell, DE
Grams Crystal Violet Solution	Merck Millipore, Darmstadt, DE
HiPerFect Transfection reagent	Qiagen, Hilden, DE
Hoechst 33258	Sigma-Aldrich, München, DE
Hydrochloride acid 1.0 M	Chemosolute, Th. Geyer, Renningen, DE
Hydrogen peroxide 30 %	Th. Geyer GmbH, Renningen, DE
LightCycler® 480 SYBR Green I Master	Roche Diagnostics, Mannheim, DE
Mayer's hemalaun solution	Applichem, Darmstadt, DE
Methanol	Chemsolute, Th. Geyer, Renningen, DE
Milk powder	Carl Roth GmbH, Karlsruhe, DE
Mounting Medium	Thermo Fischer Scientific, Schwerte, DE
Monopotassium phosphate (KH_2PO_4)	Carl Roth GmbH, Karlsruhe, DE
Opti-MEM™, reduced serum medium	Thermofisher Scientific, Darmstadt, DE
PageRuler Prestained Protein Ladder	Thermo Fischer Scientific, Schwerte, DE
Pancoll human	PAN Biotech, Aidenbach, DE
Paraformaldehyde (PFA) 4.5 % (w/v)	BUEFA Chemilkalien GmbH Co. KG, Hude, DE
Penicillin-Streptomycin (Pen/Strep)	PAA, Pasching, AT
Phosphate-buffered Saline (PBS)	Biochrom GmbH, Berlin, DE
Potassium chloride (KCl)	Chemsolute, Th. Geyer, Renningen, DE
Preserving agent for water baths	Carl Roth GmbH, Karlsruhe, DE
Rotiphorese gel 40 (37.5:1) Acrylamide/Bisacrylamide 40 % Solution (PAA)	Carl Roth GmbH, Karlsruhe, DE
Sodium chloride (NaCl)	Carl Roth GmbH, Karlsruhe, DE
Sodium dodecyl sulfate (SDS) ultra-pur	Carl Roth GmbH, Karlsruhe, DE
Tetramethylethylendiamine (TEMED)	Carl Roth GmbH, Karlsruhe, DE

Tri-Sodium Citrate Dihydrate	Carl Roth GmbH, Karlsruhe, DE
Tris-Base	Carl Roth GmbH, Karlsruhe, DE
Triton X-100	Sigma-Aldrich, München, DE
Trypan blue Solution Fluka 0.4 %	Sigma-Aldrich, München, DE
Trypsin-Ethylenediaminetetraacetic (EDTA)	PAA, Pasching, AT
Tween 20	Serva, Heidelberg, DE
Westernbright ECL substrate	Advansta, San Jose, US

2.4 Buffers und Gels

Buffer	**Formulation**
Blotto	5 % (w/v) Milk powder in TBS-T (1x)
Laemmli-Buffer (2x)	128 mM Tris-Base 4.6 % (w/v) SDS 10 % (v/v) Glycerol 1 mM Natriumorthovanadat pH 7.6
MACS-Buffer	0.5 % (w/v) BSA in PBS
PBS (10x)	1.37 M NaCl 26.8 mM KCl 97.8 mM Na_2HPO_4 x 2 H_2O 17.6 mM KH_2PO_4 pH 7.4
PBS-Tween (PBS-T)	10 % (v/v) PBS (10x) 0.05 % (v/v) Tween 20
Tris-buffered Saline (TBS; 10x)	29 mM Tris-Base 140 mM NaCl pH 7.6
TBS-Tween (TBS-T)	10 % (v/v) TBS (10x) 0.05 % Tween 20 (v/v) in ddH_2O

Elutriation	
Elutriation buffer	PBS, 1 % FCS 10 mM EDTA pH 7.4
Magnetic Activated Cell Sorting	
MACS-Sorting-Buffer	2 mM EDTA in MACS - Buffer pH 7.2
Western Blotting	
Blot buffer A	300 mM Tris-Base 20 % (v/v) Methanol pH 11
Blot buffer B	25 mM Tris-Base 20 % (v/v) methanol pH 10.6
Blot buffer C	25 mM Tris-Base 20 % (v/v) ethanol 40 mM 6-Aminocaproic acid pH 10.6
Loading dye (4x)	2.5 % (v/v) β-mercaptoethanol 0.005 % (w/v) Bromphenol blue in 2xLaemmli buffer
Running buffer	25 mM Tris-Base 192 mM Glycerol 0.1 % (w/v) SDS in ddH_20
Separating gel buffer	1.5 M Tris-Base 0.4 % (w/v) SDS pH 8.8
Stacking gel buffer	0.5 mM tris-Base 0.4 % (w/v) SDS pH 6.8

2.5 Cell biological Materials

2.5.1 Cell lines

Cell line	Information
H6c7-*pBp*, benign	Human pancreatic ductal epithelial cell line immortalised via HPV-16 E6/E7 oncogenes and transduced with the empty retroviral pBabepuro vector (Furukawa et al., 1996)
H6c7-*kras*, premalignant	Human pancreatic ductal epithelial cell line immortalised via HPV-16 E6/E7 oncogenes and transduced with the retroviral pBabepuro-Kras4B^{G12V}vector (Furukawa et al., 1996; Qian et al., 2005).

2.5.2 Cell culture additives

Cell culture additives	Manufacturer
D-Glucose	Sigma-Aldrich, München, DE
Bovine pituitary extract (BPE)	Life Technologies, Darmstadt, DE
EGF	BioLegend, Fell, DE
Fetal Calf Serum (FCS)	BioLegend, Fell, DE
GM-CSF	BioLegend, Fell, DE
Keratinocyte serum-free medium	Life Technologies, Darmstadt, DE
L-glutamine	PAA, Pasching, AT
Pen/Strep	PAA, Pasching. AT
PBS	Biochrom, Berlin, DE
Puromycin	InvivoGen, Toulouse, FR
Roswell Park Memorial Institute (RPMI) 1640 Medium, 11 mM glucose, no L-glutamine	Biochrom, Berlin, DE
Roswell Park Memorial Institute (RPMI) 1640 Medium, no glucose, 1 % L-glutamine	Lonza, Basel, CH

2.5.3 Cell culture media

Cell line	Formulation
Routine cell culture medium	
H6c7-*kras* / H6c7-*pBp*	50 % (v/v) Keratinocyte serum-free medium 50 % (v/v) RPMI 1640 5 % (v/v) FCS 0.5 % (v/v) L-glutamine 50 µg/ml BPE 5 ng/ml EGF 4 µg/ml Puromycin
Differentiation medium	
GM-CSF- stimulated monocytes	RPMI 1640 supplemented with 1 % (v/v) FCS, 1 % (v/v) L-glutamine, 1 % (v/v) Pen/Strep 50 ng/ml GM-CSF (240 U/ml)
Coculture medium	
M1-Macrophage Monoculture H6c7-*kras* - / H6c7-*pBp*- Monoculture H6c7-*kras* / M1-Coculture H6c7-*pBp* / M1-Coculture	RPMI (no Glucose, with 1 % L-glutamine), supplemented with 10 % (v/v) FCS, 5 mM or 25 mM D-Glucose
CFA-medium	
H6c7-*kras* / H6c7-*pBp*	routine cell culture medium

2.5.4 Small interfering RNA (siRNA)

siRNA	Manufacturer
Control siRNA	Santa Cruz Biotechnology, Heidelberg, DE
TGF-β1 - Receptor II siRNA	Santa Cruz Biotechnology, Heidelberg, DE

2.6 Primer for qPCR-Analysis

2.6.1 Primer from Eurofins (Ebersberg, DE)

Primer	5`-3`-Sequence		Annealing-Temperature (°C)
GAPDH	forward	TCCATGACAACTTTGGTATCGTGG	58
	reverse	GACGCCTGCTTCACCACCTTCT	

IL-1β	forward	AGTGCTCCTTCCAGGACCTGGA	58
	reverse	CACTCTCCAGCTGT AGAGTGG	
Nestin	forward	GAAACAGCCATAGAGGGCAAA	58
	reverse	TGGTTTTCCAGAGTCTTCAGTGA	
Sox-2	forward	TCCCATCACCCACAGCAAATGA	58
	reverse	TTTCTTGTCGGCATCGCGGTTT	
TGF-β1	forward	CGTGGAGCTGTACCAGAAATA	58
	reverse	TCCGGTGACATCAAAAGATAA	
TNF-α	forward	TCCTTCAGACACCCTCAACC	58
	reverse	AGGCCCCAGTTTGAATTCTT	
Zeb1	forward	TCCATGCTTAAGAGCGCTAGCT	61
	reverse	ACCGTAGTTGAGTAGGTGTATGCCA	

2.6.2 Primer from RealTimePrimers (via Biomol, Hamburg, DE)

Primer	5`-3`-Sequence		Annealing-Temperature (°C)
E-Cadherin	forward	TGCTCTTGCTGTTTCTTCGG	55
	reverse	TGCCCCATTCGTTCAAGTAG	
IL-6	forward	ATGCAATAACCACCCCTGAC	58
	reverse	GAGGTGCCCATGCTACATTT	
IL-8	forward	GTGTGAAGGTGCAGTTTTGCC	55
	reverse	AACTTCTCCACAACCCTCTGC	
IL-10	forward	AAGCCTGACCACGCTTTCTA	58
	reverse	ATGAAGTGGTTGGGGAATGA	
L1CAM	forward	GAACTGGATGTGGTGGAGAG	58
	reverse	GAGGGTGGTAGAGGTCTGGT	
Nanog	forward	ACCTACCTACCCCAGCCTTT	58
	reverse	CATGCAGGACTGCAGAGATT	
TGF-βRII	forward	TTGAGTCCTTCAAGCAGACC	58
	reverse	TCAACGTCTCACACACCATC	
Vimentin	forward	TCCAAGTTTGCTGACCTCTC	58
	reverse	TCAACGGCAAAGTTCTCTTC	
VEGF	forward	CGCTTACTCTCACCTGCTTC	58
	reverse	GGAAGGTCAACCACTCACAC	

2.6.3 Primer from Biometra (Göttingen, DE)

Primer	5`-3`-Sequence		Annealing-Temperature (°C)
Snail	forward	CTGCTCCACAAGCACCAAGAGTC	58
	reverse	CCAGCTGCCCTCCCTCCAC	
Slug	forward	ATATTCGGACCCACACATTACCT	58
	reverse	GCAAATGCTCTGTTGCAGTGA	

2.7 Antibodies

2.7.1 Antibodies for Western Blotting

Specifity (Clone)	Host (Isotype)	Stock concentration	Dilution	Manufacturer
Primary antibodies				
E-Cadherin (32A8)	mouse (IgG_1)	-	1:1000 (in BSA)	Cell Signalling, Frankfurt, DE
Hsp90 (F-8)	mouse (IgG_{2A})	200 µg/ml	1:2000	Santa Cruz Biotechnology, Heidelberg, DE
L1CAM (9.3)	mouse (IgG_3)	2.46 mg/ml	1:1000	Santa Cruz Biotechnology, Heidelberg, DE
NF-κB p-p65 (12H11)	mouse (IgG_3)	1 mg/ml	1:500	Merck Darmstadt, DE
NF-κB t-p65 (F-6)	mouse	200 µg/ml	1:500	Santa Cruz Biotechnology, Heidelberg, DE
Vimentin (V9)	mouse (IgG_1)	200 µg/ml	1:200	Santa Cruz Biotechnology, Heidelberg, DE

Secondary antibodies	Host	Dilution	Manufacturer
Mouse-IgG-HPR	horse	1:2000	Cell Signalling Frankfurt, DE

2.7.2 Blocking antibodies

Antibody	Target	Stock concentration	Final concentration	Manufacturer
Primary antibodies				
Tocilizumab	h IL-6R	2 µg/ml	1 µg/ml	kindly provided by Prof. Stefan Rose-John, Kiel, DE
sgp130Fc	IL-6/IL-6R complex	0.99 mg/ml	10 µg/ml	kindly provided by Prof. Stefan Rose-John, Kiel, DE
Control antibodies				
Rituximab	for Tocilizumab	10 mg/ml	1 µg/ml	kindly provided by Prof. Matthias Peipp Kiel, DE
Fc control	for sgp130Fc	4.443 mg/ml	10 µg/ml	kindly provided by Prof. Matthias Peipp Kiel, DE

2.8 Kits

Kit	Manufacturer
CellTrace™ CFSE Kit	Thermo Scientific, Schwerte, DE
CellTrace™ Violet Kit	Thermo Scientific, Schwerte, DE
DC™ Protein Assay	Bio-Rad Laboratories, München, DE
peqGOLD Total RNA Kit	PeqLab, Erlangen, DE
Revert Aid First Strand cDNA Synthesis Kit	Thermo Scientific, Schwerte, DE

2.9 Software

Software	Manufacturer
FUSION-CAPT 16.06	Vilber Lourmat, Eberhardzell, DE
FACScalibur CellQuest	BD Bioscience, San Jose, US
Gen5 Data Analysis Software	BioTek, Bad Friedrichshall, DE
GraphPadPRISM 7.0	GraphPad Software Inc., La Jolla, US
i-control™Microplate Reader Software	Tecan, Crailsheim, DE
LightCycler480 Software (Version 1.5)	Roche, Basel, CH
Microsoft Excel 2011	Microsoft Corporation, Redmond, US

3 Methods

3.1 Cell biological methods

3.1.1 Cell lines

The two human cell lines H6c7-*pBp* and H6c7-*kras* were used as a model for benign and premalignant pancreatic ductal epithelial cells. Both of them originate from human pancreatic duct cells which are immortalized by retroviral transduction with the oncogenes E6 and E7 of the human papilloma virus 16 (Furukawa et al., 1996). Whereas H6c7-*pBp* cells represent pancreatic duct epithelium without any of the common mutations of PDAC and were retrovirally transduced with the empty pBapepuro vector, H6c7-*kras* cells were transduced with the $Kras^{G12V}$-containing vector (Qian et al., 2005). As the mutational activation of the oncogene $Kras^{G12V}$ is already to be found in early PanIN, H6c7-*kras* cells mimic precursor lesions of PDAC.

Both the pBapepuro vector and the $Kras^{G12V}$-containing vector encode a puromycin resistance, which allows to ensure stable expression of the respective phenotype by addition of puromycin during cell culture as described in 3.1.2.

3.1.2 Cell cultivation

All cell culture work was performed at a sterile bench and only sterile material was used. All media were prewarmed in a water bath for 10 to 15 minutes prior to usage if not specified otherwise.

The cells were cultured in 75 cm^2 cell culture flasks in 10 ml of routine cell culture media and cultivated in an incubator (37 °C, 5 % CO2, humidity of 85 %). For maintenance and expansion, cells were split twice a week or when their confluency was at approximately 80 %. For this, the supernatant was aspirated and the cells incubated with 5 ml of Trypsin-ETDA for 10 minutes at 37 °C. In order to stop the enzymatic reaction, the cells were transferred into a 50 ml tube containing an equivalent amount of prewarmed cell culture media. After centrifugation (300 x g, 5 min), the supernatant was aspirated and the cell pellet resuspended in 10 ml of routine cell culture media. Depending on further planning, the cells were either counted and seeded for consecutive experiments, or split in a ratio of 1:3 or 1:4 into two new 75 cm^2 flasks. 4 µg/ml of puromycin were added per flask to ensure the selection of positively transduced clones.

The cells were kept in cultivation for approximately 15 to 20 passages, before being exchanged for new ones. Cells were regularly checked for mycoplasma contamination (MycoAlert® Mycoplasma Detection Kit); controls were negative throughout all experiments.

3.1.3 Freezing and thawing of cells

In order to prepare cells for long-term storage, they were first detached by using Trypsin-EDTA and centrifuged as described in 3.1.2. Cells were then washed with PBS and centrifugated once again. Afterwards, the cells were resuspended in 1 ml 10 % DMSO in FCS and quickly transferred into a cryo vial. This was

placed in a cryo box at -80 °C to allow a controlled cooling before it was placed in a liquid nitrogen tank for longterm storage two days later.

For the thawing of cells, these were removed from the liquid nitrogen tank and the lid of the cryo vial was slightly opened to allow pressure equalization before being incubated at 37 °C, 5 % CO_2 and 85 % humidity until completely thawed. It is important to work quickly to minimize the stress the cells are exposed to and to guarantee high survival rates. The cells were transferred into a 50 ml tube containing 5 ml of prewarmed routine cell culture media and were gently resuspended. After centrifugation (300 x g, 5 min), the supernatant was aspirated, the cell pellet resuspended in 10 ml of cell culture media and seeded into a 75 cm^2 cell culture flask. Puromycin was added for the first time the following day and then at each passaging timepoint as described in 3.1.2.

3.1.4 Determination of cell numbers

For the determination of the cell number, a Neubauer chamber was used. The cells were detached and centrifuged as described in 3.1.2, resuspended in 10 ml of cell culture media and then 10 µl of the cell suspension were pipetted into the chamber. The vital cells were counted in at least two quadrants of the chamber and the total number of cells obtained by using the following formula:

$$\text{cells per ml} = \frac{\text{vital cells counted x } 10^4}{\text{number of counted quandrants}}$$

3.1.5 Isolation of human monocytes

Monocytes were extracted from the blood of healthy donors who had given their informed consent. An approval of the ethics committee at the Faculty of Medicine and the University Hospital Schleswig-Holstein Campus Kiel is also on hand (ethics committee votum number D429/09 and A110/99).

In the context of platelet donations leukoreduction system chambers (LRS) arise as by-products. They contain highly concentrated leukocytes which include peripheral blood mononuclear cells (PBMC). Normally these chambers are discarded; the UKSH Blood Donor Centre Kiel kindly provided them for research use, allowing us to isolate monocytes for the *in vitro* generation of polarised macrophages. This is a two-step procedure: primarily, the PBMC are enriched through density gradient centrifugation and afterwards, monocytes are purified via counterflow centrifugation elutriation.

First of all, 20 ml of sterile PBS were filled into a 75 cm^2 cell culture flask. The blood of the LRS was added into the flask and diluted with PBS until a total volume of 140 ml was reached. Four 50 ml tubes were prepared with 15 ml of Pancoll solution each and 35 ml of the thoroughly mixed, diluted blood sample were carefully layered on top, avoiding a mixture of blood and Pancoll solution. The tubes were cautiously transferred into a centrifuge and centrifuged for 25 min with slow acceleration to a maximum speed of 800 x g and following deceleration without any mechanical brake at all.

During this density gradient centrifugation, cellular blood components such as erythrocytes and granulocytes are separated from the PBMCs. The former aggregate with a polysaccharide contained in the

Pancoll solution and thus accumulate at the bottom of the tube due to their high sedimentation rate. The latter, however, do not aggregate but form a so-called buffy coat at the boundary of the Pancoll and blood solution which is visible as a white ring (**Figure 8**).

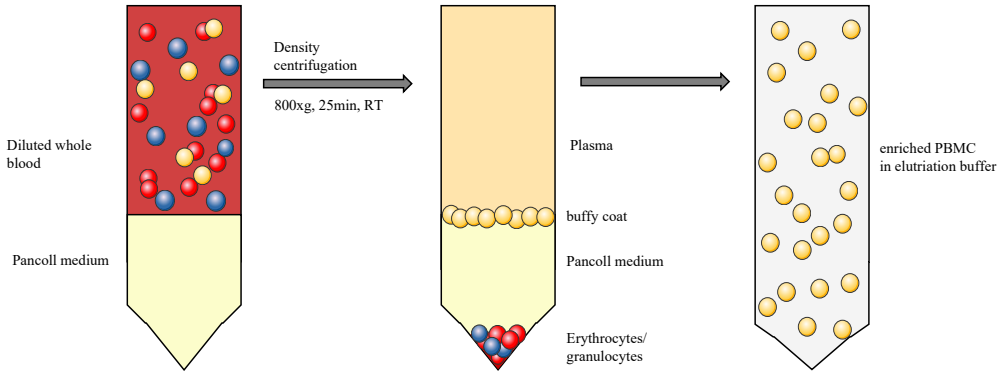

Figure 8: Schematic view of PBMC isolation out of a blood donor sample. The separation medium Pancoll and density centrifugation makes it possible to separate the PBMC based on their differing sedimentation properties. Enriched PBMC form a buffy coat at the interface of the two phases and can be separated from other blood components for further usage.

The plasma above the buffy coats was aspirated. Two of the buffy coats were then transferred into one new 50 ml tube together. The tubes were filled with cold elutriation buffer up to a total volume of 50 ml. After centrifugation (300 x g, 10 min, 4 °C), the cells were washed in 20 ml of cold elutriation buffer and centrifuged once again (300 x g, 7 min, 4 °C). In the following step the two cell pellets were united in 50 ml of elutriation buffer and the cell number was determined as described in 3.1.4. A maximum cell number of $1x10^9$ in 100 ml of elutriation buffer was used for counterflow elutriation.

Before the elutriation was started, the elutriator was rinsed with 200 ml of 70% ethanol, 300 ml of autoclaved ddH_2O and 200 ml of cold elutriation buffer at a flow rate of 65 ml/min. During this procedure, the system was freed of air bubbles by empty centrifugation at 1000 rpm (Rotor JE5, Avanti^{TM} J-20 XP Centrifuge) and cooled to 4 °C. PBMC were then loaded at 3500 rpm and a flowrate of 26 ml/min. Once all cells had entered the system and approximately 100 ml of elutriation buffer had followed, the flowrate was augmented in 2 ml/min steps per 50 ml up to a flowrate of 32 ml/min. The flow increased steps were then reduced to 1 ml/min per 50 ml. All fractions up to a flowrate of 35 ml/min were discarded whereas the following fractions of 36 to 41 were collected in prepared 50 ml tubes. The centrifuge was then switched off and a final fraction amassed (**Figure 9**).

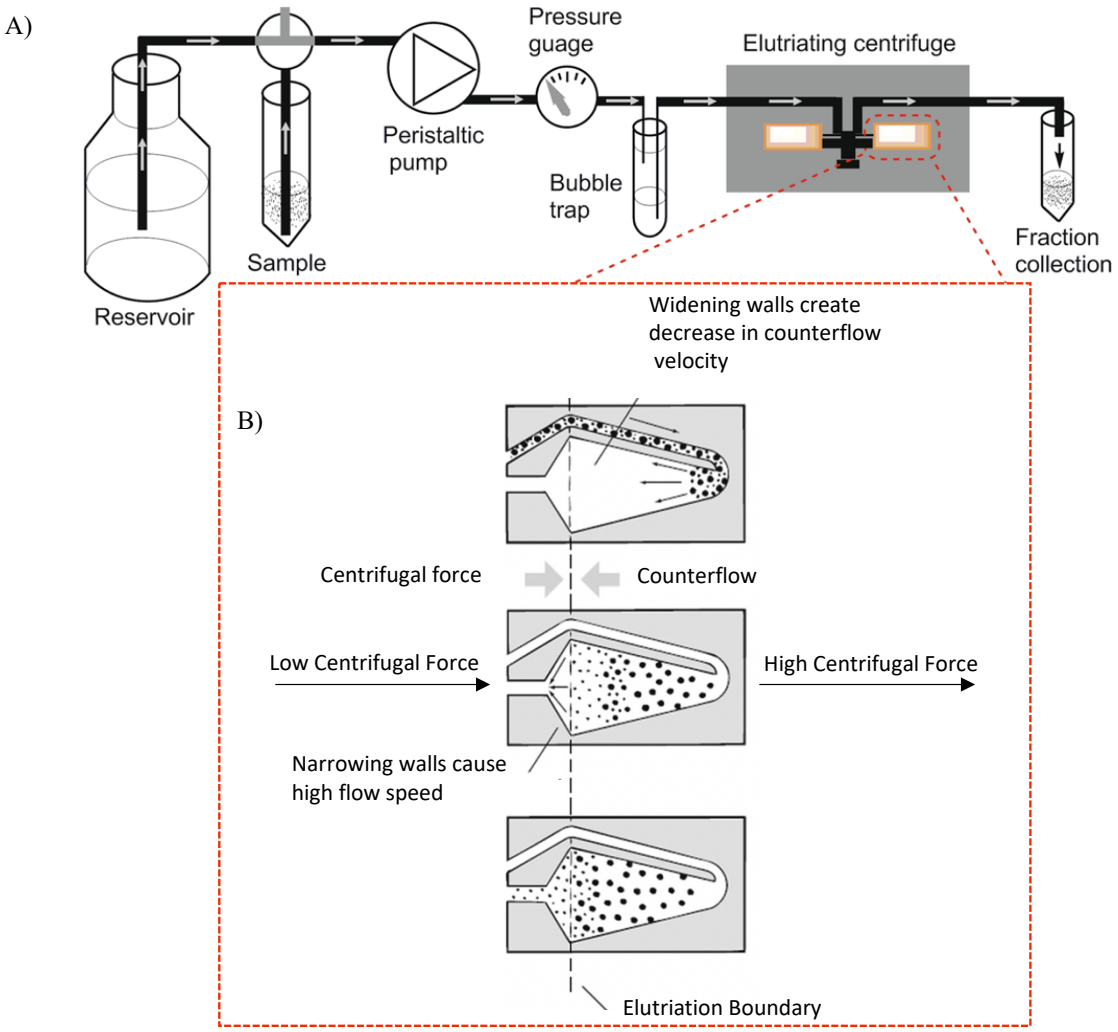

Figure 9: Schematic illustration of the elutriation procedure. (A) Elutriator construction: cells are pumped into the chamber, separated and released for subsequent collection. (B) Separation process in detail: the cells reaching the elutriator chamber are exposed to centrifugal forces and counterflow. By increasing pump pressure, counterflow slowly overcomes centrifugational forces and allows cell separation based on their size and sedimentation properties. Modified according to (Benz et al., 2017) and (Z.-J. Zhu et al., 2015).

100 µl of each fraction were transferred into flow cytometry tubes and the monocyte purity determined via forward- and sideward-scatter properties (**Figure 10**), using FACScaliburTM Flow Cytometer. Only fractions showing a purity rate of over 90 % were used for differentiation culture.

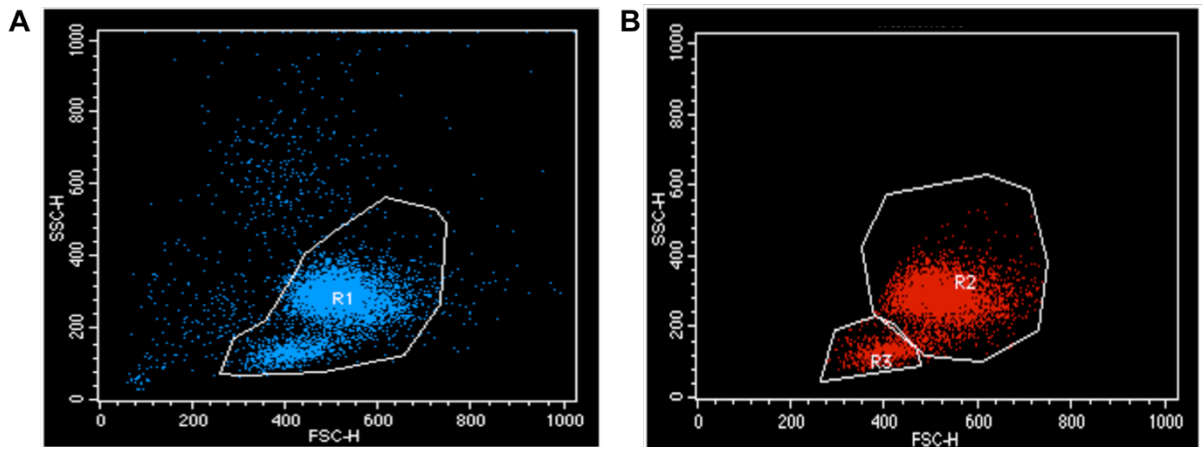

Figure 10: Representative dot plot showing cells after elutriation procedure according to their forward- and sideward-scatter. (A) Gating (R1) allows to exclude cell debris from (B) purity analysis of lymphocyte (R2) and monocyte (R3) population.

The elutriator was first rinsed with 300 ml of autoclaved ddH_20, then twice with 200 ml of Solution 555 with a 15-minute pause in between, followed by 200 ml of ddH_20 and 200 ml of 70 % ethanol. The system stayed loaded with ethanol until the next use.

3.1.6 *In vitro* generation of macrophages

For the *in vitro* generation of M1-polarized macrophages, isolated monocytes were cultivated in the presence of GM-CSF.

The chosen fractions of monocytes (see 3.1.5) were centrifuged at 300 x g and 4 °C for 10 min, the cell pellets pooled in 10 ml of differentiation media, and the cell number was determined.

Between 15 x 10^6 and 20 x 10^6 cells were resuspended in 27 ml of differentiation media. The cell suspension was carefully pipetted into VueLife cell culture bags avoiding the formation of air bubbles. Cells were then incubated at 37 °C, 5 % CO_2 and humidity of 85 % for 7 days.

3.1.7 Harvest of *in vitro* generated macrophages

Macrophages were harvested after one week of differentiation. For this, the cell bags were removed from the incubator and left on ice for an hour before being vigorously tapped onto the working surface for additional mechanical detachment. The cell suspension was poured into a 50 ml tube, the bag rinsed with 20 ml of PBS and controlled for the efficiency of detachment by microscopic inspection. Subsequently, the cells were centrifugated at 300 x g and room temperature (RT) for 10 min. The supernatant was aspirated, the cell pellet resuspended in 10 ml of macrophage medium and the cell number determined (see 3.1.4). The macrophages were now ready for coculture experiments.

3.1.8 Direct coculture of epithelial cells and macrophages

To study the interaction of pro-inflammatory macrophages and PDEC and the impact of hyperglycaemia on both cell populations, a direct coculture model was chosen.

Depending on which cell type was supposed to be analysed after 5 days of cocultivation, i.e. epithelial cells or macrophages, the respective monoculture and cocultures of H6c7-*pBp*/H6c7-*kras* and M1-macrophages (M1-MΦ) were seeded under normo- and hyperglycaemic conditions, leading to the following two possible experimental setups:

1) Experimental setup for the analysis of epithelial cells

H6c7-*pBp*	H6c7-*kras*
H6c7- *pBp* monoculture 5 mM	H6c7-*kras* monoculture 5 mM
H6c7 -*pBp* monoculture 25 mM	H6c7-*kras* monoculture 25 mM
H6c7-*pBp* / M1-MΦ coculture 5 mM	H6c7-*kras* / M1-MΦ coculture 5 mM
H6c7-*pBp* / M1-MΦ coculture 25 mM	H6c7-*kras* / M1-MΦ coculture 25 mM

2) Experimental setup for the analysis of macrophages

M1- Macrophages
M1-MΦ monoculture 5 mM
M1-MΦ monoculture 25 mM
M1-MΦ / H6c7-*pBp* coculture 5 mM
M1-MΦ / H6c7-*pBp* coculture 25 mM
M1-MΦ / H6c7-*kras* coculture 5 mM
M1-MΦ / H6c7-*kras* coculture 25 mM

For each setting at least 6 wells of a 12-well plate were used.

One day prior to the harvest of the macrophages from the culture bags (see 3.1.5), the epithelial cells were seeded in a 12-well plate in their routine cell culture medium allowing them to adhere properly overnight (**Figure 11**). To obtain a comparable ratio of PDEC and macrophages, a cell number of 2 x10^4 per well was chosen for the benign H6c7-*pBp* cells, whereas 3 x10^4 premalignant H6c7-*kras* cells were seeded per well. The well plates were stored in an incubator (37 °C, 5 % CO_2, humidity of 85 %).

The macrophages were harvested as described in 3.1.7. and resuspended in the respective coculture medium supplemented with either 5 or 25 mM of D(+)-glucose. The epithelial cells seeded a day earlier were controlled under the microscope, the supernatant of those wells designated for coculture aspirated and 2.5 x10^5 macrophages carefully added per well.

The supernatant of those wells intended for epithelial monoculture was also withdrawn and replaced by 1 ml of the respective cocultivation medium. All of the cells were then placed back in the incubator for a total of 5 days. On day 2, the cells were washed with 1 ml of PBS per well and then 1.5 ml of the equivalent cocultivation medium was given to each well.

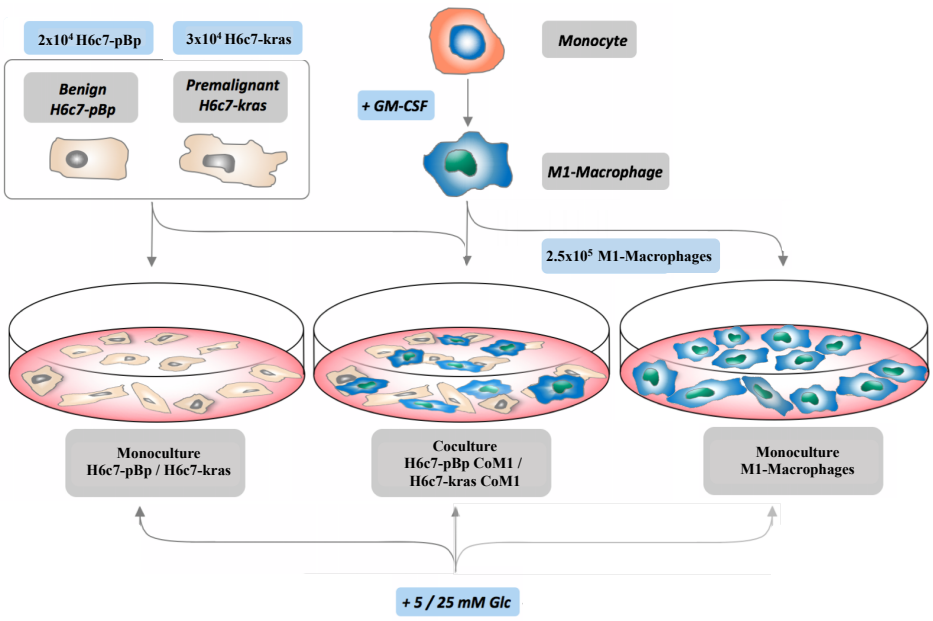

Figure 11: Schematic illustration of the experimental coculture setup. Cocultures of H6c7-*pBp* or H6c7-*kras* cells with M1-polarised macrophages were cultivated in medium supplemented with either 5 or 25 mM of glucose for 5 days. Dependent on the experiment, monocultures of PDEC or M1-macrophages were also cultivated under the same conditions serving as a control. Figure modified according to (Plundrich, 2017).

3.1.9 Magnetic Activated Cell Sorting

To investigate the effects of coculture and hyperglycaemia on macrophages and epithelial cells respectively, the two cell types needed to be separated from one another. For this, magnetic activated cell sorting (MACS) was used, a procedure allowing separation of different cell types in suspension by making use of distinct surface molecule expression. Magnetic microbeads that are conjugated to an antibody directed to a surface molecule which only one of the cell populations expresses, are added to the cell suspension. The suspension is then transferred to a column placed in a strong magnetic field. The labelled cells are held back in the column, whereas the non-labelled cell population passes through unrestrictedly.

MACS allows both positive and negative cell separation. Positive selection means that the cells of interest are labelled by microbeads and are consequently held back in the column, whereas the other cells are in the flow-through. By removing the column from the magnetic field, the labelled cells can be obtained for further usage.

For negative selection or depletion, on the other hand, microbeads are conjugated to an antibody directed to a surface molecule not present on the cell line of interest, allowing to obtain unlabelled cells; while all other cells are retained in the column.

In this study, negative selection was performed. If the epithelial cells H6c7-*pBp*/-*kras* were of interest for further analysis, microbeads linked to an antibody targeting CD11b were used; if the M1-polarized macrophages were to be investigated, microbeads attached to an anti-EpCam-antibody were utilised.

After 5 days of cocultivation, the supernatant was aspirated and the cells incubated at 37 °C with 1 ml of Trypsin-EDTA per well for 10 minutes. All cells from one experimental setup (see 3.1.8) were transferred into a 50 ml tube and the enzymatic reaction neutralised by the addition of the equivalent amount of

coculture medium. After centrifugation (300 x g, 4 °C, 5 min), the cells were carefully resuspended in 3 ml of ice-cold MACS-buffer. To singularise the cells, they were pipetted onto a pre-separation filter which was placed on a 15 ml tube and had been moistened with 500 µl of MACS-buffer beforehand. The filter was then washed three times with 500 µl of MACS buffer each before it was discarded and the cell suspension was centrifuged at 300 x g, 4 °C for 5 min. Once the supernatant was withdrawn, the cell pellet was resuspended in 80 µl of MACS-buffer and 20 µl of the respective microbeads and incubated at 4 °C for 15 min. Thereafter, 2 ml of MACS-buffer were added and the cells centrifuged once again (300 x g, 4 °C, 5 min).

In the meantime, the LD-columns were placed in the magnetic field and moistened with 2 ml of buffer. To collect the flow-through, 50 ml tubes were positioned underneath the columns. The cell pellets were resuspended in 500 µl of MACS buffer and pipetted onto the columns. To obtain as many non-labelled cells as possible, the columns were washed trice with 1 ml of buffer each. The collected cells were then centrifuged (300 x g, 4 °C, 5 min), resuspended in PBS, counted and divided for further experimental approach.

3.1.10 Colony Formation Assay

In this study, colony formation assays (CFAs) of mono- and cocultured H6c7-*pBp* and H6c7-*kras* cells of both normo- and hyperglycaemic conditions were carried out to analyse the self-renewal capacity of PDEC after the different culture conditions. Monocultured cells were detached with Trypsin-EDTA as described in 3.1.1 and washed with PBS. Cocultured cells needed to be separated from the macrophages first, which was done via MACS as described in 3.1.9. In either case, cells were then brought into solution in their routine cell culture medium and counted. Precisely 800 singularised cells were seeded in a well of a 6-well plate in duplicates or triplicates in 2 ml of cell culture media. The cells were then cultivated in an incubator (37 °C, 5 % CO_2, humidity of 85 %) for 8 to 14 days, depending on the cell line and on the treatment they had been exposed to prior to the CFA. To stop colony formation, the supernatant was discarded, the cells thoroughly washed with PBS and then fixed with 4.5 % PFA for 10 min at RT. The PFA was withdrawn and the wells rinsed twice with ddH_2O. Subsequently, the cells were incubated in 1 ml of 0.1 % crystal violet per well for 1h at RT for staining. After this, they were washed with ddH_2O at least five times or until no further crystal violet came off. The 6-well plates were left to dry overnight. For evaluation, the total number of colonies formed and the type of clone (holo-, para- or meroclone) were determined under microscopic view (**Figure 12**). For this, Evos XL Core Cell Imaging Systems was used. Only colonies containing more than 50 cells were considered.

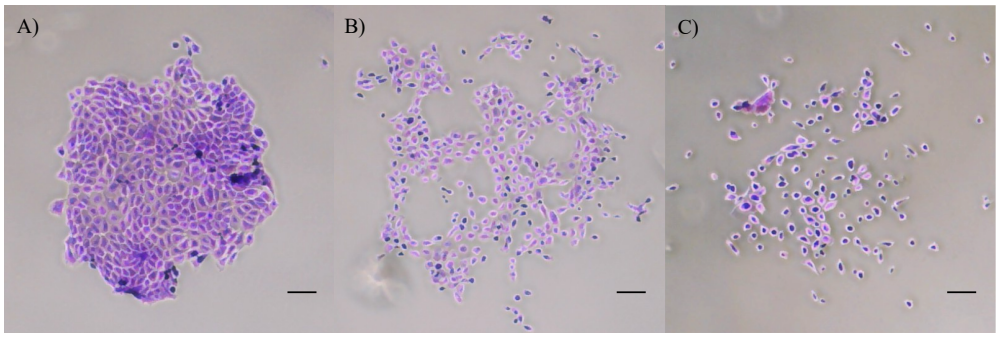

Figure 12: Representative pictures from Colony formation assay. Example of a (A) holoclone, (B) meroclone and (C) paraclone formed by H6c7-*pBp* cells are shown at 56-fold magnification. The scale bar represents 100 µm.

3.1.11 siRNA-mediated knockdown of TGF-β receptor II

Silencing of gene expression can be achieved by the introduction of small interfering RNAs (siRNA) targeting the respective messenger RNA (mRNA) and thus stopping translation into amino acids and proteins. Cells treated in that manner show reduced but not completely abolished expression levels of the respective gene.

In this study, a knockdown of the TGF-β receptor II (TGF-βRII) was chosen to analyse the contribution of TGF-β1 to the progression of EMT and the acquisition of cancer stemness related properties of H6c7-*pBp* and H6c7-*kras* cells under exposure to macrophages and/or hyperglycaemic stress. As TGF-βRII is indispensable for the successful initiation of the TGFβ-1-signalling pathway, its reduced expression levels inhibit the potential effect of the ligand TGF-β1 on the epithelial cells.

For the siRNA mediated knockdown, epithelial cells were seeded two days prior to addition of the macrophages and the cell number adapted to 1.5 x10^4 per well for the H6c7-*pBp* cells and to 2 x10^4 per well for the H6c7-*kras* cells, taking into account the prolonged cultivation time. The experimental setup using either control siRNA (ctrl siRNA) or TGF-βRII siRNA was extended to the following:

Experimental setup for TGFβRII knockdown

H6c7-*pBp*	H6c7-*kras*
Treatment with crtl siRNA	
H6c7-*pBp* / M1-MΦ coculture 5 mM	H6c7-*kr*as / M1-MΦ coculture 5 mM
H6c7-*pBp* / M1-MΦ coculture 25 mM	H6c7-*kras* / M1-MΦ coculture 25 mM
Treatment with TGFβRII siRNA	
H6c7-*pBp* / M1-MΦ coculture 5 mM	H6c7-*kras* / M1-MΦ coculture 5 mM
H6c7-*pBp* / M1-MΦ coculture 25 mM	H6c7-*kras* / M1-MΦ coculture 25 mM

For each approach, 6 wells of a 12-well plate were used.

One day after the seeding of the epithelial cells, the transfection reagent was prepared as listed below and left to incubate for 10 min at RT.

Transfection reagent (per well)
100 µl OptiMEM
6 µl HiPerfect
2 µl TGF-βRII siRNA or ctrl siRNA

In the meantime, the medium of the epithelial cells was withdrawn and replaced by 1 ml of fresh routine cell culture medium. After 10 minutes, the transfection reagent was given into the respective wells, the well plates were carefully swirled and put back into the incubator. From this point onwards, the experimental procedure was identical to the one described in 3.1.8 – 3.1.10.

The efficiency and stability of the knockdown was validated by qRT-PCR analysis. TGF-βRII levels of PDEC were analysed two, four and six days post transfection showing a stable gene suppression (data not shown). This affirmed that the established transfection protocol was convenient for subsequent coculture experiments of 5 days.

3.1.12 IL-6 blockade

To investigate the potential effect of IL-6 on the progression of EMT and the acquisition of cancer stemness related properties of H6c7-*pBp* and H6c7-*kras* cells under coculture with macrophages and/or under hyperglycaemic stress, a blockade of the IL-6 signalling pathway was performed. To consider classic and trans-signalling of lL-6 separately, two experimental setups were chosen: First of all, a blockade of IL-6 receptor via Tocilizumab was performed, blocking both signalling cascades of IL-6. Secondly, a blockade via sgp130Fc was performed, allowing the distinct analysis of the effects of IL-6 via trans-signalling.

Coculture was set up as described in 3.1.8. On day two of coculture, the wells were washed with 1 ml of PBS each and 1.5 ml of coculture medium supplemented with the equivalent blocking reagent was given to each well. Tocilizumab and its control antibody Rituximab were added at a concentration of 1 µg/ml, whereas gp130Fc and its control-Fc were used at a concentration of 10 µg/ml. Coculture was continued for four further days before separating the epithelial cells from the macrophages as described in 3.1.9 and using them for qPCR and CFA analysis.

Successful blocking of the downstream signalling pathways was verified by western blot analysis of phosphorylated STAT3 in PDEC two and five days after the addition of the respective blocking reagents. As the phosphorylation of the IL-6 downstream target was still visibly reduced five days post Tocilizumab or sgp130FC treatment (data not shown) the protocol was proven to be adequate for all experimental settings.

3.1.13 Scratch Assay

For further analysis of the impact of TGF-βRII knockdown and blockade of IL-6 signalling on EMT progression, scratch assays were performed allowing to evaluate potential changes in the cells' mobility capacity upon the different treatments. For this, the experimental setup was as described in chapter 3.1.11 (TGF-βRII knockdown) or 3.1.12 (blockade of IL-6 signalling), however, only one well per treatment was seeded. After 5 days of coculture with M1-polarised macrophages under normo- or hyperglycaemic conditions, a scratch was applied in each well with a 100 µl pipette tip. The cells were then immediately photographed with the Lionheart FX Automated Microscope, designating this as timepoint zero (t=0). Further pictures were taken 9 and 24 hours after the scratch had been applied. For analysis of the cellular confluence, the wound surfaces at these timepoints were compared to the equivalent surface at t=0 using the Gen5 Data Analysis Software.

3.2 Molecular biological methods

3.2.1 RNA isolation

For the analysis of gene expression of PDEC and macrophages after mono- or coculture and after exposition to normo- or hyperglycaemia, RNA was isolated. For this, cells were harvested, separated via MACS where applicable (see chapter 3.1.9), washed with PBS and then centrifuged (300 x g, RT, 5 min). The cell pellet was resuspended in 300 µl of lysis buffer T from the peqGOLD Total RNA Kit (PeqLab, Erlangen, DE). All the following steps of RNA isolation were performed according to the manufacturer's instruction. First of all, the lysate was pipetted onto the DNA removing column and centrifugated at 12.000 x g and RT for 1 min. The column holding back DNA and other debris was discarded, the flow-through containing the RNA was washed with 300 µl of 70 % ethanol and pipetted onto the PerfectBind RNA column. Centrifugation at 10.000 x g and RT for 1 min followed. The RNA was now bound to the column, which was washed twice, once with 500 µl of Wash buffer I and, after repeated centrifugation (10.000 x g, RT, 1 min), with 600 µl of Wash buffer II. A further centrifugation step followed to eliminate any remaining fluid from the column (10.000 x g, RT, 2 min). Finally, the PerfectBind RNA column was placed into a 1.5 ml reaction tube, 40 µl of nuclease-free ddH_2O were pipetted directly onto the matrix and left to rest for 3 min. The isolated RNA was then eluted from the column by centrifugation for 1 min at 5.000 x g and RT.

Nucleic acid concentration was measured by using an Infinite 200 PRO Microplate Reader. To assure a high purity degree of the RNA samples, the ratio of absorbances at the wavelengths 260 nm and 280 nm, representing the absorbance maxima of nucleid acids and proteins, respectively, was controlled and made sure to be close to 2. RNA samples were then stored at -80 °C until further usage.

3.2.2 cDNA synthesis

Complementary DNA (cDNA) was generated from isolated RNA (see chapter 3.2.1) by using the RevertAid Strand cDNA Synthesis Kit (Thermo Scientific, Schwerte, DE) according to the manufacturer's instruction. For this, 100 to 500 ng of RNA were diluted with nuclease-free ddH_2O up to a total volume of 11.5 µl. One µl of oligo $(dT)_{18}$ primer was added to each sample, the solution thoroughly mixed and incubated at 65 °C for 5 min. Subsequently, the samples were cooled on ice, mixed and briefly centrifugated before following components were added:

Reaction mixture per RNA sample
4.0 µl 5x reaction buffer
0.5 µl RiboLock RNase Inhibitor
2.0 µl 10 mM dNTP mix
1.0 µl RevertAid

The solution was mixed and incubated at 42 °C for 1 h. To stop the reaction, a final incubation step followed at 70 °C for 5 min. The cDNA was then diluted with nuclease-free water in a ratio of 1:4 and stored at -20 °C until further usage.

3.2.3 Quantitative Realtime-Polymerase Chain Reaction

To evaluate specific gene expression of macrophages or H6c7-*pBp /-kras* cells under specific cultivation conditions, quantitative Realtime-Polymerase Chain Reaction (qRT-PCR) was performed. All the following steps were carried out on ice. First of all, 2.5 µl of cDNA were pipetted into one well of a LightCycler 96-well microtiter plate in duplicates and supplemented by 7.5 µl of a reaction mixture. The reaction mixture was prepared as specified below, depending on the provider of the primer.

Reaction mixture for Eurofins Primers (per cDNA sample)	**Reaction mixture for RealTimePrimers (per cDNA sample)**
5 µl SYBR Green I Mastermix(2x)	5 µl SYBR Green I Mastermix(2x)
1 µl Forward Primer	1 µl Primer Mastermix
1 µl Reverse Primer	1.5 µl nuclease-free ddH_20
0.5 µl nuclease-free ddH_20	

Reaction mixture for Biometra Primers (per cDNA sample)
5 µl SYBR Green I Mastermix(2x)
0.0375 µl Forward Primer
0.0375 µl Reverse Primer
1.425 µl nuclease-free ddH_20

Then, the microtiter plate was sealed with a translucent adhesive film and centrifuged at 300 x g and 4 °C for 2 min. The qRT-PCR was carried out using a LightCycler 480 II with a maximum of 50 cycles and a subsequent analysis of the melting curve for PCR quality control.
A detailed qPCR protocol is listed below; the corresponding annealing temperature for the different gene specific primers can be found in 2.6.1-2.6.3.

qPCR protocol			
1) Initial Denaturation	5 min	95 °C	
2) Denaturation	10 sec	95 °C	40-50 cycles of step 2-4
3) Annealing	20 sec	58-61 °C (see 2.6.1-2.6.3)	
4) Elongation	30 sec	72 °C	
5) Final Extension	10 min		
6) Melting Curve		72 °C	
7) Cooling		4 °C	

The duration of the annealing phase was prolonged to 45 sec for analysation of L1CAM, Nanog and TGF-βRII.
Subsequent evaluation was performed using the LightCycler 480 software and Microsoft Excel. The relative expression level of the evaluated genes was calculated using the 2ΔΔ- method and the expression of the housekeeper gene GAPDH as a normalisation reference.

3.3 Biochemical methods

3.3.1 Generation of whole cell lysates

For the isolation of whole cell lysates of H6c7-*pBp* and H6c7-*kras* cells after mono- or coculture and exposition to normo- or hyperglycaemia, cells were harvested and, where applicable, separated from macrophages via MACS as described in 3.1.9. The cells were centrifuged at 300 x g and RT for 5 min, and then resuspended in 80-100 µl of 2xLaemmli buffer. The lysates were briefly sonicated three times, ensuring complete disruption of the cell membrane. The samples were stored at -20 °C until further usage.

3.3.2 Determination of protein concentration

To determine the concentration of proteins within whole cell lysates, the DC Protein Assay (Bio-Rad Laboratories, München, DE) was used according to the manufacturer's instructions.

First of all, all reagents were prewarmed to RT to avoid precipitation and thus to allow precise calorimetric reaction. Five µl of each sample and of a standard row with concentrations ranging from 0.193 g/ml to 1.55 mg/ml were pipetted into the wells of a translucent 96-well flat bottom plate in duplicates. Then, 25 µl of reagent A` (1:50 dilution of reagent S in reagent A) and subsequently 200 µl of reagent B were added into each well and the plate left to incubate in the dark for 15 min at RT. After this time, the protein concentration was measured by using the Tecan Infinite M200PRO spectrophotometer with a wavelength of 680 nm.

3.3.3 Western Blotting

3.3.3.1 Sodium dodecyl sulfate polyacrylamide gel electrophoresis (SDS-PAGE)

Sodium dodecyl sulfate polyacrylamide gel electrophoresis (SDS-PAGE) enables the separation of proteins according to their molecular weight. For this, 10 µg of protein were diluted with 2xLaemmli buffer ensuring that all samples were brought up to the same final volume. Loading dye (4x) was added to each sample at a ratio of 1:4 before samples were heated to 95 °C for 5 min. Samples were then cooled on ice and spun down.

In the meantime, a separation gel was prepared as shown in the list below and topped with isopropanol. Once it was polymerised, the isopropanol was withdrawn, a stacking gel layered above (see components below) and a suitable sample comb carefully inserted avoiding formation of air bubbles.

Separation gel (10 %)	Stacking gel
4.0 ml ddH_20	2000 µl ddH_20
2.0 ml separation gel buffer	765 µl stacking gel buffer
2.0 ml PAA	31 µl PAA
30 µl 10 % APS	20 µl 10 % APS
6.0 µl TEMED	3.0 µl TEMED

After complete polymerisation, the gel was placed into a running chamber, covered with running buffer and the comb cautiously pulled out. The samples and at least one PageRulerTM Plus Prestained Protein Ladder per gel were loaded into the pockets. Electrophoretic separation was carried out at a voltage of 90 mV until the samples had reached the separation gel, then the voltage was increased to 130 mV.

3.3.3.2 Protein transfer

After completed segregation of the proteins, gels were transferred onto a polyvinylidene fluoride (PVDF) membrane in a semidry blotting chamber. First of all, the PVDF membrane was activated by incubation in 100 % methanol for 1 min and subsequently rinsed in ddH_2O. In a second step, the SDS-gel was carefully

withdrawn from the running chamber and placed onto the PVDF membrane. Both membrane and gel were then enclosed in between Whatman paper soaked in Blotting buffer as shown in **Figure 13**.

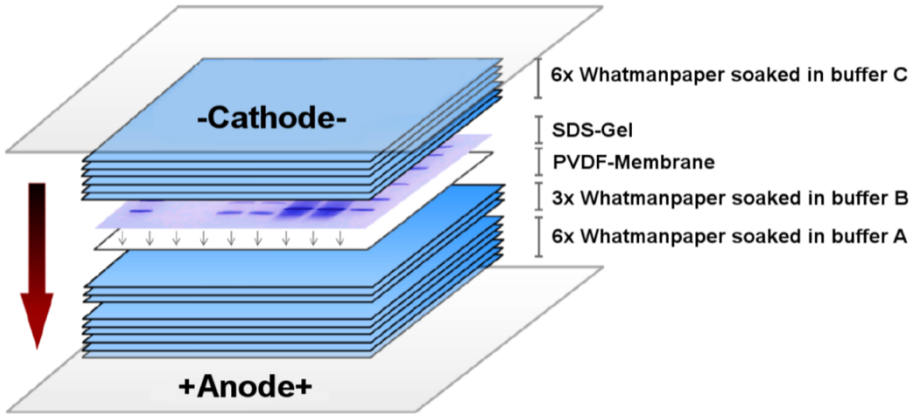

Figure 13: Schematic depiction of semidry blotting technique. Six sheets of Whatmanpapers were soaked in blot buffer A and placed onto the anode of the blotting system. Three Whatmanpapers trenched in blot buffer B and the activated PVDF membrane followed. Next, the SDS-gel was carefully stacked on top and 6 Whatmanpapers soaked in blot buffer C. Once the cathode was placed on top, the system was ready for protein transfer. Figure according to (Lenk, 2017).

The blotting chamber was closed, and the proteins transferred onto the membrane by application of an electric current of 70 mA per gel for 1 h.

3.3.3.3 Immunodetection of proteins

Once the protein transfer onto the PVDF-membrane was terminated, the blotting chamber was disassembled and the membrane washed in TBS-T for 10 min on a shaker.

To decrease unspecific binding of proteins, the PVDF membrane was blocked with Blotto for at least 1 h at RT. Subsequently, the membrane was transferred into a 50 ml tube containing the respective primary antibody diluted in Blotto if not specified otherwise (see chapter 2.7.1) and was left to incubate on a roll mixer at 4 °C overnight. The following day, the membrane was washed in TBS-T three times before being transferred into the according secondary antibody (see chapter 2.7.1). Secondary antibodies are linked to horseradish peroxidase allowing luminescent detection. After 1 h of incubation at RT on a roll mixer, the membrane was once again washed in TBS-T three times for 10 min each before being incubated in WesternBright ECL substrate for 3 min in the dark. The emerging chemiluminescent signal was detected using the Fusion SL Detection System. The PageRulerTM Plus Prestained Protein Ladder allowed control of protein size. Heat Shock Protein 90 (Hsp90) was used as loading control.

3.4 Statistical Analysis

Statistical analysis was performed using GraphPadPRISM Version 7.0a. Normal distribution was tested via the Shapiro-Wilk-Test. Parametric data were either analysed by unpaired t-test or one-way analysis of variance (one-way ANOVA) if comparing the impact of multiple factors. Data are represented by their mean and their standard error of mean (SEM). Non-parametric data were analysed by Kruskal-Wallis one-way ANOVA on ranks and their median and interquartile range are represented. Results were considered as statistically significant for p-values < 0,05. Significance of results is indicated as follows:

*: 0,05 > p > 0,0332 **: =0,0331 > p> 0,0021 ***=: 0,002 > p> 0,0001 ****: p <0,0001

4 Results

4.1 The impact of hyperglycaemia and PDEC on macrophages

Previous experiments revealed that high glucose levels increase the pro-inflammatory character of M1-polarised macrophages. It could also be shown that PDEC which are simultaneously exposed to M1-macrophages and hyperglycaemia are influenced in their EMT-properties. First findings suggested that this gain of tumourigenesis-associated characteristics may be attributed to elevated TNF-α levels expressed by macrophages (Plundrich, 2017). However, so far only little is known about the impact of the mentioned interplay between pro-inflammatory M1-macrophages and PDEC in T2DM-associated hyperglycaemic conditions on macrophages themselves. To elucidate this and to gain further insights on macrophages' potential contribution to the findings of Plundrich *et al.*, a direct coculture system of PDEC and macrophages was conducted and the gene expression level of several pro- and anti-inflammatory cytokines and growth factors in macrophages was analysed.

4.1.1 The presence of PDEC and high glucose levels alters the cytokine profile of macrophages

In a first step, the combined impact of hyperglycaemia and coculture with PDEC on macrophages was analysed. For this, macrophages were cultivated with H6c7-*pBp* or H6c7-*kras* cells in coculture medium supplemented with either 5 or 25 mM glucose for 5 days. As a control, macrophages were monocultured in normo- or hyperglycaemic settings. After 5 days, macrophages were separated from coculture via EpCam MACS-depletion of PDEC or harvested from monoculture and their relative gene expression levels of pro- and anti-inflammatory cytokines and growth factors were evaluated. Indeed, macrophages that had been cocultured with PDEC were influenced in their expression level of the analysed EMT- and CSC-inducing mediators. Here, IL-6 levels were altered most impressively: normoglycaemic coculture with H6c7-*pBp* cells led to a 263-fold, and hyperglycaemic coculture to a 229-fold increase compared to monocultured macrophages under similar glycaemic conditions (**Figure 14** A). In macrophages cocultured with H6c7-*kras* cells, elevated glucose levels had a synergistic effect causing a 297-fold increase in hyperglycaemic while a 231-fold increase in normoglycaemic settings could be observed compared to respectively monocultured macrophages (**Figure 14** A).

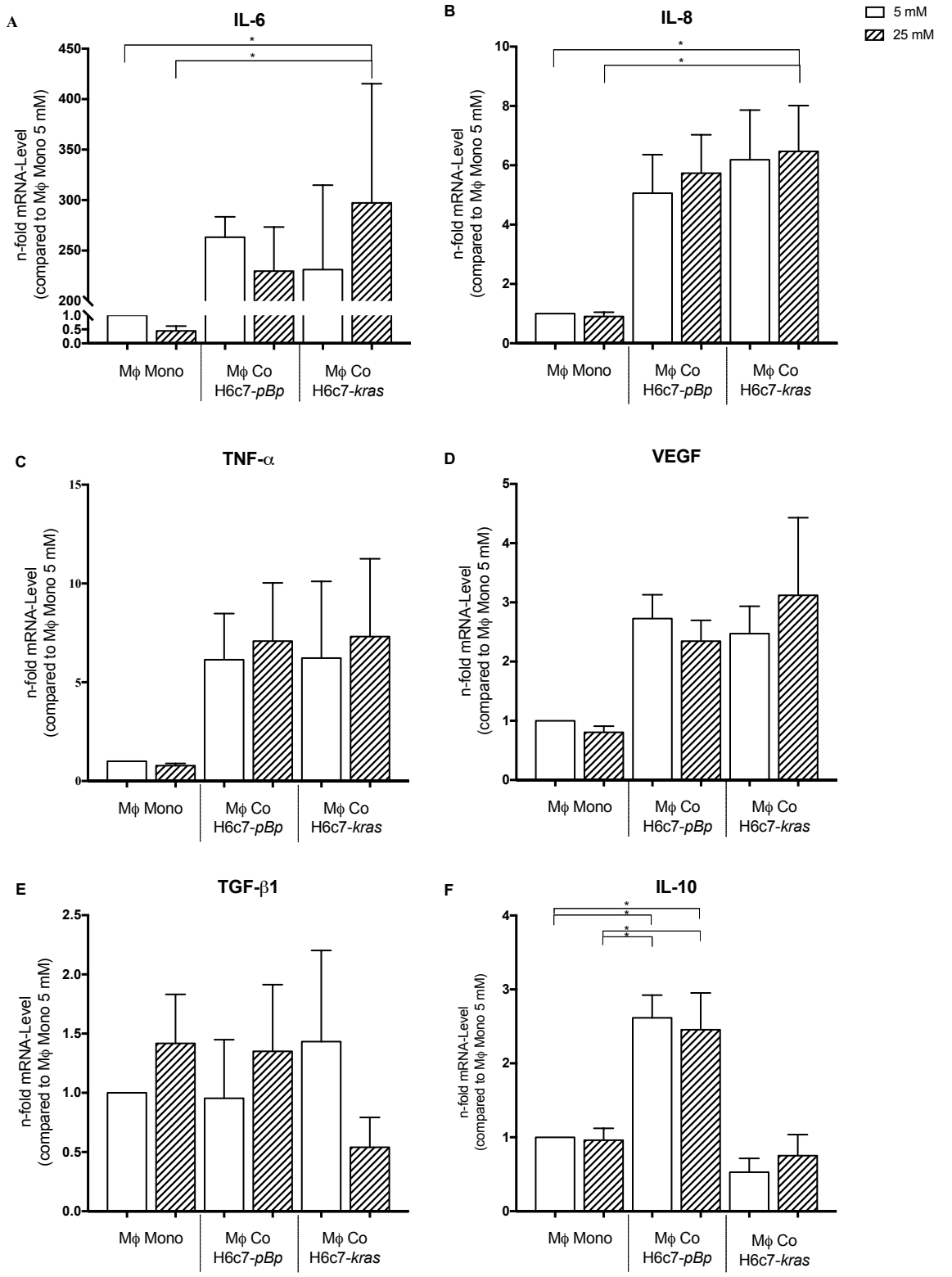

Figure 14: The presence of benign and premalignant PDEC and high glucose levels alters the gene expression level of pro- and anti-inflammatory cytokines and growth factors in macrophages (MΦ). M1-polarised macrophages were cultivated in mono- or coculture with H6c7-*pBp* or H6c7-*kras* cells for 5 days under normo- or hyperglycaemic conditions (5 or 25 mM glucose). MΦ were separated from direct coculture with epithelial cells via EpCam-MACS depletion of PDEC or harvested from monoculture and used for qRT-PCR analysis. The relative gene expression levels of IL-6 (A), IL-8 (B), TNF-α (C), VEGF (D), TGF-β1 (E) and IL-10 (F) are depicted, normalised to the housekeeping gene GAPDH and presented as n-fold expression compared to the normoglycaemic monocultured MΦ sample. Data are presented as mean and standard error of mean; one-way ANOVA was performed for statistical analysis. * :0,05>p>0,0332; n=5

The mRNA levels of the pro-inflammatory cytokines IL-8 and TNF-α were very similarly impacted by coculture with PDEC and high glucose levels. Both mediators were elevated in a coculture-dependent manner and hyperglycaemia further aggravated this upregulation (**Figure 14** B and C). In general, the effect induced through coculture with the premalignant H6c7-*kras* cells was slightly more pronounced than the one evoked through coculture with the benign H6c7-*pBp* cells (IL-8 levels: 5.0- and 5.7-fold increase through normo- and hyperglycaemic coculture with H6c7-*pBp*; 6.2- and 6.5-fold increase through normo- and hyperglycaemic coculture with H6c7-*kras* cells. TNF-α levels: 6.1- and 7.1-fold increase through normo- and hyperglycaemic coculture with H6c7-*pBp*; 6.2- and 7.3-fold increase normo- and hyperglycaemic coculture with H6c7-*kras* cells).

VEGF, which is known to be an important factor in the context of vasculogenesis and angiogenesis (Luo et al., 2001) as well as in the stimulation of monocyte and macrophage migration (Wheeler et al., 2018), was also clearly upregulated through coculture with both PDEC lines, irrespective of the glucose level (**Figure 14** D).

The mRNA level of TGF-β1 in macrophages was less impacted by coculture than had been the case for the other cytokines analysed (**Figure 14** E). Whereas normoglycaemic coculture with the benign PDEC line did not influence the gene expression level at all, hyperglycaemic coculture led to a 1.5-fold increase compared to normoglycaemic monoculture. A similar increase of nearly 50 % was evoked through normoglycaemic coculture with the premalignant PDEC line, whereas hyperglycaemic coculture intriguingly led to a reduction of 62 % compared to macrophages from normoglycaemic coculture.

Remarkably, IL-10 showed significantly increased mRNA levels in macrophages cocultured with H6c7-*pBp* cells irrespective of the glucose level, whereas macrophages cocultured with the premalignant H6c7-*kras* cells showed diminished mRNA levels of this factor (**Figure 14** F). The diminution was slightly more pronounced under normoglycaemic than under hyperglycaemic coculture conditions.

Altogether, these data show that the gene expression level of pro- and anti-inflammatory cytokines of macrophages are clearly impacted by the presence of PDEC and hyperglycaemia. Especially the presence of the premalignant H6c7-*kras* cells and high glucose levels promote a pro-inflammatory phenotype of macrophages with high expression levels of IL-6, IL-8, TNF-α and VEGF and simultaneously low expression levels of the anti-inflammatory TGF-β1 and IL-10.

4.1.2 High glucose levels faintly promote the pro-inflammatory phenotype of macrophages cocultured with PDEC

In order to better discriminate whether elevated glucose levels or the presence of PDEC account for the aggravation of a pro-inflammatory phenotype in macrophages, the alone effect of glucose on macrophages that had either been monocultured or cocultured with H6c7-*pBp* or H6c7-*kras* cells was analysed in a second step. For this, the experimental setup was identical to the one mentioned in section 4.1.1, but for analysis the relative gene expression level of the pro- and anti-inflammatory cytokines and growth factors of the cells cultivated under hyperglycaemic conditions were compared to the equivalent cells from normoglycaemic cultivation conditions. Interestingly, monocultured macrophages showed a significant decrease in the gene expression level of IL-6 (**Figure 15** A) through high glucose and tendencies of decrease for IL-8, TNF-α, VEGF and IL-10 (**Figure 15** B, C, D, F). TGF-β1 expression, on the other hand, was slightly upregulated through hyperglycaemia in monocultured macrophages (**Figure 15** E).

In contrast, macrophages that had been cocultured with either epithelial cell line showed tendencies of increase in the mRNA levels of all pro-inflammatory cytokines and growth factors through elevated glucose levels (**Figure 15** A-C). Hyperglycaemia induced a 2.7-fold elevation in the expression level of VEGF in macrophages from coculture with the premalignant cells, whereas it did not alter the expression in macrophages from coculture with the benign PDEC. The immunosuppressive cytokines and growth factors did not show uniform effects: TGF-β1 expression was increased through high glucose levels in macrophages from coculture with H6c7-*pBp* cells but decreased in those from coculture with H6c7-*kras* cells. The gene expression level of IL-10 was only affected in macrophages arising from coculture with the premalignant PDEC showing a slight glucose-dependent increase (**Figure 15** E and F).

Thus, overall, glucose alone only faintly impacted on the gene expression level of the analysed potential EMT- and CSC- inducers. This leads to the assumption that the effects seen in section 4.1.1 are mainly caused by the interaction between macrophages and PDEC. Therefore, the effect of coculture with PDEC on its own on the gene expression level of macrophages was analysed.

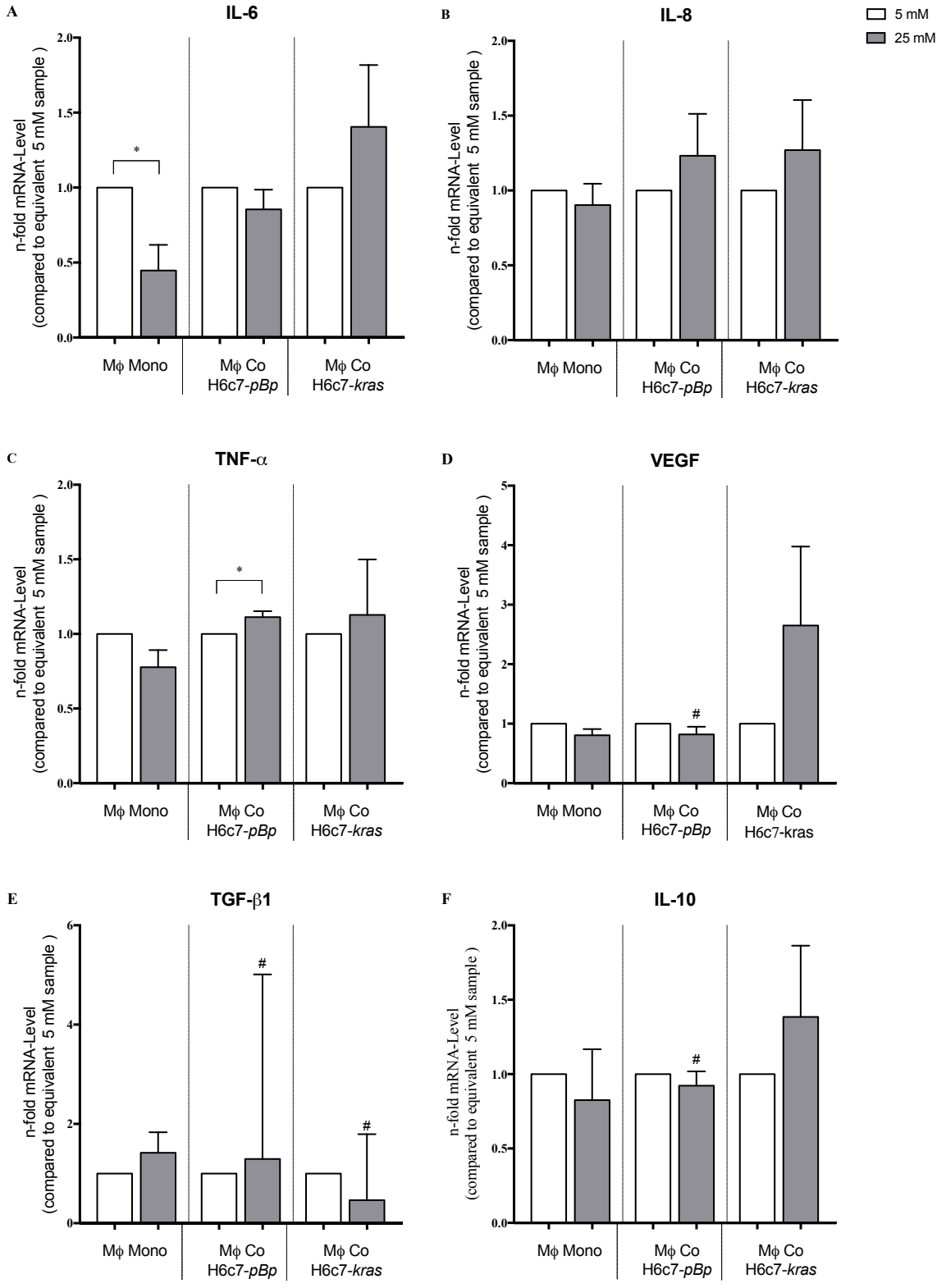

Figure 15: High glucose levels faintly amplify the pro-inflammatory phenotype of macrophages (MΦ) cocultured with PDEC. M1-polarised MΦ were cultivated under normo- or hyperglycaemic conditions (5 or 25 mM of glucose) for 5 days in mono- or coculture with H6c7-*pBp* or H6c7-*kras* cells. MΦ were separated from direct coculture with epithelial cells via EpCam-MACS depletion or harvested from monoculture and used for qRT-PCR analysis. The relative gene expression levels of IL-6 (A), IL-8 (B), TNF-α (C), VEGF (D), TGF-β1 (E) and IL-10 (F) are depicted, normalised to the housekeeping gene GAPDH and presented as n-fold expression compared to the equivalent sample arising from the normoglycaemic setting. Normally distributed data are presented as mean and standard error of mean, unpaired t-test was performed for statistical analysis. Not normally distributed data (indicated via (#)) are shown as median and interquartile range. Wilcoxon Signed Rank Test was used for statistical analysis. *: 0,05>p>0,0332; n=5

4.1.3 The presence of PDEC strengthens the pro-inflammatory phenotype of macrophages

After having analysed the combined effect of glucose and coculture with PDEC on macrophages and the one of glucose alone, the effect of coculture on its own was now to be investigated. For this, the experimental setup was the same as described in section 4.1.1, but the monocultured macrophages of the equivalent glucose condition served as a control for comparative analysis.

The gene expression level of IL-6 was markedly elevated through coculture with both pancreatic epithelial cell lines, irrespective of the glucose level. Interestingly, the statistically most significant increase was evoked through coculture with H6c7-*pBp* cells under normoglycaemic conditions (263-fold increase compared to normoglycaemic monoculture). But also normoglycaemic H6c7-*kras* cell coculture and hyperglycaemic H6c7-*pBp* cell coculture led to a significant elevation of the pro-inflammatory cytokine (231-fold increase, and 838-fold increase, respectively) (**Figure 16** A).

Similar effects were also detected for all other analysed pro-inflammatory cytokines and growth factors. Even though the effects were not as pronounced as for IL-6, a clear coculture-induced amplification on mRNA level could be observed (**Figure 16** B-D). Under normoglycaemic conditions IL-8 mRNA levels showed significant 5.06-fold and 6.19-fold increases upon coculture with the benign and premalignant PDEC, respectively (**Figure 16** B). Hyperglycaemic coculture further intensified these increases (6.64-fold and 8.36-fold for coculture with benign and premalignant PDEC, respectively, compared to monoculture). TNF-α expression showed a significant 9.17-fold increase through coculture with H6c7-*pBp* cells under high glucose levels (**Figure 16** C).Macrophages' VEGF levels were elevated by the factor 2.73 or 3.06 upon exposure to normo- or hyperglycaemic coculture with H6c7-*pBp* cells, respectively, and also coculture with H6c7-*kras* cells led to 2.47- and 3.75-fold increases (**Figure 16** D). TGF-β1 levels of macrophages were not influenced by coculture with the benign H6c7-*pBp* cells, suggesting that hyperglycaemia was the main mediator of the effects seen upon exposure to coculture and high glucose levels in section 4.1.1. Coculture with the premalignant H6c7-*kras* cells, however, did impact on the TGF-β1 levels of macrophages: normoglycaemic coculture led to a 1.4-fold increase on mRNA level, whereas hyperglycaemic coculture evoked a significant decrease of 60 % compared to monocultured macrophages (**Figure 16** E).

As for IL-10, coculture with benign H6c7-*pBp* cells evoked a significant increase in gene expression irrespective of the glucose level the cells were subjected to (2.62-fold increase for normoglycaemic and 2.79-fold for hyperglycaemic coculture) (**Figure 16** F). Contrary to this, coculture with H6c7-*kras* cells decreased the mRNA level of IL-10, reaching statistical significance under normoglycaemic settings with a reduction of 49 %.

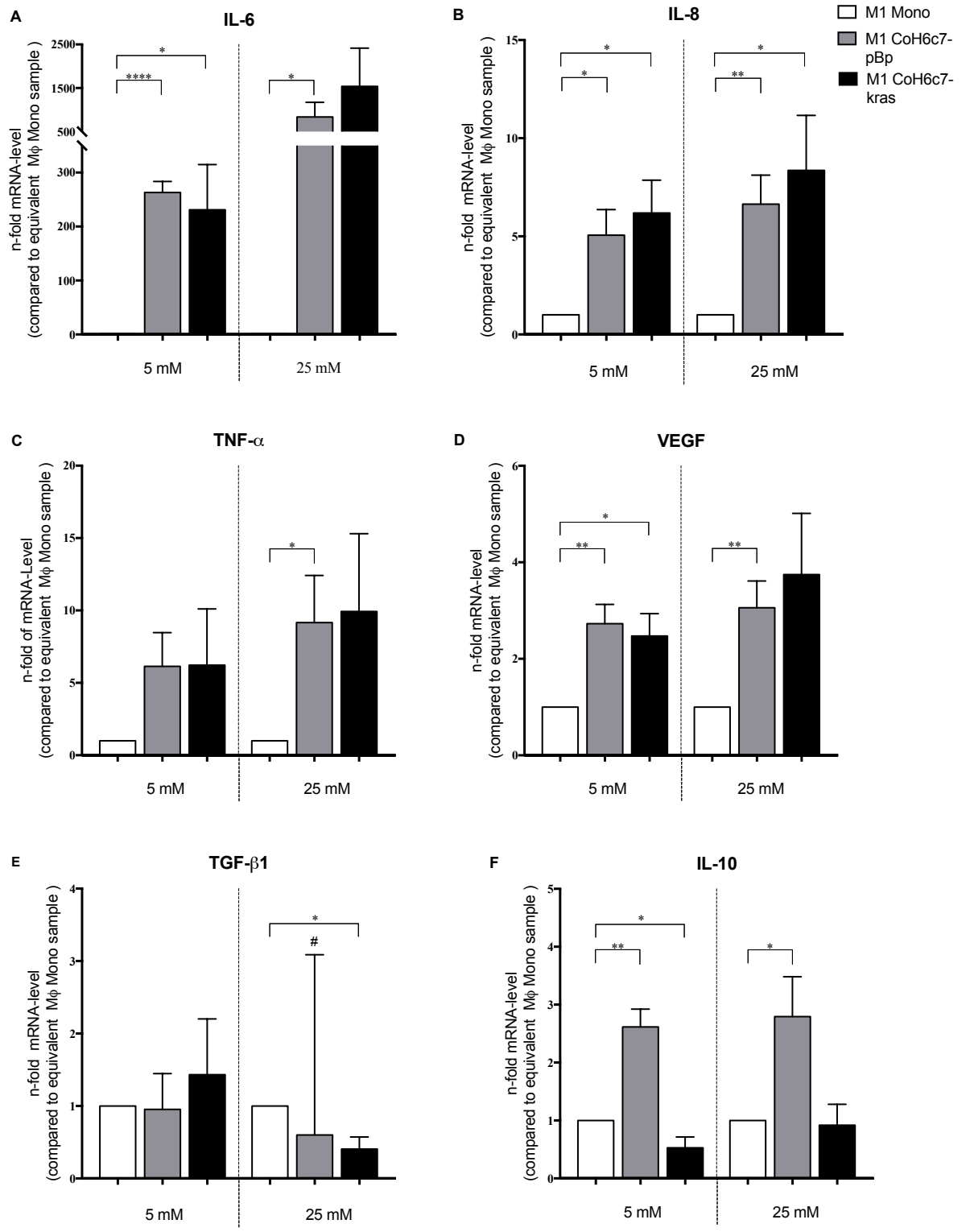

Figure 16: The presence of PDEC amplifies the pro-inflammatory phenotype of macrophages (MΦ). M1-polarised MΦ were cultivated in mono- or coculture with H6c7-*pBp* or H6c7-*kras* cells for 5 days under normo- or hyperglycaemic conditions (5 or 25 mM of glucose). MΦ were separated from direct coculture with epithelial cells via EpCam-MACS depletion of PDEC or harvested from monoculture and used for qRT-PCR analysis. The relative gene expression levels of IL-6 (A), IL-8 (B), TNF-α (C), VEGF (D), TGF-β1 (E) and IL-10 (F) are depicted, normalised to the housekeeping gene GAPDH and presented as n-fold expression compared to the equivalent monocultured sample. Normally distributed data are presented as mean and standard error of mean, unpaired t-test was performed for statistical analysis. Not normally distributed data (indicated via (#)) are shown as median and interquartile range. Wilcoxon Signed Rank Test was used for statistical analysis.
*: 0,05>p>0,0332 **: =0,0331>p>0,0021 ***=: 0,002>p>0,0001 ****: p<0,0001; n=5

Altogether, these findings suggest that the shift towards a more pro-inflammatory phenotype in the presence of high glucose levels and - especially premalignant - PDEC seen on the mRNA level of macrophages in Figure 14 was mainly triggered by coculture with PDEC. Hyperglycaemia alone led to similar tendencies, but these were rather minor, thereby excluding high glucose levels as the sole mediator of the observed effects. Exposure to hyperglycaemia, however, further amplified several of the coculture-dependent increases in gene expression. Only mRNA levels of the important EMT-inducer TGF-β1 seemed to be more impacted by high glucose levels than by coculture. Remarkably, IL-10 gene expression levels showed a divergent reaction upon exposure to H6c7-*pBp* or -*kras* cells.

4.2 The impact of hyperglycaemia and macrophages on PDEC

Previous studies investigated the impact of a two-day exposure to hyperglycaemia and M1-polarised macrophages on both benign and premalignant PDEC. On gene expression level, EMT induction was asserted identifying TNF-α as a potential mediator of these effects (Plundrich, 2017). Promotion of CSC-properties was detected to a lesser extent, raising the question whether a longer subjection to a hyperglycaemic and inflammatory microenvironment may also promote stemness characteristics in PDEC. Furthermore, it was suggested that a prolonged exposure of PDEC to hyperglycaemia and macrophages might corroborate the previous findings by also showing EMT- and CSC-associated changes on protein level. In preliminary experiments EMT- and CSC-associated characteristics in PDEC were analysed upon short- (2 days) and long-term (5 days) exposure to a hyperglycaemic and inflammatory environment. These experiments revealed that some EMT-associated alterations in gene expression were initiated upon short-term exposure to hyperglycaemia and macrophages but amplified over time (especially in the premalignant H6c7-*kras* cells) (data not shown). This indicates a time-dependence in the acquisition of malignancy-associated characteristics upon exposure to glucose and macrophages. Therefore, further coculture experiments were performed for 5 days and alterations in EMT- and CSC-associated characteristics of PDEC upon exposure to a hyperglycaemic inflammatory microenvironment were analysed on gene level (chapter 4.2.1), protein level (chapter 4.2.2) and through colony formation assays (chapter 4.2.3).

4.2.1 Impact of hyperglycaemia and macrophages on the gene expression levels of EMT- and CSC-associated genes in PDEC

To elucidate the impact of a T2DM-associated microenvironment on the gene expression level of PDEC, H6c7-*pBp* and H6c7-*kras* cells were cultivated in mono- or coculture with M1-polarised macrophages under normo- or hyperglycaemic conditions for five days. The epithelial cells were then separated from the direct coculture via CD11b-MACS depletion or harvested from monoculture and used for qRT-PCR analysis.

As in previous studies (Plundrich, 2017), IL-6, IL-8, TNF-α and TGF-β1 were analysed as potential EMT-inducing cytokines and growth factors. Slug, Snail and Zeb1 mRNA level were analysed as EMT- and CSC-inducing transcriptional factors. E-Cadherin, Vimentin and L1CAM were chosen as EMT markers and finally Nestin and Nanog were analysed representing typical CSC markers.

In a first step, analysis focused on the combined effect of glucose and macrophages on the gene expression level of PDEC (4.2.1.1). In a second step, the sole effect of glucose on PDEC was analysed (4.2.1.2) and finally the effect of coculture alone on the gene expression level of PDEC was evaluated (4.2.1.3).

4.2.1.1 Combined impact of glucose and coculture on PDEC

To analyse the impact of a T2DM-associated microenvironment – that is the combined impact of glucose and coculture with M1-polarised macrophages – on PDEC, the experimental setup was as described in 4.2.1. For analysis, the relative gene expression levels of EMT- and CSC-associated mediators and transcription factors of PDEC arising from the different conditions were compared to the equivalent cells from normoglycaemic monoculture.

4.2.1.1.1 Hyperglycaemia and the presence of macrophages reduce the expression of pro-inflammatory mediators in benign and elevates them in premalignant PDEC

Compared to monocultured benign H6c7-*pBp* cells, those that had been exposed to macrophages showed a decrease in their relative gene expression level of the pro-inflammatory cytokines IL-6, IL-8 and TNF-α (**Figure 17**A, C, E). This effect was highly significant for IL-8 irrespective of the glucose level: a reduction of 70% in normoglycaemic and of 68% in hyperglycaemic coculture compared to the equivalent monoculture was to be observed. As for the gene expression level of TNF-α, only hyperglycaemic coculture settings evoked a statistically significant decrease of roughly 56% compared to the equivalent monoculture setting.

Remarkably, the coculture-induced effects seen on the gene expression level of the benign PDEC for IL-6 and TNF-α were contrary to those in the premalignant cells. Both factors were upregulated on the mRNA level in H6c7-*kras* cells that had been exposed to macrophages (**Figure 17** B and F). The effects were more explicit for TNF-α, reaching statistical significance irrespective of the glucose level (3.1-fold elevation in normoglycaemic coculture and 2.4-fold elevation in hyperglycaemic coculture compared to normoglycaemic monoculture). The expression level of IL-8, on the other hand, was not affected at all through hyperglycaemia and macrophage coculture in H6c7-*kras* cells (**Figure 17** D).

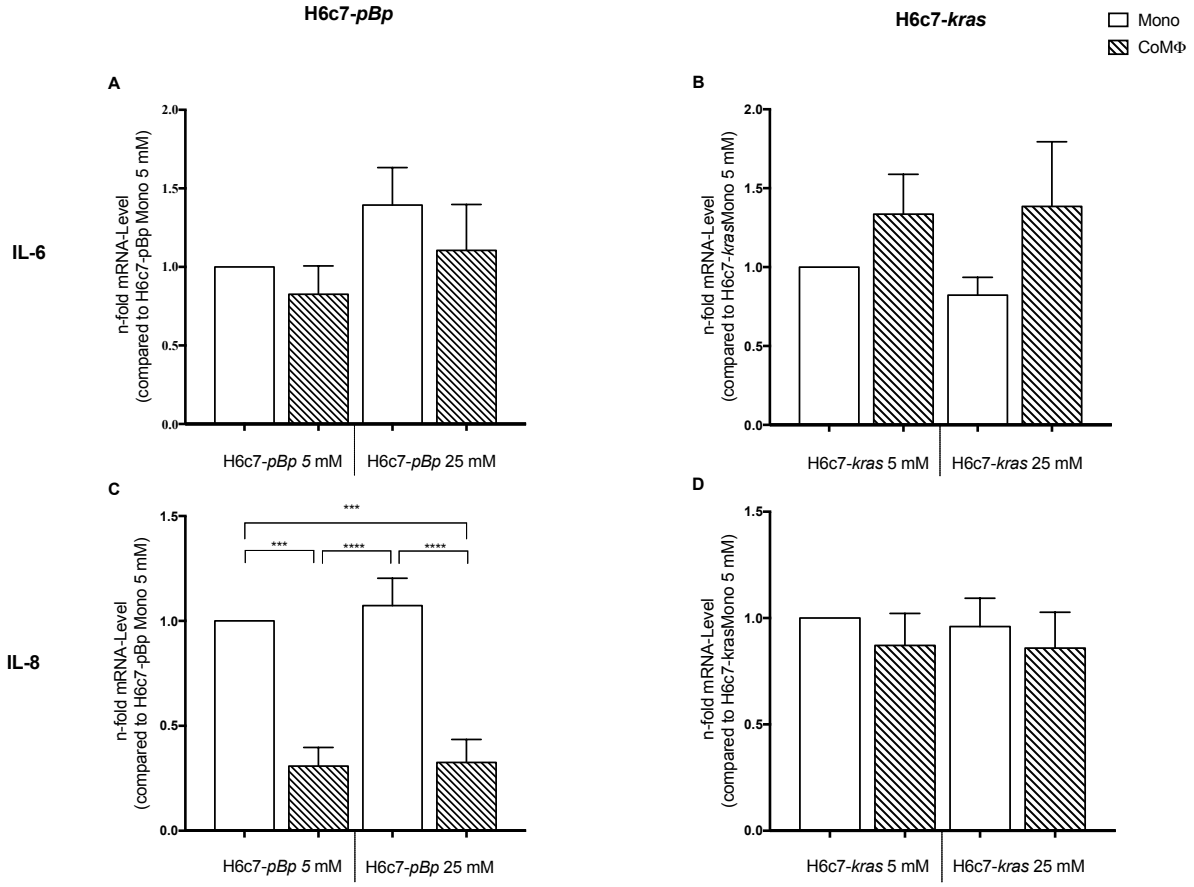

Figure17: **Combined impact of glucose and coculture on the gene expression level of EMT- and CSC-inducing IL-6, IL-8, TNF-α and TGF-β1 in H6c7-*pBp* and H6c7-*kras* cells.** (to be continued on next page)

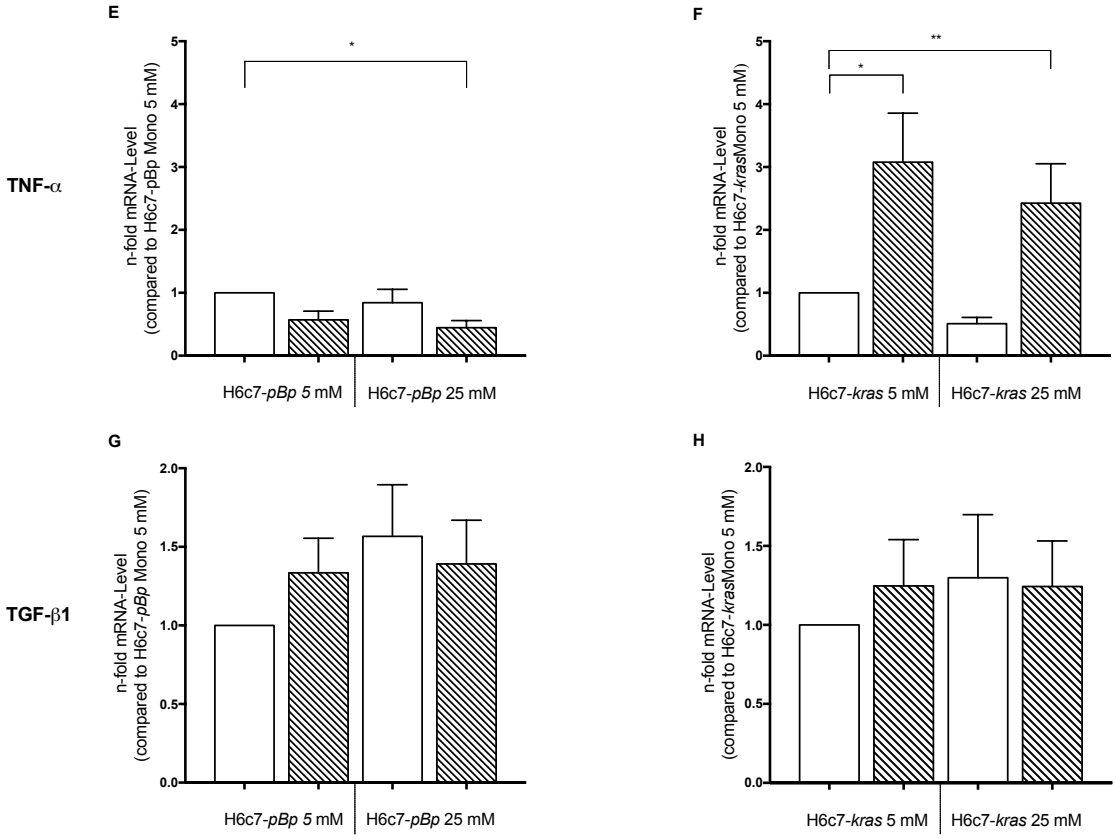

Figure 17: Combined impact of glucose and coculture on the gene expression level of EMT- and CSC-inducing IL-6, IL-8, TNF-α and TGF-β1 in H6c7-*pBp* and H6c7-*kras* cells. (continued) H6c7-*pBp* or H6c7-*kras* cells were mono- or cocultured with M1-polarised macrophages (MΦ) for 5 days in normo-or hyperglycaemic settings (5 or 25 mM of glucose). The epithelial cells were separated from direct coculture via CD11b-MACS depletion of M1-MΦ or harvested from monoculture and used for qRT-PCR analysis. The relative gene expression levels of IL-6 (A and B), IL-8 (C and D), TNF-α (E and F) and TGF-β1 (G and H) of both cell lines are depicted, normalised to the housekeeping gene GAPDH and presented as n-fold expression compared to the monocultured sample from normoglycaemic settings. Normally distributed data are presented as mean and standard error of mean and one-way ANOVA was performed for statistical analysis.
*: 0,05>p>0,0332 **: =0,0331>p>0,0021 ***=: 0,002>p>0,0001 ****: p<0,0001; n=7

The impact of a T2DM-associated microenvironment on the gene expression level of the anti-inflammatory TGF-β1 was similar in both cell lines. Exposure to macrophages led to tendencies of elevation and hyperglycaemia evoked a slight increase in monocultured cells (**Figure 17** G and H).

4.2.1.1.2 The EMT- and CSC-associated transcription factor Zeb1 is elevated through hyperglycaemia and the presence of macrophages in PDEC

Next, the gene expression levels of the EMT- and CSC-associated transcription factors Snail, Slug and Zeb1 were analysed.

Whereas hyperglycaemia and coculture did not influence the gene expression level of Snail in H6c7-*pBp* cells (**Figure 18** A), they did lead to an elevated level in H6c7-*kras* cells (**Figure 18** B). The most explicit increase was to be seen under hyperglycaemic coculture conditions (1.75-fold elevation compared to normoglycaemic monoculture conditions).

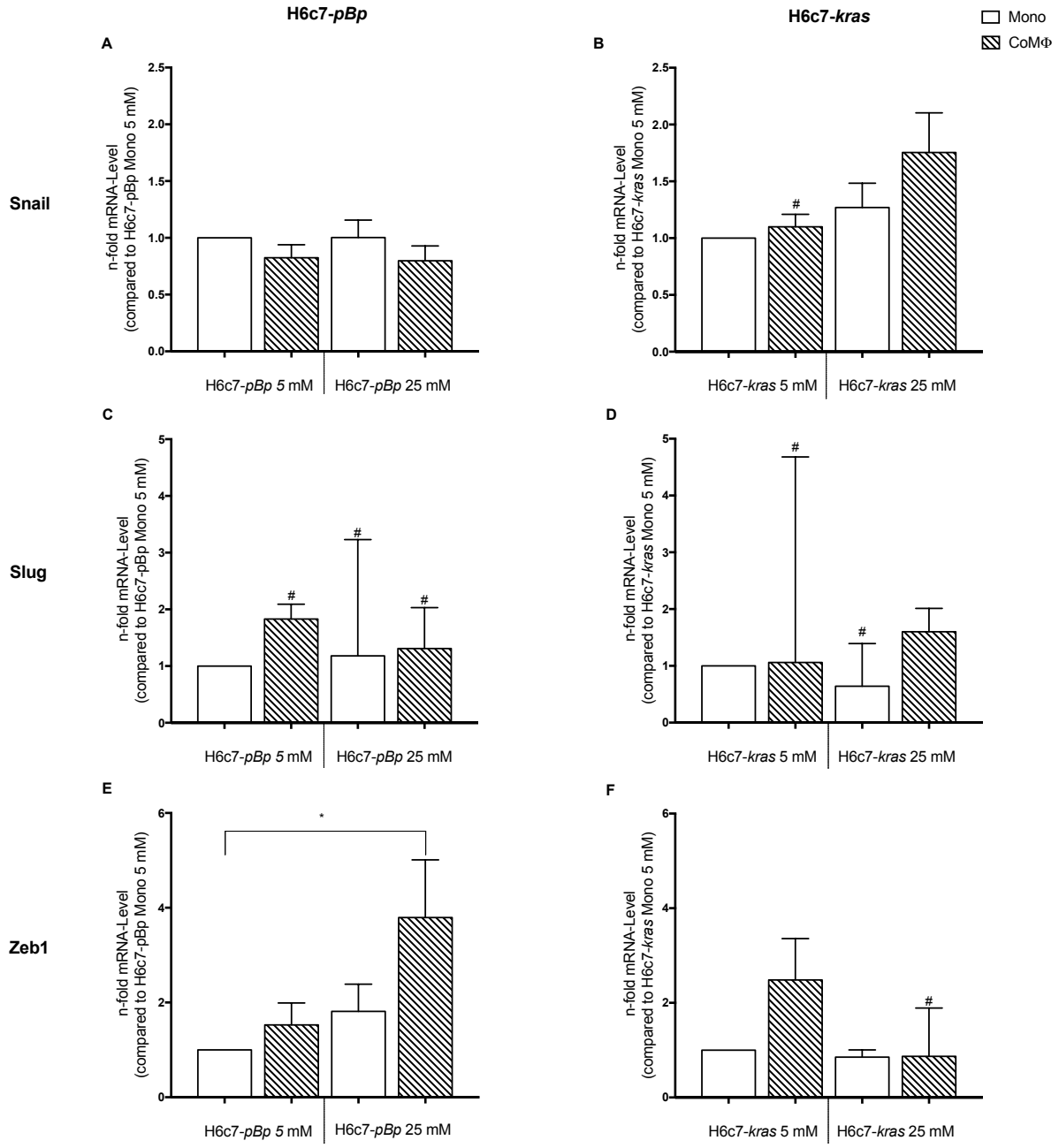

Figure 18: Combined impact of glucose and coculture on the gene expression level of EMT- and CSC-associated transcription factors. H6c7-*pBp* or H6c7-*kras* cells were monocultured or cocultured with M1-polarised macrophages (MΦ) for 5 days in normo- or hyperglycaemic settings (5 or 25 mM of glucose). The epithelial cells were separated from direct coculture via CD11b-MACS depletion of M1-MΦ or harvested from monoculture and used for qRT-PCR analysis. The relative gene expression levels of Snail (A and B), Slug (C and D) and Zeb1 (E and F) of both cell lines are depicted, normalised to the housekeeping gene GAPDH and presented as n-fold expression compared to the monocultured sample from normoglycaemic settings. Normally distributed data are presented as mean and standard error of mean and one-way ANOVA was performed for statistical analysis. Not normally distributed data (indicated via #) are shown as median and interquartile range. Kruskal-Wallis one-way ANOVA on ranks was used for statistical analysis. *: 0,05>p>0,0332; n=7

The impact on the mRNA level of Slug was similar in both cell lines: a coculture-dependent elevation, slightly more pronounced under normoglycaemic conditions in the benign PDEC and under hyperglycaemic conditions in the premalignant PDEC (**Figure 18** C and D). Interestingly, H6c7-*pBp* cells showed an upregulation of Zeb1 on mRNA level throughout all samples (**Figure 18** E). Normoglycaemic coculture led to a 1.53-fold; hyperglycaemic monoculture to a 1.81-fold elevation compared to normoglycaemic

monoculture, respectively. Hyperglycaemic coculture conditions even led to statistically significant changes compared to the monocultured normoglycaemic cells (3.79-fold upregulation). In H6c7-*kras* cells, only coculture under normoglycaemic conditions led to elevated Zeb1 levels (2.48-fold compared to normoglycaemic monoculture); cells mono- or cocultured in hyperglycaemia did not show any changes (**Figure 18** F).

4.2.1.1.3 Hyperglycaemia and macrophages promote changes in the expression of EMT markers in PDEC

The epithelial marker E-Cadherin and the two mesenchymal markers Vimentin and L1CAM were chosen as indicators for potential EMT-associated alteration in PDEC. Both cell lines were characterised by a loss of epithelial and a gain of mesenchymal markers through the impact of hyperglycaemia and macrophages. However, the reduction of E-Cadherin was more pronounced in H6c7-*kras* than in H6c7-*pBp* cells, with a maximum reduction of 50 % provoked by hyperglycaemic coculture (**Figure 19** A and B).

The increase of the mesenchymal marker Vimentin, on the other hand, was more pronounced in the benign PDEC. Here, normoglycaemic coculture led to a 15.2-fold, and hyperglycaemic coculture to a 13.6-fold increase in H6c7-*pBp* cells compared to cells of the normoglycaemic monoculture (**Figure 19 C**). In the premalignant cells, Vimentin levels were elevated by the factors 3.4 and 2.5, respectively (**Figure 19** D).

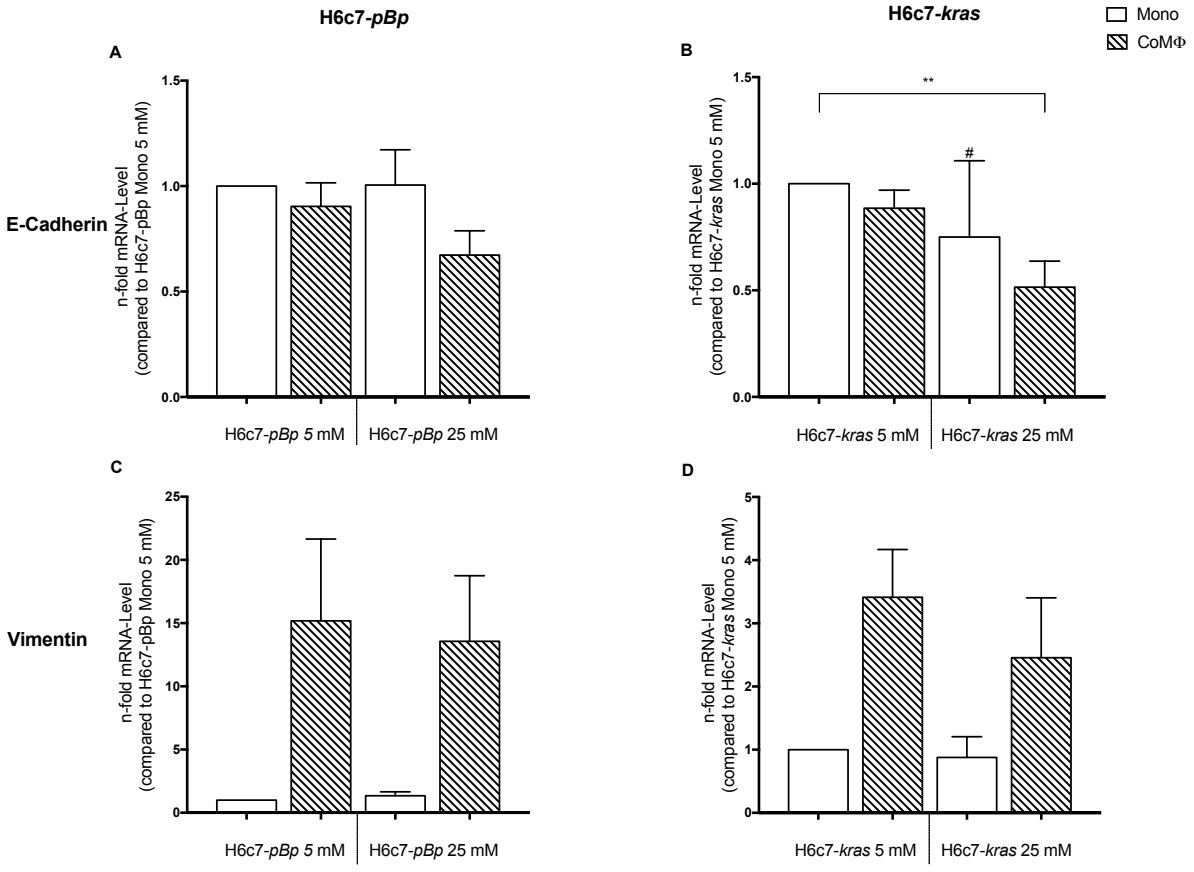

Figure 19: Combined impact of glucose and coculture on the gene expression level of EMT markers in PDEC. (to be continued on next page)

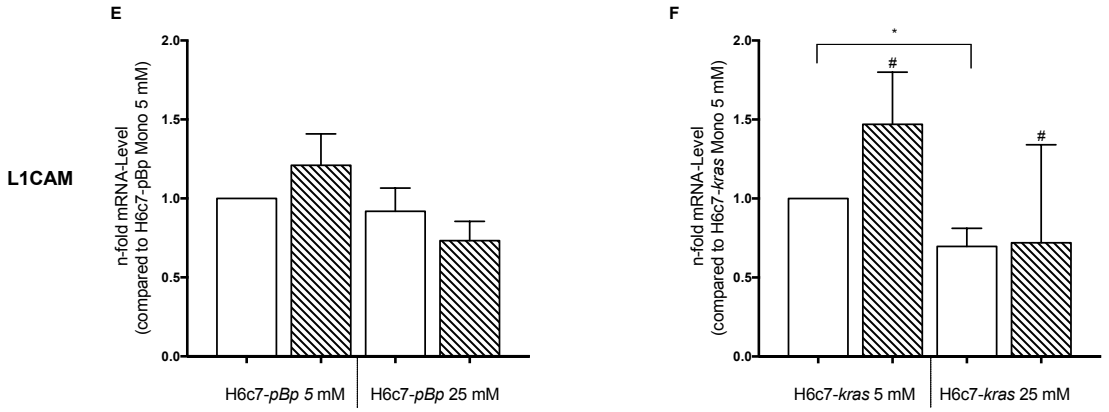

Figure 19: Combined impact of glucose and coculture on the gene expression level of EMT markers in PDEC. (continued) H6c7-*pBp* or H6c7-*kras* cells were mono- or cocultured with M1-polarised macrophages (MΦ) for 5 days in normo- or hyperglycaemic settings (5 or 25 mM of glucose). The epithelial cells were separated from direct coculture via CD11b-MACS depletion of M1-MΦ or harvested from monoculture and used for qRT-PCR analysis. The relative gene expression levels of E-Cadherin (A and B), Vimentin (C and D), and L1CAM (E and F) of both cell lines are depicted, normalised to the housekeeping gene GAPDH and presented as n-fold expression compared to the monocultured sample from normoglycaemic settings. Normally distributed data are presented as mean and standard error of mean and one-way ANOVA was performed for statistical analysis. Not normally distributed data (indicated via #) are shown as median and interquartile range. Kruskal-Wallis one-way ANOVA on ranks was used for statistical analysis. *: 0,05>p>0,0332 **: =0,0331>p>0,0021; n=7

The effects on the gene expression level of mesenchymal L1CAM were similar in both cell lines, but slightly more pronounced in the premalignant PDEC. A coculture-dependent upregulation under normoglycaemic settings could be observed. High glucose levels, however, rather decreased the mRNA level of L1CAM in monocultured cells and neutralised the coculture-dependent increase (**Figure 19** E and F).

4.2.1.1.4 Stemness markers Nestin and Nanog in PDEC are heterogeneously impacted by a T2DM-associated microenvironment

As indicators for stemness, Nestin and Nanog expression levels were evaluated. Interestingly, Nestin showed a coculture-dependent decrease in its expression level in the benign PDEC (**Figure 20** A). In contrast, the mRNA level of Nestin in the premalignant PDEC was increased through both glucose and coculture, the strongest effect to be seen in those cells cultivated in hyperglycaemic coculture (3.5-fold increase compared to normoglycaemic monoculture) (**Figure 20** B).

Monocultured H6c7-*pBp* cells exposed to high glucose levels showed a 1.53-fold increase in Nanog level compared to the normoglycaemic monoculture (**Figure 20** C). A less explicit increase was evoked through normoglycaemic coculture. Remarkably, hyperglycaemic coculture with M1-polarised macrophages had the opposite effect on the benign epithelial cells so that the mRNA level was reduced by 40 %.

A similar reduction of Nanog was also observed on the mRNA level of the premalignant H6c7-*kras* cells arising from hyperglycaemic coculture (**Figure 20** D). Gene expression levels were reduced by 55 % compared to the normoglycaemic monoculture. Contrary to the effects seen in H6c7-*pBp* cells, however, hyperglycaemic monoculture led to slight tendencies of decrease in the expression level of Nanog compared to normoglycaemic monoculture, whereas coculture in low glucose levels did not affect Nanog expression at all.

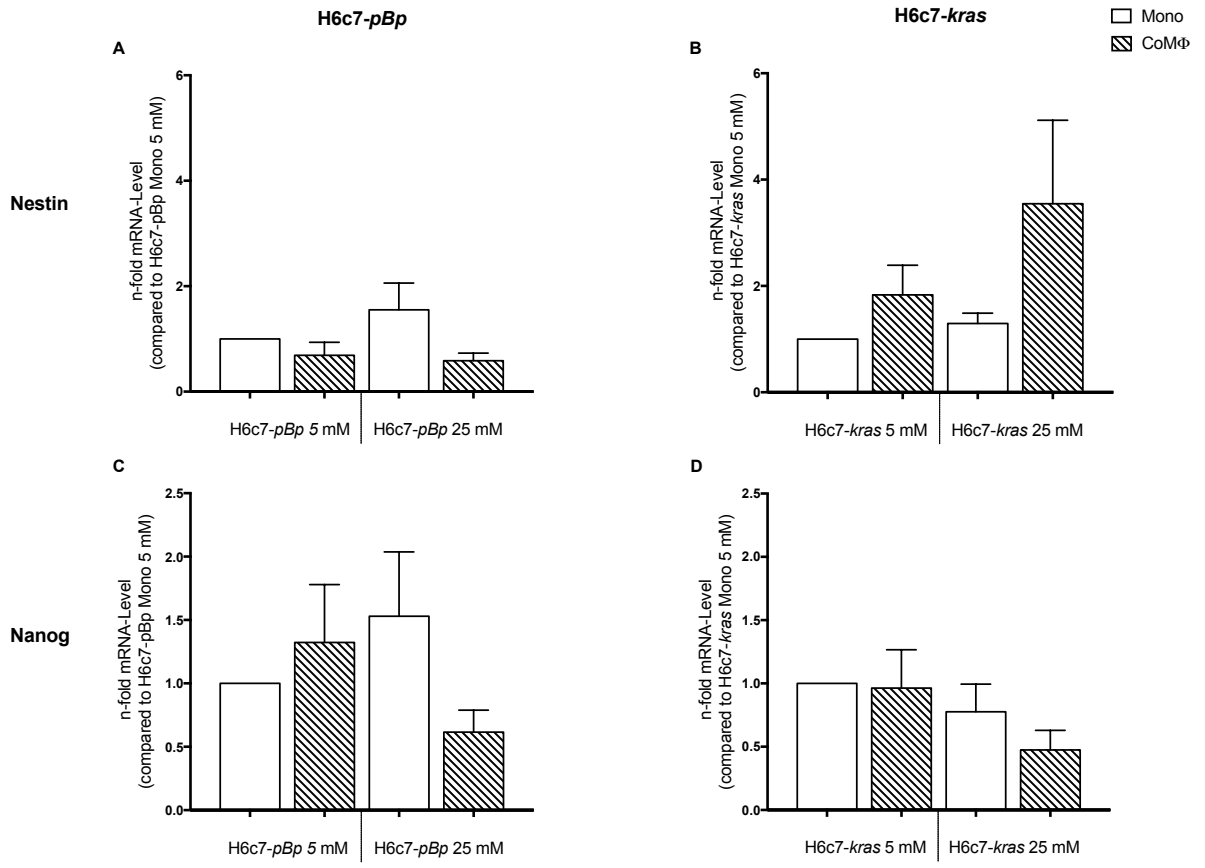

Figure 20: Combined impact of glucose and coculture on the gene expression level of stemness markers in PDEC. H6c7-*pBp* or H6c7-*kras* cells were mono- or cocultured with M1-polarised macrophages (MΦ) for 5 days in normo- or hyperglycaemic settings (5 or 25 mM of glucose). The epithelial cells were separated from direct coculture via CD11b-MACS depletion of M1-MΦ or harvested from monoculture and used for qRT-PCR analysis. The relative gene expression levels of Nestin (A and B) and Nanog (C and D) of both cell lines are depicted, normalised to the housekeeping gene GAPDH and presented as n-fold expression compared to the monocultured sample from normoglycaemic settings. Normally distributed data are presented as mean and standard error of mean and one-way ANOVA was performed for statistical analysis. n=7

Altogether, these data demonstrate that an inflammatory and hyperglycaemic microenvironment impacts on the expression level of both EMT- and CSC-associated genes in PDEC. Especially a loss of epithelial markers and a gain of mesenchymal ones was to be observed, indicating a glucose and coculture-dependent promotion of EMT. Furthermore, it is to note that the combined effect of glucose and M1-polarised macrophages was not always uniform in both cell lines. The effect on EMT markers was more pronounced in H6c7-*pBp* cells, whereas the one on the EMT- and CSC-associated transcription factors was stronger in H6c7-*kras* cells. The gene expression levels of the pro-inflammatory cytokines IL-6, IL-8 and TNF-α were even contrarily affected in H6c7-*pBp* and H6c7-*kras* cells. Elevated gene expression level of Nestin, suggesting a gain of CSC-properties, was seen in both cell lines. This effect, however, was exclusively glucose-dependent in the benign but coculture- and glucose-dependent in the premalignant PDEC.

These findings suggest that some CSC- and EMT-associated alterations in PDEC are rather glucose-dependent than coculture-dependent and vice versa. The genetic constitution might influence this behaviour, as differences were seen between the benign H6c7-*pBp* cells and the premalignant H6c7-*kras* cells which harbour the PDAC-associated early mutation in the *kras*-oncogene.

4.2.1.2 Impact of glucose alone on PDEC

The qRT-PCR analysis revealed an impact of a pro-inflammatory and hyperglycaemic microenvironment on EMT induction in PDEC, a gain of CSC-related properties and an induction of pro-inflammatory factors especially in the premalignant PDEC. However, some gene expression levels seemed to be rather affected through coculture with M1-polarised macrophages, mimicking the inflammatory surrounding, whereas other genes were more influenced by the differing glucose conditions. Therefore, the effect of glucose alone on the gene expression level in PDEC was to be analysed in a next step. For this, the experimental setup was identical to the one mentioned in 4.2.1, but cells arising from normoglycaemic settings now served as a control for those exposed to hyperglycaemia under each culture condition.

4.2.1.2.1 Hyperglycaemia increases TGFß-1 levels in PDEC

In accordance with the findings in 4.2.1.1, high glucose levels only slightly increased the gene expression of the pro-inflammatory cytokine IL-6 in H6c7-*pBp* cells (in mono-and coculture equally) but did not alter it in H6c7-*kras* cells (**Figure 21** A and B).

Likewise, IL-8 mRNA levels in PDEC were not affected at all by hyperglycaemia (**Figure 21** C and D).

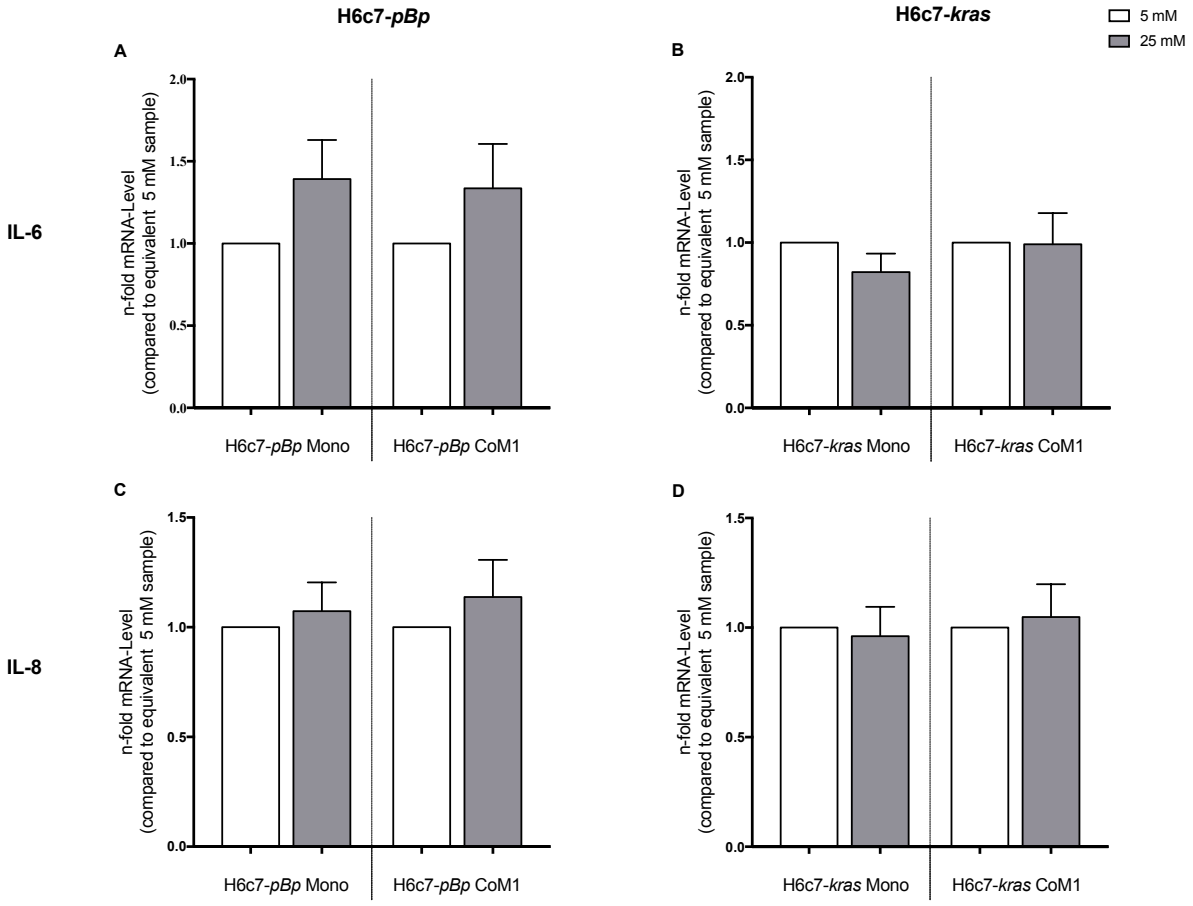

Figure 21: Impact of hyperglycaemia on the expression level of EMT- and CSC-inducing mediators in mono- and cocultured PDEC. (to be continued on next page)

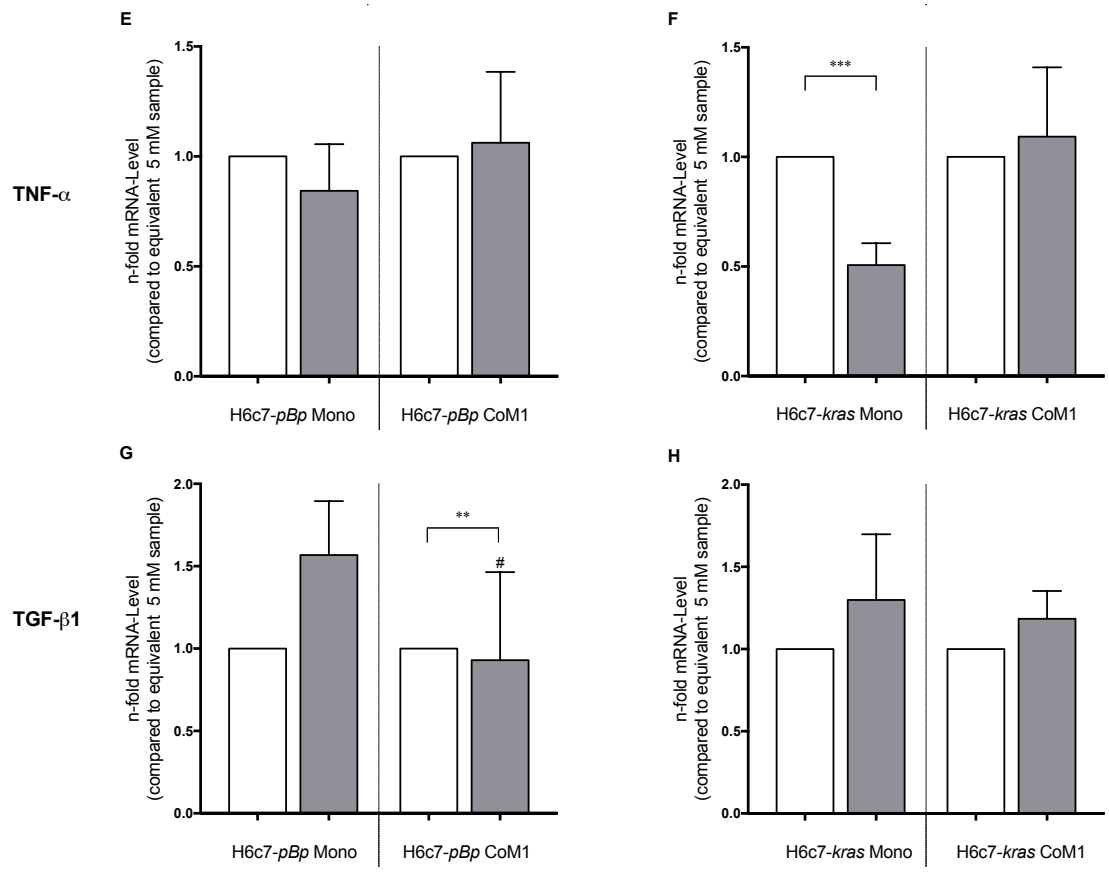

Figure 21: Impact of hyperglycaemia on the expression level of EMT- and CSC-inducing mediators in mono- and cocultured PDEC. (continued) H6c7-pBp or H6c7-kras cells were cultivated in normo- or hyperglycaemic conditions (5 or 25 mM of glucose) in mono- or coculture with M1-polarised macrophages (MΦ). The epithelial cells were separated from direct coculture with macrophages via CD11b-MACS depletion of M1-MΦ or harvested from monoculture and used for qRT-PCR analysis. The relative gene expression levels of IL-6 (A and B), IL-8 (C and D), TNF-α (E and F) and TGF-β1 (G and H) for both cell lines are depicted, normalised to the housekeeping gene GAPDH and presented as n-fold expression compared to the equivalent sample arising from normoglycaemic setting. Normally distributed data are presented as mean and standard error of mean, unpaired t-test was performed for statistical analysis. Not normally distributed data (indicated via #) are shown as median and interquartile range. Wilcoxon Signed Rank Test was used for statistical analysis.
*: 0,05>p>0,0332 **: =0,0331>p>0,0021 ***=: 0,002>p>0,0001; n=7

There were also no visible changes for TNF-α levels in the benign PDEC nor in cocultured premalignant H6c7-*kras* cells. However, exposure to hyperglycaemia resulted in a significant decrease in TNF-α levels in monocultured H6c7-*kras* cells (roughly 50%) (**Figure 21** E and F). The important EMT-inducer TGF-β1 was expressed at a slightly higher level in cells subjected to high glucose levels, the effect being slightly stronger in the benign (1.6-fold increase in hyperglycaemic compared to normoglycaemic monoculture) than in the premalignant cell line (1.3-fold increase in monoculture upon exposure to hyperglycaemia) (**Figure 21** G and H).

4.2.1.2.2 High glucose levels increase Zeb1 expression in benign and Snail in premalignant PCEC

The gene expression level of Snail in H6c7-*pBp* cells was not affected by exposure to hyperglycaemia (**Figure 22** A), whereas it was weakly increased in H6c7-*kras* cells from hyperglycaemic conditions (**Figure 22** B). This effect was slightly more dominant in cocultured premalignant cells than in

monocultured ones (1.40 and 1.30-fold increase compared to normoglycaemic conditions, respectively). Expression levels of Slug were slightly increased in monocultured H6c7-*pBp* cells upon exposure to high glucose levels (1.32-fold increase compared to normoglycaemic monoculture), whereas cocultured H6c7-*pBp* cells showed diminished expression levels of Slug (0.75-fold) in hyperglycaemic settings (**Figure 22** C). In H6c7-*kras* cells, on the other hand, expression levels of Slug showed a glucose-dependent decrease of similar strength in mono- and cocultured cells (**Figure 22** D). As for Zeb1, expression levels were increased in a glucose-dependent manner in the benign PDEC, reaching statistical significance in H6c7-*pBp* cells cocultured with M1-macrophages (2.21-fold elevation in cocultured; 1.81-fold elevation in monocultured cells compared to the equivalent normoglycaemic sample) (**Figure 22** E). In the premalignant cells, however, no glucose-dependent influence was visible on expression levels of Zeb1(**Figure 22** F)

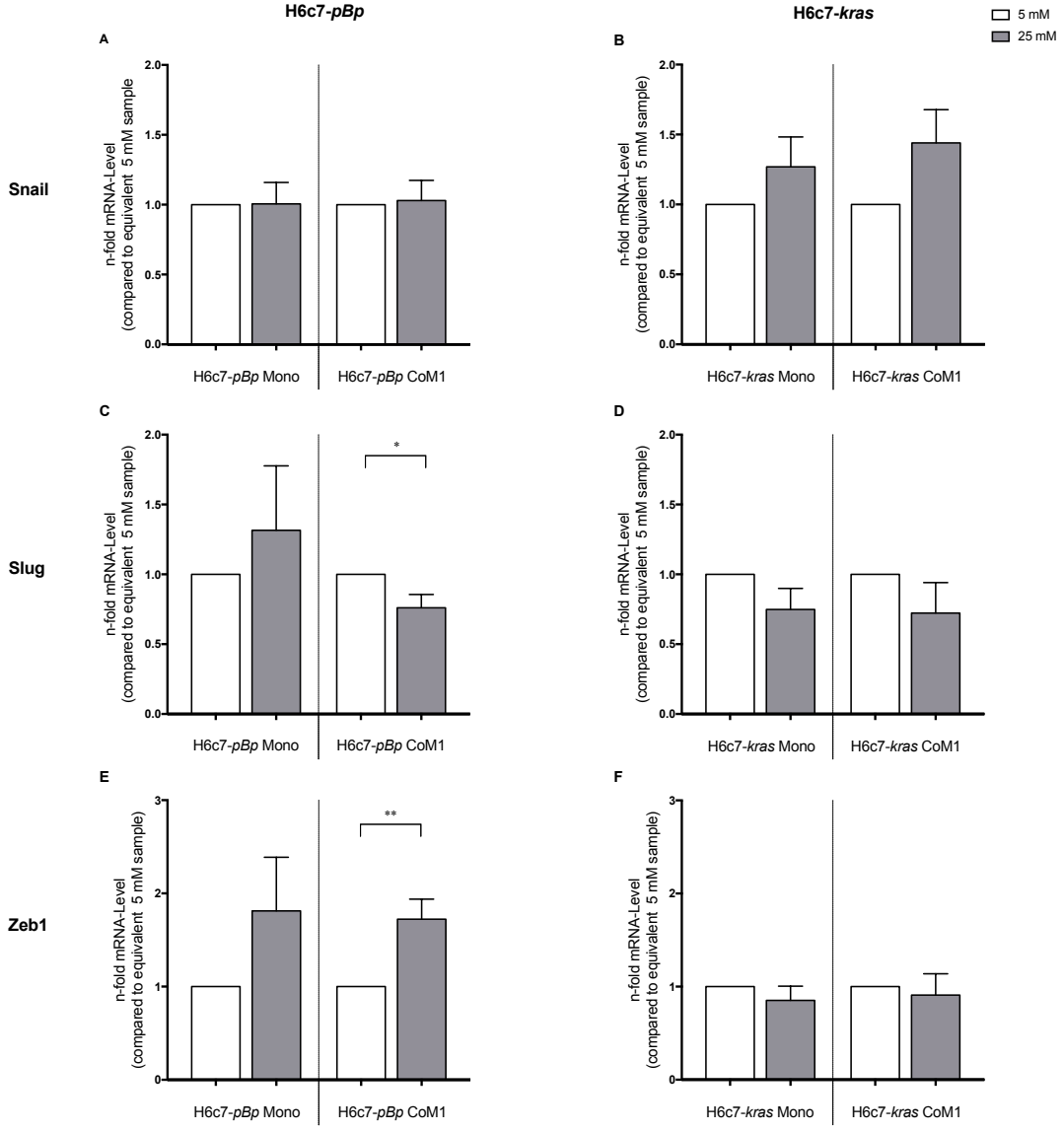

Figure 22: Impact of hyperglycaemia on the expression level of EMT- and CSC-associated transcription factors of mono- and cocultured PDEC. H6c7-*pBp* or H6c7-*kras* cells were cultivated in normo- or hyperglycaemic conditions (5 or 25 mM of glucose) in mono- or coculture with M1-polarised macrophages (MΦ). The epithelial cells were separated from direct coculture with macrophages via CD11b-MACS depletion of M1-MΦ or harvested from monoculture and used for qRT-PCR analysis. The relative gene expression levels of Snail (A and B), Slug (C and D) and Zeb1(E and F) for both cell lines are depicted, normalised to the housekeeping gene GAPDH and presented as n-fold expression compared to the equivalent sample arising from normoglycaemic setting. Normally distributed data are presented as mean and standard error of mean, unpaired t-test was performed for statistical analysis.
*: 0,05>p>0,0332 **: =,331>p>0,0021; n=7

4.2.1.2.3 High glucose levels alter the expression of EMT markers in PDEC

The impact of glucose on the gene expression levels of the EMT markers E-Cadherin, Vimentin and L1CAM was more pronounced in the premalignant than in the benign PDEC.

With the exception of monocultured H6c7-*pBp* cells, PDEC from all other culture conditions were characterised by a significant loss of the epithelial marker E-Cadherin when subjected to hyperglycaemia (**Figure 23** A and B).

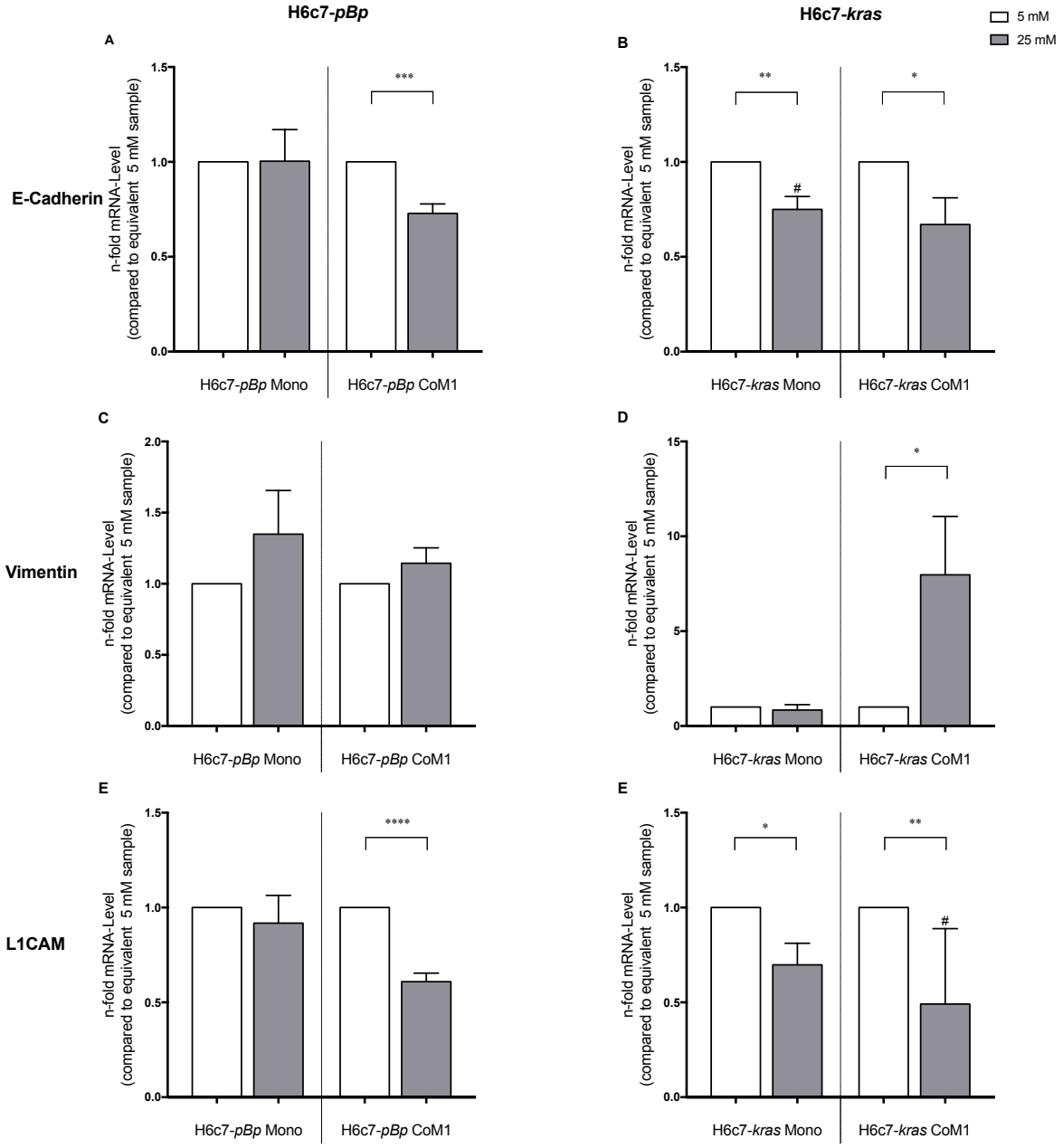

Figure 23: Impact of hyperglycaemia on the expression level of EMT markers of mono- and cocultured PDEC. H6c7-*pBp* or H6c7-*kras* cells were cultivated in normo- or hyperglycaemic conditions (5 or 25 mM of glucose) in mono- or coculture with M1-polarised macrophages (MΦ). The epithelial cells were separated from direct coculture with macrophages via CD11b-MACS depletion of M1-MΦ or harvested from monoculture and used for qRT-PCR analysis. The relative gene expression levels of E-Cadherin (A and B), Vimentin (C and D) and L1CAM (E and F) for both cell lines are depicted, normalised to the housekeeping gene GAPDH and presented as n-fold expression compared to the equivalent sample arising from normoglycaemic setting. Normally distributed data are presented as mean and standard error of mean, unpaired t-test was performed for statistical analysis. Not normally distributed data (indicated via #) are shown as median and interquartile range. Wilcoxon Signed Rank Test was used for statistical analysis. *: 0,05>p>0,0332 **: =0,0331>p>0,0021 ***=: 0,002>p>0,0001 ****: p<0,0001; n=7

Exposure to high glucose levels also resulted in an upregulation of Vimentin expression levels (**Figure 23** C and D). This effect was most impressive in cocultured H6c7-*kras* cells which showed an 8.0-fold increase compared to the equivalent normoglycaemic sample.

Surprisingly, the mesenchymal marker L1CAM was significantly downregulated by hyperglycaemia in cocultured H6c7-*pBp* cells and in both mono- and cocultured H6c7-*kras* cells (**Figure 23** E and F). This decrease was slightly more pronounced in the cocultured than in the monocultured premalignant cells.

4.2.1.2.4 Hyperglycaemia increases Nestin levels but decreases Nanog expression in PDEC

The PDAC-associated stem cell marker Nestin showed upregulated expression levels upon exposure to hyperglycaemia in both cell lines (**Figure 24** A and B). This effect was most pronounced in the cocultured premalignant H6c7-*kras* cells with a 1.9-fold elevation compared to the equivalent normoglycaemic sample (1.3-fold glucose-dependent elevation in monocultured H6c7-*kras* cells, 1.6-fold in cocultured and 1.4-fold in monocultured H6c7-*pBp* cells).

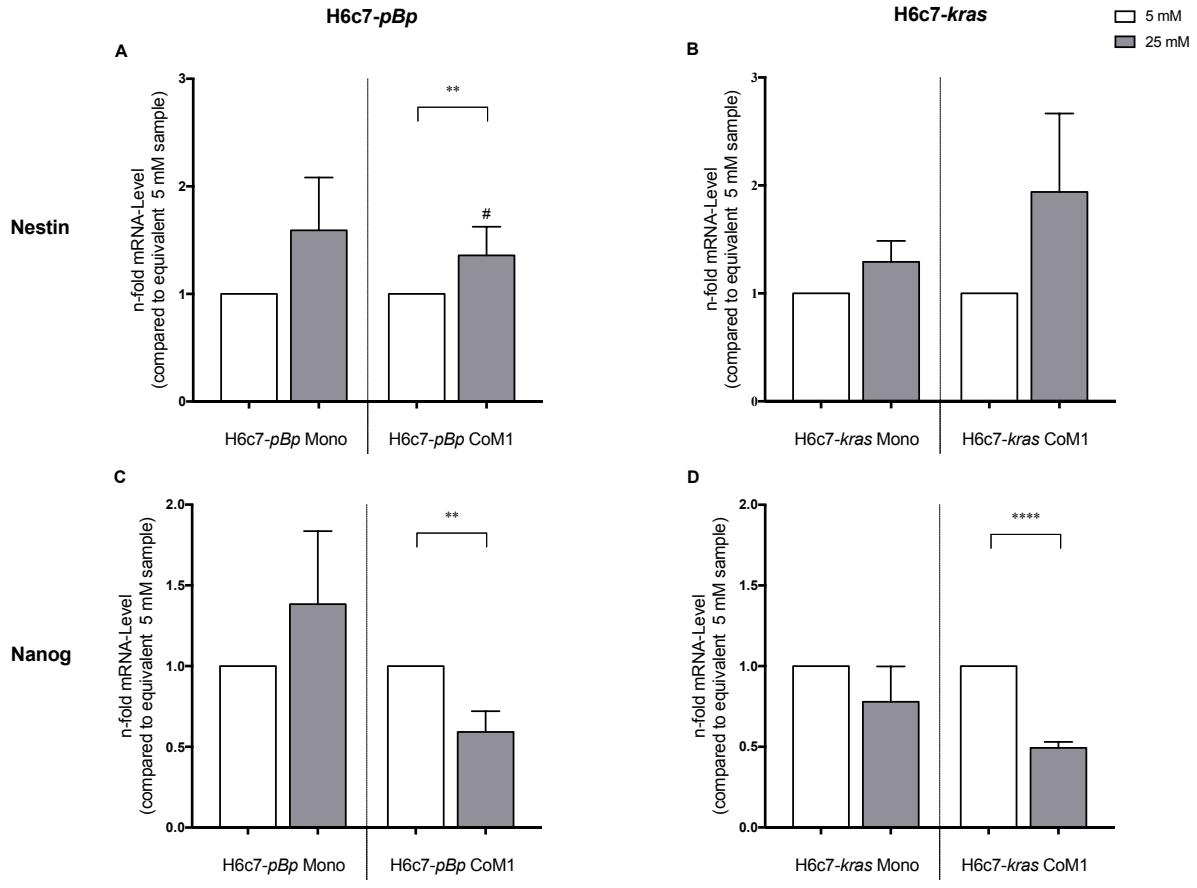

Figure 24: Impact of hyperglycaemia on the expression level of CSC markers of mono- and cocultured H6c7-*pBp* and H6c7-*kras* cells. H6c7-*pBp* or H6c7-*kras* cells were cultivated in normo-or hyperglycaemic conditions (5 or 25 mM of glucose) in mono- or coculture with M1-polarised MΦ. The epithelial cells were separated from direct coculture with macrophages via CD11b-MACS depletion of M1-MΦ or harvested from monoculture and used for qRT-PCR analysis. The relative gene expression levels of Nestin (A and B) and Nanog (C and D) for both cell lines are depicted, normalised to the housekeeping gene GAPDH and presented as n-fold expression compared to the equivalent sample arising from normoglycaemic setting. Normally distributed data are presented as mean and standard error of mean, unpaired t-test was performed for statistical analysis. Not normally distributed data (indicated via #) are shown as median and interquartile range. Wilcoxon Signed Rank Test was used for statistical analysis.
**: =0,0331>p>0,0021 ****: p<0,0001; n=7

Nanog, on the other hand, was not impacted that uniformly. Whereas its expression rate was slightly increased in monocultured benign PDEC upon exposure to high glucose levels (1.53-fold compared to normoglycaemic conditions), it was significantly decreased by roughly 40% in cocultured H6c7-*pBp* cells when subjected to high glucose (**Figure 24** C). Hyperglycaemia also decreased the mRNA level of Nanog in H6c7-*kras* cells. This effect was more pronounced in co- than in monocultured premalignant PDEC, glucose leading to a significant loss of 51% compared to normoglycaemic coculture (**Figure 24** D).

Collectively, these experiments showed that hyperglycaemia predominantly influences EMT- and only slightly CSC-associated marker genes in PDEC. A glucose-mediated EMT induction was observed in both H6c7-*pBp* and H6c7-*kras* cells. This effect was more pronounced in the premalignant than in the benign PDEC. Hyperglycaemia also led to slightly increased TGF-β1 levels in both cell lines, whereas no distinctive glucose-dependent effect was observed on the gene expression level of IL-6, IL-8 or TNF-α. Finally, an elevation of the stem cell marker Nestin was seen in both H6c7-*pBp* and H6c7-*kras* cells when exposed to high glucose levels. Again, this impact was more pronounced in the premalignant H6c7-*kras* cells than in the benign H6c7-*pBp* cells.

4.2.1.3 Impact of coculture alone on PDEC

In a final step, the exclusive impact of exposure to M1-polarised macrophages in PDEC was investigated. The aim was to elucidate the macrophages' contribution to the effects observed above on EMT and CSC marker gene expression of PDEC upon exposition to T2DM-associated microenvironment. The experimental setup was the same as the one in section 4.2.1, but the monocultured epithelial cells of each glucose condition served as a reference compared to cocultured ones.

4.2.1.3.1 The presence of macrophages reduces pro-inflammatory cytokine expression in benign PDEC and increases them in premalignant cells

H6c7-*pBp* cells and H6c7-*kras* cells showed rather different reactions upon exposure to M1-macrophages in their gene expression level of IL-6, IL-8, TNF-α and TGF-β1.

The benign PDEC did not show relevant changes on mRNA level for IL-6, but a statistically highly significant decrease in gene expression level of IL-8 upon exposure to macrophages (**Figure 25** A and C). Interestingly, this effect was slightly more pronounced under hyperglycaemic cultivation conditions (0.27-fold in 25 mM of glucose, 0.31-fold in 5 mM of glucose), even though no glucose-dependent effect had been seen in 4.2.1.2.1. Similar results were obtained for TNF-α in H6c7-*pBp* cells: coculture with macrophages significantly diminished gene expression level of this pro-inflammatory cytokine (**Figure 25** E). The effect was also slightly more marked under high glucose levels (reduction of 46% and 43%, respectively, compared to the equivalent monocultured cells). Gene expression levels of TGF-β1, on the other hand, were slightly elevated in the presence of macrophages in normoglycemia, but not in hyperglycaemia (**Figure 25** G).

In the premalignant H6c7-*kras* cells, IL-6 levels were slightly increased, whereas IL-8 was not affected at all by exposure to macrophages (**Figure 25** B and D). Surprisingly, coculture showed contrary effects on the gene expression level of TNF-α in H6c7-*kras* cells compared to their benign counterpart. Here, TNF-α was significantly increased in cocultured cells and the effect more distinct under hyperglycaemia than normoglycaemia (3.9-fold and 3.1-fold elevation respectively compared to the equivalent monocultured cells) (**Figure 25** F). Coculture with pro-inflammatory macrophages also led to a weak increase in the gene expression level of TGF-β1, irrespective of the glucose level (**Figure 25** H).

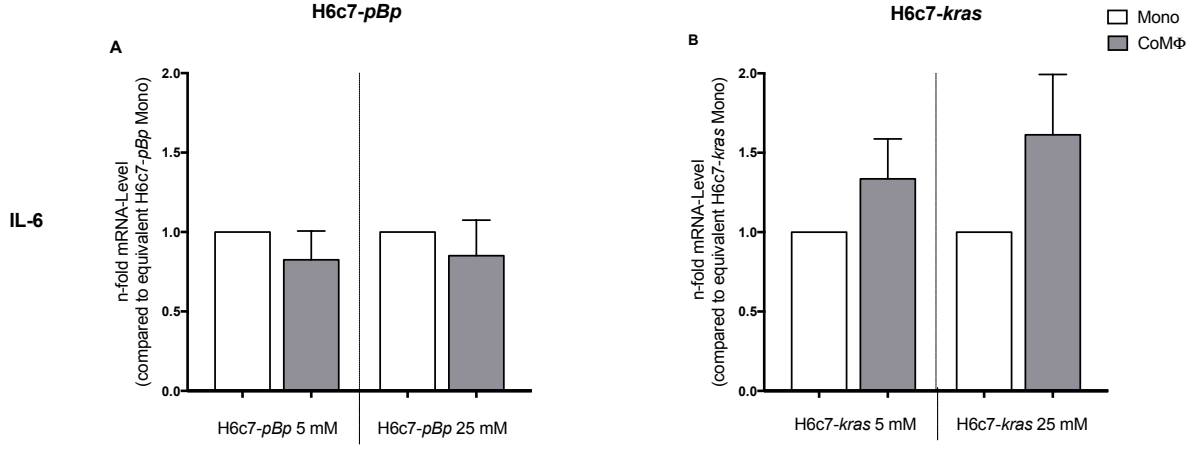

Figure 25: Coculture with macrophages (MΦ) impacts on the expression level of pro- and anti-inflammatory cytokines and growth factors of PDEC. (to be continued on next page)

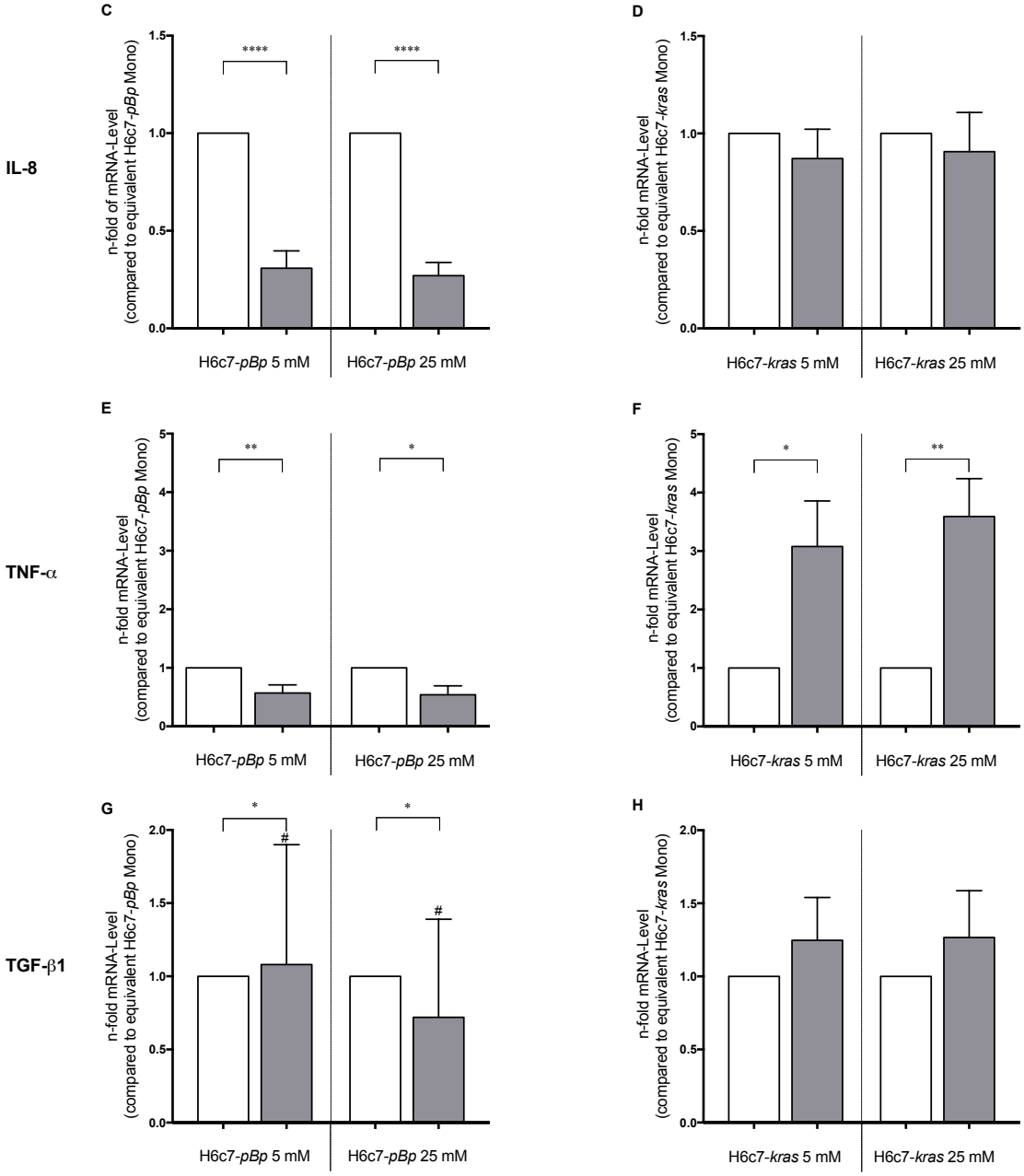

Figure 25: Coculture with macrophages (MΦ) impacts on the expression level of pro- and anti-inflammatory cytokines and growth factors of PDEC. (continued) H6c7-*pBp* or H6c7-*kras* cells were mono- or cocultured with M1-polarised MΦ for 5 days in normo- or hyperglycaemic settings (5 or 25 mM of glucose). The epithelial cells were separated from direct coculture via CD11b-MACS depletion pf M1-MΦ or harvested from monoculture and used for qRT-PCR analysis. The relative gene expression levels of IL-6 (A and B), IL-8 (C and D), TNF-α (E and F) and TGF-β1 (G and H) are depicted for both cell lines, normalised to the housekeeping gene GAPDH and presented as n-fold expression compared to the equivalent monocultured sample. Normally distributed data are presented as mean and standard error of mean, unpaired t-test was performed for statistical analysis. Not normally distributed data (indicated via #) are shown as median and interquartile range. Wilcoxon Signed Rank Test was used for statistical analysis.
*: 0,05>p>0,0332 **: =0,0331>p>0,0021 ***=: 0,002>p>0,0001 ****: p<0,0001; n=7

4.2.1.3.2 Macrophages lead to enhanced Zeb1 and Slug expression in PDEC

qRT-PCR analysis of EMT- and CSC-associated transcription factors upon exposure to macrophages showed analogous results in both cell lines, albeit all effects were slightly more dominant in H6c7-*kras* cells. The gene expression level of Snail did not show clear coculture impacts, only faint tendencies of increase in H6c7-*kras* cells stemming from hyperglycaemic coculture (**Figure 26** A and B).

mRNA levels of Slug, on the other hand, were upregulated, reaching statistical significance in normoglycaemic coculture conditions for H6c7-*pBp* cells and in both normo- and hyperglycaemic coculture conditions for H6c7-*kras* cells (**Figure 26** C and D). Similar results were obtained for Zeb1: gene expression was increased in cocultured PDEC and this effect was slightly more pronounced under additional exposure to high glucose levels (**Figure 26** E and F).

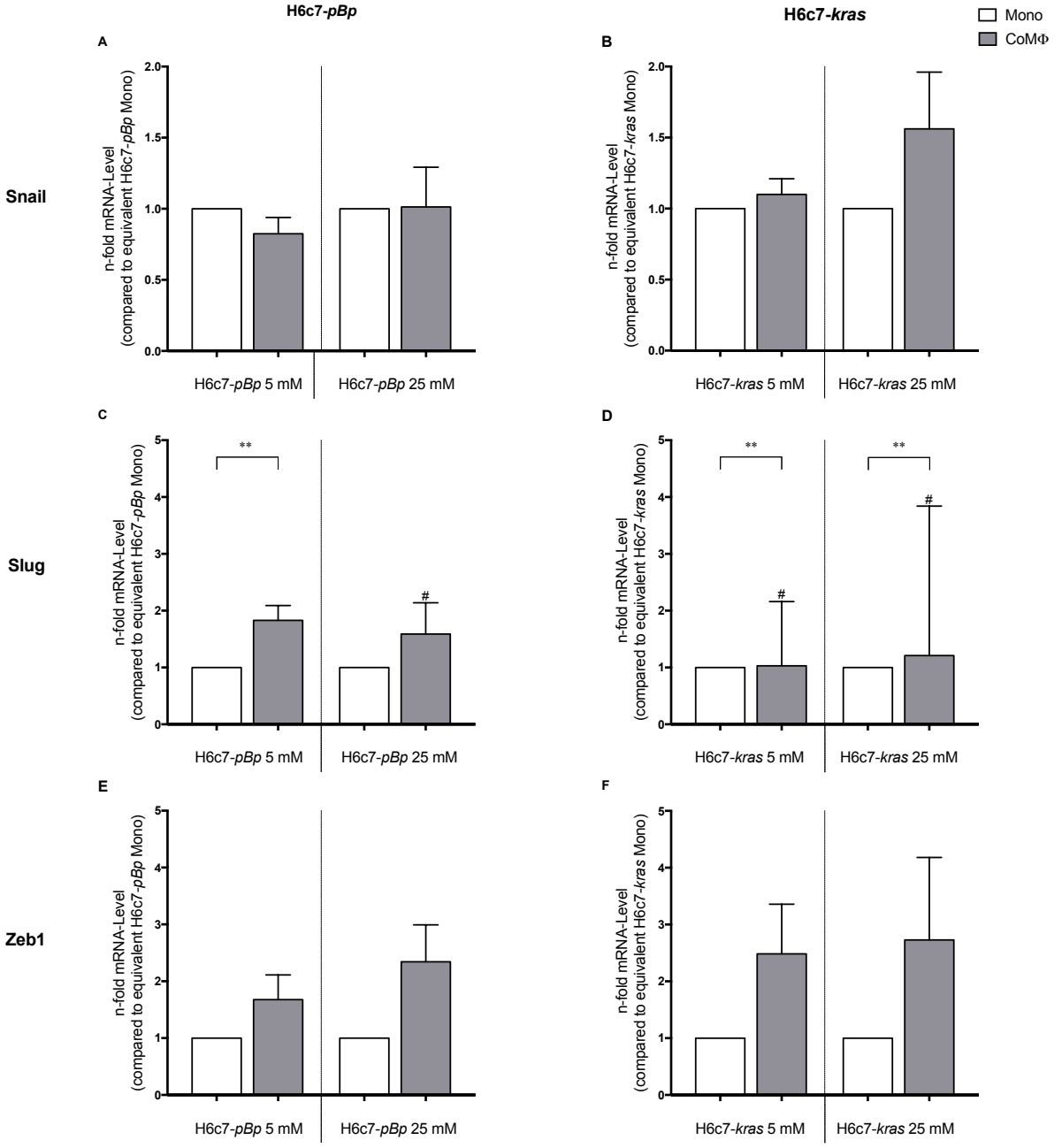

Figure 26: Coculture with macrophages (MΦ) enhances the expression level of EMT- and CSC-associated transcription factors in PDEC. H6c7-*pBp* or H6c7-*kras* cells were mono- or cocultured with M1-polarised MΦ for 5 days in normo- or hyperglycaemic settings (5 or 25 mM of glucose). The epithelial cells were separated from direct coculture via CD11b-MACS depletion of M1-MΦ or harvested from monoculture and used for qRT-PCR analysis. The relative gene expression levels of Snail (A and B), Slug (C and D) and Zeb1 (E and F) of both cell lines are depicted, normalised to the housekeeping gene GAPDH and presented as n-fold expression compared to the equivalent monocultured sample. Normally distributed data are presented as mean and standard error of mean, unpaired t-test was performed for statistical analysis. Not normally distributed data (indicated via #) are shown as median and interquartile range. Wilcoxon Signed Rank Test was used for statistical analysis.
**: =0,0331>p>0,0021; n=7

4.2.1.3.3 Macrophages alter the expression level of EMT markers in PDEC

Coculture with M1-polarised macrophages clearly led to a downregulation of epithelial markers and an upregulation of genes linked to a more motile phenotype in PDEC. The EMT-inducing effect, which had been seen in 4.2.1.1.3 upon exposition to a pro-inflammatory and hyperglycaemic microenvironment, thus seems to be a predominately coculture-induced one being reinforced by hyperglycaemia in some cases.

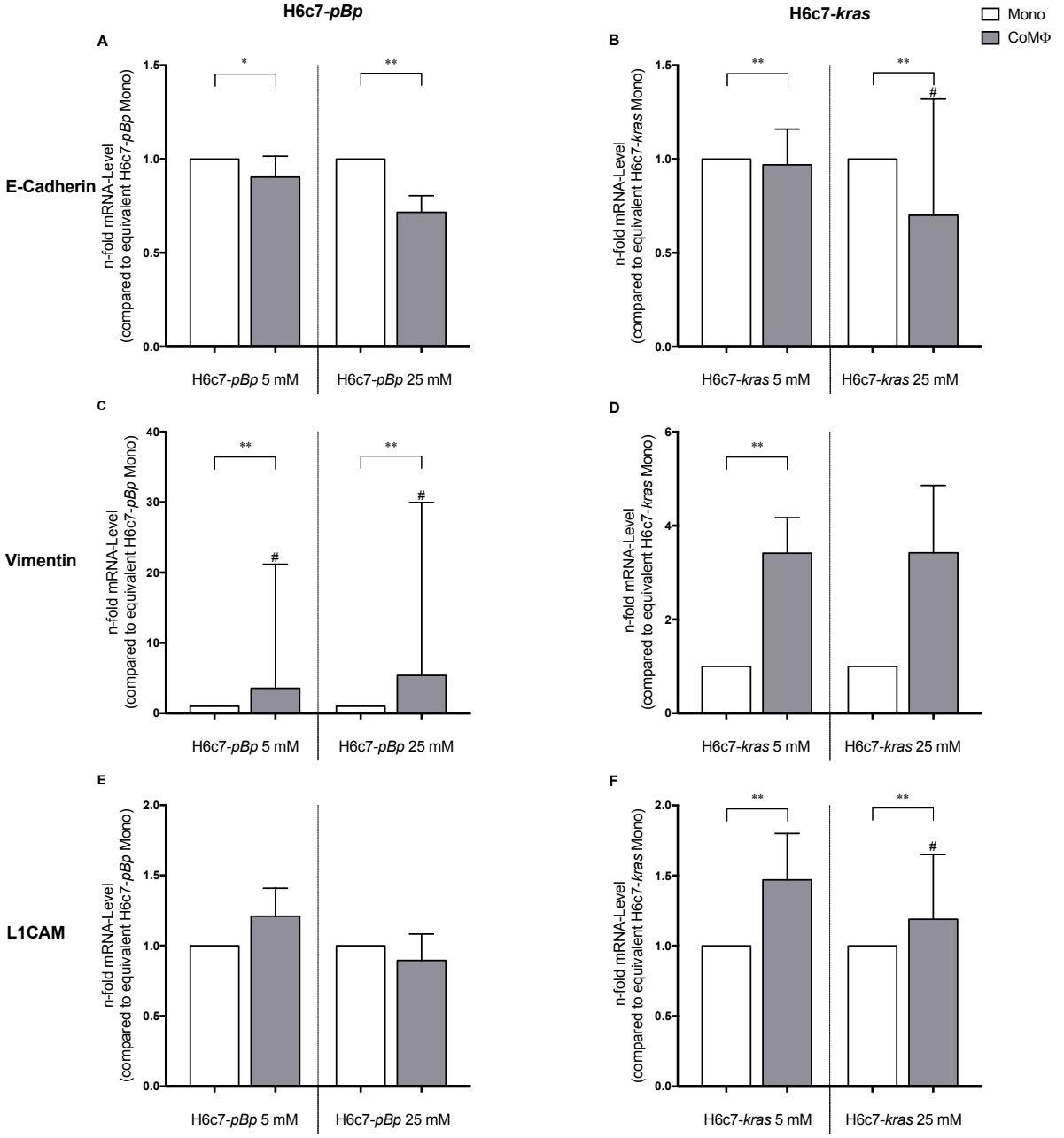

Figure 27: Coculture with macrophages (MΦ) leads to loss of epithelial and gain of mesenchymal marker expression in PDEC. H6c7-*pBp* or H6c7-*kras* cells were mono- or cocultured with M1-polarised MΦ for 5 days in normo- or hyperglycaemic settings (5 or 25 mM of glucose). The epithelial cells were separated from direct coculture via CD11b-MACS depletion of M1-MΦ or harvested from monoculture and used for qRT-PCR analysis. The relative gene expression levels of E-Cadherin (A and B), Vimentin (C and D) and L1CAM (E and F) of both cell lines are depicted, normalised to the housekeeping gene GAPDH and presented as n-fold expression compared to the equivalent monocultured sample. Normally distributed data are presented as mean and standard error of mean, unpaired t-test was performed for statistical analysis. Not normally distributed data (indicated via #) are shown as median and interquartile range. Wilcoxon Signed Rank Test was used for statistical analysis.
*: 0,05>p>0,0332 **: =0,0331>p>0,0021; n=7

A coculture-dependent decrease in the gene expression level of E-Cadherin was seen in both cell lines but was even more explicit in the premalignant H6c7-*kras* cells (**Figure 27** A and B). In accordance with the findings in 4.2.1.2.3, the downregulation was stronger under hyperglycaemic conditions in both cell lines.
The mesenchymal marker Vimentin was significantly increased in both H6c7-*pBp* and H6c7-*kras* cells upon exposure to macrophages (**Figure 27** C and D). Interestingly, this increase was more manifest under hyperglycaemia in the benign cells (5.39-fold versus 3.56-fold increase), but of similar strength in both glucose conditions in the premalignant cells (3.4-fold). It is also important to note that the coculture-dependent changes for Vimentin were more distinct in H6c7-*pBp* cells, which are characterised by a significantly lower basal expression than their premalignant counterpart (data not shown).
mRNA levels of L1CAM were not impacted by coculture in H6c7-*pBp* cells. In H6c7-*kras* cells, on the other hand, a clear coculture-related induction of the gene expression level of L1CAM was to be noted in both glucose conditions (**Figure 27** E and F).

To sum up, the results obtained are all in favour of the view that the induction of the EMT-program on mRNA level is predominantly coculture-dependent in PDEC. The coculture-induced effect in gene expression levels of Vimentin was more pronounced in H6c7-*pBp* cells, the effect on gene expression levels of E-Cadherin and L1CAM, however, more implicit in H6c7-*kras* cells.

4.2.1.3.4 Macrophages impact heterogeneously on the expression levels of CSC markers in benign and premalignant PDEC

Contrary to the glucose-dependent upregulation that had been seen in 4.2.1.2.4 on the gene expression level of Nestin, coculture decreased the mRNA level of this CSC-associated gene in H6c7-*pBp* cells (**Figure 28** A). In H6c7-*kras* cells, a coculture-induced increase on the mRNA level of Nestin was to be observed, in line with the glucose-dependent findings (**Figure 28** B).
As for expression levels of Nanog, hyperglycaemic coculture resulted in a significant decrease in both cell lines. Normoglycaemic coculture, on the other hand, slightly increased the mRNA level in H6c7-*pBp* cells, whereas it faintly decreased the level in H6c7-*kras* cells (**Figure 28** C and D).

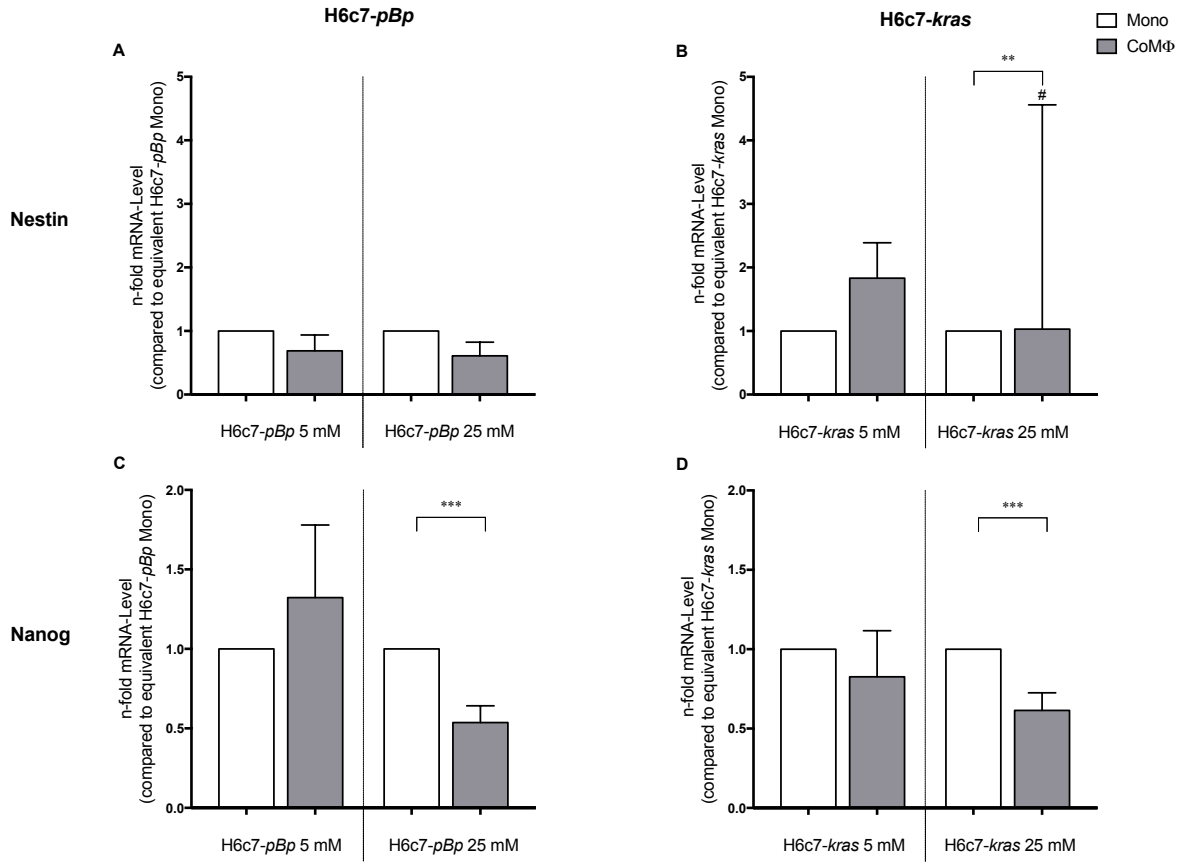

Figure 28: Impact of coculture on the expression level of CSC marker of PDEC. H6c7-*pBp* or H6c7-*kras* cells were mono- or cocultured with M1-polarised macrophages (MΦ) for 5 days in normo- or hyperglycaemic settings (5 or 25 mM of glucose). The epithelial cells were separated from direct coculture via CD11b-MACS depletion of M1-MΦ or harvested from monoculture and used for qRT-PCR analysis. The relative gene expression levels of Nestin (A and B) and Nanog (C and D) of both cell lines are depicted, normalised to the housekeeping gene GAPDH and presented as n-fold expression compared to the equivalent monocultured sample. Normally distributed data are presented as mean and standard error of mean, unpaired t-test was performed for statistical analysis. Not normally distributed data (indicated via #)) are shown as median and interquartile range. Wilcoxon Signed Rank Test was used for statistical analysis. *: 0,05>p>0,0332 **: =0,0331>p>0,0021 ***=: 0,002>p>0,0001; n=7

Altogether, these findings demonstrate the promotion of malignancy-associated features in both PDEC lines through exposure to a hyperglycaemic und inflammatory microenvironment. However, glucose- and coculture-dependent effects have to be taken into account and considered separately as they seem of varying importance for the different markers and also for the two cell lines.

Whereas the important EMT-inducer TGF-β1 was elevated in a glucose-dependent manner in both cell lines, the other cytokines analysed where influenced in a coculture-dependent manner. However, the effects were inverse in the benign and premalignant PDEC, showing decreased levels in H6c7-*pBp* but increased levels in H6c7-*kras* cells.

The transcriptional factors Zeb1 and Slug were influenced in a coculture- rather than a glucose-dependent manner.

Increases in the expression level of Nestin also indicate enhanced acquisition of properties associated with cancer stemness in PDEC. In the benign cells, the elevation was glucose-dependent, whereas in the premalignant cells, glucose and macrophages showed synergistic effects, evoking the most pronounced elevation in those cells that were exposed to hyperglycaemia and inflammation.

4.2.2 Exposure to macrophages and hyperglycaemia induces mesenchymal phenotype in PDEC on protein level

To obtain further insights into the kinetics of EMT induction in PDEC upon exposure to hyperglycaemia and/or macrophages, several EMT markers were also investigated on protein level. Additionally, protein levels of phosphorylated-p65 (p-p65) and total-p65 (t-p65) were analysed to explore the contribution of activation of NF-κB, the central inflammatory signalling pathway, to EMT induction. Upon binding of e.g. TNF-α to its receptor, inhibitor of kappa B (IκB) is phosphorylated and ubiquitinated by the activated IκB kinase. This leads to IκBs degradation with subsequent release of the NF-κB subunit p65 which can then translocate into the nucleus and initiate signalling cascades involved in the regulation of apoptosis, proliferation and invasiveness (Hayden and Ghosh, 2004; Maier et al., 2010).

In the benign cells, a coculture- and glucose-dependent loss of E-Cadherin was clearly to be seen (**Figure 29** A). The strongest diminution of E-Cadherin was to be observed in cells arising from hyperglycaemic coculture, in which E-Cadherin could not be detected any more.

The protein levels of the mesenchymal markers L1CAM and Vimentin were elevated in a coculture-dependent manner. Whereas this coculture-dependent upregulation was further amplified by high glucose levels in L1CAM, no such additive glucose-dependent effect was to be observed in Vimentin levels.

Phosphorylated p65 displayed clear coculture-dependent increases on protein level. Total-p65, on the other hand, was decreased in cocultured H6c7-*pBp* cells and high glucose levels further strengthened this effect.

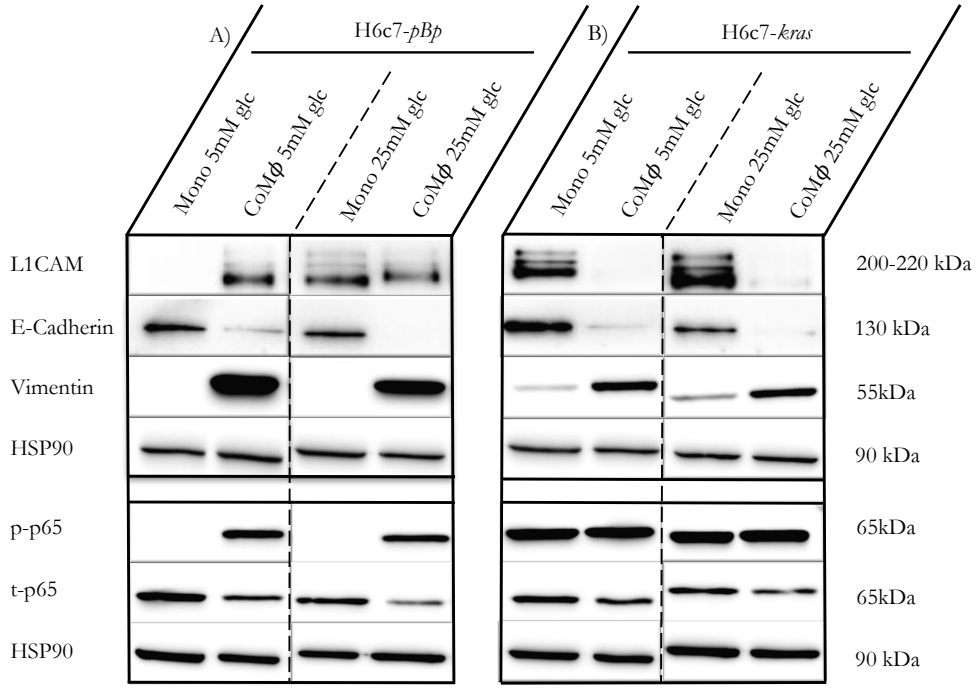

Figure 29: Exposure to hyperglycaemia and macrophages (MΦ) promotes EMT-associated changes on protein levels in PDEC. H6c7-*pBp* or H6c7-*kras* cells were cultivated in mono- or coculture with M1-polarised MΦ under normo- or hyperglycaemic conditions (5 or 25 mM of glucose). Epithelial cells were separated from direct coculture with macrophages via CD11b-MACS depletion of M1-MΦ or harvested from monoculture and used as whole cell lysates for Western Blot analysis. The protein levels of L1CAM, E-Cadherin, Vimentin, p-p65 and t-p65 in H6c7-*pBp* (A) and H6c7-*kras* cells (B) were analysed. Hsp90 was used as loading control. A representative of three independent experiments is shown.

In the premalignant cells, the protein level of E-Cadherin was also clearly decreased upon exposure to high glucose levels and/or macrophages (**Figure 29** B). In line with the findings for H6c7-*pBp* cells, this effect was most pronounced upon exposure to a hyperglycaemic and inflammatory micromilieu.
Coculture with macrophages also led to clearly elevated protein levels of Vimentin in H6c7-*kras* cells. However, this increase did not reach the intensity of the one observed in the benign PDEC upon exposure to macrophages (**Figure 29** A). This finding is in line with the coculture-dependent increase of Vimentin observed on mRNA level which was also more pronounced in the benign than in the premalignant cells (**Figure 27** C and D).
Exposure to glucose also promoted protein levels of Vimentin in monocultured premalignant PDEC.
Remarkably, L1CAM was decreased in a coculture-dependent manner on protein level, which stands in contrast to the effects observed on mRNA level. Also differing from the qRT-PCR results, hyperglycaemia promoted L1CAM expression in monocultured H6c7-*kras* cells.
Very similar to their benign counterpart, premalignant PDEC showed a coculture-dependent increase in protein levels of p-p65. However, even monocultured H6c7-*kras* cells showed clear expression levels of p-p65 whereas no signal could be detected in monocultured H6c7-*pBp* cells. For t-p65, protein levels were decreased in a coculture-dependent manner, and no glucose-induced effect was to be observed.

Overall, the findings favour the view of EMT induction in PDEC through exposure to a hyperglycaemic and inflammatory surrounding. The key step of EMT induction is the loss of E-Cadherin, which was predominantly coculture-dependent in both PDEC lines and amplified by glucose. Furthermore, elevated levels of p-p65 indicate promoted inflammatory signalling especially in PDEC arising from coculture with macrophages.

4.2.3 Exposure to macrophages and high glucose levels leads to an increased colony formation capacity of PDEC and promotion of colonies with high CSC-potential

For the analysis of the acquisition of CSC-properties on a functional level, colony formation assays were performed. The cells' ability to form clones upon exposure to macrophages and/or hyperglycaemia was investigated. In detail, the total number of clones formed per well and the quality of clones (para-, mero- or holoclones) were evaluated. To get an insight on the impact of glucose environment on the colony formation abilities of PDEC, results were normalised to the equivalent sample arising from cultivation under normoglycaemic conditions. It was decided not to compare cells from mono- and coculture settings, as first experiments showed that MACS-separation affected the colony formation. Cells that had been exposed to the stress of a magnetic cell separation procedure, showed a shift in quality of clones formed towards more holoclones, thus, counterfeiting an increased gain in CSC-associated properties (data not shown). Therefore, cells arising from coculture were only compared among themselves for analysis of the impact of glucose.
The total number of colonies formed was slightly decreased by the factor 0.92 upon exposure to high glucose levels in monocultured benign PDEC. In cocultured benign PDEC, on the other hand, exposure to glucose marginally increased the total number of colonies formed (**Figure 30** A).

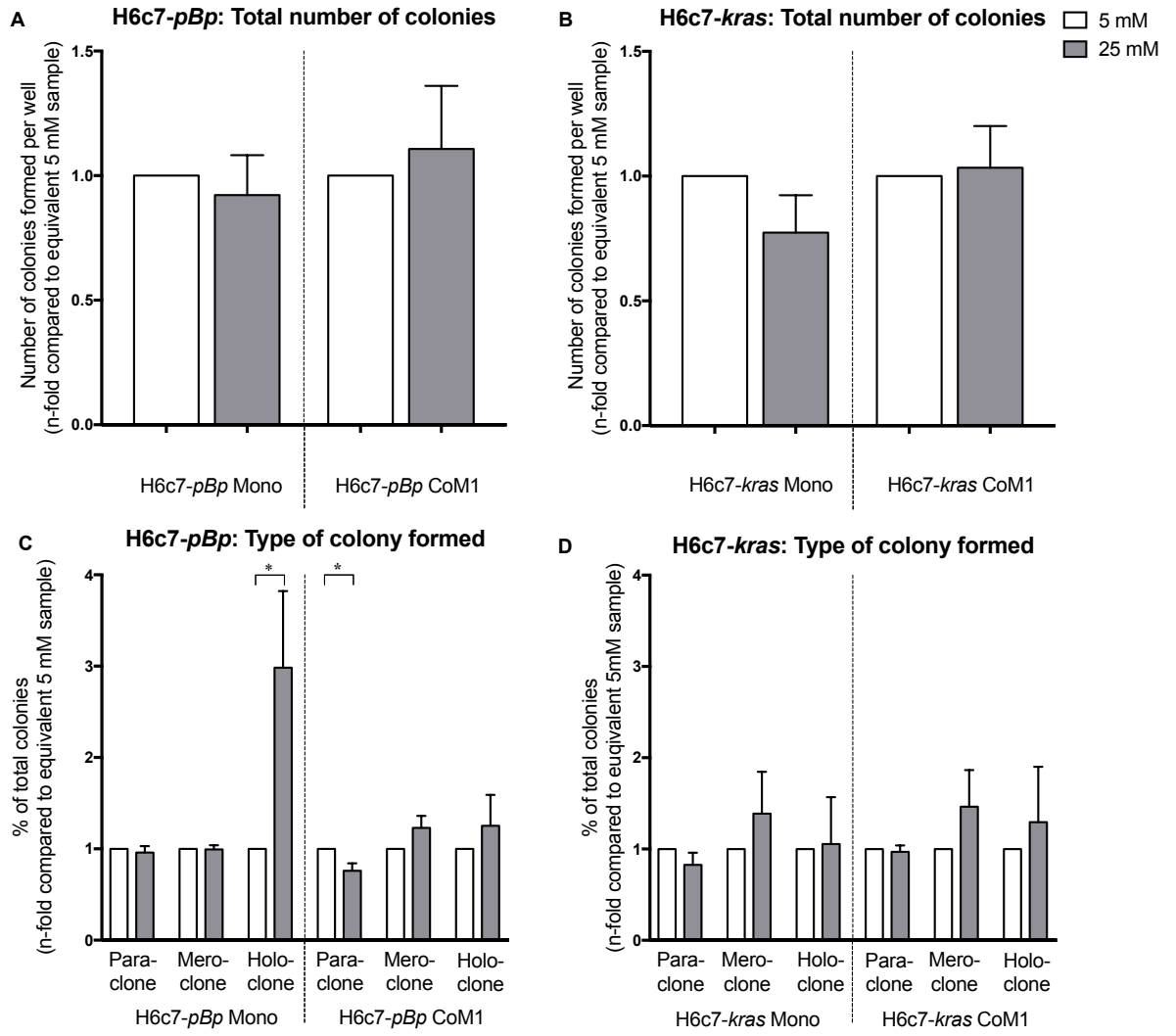

Figure 30: Hyperglycaemia promotes the formation of colonies with high CSC-potential in mono- and cocultured PDEC. H6c7-*pBp* and H6c7-*kras* cells were cultivated in normo- or hyperglycaemic conditions (5 or 25 mM of glucose) in mono- or coculture with M1-polarised macrophages (MΦ). The epithelial cells were separated from direct coculture with macrophages via CD11b-MACS depletion of M1-MΦ or harvested from monoculture and used for colony formation assays. For this, 800 cells/well were seeded in duplicates and cultivated for 8 to 14 days. After fixation and staining, colonies of more than 50 cells were analysed. The total number of colonies per well (A and B) and the quality of colonies (C and D) formed under the differing glycaemic conditions are shown. Data are depicted as n-fold to the equivalent sample arising from normoglycaemic settings. Normally distributed data are presented as mean and standard error of mean, unpaired t-test was performed for statistical analysis.
*: 0,05>p>0,0332; n=6

In monocultured H6c7-*kras* cells, exposure to high glucose levels led to an 0.77-fold reduction in the number of colonies formed compared to normoglycaemic conditions. H6c7-*kras* cells cocultured with M1-polarised macrophages, however, were not impacted in their ability of colony formation through hyperglycaemia (**Figure 30** B).

Even though the total number of colonies formed was reduced, a significant 2.98-fold increase in holoclones was observed after exposure to high glucose levels in monocultured benign PDEC (**Figure 30** C). In cocultured H6c7-*pBp* cells, glucose also led to a slight shift towards mero- and holoclone (1.23-fold and 1.25-fold increase, respectively, compared to the equivalent normoglycaemic cells) at the expense of paraclones (0.76-fold decrease compared to normoglycaemic cells).

The impact of glucose on the type of colonies was similar in mono- and cocultured premalignant PDEC. Both showed a greater proportion of mero- and holoclones after subjection to high glucose levels and thus fewer paraclones (**Figure 30** D). This effect was slightly more pronounced in H6c7-*kras* cells arising from coculture settings (1.50-fold increase in meroclones and 1.30-fold increase in holoclones compared to the normoglycaemic coculture) than in cells from monoculture (1.40-fold increase in mero- and 1.1-fold in holoclones compared to normoglycaemic monoculture).

Together, these findings suggest that hyperglycaemia promotes cancer stemness characteristics in both H6c7-*pBp* and H6c7-*kras* cells. Whereas the glucose-induced acquisition of CSC-associated properties was more pronounced in monocultured benign PDEC, the premalignant PDEC are similarly impacted in both cultivation conditions.

4.3 TGF-βIIR Knockdown

TGF-β1 is regarded as a potent inducer of EMT- and CSC-properties and is attributed an important role in the process of metastatic spreading (J. Xu et al., 2009; Jing et al., 2011). We could show that gene expression levels of TGF-β1 were increased in PDEC exposed to a hyperglycaemic and inflammatory microenvironment (**Figure 17**). To analyse whether enhanced TGF-β1-signalling is responsible for the glucose- and coculture-dependent alterations in malignancy-associated properties of PDEC, TGF-βRII expression was supressed by transfection with siRNA. TGF-β-signalling depends on the association of TGF-βRI and TGF-βRII upon the activation by the TGF-β ligand. TGF-βRII then phosphorylates TGF-βRI and permits subsequent downstream action of TGF-β (Feng and Derynck, 2005; Jakowlew, 2006). Therefore, suppression of TGF-βRII disables functional TGF-β1-signalling.

The knockdown of TGF-βRII was performed in H6c7-*pBp* and H6c7-*kras* cells one day prior to coculture in normo- and hyperglycaemic conditions.

Prior to these experiments, the stability of the knockdown was analysed to ensure that TGF-βRII signalling was suppressed throughout the whole experimental time span, this is up to 6 days post-transfection. To this end, TGF-βRII mRNA levels were clearly reduced on day 2, 4 and 6 after transfection with TGF-βRII siRNA (data not shown).

4.3.1 Impact of TGF-βRII knockdown on gene expression levels of EMT- and CSC-associated genes in cocultured PDEC

To evaluate whether the knockdown of TGF-βRII impacts on the gene expression level of EMT- and stemness-associated genes in PDEC, H6c7-*pBp* and H6c7-*kras* cells were transfected with either TGF-βRII siRNA or control (ctrl) siRNA and cocultured with M1-polarised macrophages in normo- or hyperglycaemic conditions for 5 days. The epithelial cells were then separated from the direct coculture via CD11b-MACS depletion of macrophages and used for qRT-PCR analysis. Cells arising from the equivalent coculture setting but transfected with ctrl siRNA served as a control.

4.3.1.1 TGF-βRII knockdown reduces gene expression levels of IL-6, TNF-α and TGF-β1 in PDEC

In a first step, it was evaluated whether the knockdown of TGF-βRII impacts the gene expression level of EMT- and stemness-inducing factors in PDEC arising from normo- or hyperglycaemic coculture with M1-polarised macrophages.

Knockdown of TGF-βRII reduced the gene expression level of IL-6 by 53% in benign PDEC arising from normoglycaemic coculture. This effect was less explicit under hyperglycaemic coculture conditions, showing a reduction of 26% (**Figure 31** A). In the premalignant PDEC, the knockdown also led to a reduction of roughly 32% in both coculture settings (**Figure 31** B). Gene expression levels of IL-8, on the other hand, were not affected at all through knockdown of TGF-βRII, neither in H6c7-*pBp* nor in H6c7-*kras* cells under either condition (**Figure 31** C and D). Transfection with TGF-βRII siRNA led to a reduction in gene

expression of TNF-α levels in H6c7-*pBp* cells, which was strengthened by high glucose levels (0.53-fold decrease) compared to low glucose levels (0.81-fold decrease) (**Figure 31** E). In H6c7-*kras* cells, on the other hand, TGF-βRII knockdown led to elevated levels of TNF-α in cells from normoglycaemic coculture, whereas cells arising from coculture with high glucose levels did not show any alteration in their gene expression level of TNF-α (**Figure 31** F). Finally, TGF-β1 expression was significantly reduced in H6c7-*pBp* cells from normoglycaemic coculture upon knockdown of TGF-βRII (0.76-fold compared to the equivalent sample transfected with ctrl siRNA); tendencies of increase were observed in the gene expression level of TGF-β1 after knockdown of TGF-βRII under hyperglycaemic conditions (**Figure 31** G). H6c7-*kras* cells showed a weak decrease of TGF-β1 expression upon transfection with TGF-βRII siRNA under either condition (**Figure 31** H).

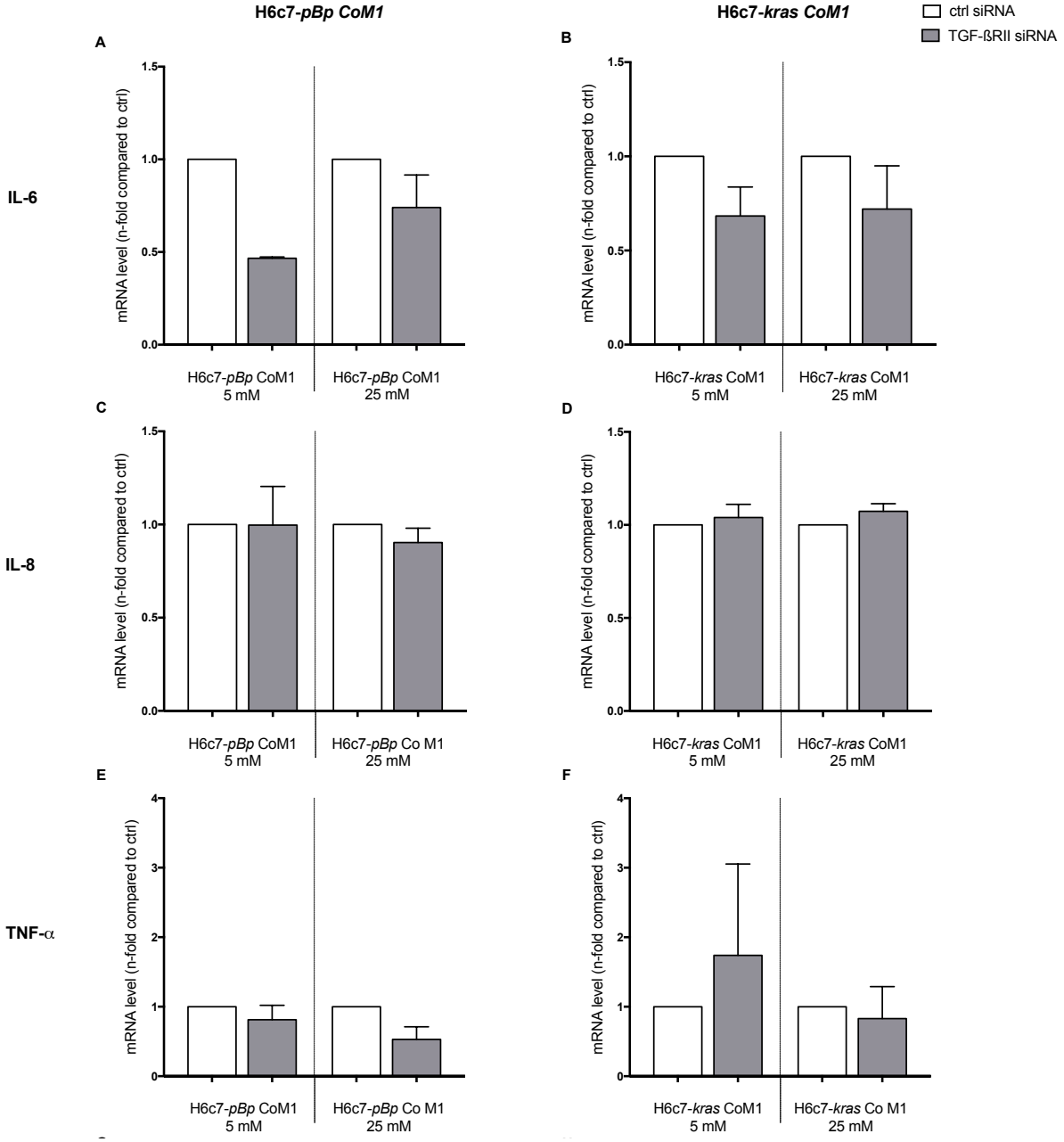

Figure 31: TGF-βRII knockdown reduces the expression of EMT- and CSC-inducing factors in cocultured PDEC. (to be continued on next page)

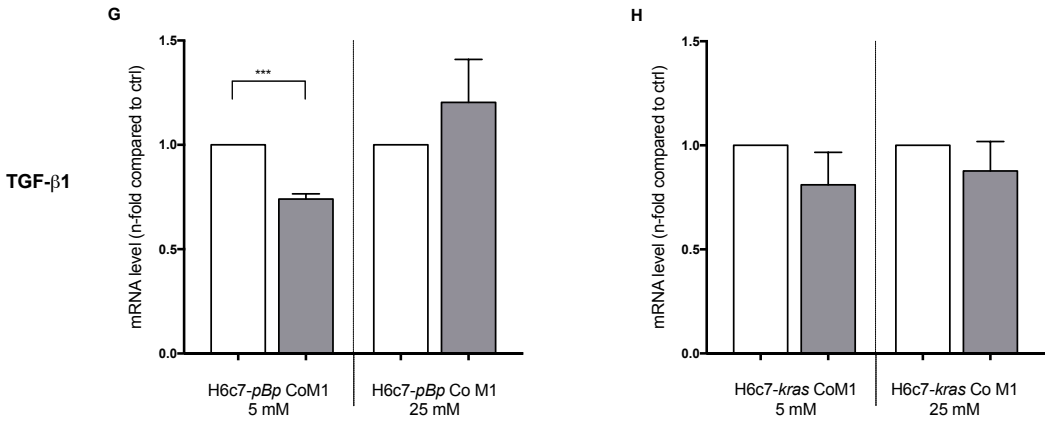

Figure 31: TGF-βRII knockdown reduces the expression of EMT- and CSC-inducing factors in cocultured PDEC. (continued) H6c7-*pBp* or H6c7-*kras* cells were cocultured with M1-polarised macrophages (MΦ) for 5 days in normo- or hyperglycaemic settings (5 or 25 mM of glucose) and transfected with TGF-βRII-siRNA or ctrl siRNA. The epithelial cells were separated from direct coculture via CD11b-MACS depletion of M1-MΦ and used for qRT-PCR analysis. The relative gene expression levels of IL-6 (A and B), IL-8 (C and D), TNF-α (E and F) and TGF-β1 (G and H) of both cell lines are depicted, normalised to the housekeeping gene GAPDH and presented as n-fold expression compared to the equivalent ctrl siRNA sample. Normally distributed data are presented as mean and standard error of mean, unpaired t-test was performed for statistical analysis. ***=: 0,002>p>0,0001; n=3

4.3.1.2 TGF-βRII knockdown heterogeneously impacts on EMT- and CSC-associated transcription factors

Next, the gene expression levels of the EMT- and CSC-associated transcription factors Snail, Slug and Zeb1 were analysed in PDEC which had been transfected with TGF-βRII siRNA or ctrl siRNA and cocultured with M1-polarised macrophages under normo- or hyperglycaemic conditions.

TGF-βRII knockdown hardly affected the gene expression level of Snail in both PDEC lines, irrespective of the glucose level at which the cells had been cocultured (**Figure 32** A and B). mRNA levels of the transcription factor Slug were not affected in H6c7-*pBp* cells transfected with TGF-βRII siRNA under normoglycaemic conditions. However, H6c7-*pBp* cells transfected with TGF-βRII siRNA cells and arising from hyperglycaemic coculture showed 1.82-fold elevated mRNA levels of Slug compared to the equivalent cells transfected with ctrl siRNA (**Figure 32** C). In H6c7-*kras* cells, Slug levels were elevated in all samples after TGF-βRII knockdown; with a more pronounced effect in cells from normoglycaemic than from hyperglycaemic coculture (2.26- and 1.49-fold increase respectively) (**Figure 32** D).

Finally, the knockdown did not impact on gene expression level of Zeb1 in the benign cells, nor in the premalignant cells arising from normoglycaemic coculture (**Figure 32** E and F). However, benign PDEC transfected with TGF-βRII siRNA and exposed to high glucose levels showed significantly reduced expression levels of Zeb1 (0.54-fold compared to the equivalent cells transfected with ctrl siRNA) (**Figure 32** E).

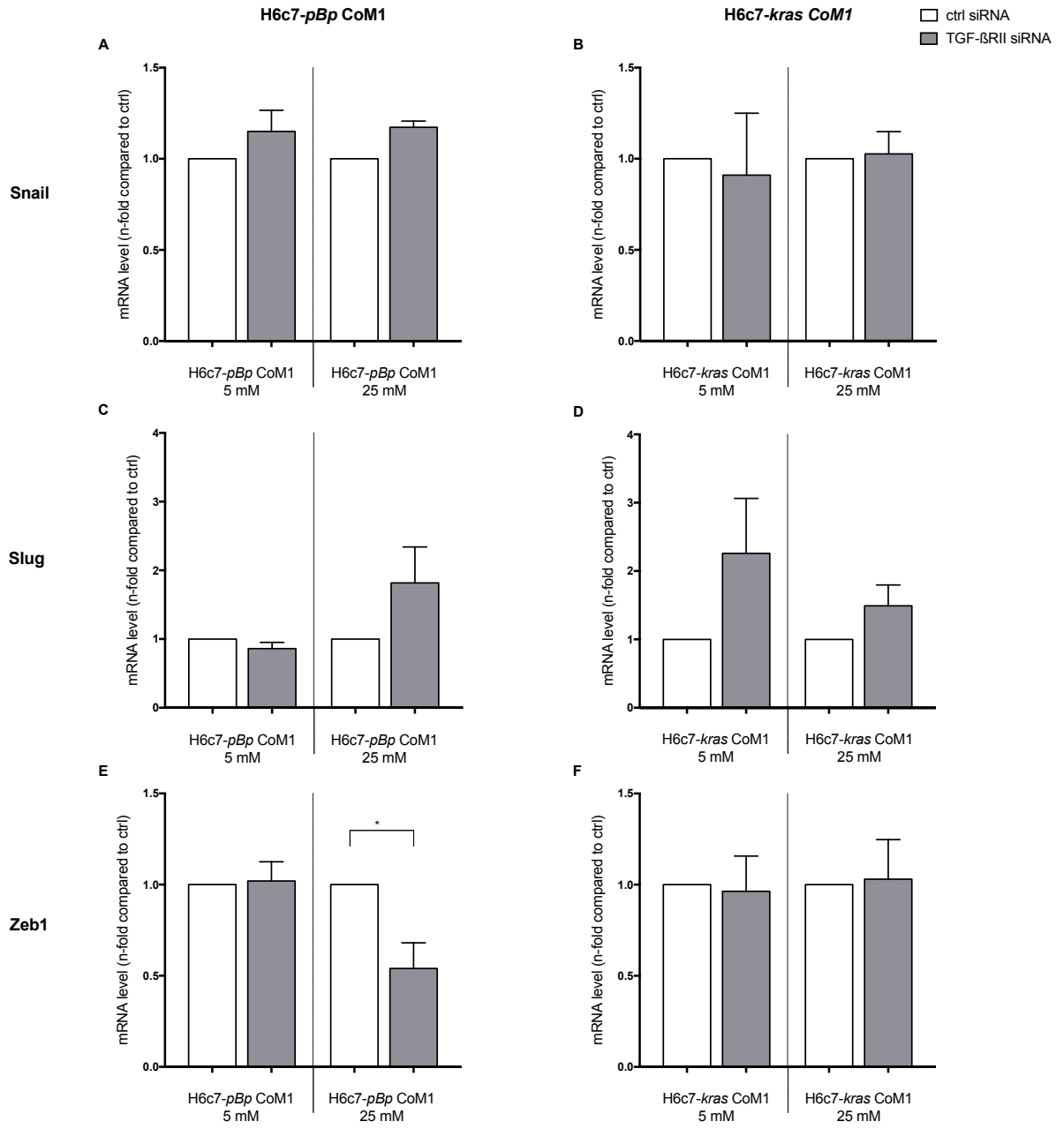

Figure 32: Impact of TGF-βRII knockdown on the gene expression levels of EMT- and CSC-associated transcription factors in PDEC. H6c7-*pBp* or H6c7-*kras* cells were cocultured with M1-polarised macrophages (MΦ) for 5 days in normo- or hyperglycaemic settings (5 or 25 mM of glucose) and transfected with TGF-βRII-siRNA or ctrl siRNA. The epithelial cells were separated from direct coculture via CD11b-MACS depletion of M1-MΦ and used for qRT-PCR analysis. The relative gene expression levels of Snail (A and B), Slug (C and D) and Zeb1 (E and F) of both cell lines are depicted, normalised to the housekeeping gene GAPDH and presented as n-fold expression compared to the equivalent ctrl sample. Normally distributed data are presented as mean and standard error of mean, unpaired t-test was performed for statistical analysis. *: 0,05>p>0,0332; n=4

4.3.1.3 TGF-βRII knockdown promotes gene expression level of the epithelial marker E-Cadherin in PDEC

In a next step, the impact of TGF-β1-signalling suppression on the gene expression level of EMT-markers in PDEC cocultured with M1-polarised macrophages under normo- or hyperglycaemic conditions was analysed.

Knockdown of TGF-βRII led to clearly elevated expression levels of the epithelial marker E-Cadherin in both cell lines arising from normoglycaemic conditions. While an increase was also observed in H6c7-*pBp* cells under hyperglycaemic coculture (1.6-fold compared to equivalent cells transfected with ctrl siRNA), TGF-βRII suppression did not impact E-Cadherin expression in H6c7-*kras* cells under comparable conditions (**Figure 33** A and B).

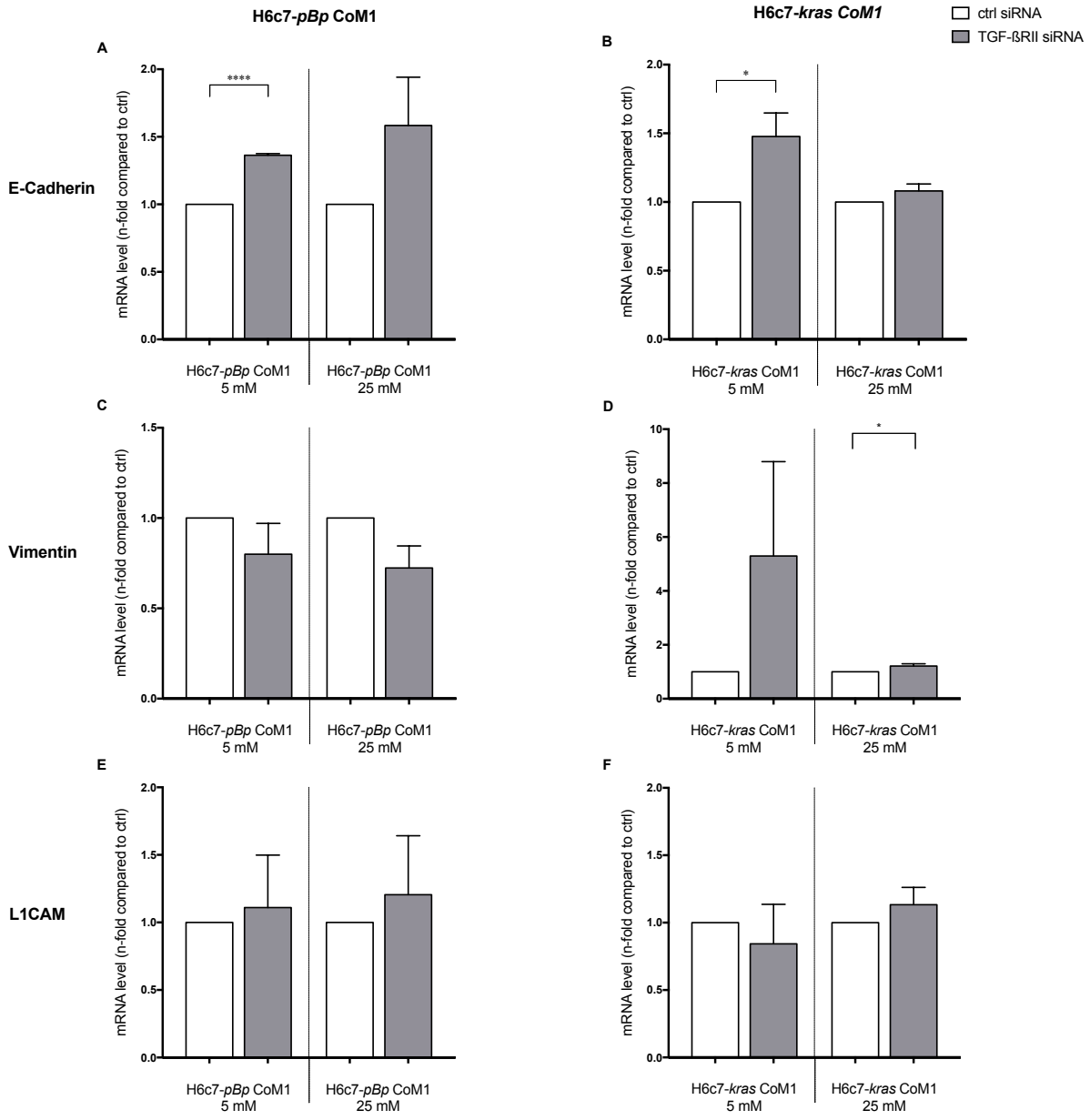

Figure 33: TGF-βRII knockdown promotes the expression of the epithelial marker E-Cadherin in PDEC. H6c7-*pBp* or H6c7-*kras* cells were cocultured with M1-polarised macrophages (MΦ) for 5 days in normo- or hyperglycaemic settings (5 or 25 mM of glucose) and transfected with TGF-βRII-siRNA or ctrl siRNA. The epithelial cells were separated from direct coculture via CD11b-MACS depletion of M1-MΦ and used for qRT-PCR analysis. The relative gene expression levels of E-Cadherin (A and B), Vimentin (C and D) and L1CAM (E and F) of both cell lines are depicted, normalised to the housekeeping gene GAPDH and presented as n-fold expression compared to the equivalent ctrl sample. Normally distributed data are presented as mean and standard error of mean, unpaired t-test was performed for statistical analysis. *: 0,05>p>0,0332 ****: p<0,0001; n=4

Intriguingly, the gene expression level of the mesenchymal marker Vimentin was slightly reduced through transfection with TGF-βRII siRNA in the benign PDEC (**Figure 33** C), whereas it was elevated in the

premalignant cells under both glucose conditions. This effect was even more pronounced in normoglycaemic coculture (5.30-fold elevation compared to equivalent cells transfected with ctrl siRNA) than in hyperglycaemic coculture (1.25-fold increase compared to equivalent cells transfected with ctrl siRNA) (**Figure 33** D).

Finally, L1CAM gene expression levels were hardly affected by the knockdown of TGF-βRII, but showed a slight increase in all samples except in H6c7-*kras* cells arising from normoglycaemic coculture (**Figure 33** E and F).

4.3.1.4 TGF-βRII knockdown impacts on the expression of CSC markers in PDEC

Finally, the impact of TGF-βRII knockdown on the expression level of the stemness indicators Nestin and Nanog were evaluated in PDEC arising from normo- or hyperglycaemic coculture with M1-polarised macrophages.

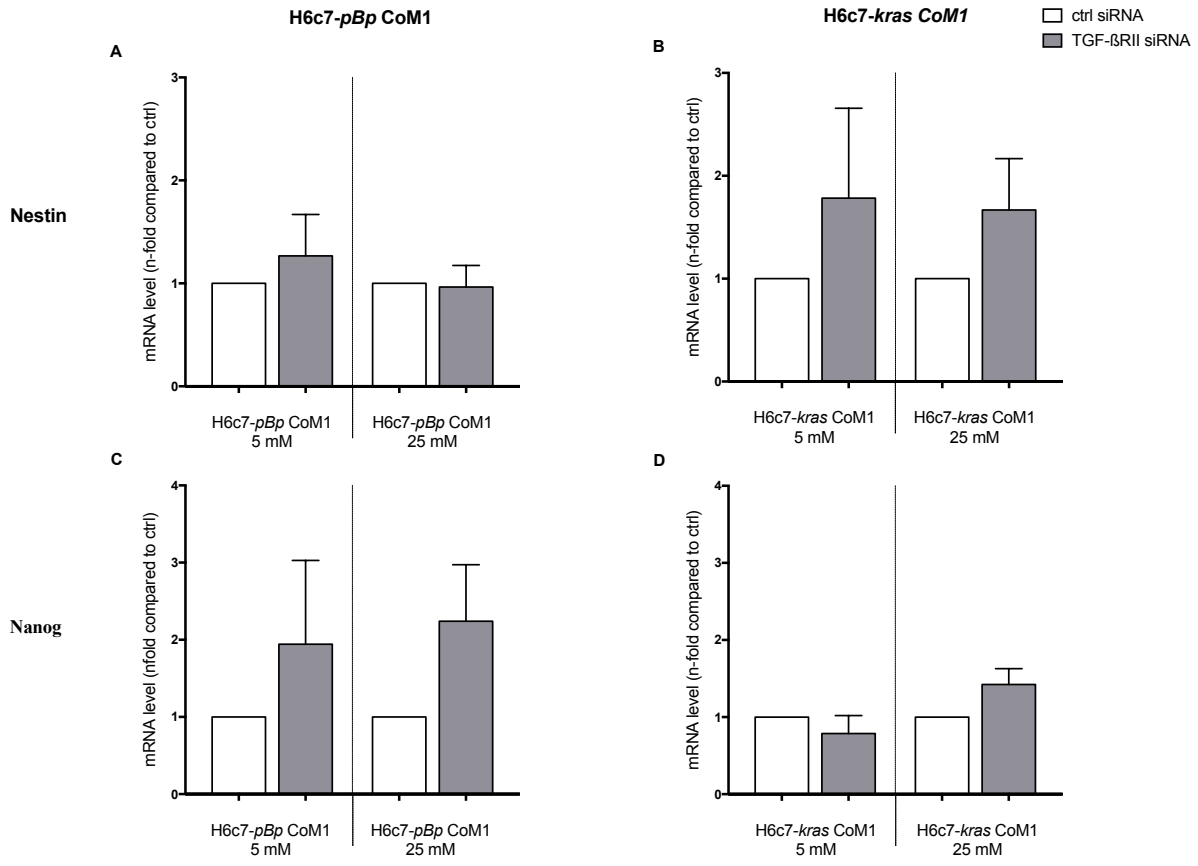

Figure 34: Impact of TGF-βRII knockdown on the expression of CSC markers in PDEC. H6c7-*pBp* or H6c7-*kras* cells were cocultured with M1-polarised macrophages (MΦ) for 5 days in normo- or hyperglycaemic settings (5 or 25 mM of glucose) and transfected with TGF-βRII-siRNA or ctrl siRNA. The epithelial cells were separated from direct coculture via CD11b-MACS depletion of M1-MΦ and used for qRT-PCR analysis. The relative gene expression levels of Nestin (A and B) and Nanog (C and D) of both cell lines are depicted, normalised to the housekeeping gene GAPDH and presented as n-fold expression compared to the equivalent ctrl sample. Normally distributed data are presented as mean and standard error of mean, unpaired t-test was performed for statistical analysis. n=4

Whereas only H6c7-*pBp* cells from normoglycaemic coculture showed slightly elevated gene expression levels of Nestin upon transfection with TGF-βRII siRNA (**Figure 34** A), mRNA levels of Nestin were

elevated in H6c7-*kras* transfected with TGF-βRII siRNA irrespective of the glucose level (1.78- and 1.67-increase for normo-and hyperglycaemic coculture settings compared to the equivalent cells transfected with ctrl siRNA) (**Figure 34** B).

mRNA levels of Nanog were elevated in H6c7-*pBp* cells arising from normo- and hyperglycaemic knockdown samples (1.94- and 2.24-fold increase, respectively, compared to the equivalent cells transfected with ctrl siRNA) (**Figure 34** C). In H6c7-*kras* cells, however, TGF-βRII knockdown also led to increased Nanog expression in hyperglycaemic coculture settings (1.42-fold compared to cells from hyperglycaemic coculture transfected with ctrl siRNA), but to slightly decreased Nanog levels in normoglycaemic conditions (0.79-fold compared to the equivalent cells transfected with ctrl siRNA) (**Figure 34** D).

4.3.2 TGF-βRII knockdown reduces the fraction of holoclones formed by PDEC arising from coculture with M1-polarised macrophages under hyperglycaemic conditions

In a next step, colony formation assays were performed to analyse the effect of the TGF-βRII knockdown on the acquisition of CSC-properties in PDEC on a functional level. For this, the ability of PDEC cocultured with M1-polarised macrophages under normo- or hyperglycaemic conditions and transfected with either TGF-βRII siRNA or ctrl siRNA to form clones of more than 50 cells was compared and the type of clones formed was evaluated.

Whereas the total number of colonies formed was hardly affected by the knockdown of TGF-βRII in both PDEC lines (**Figure 35** A and B), the type of colonies was altered.

In detail, H6c7-*pBp* cells arising from the hyperglycaemic coculture and transfected with TGF-βRII siRNA formed significantly fewer holoclones (0.37-fold reduction compared to the control sample), but more paraclones, whereas the fraction of meroclones was constant. H6c7-*pBp* cells arising from the normoglycaemic coculture, on the other hand, formed more holoclones upon transfection with TGF-βRII siRNA (1.38-fold elevation compared to the equivalent control), whereas the fraction of para-and meroclones were hardly impacted (**Figure 35** C).

H6c7-*kras* cells arising from the hyperglycaemic coculture and transfected with TGF-βRII siRNA also showed a proportional reduction of holoclones (0.49-fold decrease compared to the equivalent cells transfected with ctrl siRNA), while H6c7-*kras* cells arising from normoglycaemic coculture formed slightly more mero- and holoclones after knockdown of TGF-βRII (**Figure 35** D).

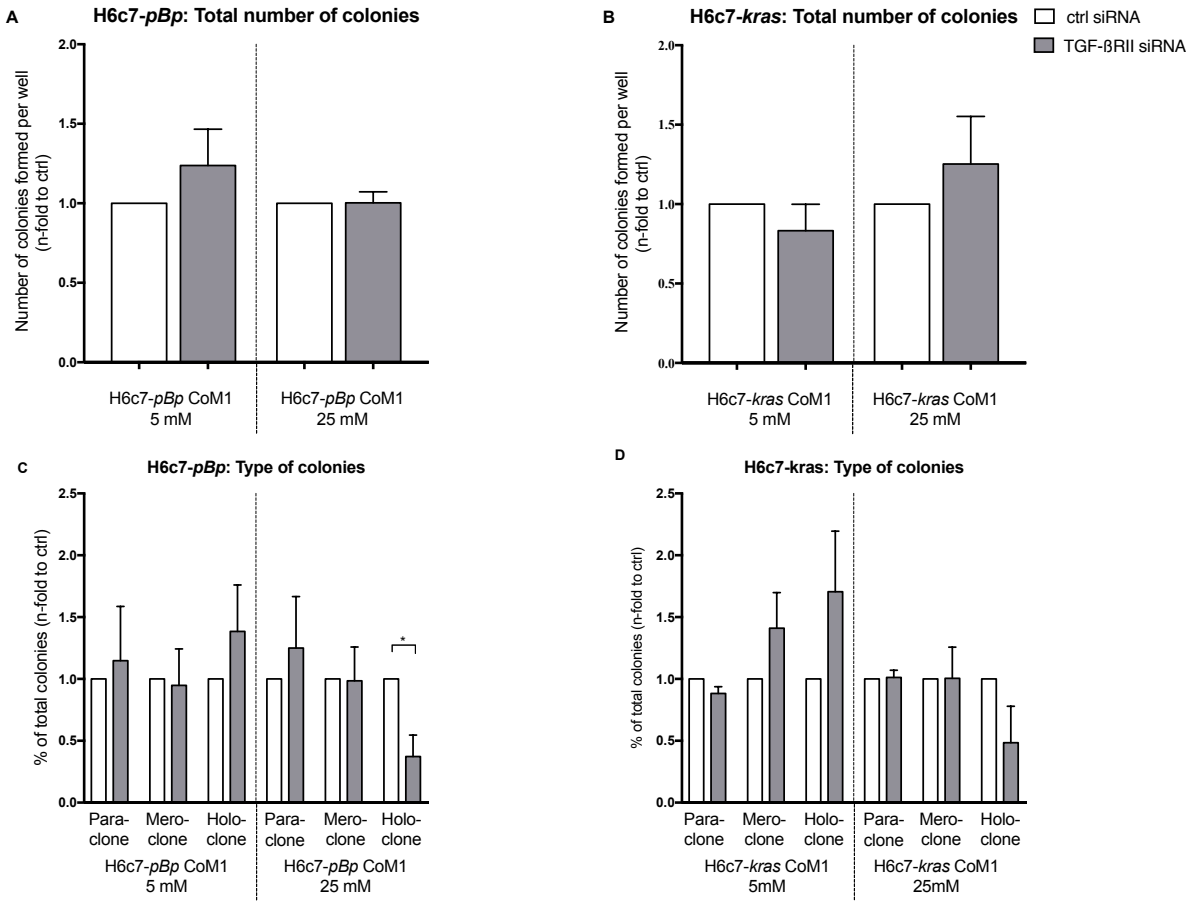

Figure 35: TGF-βRII knockdown reduces the fraction of holoclones formed by H6c7-*pBp* and H6c7-*kras* cells arising from hyperglycaemic coculture with M1-polarised macrophages (MΦ). H6c7-*pBp* and H6c7-*kras* cells were cocultured with M1-polarised MΦ for 5 days in normo- or hyperglycaemic settings (5 or 25 mM of glucose) transfected with TGF-βRII-siRNA or ctrl siRNA. The epithelial cells were separated from direct coculture with macrophages via CD11b-MACS depletion of M1-MΦ and used for colony formation assays. For this, 800 cells/well were seeded in duplicates and cultivated for 8 to 14 days. After fixation and staining, colonies of more than 50 cells were analysed. The total number of colonies per well (A and B) and the quality of colonies (C and D) formed under the differing treatments are shown. Data are depicted as n-fold compared to the equivalent ctrl sample. Normally distributed data are presented as mean and standard error of mean, unpaired t-test was performed for statistical analysis. *: 0,05>p>0,0332; n=4

4.3.3 Knockdown of TGF-βRII reduces the migratory potential of PDEC arising from normoglycaemic coculture with M1-polarised macrophages

To analyse possible changes in the migratory potential of PDEC through the knockdown of TGF-βRII, a scratch assay was performed with PDEC transfected with either TGF-βRII siRNA or ctrl siRNA and cocultured with M1-polarised macrophages under normoglycaemic conditions.

At the early timepoint of evaluation (t=9h), benign PDEC transfected with TGF-βRII siRNA showed a slightly pronounced gap closure compared to the equivalent control (22.38% and 17.65% compared to t=0, respectively) (**Figure 36** A). After 24 hours, however, this effect was reversed. TGF-βRII knockdown led to a reduced closure of the scratch in H6c7-*pBp* cells cocultured with M1-polarised macrophages, indicating a diminished migratory potential. (30.4 % of the gap were closed compared to 37% in the equivalent control).

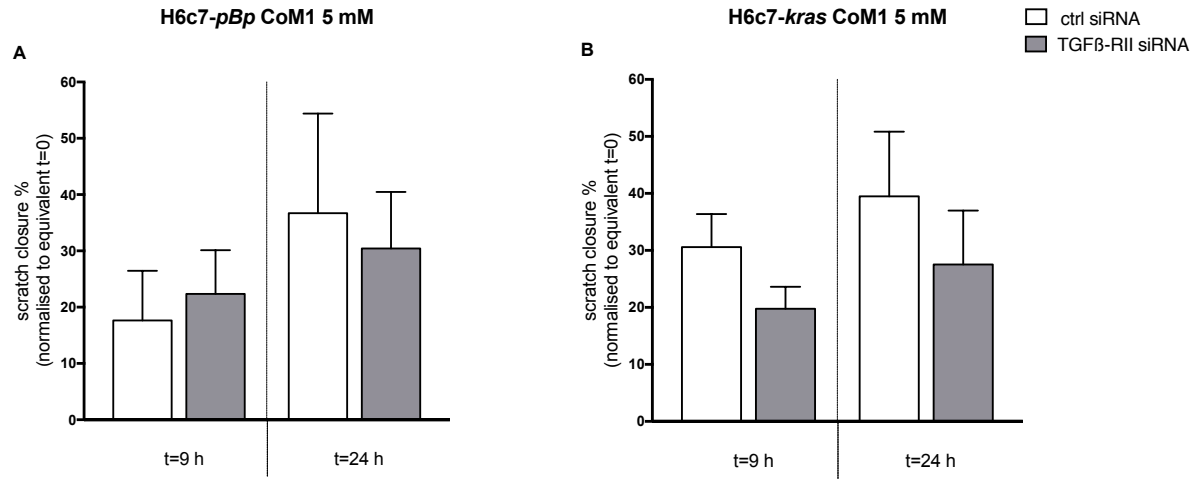

Figure 36: Knockdown of TGF-βRII reduces the migratory potential of PDEC arising from normo- or hyperglycaemic coculture with M1-polarised macrophages (MΦ). H6c7-*pBp* and H6c7-*kras* cells were cocultured with M1-polarised MΦ for 5 days in normo- or hyperglycaemic settings (5 or 25 mM of glucose) and transfected with TGF-βRII siRNA or ctrl siRNA. The migratory potential of PDEC was evaluated via scratch assay using Lionheart FX Automated Microscope. Scratch closure was assessed at t=0, t=9h and t=24h for H6c7-*pBp* CoM1 (A) and H6c7-*kras* CoM1 cells (B). The percentage of closure was evaluated with the Gen5 Data Analysis Software. Normally distributed data are presented as mean and standard error of mean, unpaired t-test was performed for statistical analysis. n=4

Similarly, cellular migration was also reduced in premalignant PDEC upon knockdown of TGF-βRII. However, contrary to the benign PDEC, this reduction in migratory potential was already visible after 9 hours: H6c7-*kras* transfected with TGF-βRII siRNA showed a closure of 19.77% and 27,52% after 9 and 24 hours, respectively (compared to t=0) compared to cells from the equivalent control (30.57% and 39.48% after 9 and 12 hours) (**Figure 36** B).

In summary, the knockdown of TGF-βRII revealed that TGF-β1 signalling is involved in the glucose- and M1-MΦ-dependent alterations of malignancy-associated properties of PDEC.

The knockdown of TGF-βRII led to reduced mRNA levels of the EMT- and CSC- inducing factors IL-6, TNF-α and TGF-β1 in both PDEC lines. Furthermore, the important epithelial marker E-Cadherin showed elevated expression levels upon transfection with TGF-βRII siRNA, indicating a role of TGF-β-signalling in glucose- and inflammation-mediated EMT in these cells. The reduced cellular motility of PDEC after knockdown of TGF-βRII underlines these findings. However, gene expression levels of the mesenchymal marker Vimentin were also elevated, indicating that EMT induction is not completely reversed by the knockdown.

Finally, the decrease in the number of holoclones formed by PDEC transfected with TGF-βRII siRNA indicates a role of TGF-β1-signalling in the acquisition of CSC-properties under hyperglycaemic inflammatory conditions.

4.4 Blockade of IL-6 signalling pathway

IL-6-dependent signalling pathways are closely linked to inflammatory processes (Mauer et al., 2014; Scheller et al., 2014). Extremely high levels of IL-6 have been reported within inflammatory tissues (Robak et al., 1998; Rose-John et al., 2006), which is in accordance with the impressive gene expression levels of IL-6 we observed in macrophages upon exposure to PDEC and/or glucose (section 4.1). To elucidate whether this pro-inflammatory cytokine is involved in the EMT- and CSC-associated alterations in PDEC upon exposure to a T2DM-associated inflammatory microenvironment, IL-6 signalling was blocked in coculture experiments.

IL-6 is characterised by a complex signalling pathway. A classic-signalling pathway is distinguished from a trans-signalling one. For the initiation of the classic-signalling cascade, IL-6 needs to bind to a membrane-bound IL-6 receptor (IL-6R). This receptor is only expressed on a few cells, e.g., on monocytes and macrophages as well as on hepatocytes. Once the IL-6-IL-6R-complex is formed, various pathways, such as Ras/Raf/MAPK, PI3K are activated (Rose-John, 2012).

Trans-signalling, on the other hand, is not reliant on the membrane bound IL-6R but on a soluble IL-6 receptor (sIL-6R). Once IL-6 binds to the sIL-6R, the complex can initiate downstream signalling (Rose-John, 2012).

Several studies assume that classic-signalling initiates anti-inflammatory activities of IL-6, whereas trans-signalling promotes pro-inflammatory reactions (Atreya et al., 2000; Barkhausen et al., 2011; Rose-John, 2012).

In a first step, both pathways of IL-6-signalling were blocked by the antibody Tocilizumab which binds to IL-6R (chapter 4.4.1). Rituximab was used as a control antibody. In a second step, just trans-signalling was disabled via sgp130Fc (chapter 4.4.2). Sgp130Fc only binds to IL-6 that is bound to the sIL-6R and does not interfere with the classic-signalling via the membrane bound IL-6R. Ctrl-Fc was used as a control in these experiments.

4.4.1 Complete blockade of IL-6-signalling via Tocilizumab

4.4.1.1 Impact of IL-6 blockade via Tocilizumab on the gene expression levels of EMT-and CSC-associated genes in cocultured PDEC

To evaluate whether the blockade of IL-6 signalling impacts the gene expression level of EMT- and stemness-associated mediators in PDEC, H6c7-*pBp* and H6c7-*kras* cells were treated with either Tocilizumab or Rituximab and cocultured with M1-polarised macrophages in normo- or hyperglycaemic conditions for 5 days. The epithelial cells were then separated from direct coculture via CD11b-MACS depletion of macrophages and used for qRT-PCR analysis. Cells arising from the equivalent coculture setting treated with Rituximab served as a control.

4.4.1.1.1 Tocilizumab increases expression levels of EMT- and CSC- inducing mediators in hyperglycaemic cocultured H6c7-*kras* cells

In a first step, it was evaluated whether the blockade of both IL-6 trans- and IL-6 classic-signalling via Tocilizumab impacts the gene expression level of EMT- and stemness inducing factors in PDEC arising from normo- or hyperglycaemic coculture with M1-polarised macrophages.

The benign PDEC were not impacted in their gene expression of IL-6, IL-8 or TGF-β1 through blockade via Tocilizumab (**Figure 37** A, C and G). Only the pro-inflammatory cytokine TNF-α showed a 1.5-fold increase upon IL-6 blockade in normoglycaemic coculture conditions compared to the control sample. Under hyperglycaemic conditions, however, no Tocilizumab-induced effect was to be seen (**Figure 37** E). H6c7-*kras* cells from normoglycaemic coculture with macrophages were also not affected in their expression level of these mediators by Tocilizumab. However, cells arising from hyperglycaemic coculture showed increased levels for IL-6 (1.8-fold (**Figure 37** B)), IL-8 (1.78-fold (**Figure 37** D)), TNF-α (1.66-fold (**Figure 37** F)) and TGF-β1 (1.66-fold (**Figure 37** H)) upon treatment with Tocilizumab.

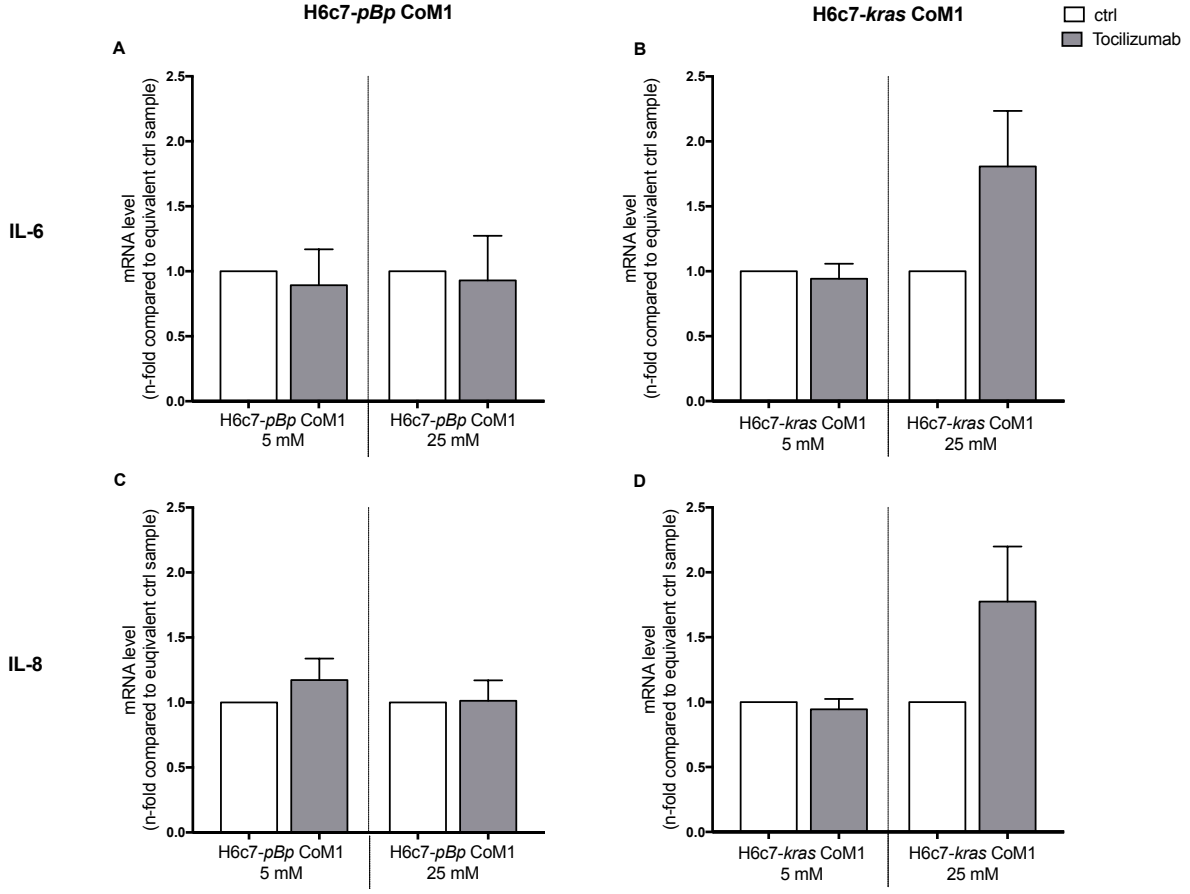

Figure 37: Blockade of IL-6 signalling via Tocilizumab leads to an elevation of EMT- and CSC-associated mediators in cocultured hyperglycaemic H6c7-*kras* cells. (to be continued on next page)

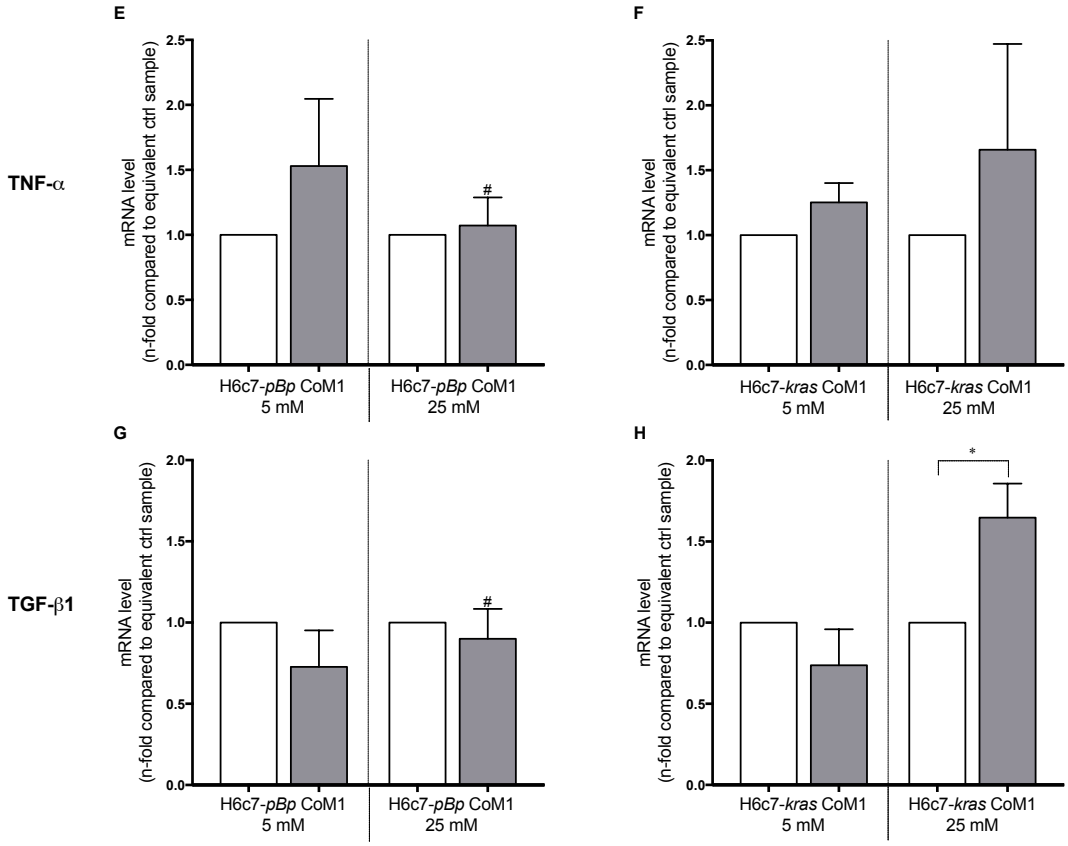

Figure 37: Blockade of IL-6 signalling via Tocilizumab leads to an elevation of EMT- and CSC-associated mediators in cocultured hyperglycaemic H6c7-*kras* cells. (continued) H6c7-*pBp* or H6c7-*kras* cells were cocultured with M1-polarised macrophages (MΦ) for 5 days in normo- or hyperglycaemic settings (5 or 25 mM of glucose) and treated with 1 µg/ml of Tocilizumab or Rituximab (ctrl). The epithelial cells were separated from direct coculture via CD11b-MACS depletion of M1-MΦ and used for qPCR analysis. The relative gene expression levels of IL-6 (A and B), IL-8 (C and D), TNF-α (E and F) and TGF-ß1 (G and H) of both cell lines are depicted, normalised to the housekeeping gene GAPDH and presented as n-fold expression compared to the equivalent ctrl sample. Normally distributed data are presented as mean and standard error of mean, unpaired t-test was performed for statistical analysis. Not normally distributed data (indicated via #) are shown as median and interquartile range. Wilcoxon Signed Rank Test was used for statistical analysis. *: 0,05>p>0,0332; n=4

4.4.1.1.2 Tocilizumab treatment promotes Zeb1 expression in hyperglycaemic cocultured H6c7-*kras* cells

Next, the gene expression levels of the EMT- and CSC-associated transcription factors Snail, Slug and Zeb1 were analysed in PDEC treated with Tocilizumab or Rituximab and cocultured with M1-polarised macrophages under normo- or hyperglycaemic conditions.

Tocilizumab hardly influenced the benign PDEC in their gene expression level of the EMT- and CSC-associated transcription factors irrespective of the coculture condition (**Figure 38** A, C, E).

In contrast, slight increases were observed in the premalignant PDEC line from hyperglycaemic coculture treated with Tocilizumab for Snail and Slug (1.32-fold increase for both transcription factors compared to the equivalent control samples) (**Figure 38** B and D), and a significant 1.87-fold increase was observed for Zeb1 compared to the equivalent hyperglycaemic control (**Figure 38** F).

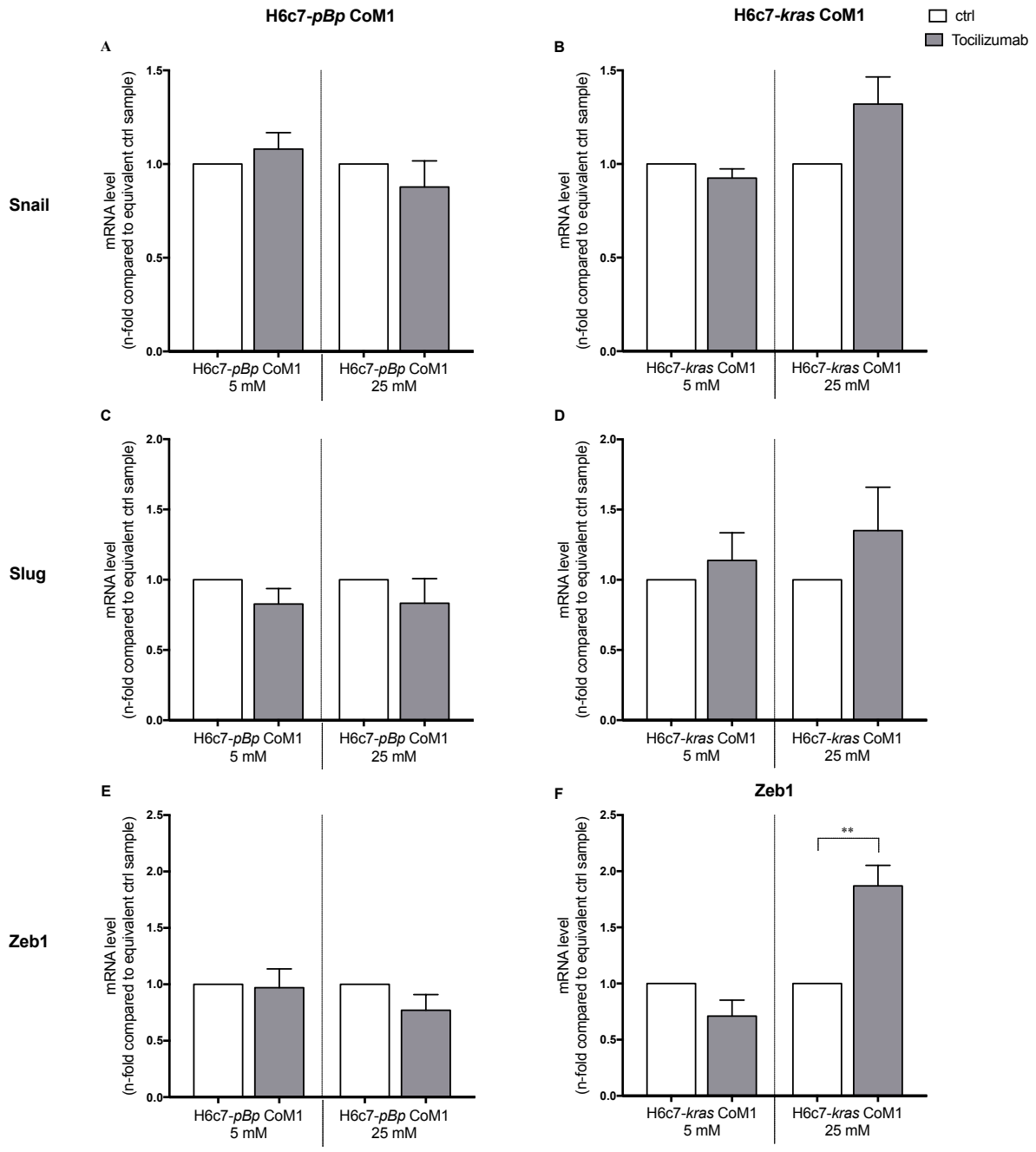

Figure 38: Blockade of IL-6 signalling via Tocilizumab increases Snail, Slug and Zeb1 expression in cocultured hyperglycaemic H6c7-*kras* cells. H6c7-*pBp* or H6c7-*kras* cells were cocultured with M1-polarised macrophages (MΦ) for 5 days in normo- or hyperglycaemic settings (5 or 25 mM of glucose) and treated with 1 µg/ml of Tocilizumab or Rituximab (ctrl). The epithelial cells were separated from direct coculture via CD11b-MACS depletion of M1-MΦ and used for qPCR analysis. The relative gene expression levels of Snail (A and B), Slug (C and D) and Zeb1 (E and F) of both cell lines are depicted, normalised to the housekeeping gene GAPDH and presented as n-fold expression compared to the equivalent ctrl sample. Normally distributed data are presented as mean and standard error of mean, unpaired t-test was performed for statistical analysis. **: =0,0331>p>0,0021; n=4

4.4.1.1.3 Tocilizumab increases expression of epithelial and mesenchymal markers in H6c7-*kras* cells from hyperglycaemic coculture

In a next step, the impact of the blockade of IL-6-signalling on the gene expression level of EMT markers in PDEC cocultured with M1-polarised macrophages under normo- or hyperglycaemic conditions was analysed.

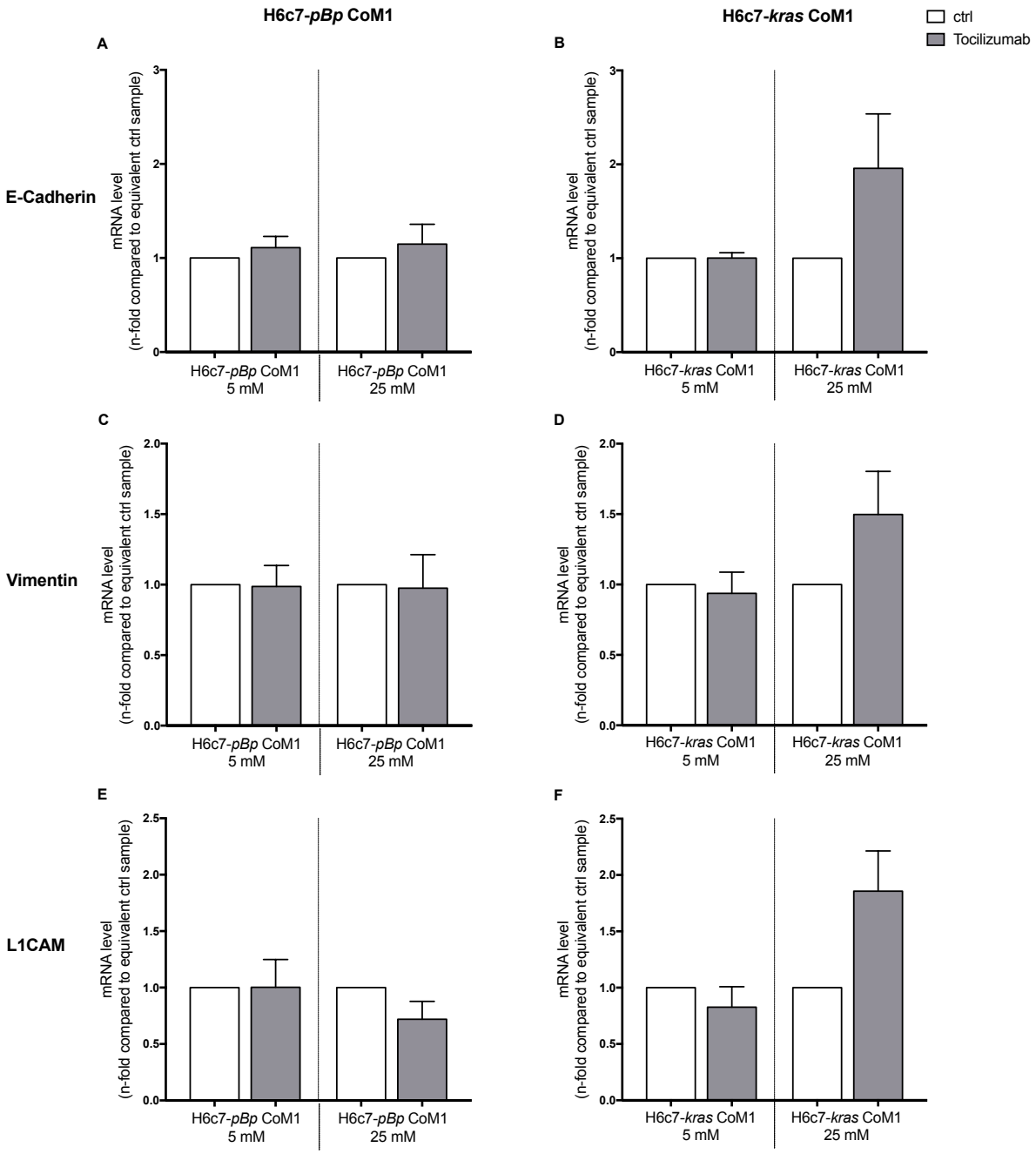

Figure 39: **Blockade of IL-6 signalling via Tocilizumab increases epithelial and mesenchymal markers in cocultured hyperglycaemic H6c7-*kras* cells**. H6c7-*pBp* or H6c7-*kras* cells were cocultured with M1-polarised macrophages (MΦ) for 5 days in normo- or hyperglycaemic settings (5 or 25 mM of glucose) and treated with 1 µg/ml of Tocilizumab or Rituximab (ctrl). The epithelial cells were separated from direct coculture via CD11b-MACS depletion of M1-MΦ and used for qPCR analysis. The relative gene expression levels of E-Cadherin (A and B), Vimentin (C and D) and L1CAM (E and F) of both cell lines are depicted, normalised to the housekeeping gene GAPDH and presented as n-fold expression compared to the equivalent ctrl sample. Normally distributed data are presented as mean and standard error of mean, unpaired t-test was performed for statistical analysis. n=4

Similar to the effects of Tocilizumab treatment on the expression of EMT-associated mediators and transcription factors of H6c7-*pBp* cells, gene expression levels of the EMT markers E-Cadherin and Vimentin were also not influenced by blockade of IL-6 signalling (**Figure 39** A and C). Only L1CAM levels were slightly diminished in H6c7-*pBp* cells arising from hyperglycaemic coculture treated with Tocilizumab (**Figure 39** E) (reduction of 28% compared to the equivalent control).

Interestingly, Tocilizumab treatment evoked an increase in both epithelial and mesenchymal markers in premalignant H6c7-*kras* cells under hyperglycaemic coculture. E-Cadherin levels showed a 1.96 -fold elevation compared to the control (**Figure 39** B); Vimentin a 1.5-fold (**Figure 39** D) and L1CAM a 1.86-fold elevation (**Figure 39** F).

4.4.1.1.4 Tocilizumab slightly increases the expression of stemness markers in PDEC

Finally, the impact of Tocilizumab treatment on the expression level of the stemness indicators Nestin and Nanog were evaluated in PDEC arising from normo- or hyperglycaemic coculture with M1-polarised macrophages.

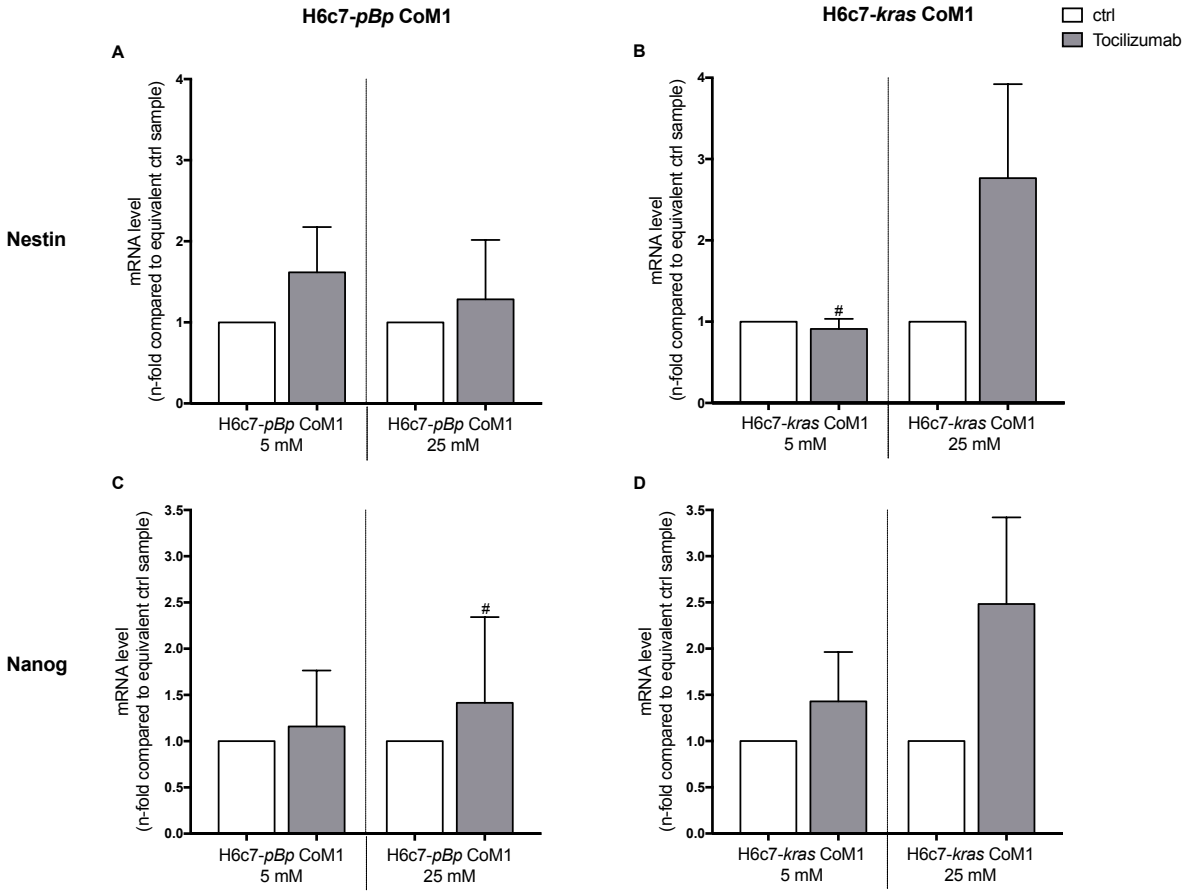

Figure 40: Blockade of IL-6 signalling via Tocilizumab slightly increases the expression of CSC-marker in PDEC. H6c7-*pBp* or H6c7-*kras* cells were cocultured with M1-polarised macrophages (MΦ) for 5 days in normo- or hyperglycaemic settings (5 or 25 mM of glucose) and treated with 1 µg/ml of Tocilizumab or Rituximab (ctrl). The epithelial cells were separated from direct coculture via CD11b-MACS depletion of M1-MΦ and used for qPCR analysis. The relative gene expression levels of Nestin (A and B) and Nanog (C and D) of both cell lines are depicted, normalised to the housekeeping gene GAPDH and presented as n-fold expression compared to the equivalent ctrl sample. Normally distributed data are presented as mean and standard error of mean, unpaired t-test was performed for statistical analysis. Not normally distributed data (indicated via (#)) are shown as median and interquartile range. Wilcoxon Signed Rank Test was used for statistical analysis. n=7

Nestin showed a 1.62-fold elevation in H6c7-*pBp* cells from normoglycaemic coculture treated with Tocilizumab, whereas H6c7-*pBp* cells from hyperglycaemic coculture were not impacted (**Figure 40** A). Moreover, gene expression levels of Nanog in the benign PDEC were not influenced by Tocilizumab at all (**Figure 40** C).

In the premalignant H6c7-*kras* cells, Nestin levels were not influenced by Tocilizumab in normoglycaemic coculture settings, whereas Nanog levels were slightly increased (1.43-fold elevation compared to normoglycaemic control). In hyperglycaemic coculture settings, on the other hand, the premalignant cells showed enhanced levels of both Nestin (2.77-fold) and Nanog (2.48-fold) upon Tocilizumab treatment (**Figure 40** B and D).

Altogether, these data indicate that while benign H6c7-*pBp* cells were hardly affected by Tocilizumab, Tocilizumab predominantly influences H6c7-*kras* cells when exposed to hyperglycaemic coculture with M1-polarised macrophages. In these cells, Tocilizumab treatment increases the expression of EMT- and CSC-inducing mediators and transcription factors along with the expression of epithelial, mesenchymal and stemness markers. Interestingly, these effects were not to be observed in H6c7-*kras* cells cultivated under normoglycaemic inflammatory settings.

4.4.1.2 Impact of Tocilizumab on the colony formation ability of cocultured PDEC

Tocilizumab's impact on the stemness ability of PDEC from normo-and hyperglycaemic coculture with M1-polarised macrophages was additionally analysed via colony formation assays. For this, the quantity and quality of colonies formed by PDEC treated with either Tocilizumab or with the control antibody under the respective conditions were investigated.

H6c7-*pBp* cells arising from normoglycaemic settings showed a 1.22-fold increase in the total number of colonies formed when treated with Tocilizumab compared to cells treated with the control antibody (**Figure 41** A). H6c7-*pBp* cells from hyperglycaemic coculture, on the other hand, formed similar quantities of colonies irrespective of the antibody treatment. The fact that cells exposed to high glucose levels beforehand showed a decline in the total number of colonies compared to cells cultured in normoglycaemic settings (data not shown) is in line with the findings mentioned in section 4.2.3 (**Figure 30**).

Normoglycaemic premalignant PDEC treated with Tocilizumab showed a marginal reduction of colonies formed compared to the equivalent cells treated with the control antibody (0.94-fold). However, hyperglycaemic H6c7-*kras* cells showed a 1.73-fold increase in the quantity of colonies formed upon blockade of IL-6-signalling via Tocilizumab (**Figure 41** B).

Interestingly, Tocilizumab had a more pronounced impact on the type of colonies formed by the benign than by the premalignant PDEC. In normoglycaemic H6c7-*pBp* cells treated with Tocilizumab, a 1.5-fold increase in the percentage of holoclones was observed (**Figure 41** C). This occurred at the expense of meroclones, which showed a 0.88-fold decrease, whereas the proportion of paraclones remained stable. In hyperglycaemic H6c7-*pBp* cells, Tocilizumab predominantly led to a larger amount of paraclones (1.51-fold increase compared to the control samples), whereas the percentage of holo- and meroclones was unchanged.

In the premalignant PDEC Tocilizumab treatment in normoglycaemic setting evoked almost no alterations in the composition of the colonies formed (**Figure 41** D), while a slight increase in holoclones and no alterations in para- and meroclones could be observed in hyperglycaemic conditions.

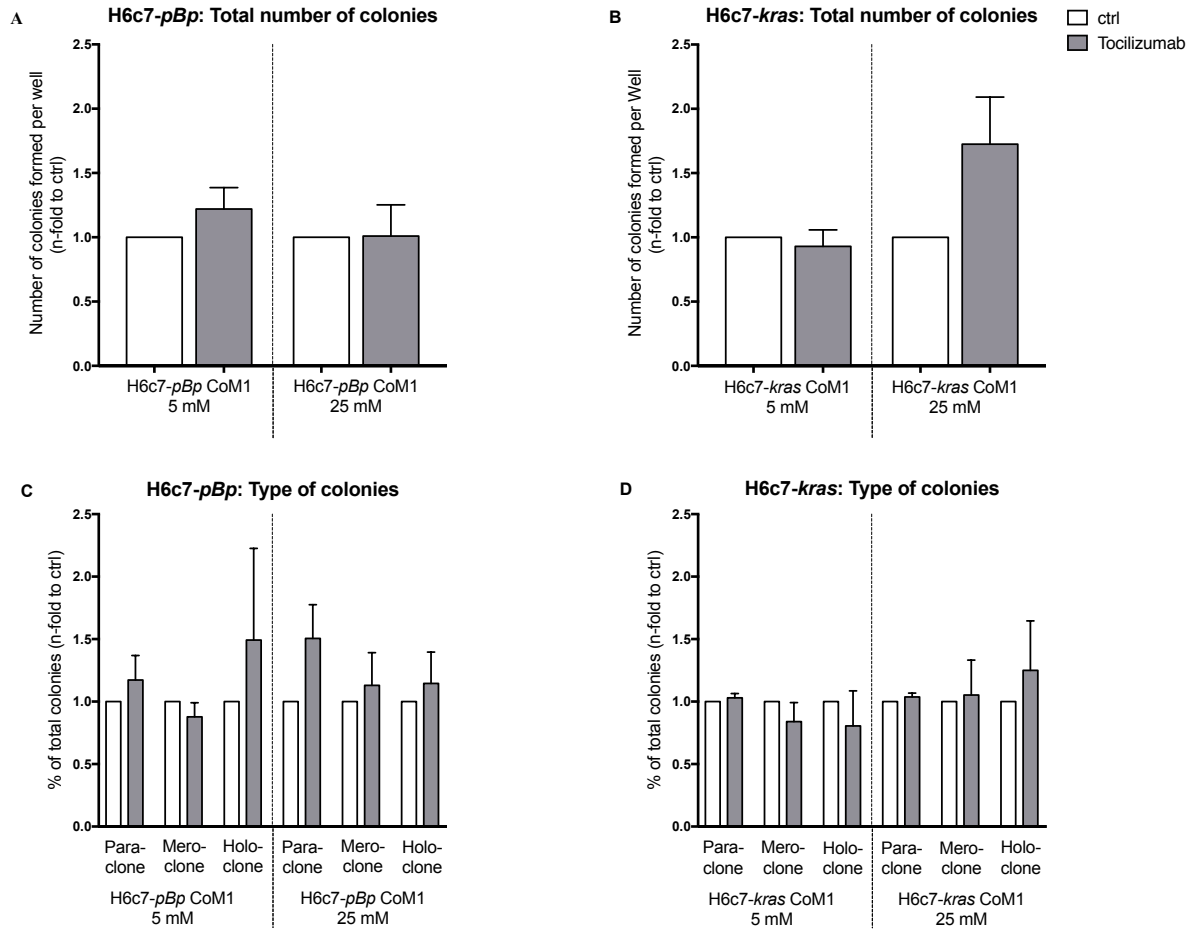

Figure 41: Impact of Tocilizumab on the colony formation ability of PDEC arising from normo- or hyperglycaemic coculture with M1-polarised macrophages (MΦ). H6c7-*pBp* and H6c7-*kras* cells were cocultured with M1-polarised MΦ for 5 days in normo- or hyperglycaemic settings (5 or 25 mM of glucose) and treated with 1 µg/ml Tocilizumab or Rituximab (ctrl). The epithelial cells were separated from direct coculture with macrophages via CD11b-MACS depletion of M1-MΦ and used for colony formation assays. For this, 800 cells/well were seeded in duplicates and cultivated for 8 to 14 days. After fixation and staining, colonies of more than 50 cells were analysed. The total number of colonies per well (A and B) and the quality of colonies (C and D) formed under the differing treatments are shown. Data are depicted as n-fold compared to the equivalent ctrl sample. Normally distributed data are presented as mean and standard error of mean, unpaired t-test was performed for statistical analysis. n=6

To sum up, Tocilizumab treatment especially impacted on H6c7-*pBp* cells from normoglycaemic coculture and on H6c7-*kras* cells from hyperglycaemic coculture. In these conditions, Tocilizumab led to an increase in the total number of colonies and to an increase in the percentage of holoclones.

4.4.1.3 Blockade of IL-6 signalling via Tocilizumab reduces the migratory potential of H6c7-kras cells arising from hyperglycaemic coculture with M1-polarised macrophages

To visualise possible changes in the migratory potential of PDEC through the blockade of IL-6 signalling, a scratch assay was performed in PDEC treated with either Tocilizumab or Rituximab and cocultured with M1-polarised macrophages under normo- or hyperglycaemic conditions.

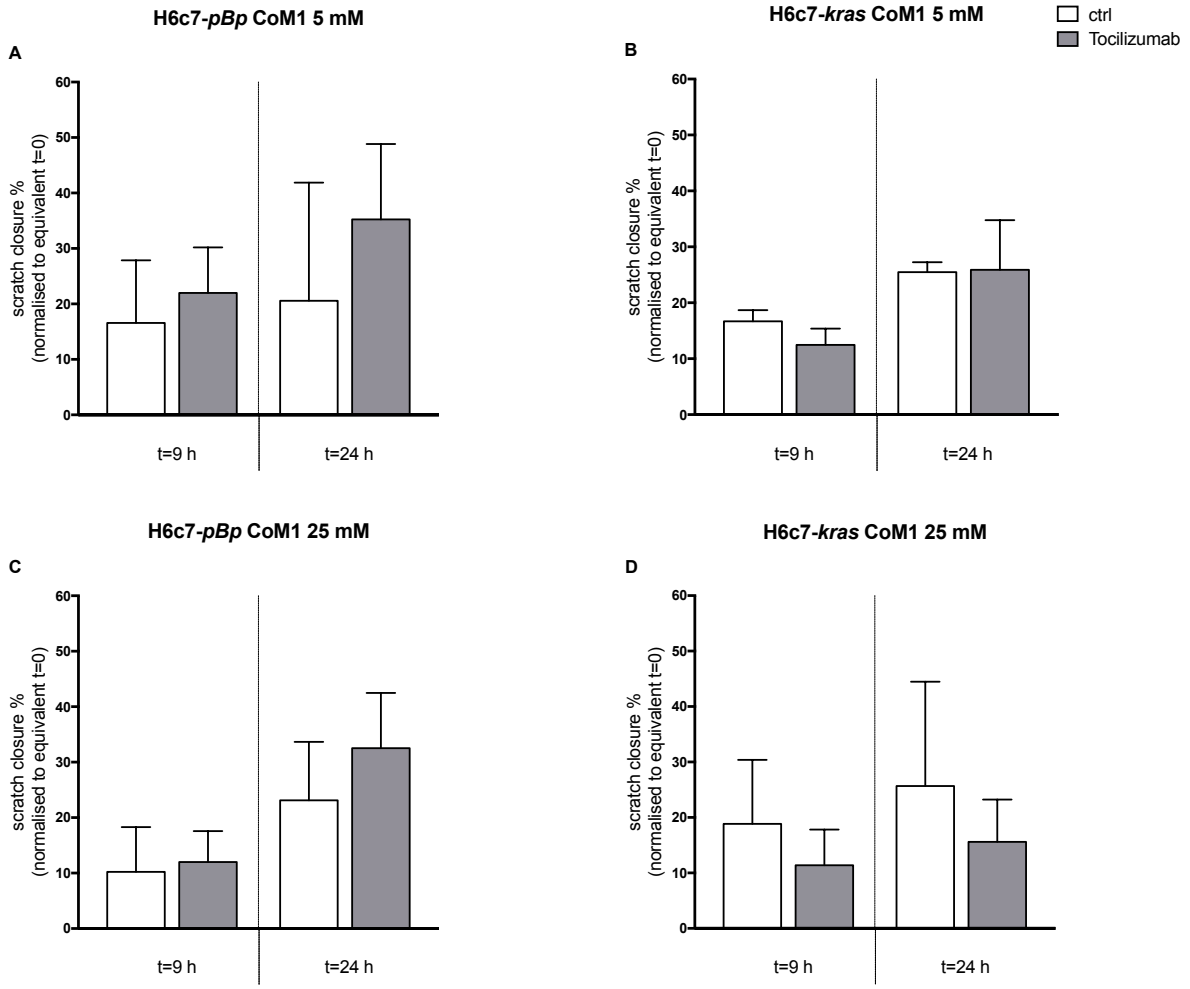

Figure 42: Blockade of IL-6 signalling via Tocilizumab reduces the migratory potential of H6c7-*kras* cells arising from hyperglycaemic coculture with M1-polarised macrophages (MΦ). H6c7-*pBp* and H6c7-*kras* cells were cocultured with M1-polarised MΦ for 5 days in normo- or hyperglycaemic settings (5 or 25 mM of glucose) and treated with Tocilizumab or Rituximab (ctrl). The migratory potential of PDEC was then evaluated via scratch assay using the Lionheart FX Automated Microscope. Scratch closure was assessed at t=0, t=9h and t=24h for normo- and hyperglycaemic H6c7-*pBp* CoM1 (A and C) and H6c7-*kras* CoM1 (B and D). The percentage of closure was evaluated with the Gen5 Data Analysis Software Normally distributed data are presented as mean and standard error of mean; unpaired t-test was performed for statistical analysis. n=4

In H6c7-*pBp* cells, the blockade of IL-6 signalling led to an increase in their migratory potential irrespective of the glucose conditions. 24 hours after the scratch was performed, 35.24% of the scratch were closed by the benign PDEC arising from normoglycaemic coculture treated with Tocilizumab, whereas only 20.55% were closed by the equivalent cells treated with the control antibody (**Figure 42** A). In hyperglycaemic coculture conditions, 32.53% of the scratch were closed after 24 hours by benign PDEC treated with Tocilizumab but only 23.13% by the equivalent control (**Figure 42** C).

Tocilizumab treatment only marginally influenced the migratory potential of H6c7-*kras* cells from normoglycaemic coculture (**Figure 42** B). After 9 hours the scratch closure was slightly less pronounced in cells treated with Tocilizumab compared to the equivalent control (12.48% and 16.68% of closure compared to t=0, respectively). After 24 hours, however, the scratch was closed to roughly 25%, irrespective of the antibody treatment. Together, these findings show that Tocilizumab leads to a slower migration of H6c7-*kras* cells in normoglycaemic coculture conditions but does not impact on the overall migratory potential.
In hyperglycaemic coculture conditions, on the other hand, Tocilizumab treatment led to a reduced closure of the scratch at both evaluated timepoints, indicating a reduction of migratory potential (**Figure 42** D). 15.61% of the scratch were closed by H6c7-*kras* treated with Tocilizumab and cocultured with M1-polarised macrophages in hyperglycaemic conditions, whereas the equivalent control showed a scratch closure of 25.68% after 24 hours.

4.4.2 Blockade of IL-6 trans-signalling via sgp130Fc

4.4.2.1 Impact of IL-6 blockade by gp130Fc on the gene expression levels of EMT- and CSC-associated genes in cocultured PDEC

After having evaluated the impact of the blockade of both IL-6 signalling pathways, changes on the gene expression level of EMT- and stemness-associated genes in PDEC were now investigated after the exclusive blockade of IL-6 trans-signalling. For this, H6c7-*pBp* and H6c7-*kras* cells were treated with either sgp130Fc or ctrlFc and cocultured with M1-polarised macrophages in normo- or hyperglycaemic conditions for 5 days. The epithelial cells were then separated from direct coculture via CD11b-MACS depletion of macrophages and used for qRT-PCR analysis. Cells arising from the equivalent coculture setting treated with ctrlFc served as a control.

4.4.2.1.1 sgp130Fc increases expression levels of EMT- and CSC-inducing mediators in PDEC

Both benign and premalignant PDEC were similarly impacted in their gene expression levels of IL-6, IL-8, TGF-β1 and TNF-α through the blockade of IL-6 trans-signalling via gp130Fc.
IL-6 levels were clearly elevated in H6c7-*pBp* cells arising von normoglycaemic coculture blocked via sgp130Fc (6.88-fold elevation compared to the control sample) (**Figure 43** A). This effect also occurred but was less explicit in H6c7-*pBp* cells from hyperglycaemic coculture (2.4-fold increase compared to the control sample). In H6c7-*kras* cells, blockade of IL-6 trans-signalling also showed elevated IL-6 expression levels irrespective of the glucose level (**Figure 43** B). However, the increase was not as pronounced as in the H6c7-*pBp* cells.
Similarly, gene expression level of IL-8 was clearly elevated in H6c7-*pBp* cells upon treatment with sgp130Fc and this elevation seemed to be independent of the glucose level (2.36- and 2.65-fold elevation compared to the equivalent control) (**Figure 43** C). In H6c7-*kras* cells, the blockade of IL-6 trans-signalling led to similar results, but again, the elevation in gene expression level was less pronounced than in their benign counterpart (**Figure 43** D).

Gene expression levels of TNF-α were only influenced in PDEC arising from hyperglycaemic coculture settings: a 1.65-fold elevation in benign and a 1.63-fold in premalignant PDEC compared to the equivalent control was to be observed here upon blockade via gp130Fc (**Figure 43** E and F).

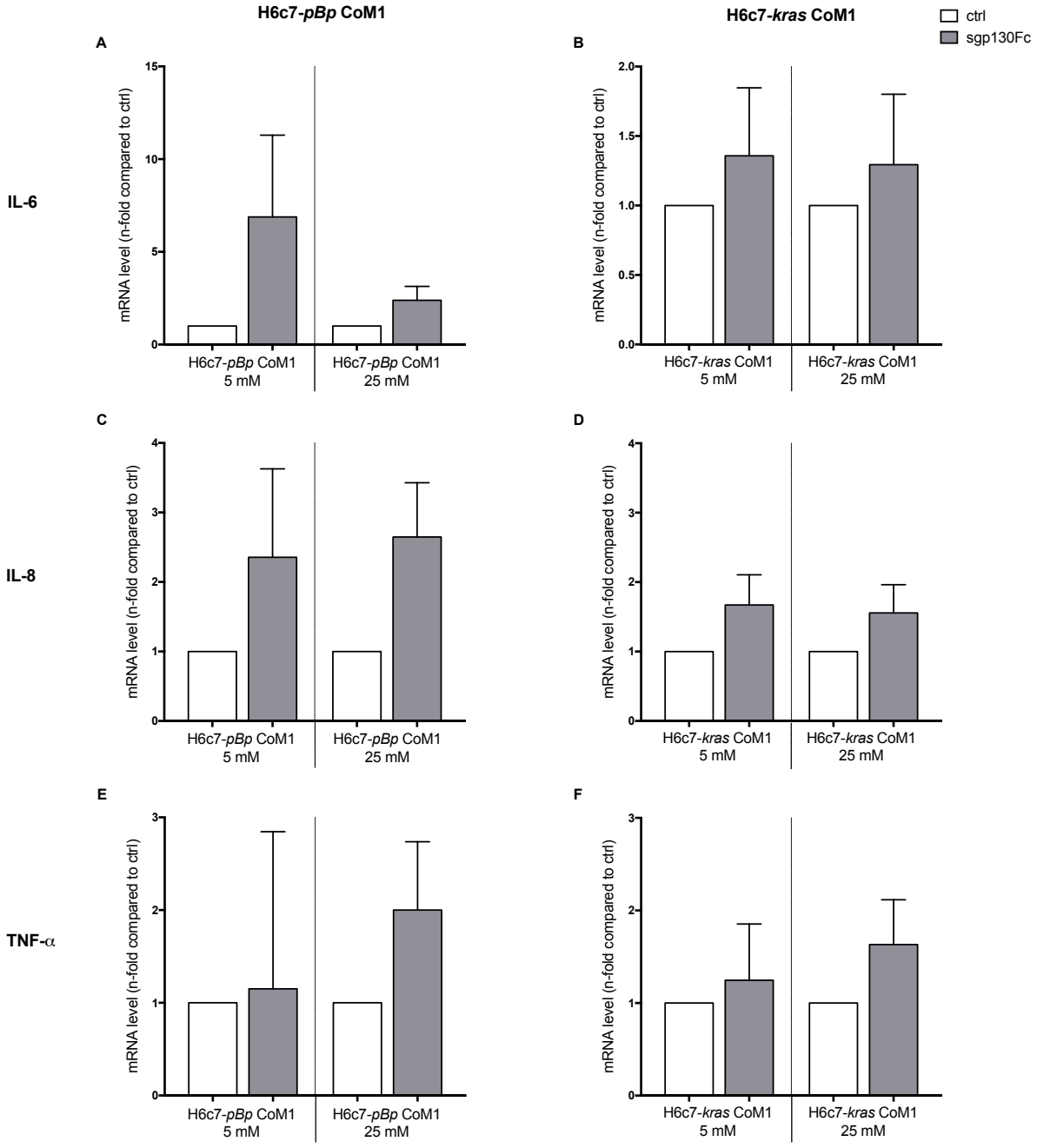

Figure 43: Blockade of IL-6 trans-signalling via sgp130Fc promotes the expression of EMT- and CSC-inducing mediators in PDEC. (to be continued on next page)

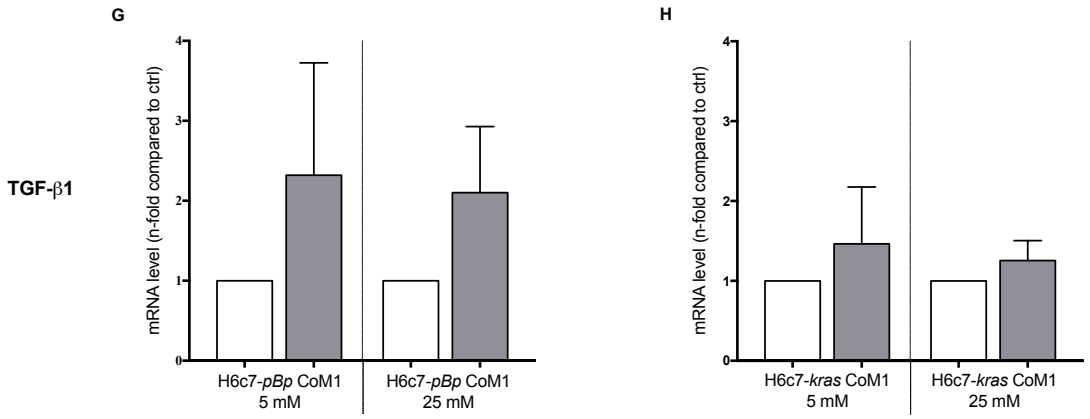

Figure 43: Blockade of IL-6 trans-signalling via sgp130Fc promotes the expression of EMT- and CSC-inducing mediators in PDEC. (continued) H6c7-pBp or H6c7-kras cells were cocultured with M1-polarised macrophages (MΦ) for 5 days in normo- or hyperglycaemic settings (5 or 25 mM of glucose) and treated with 10 µg/ml of sgp130Fc or ctrlFc (ctrl). The epithelial cells were separated from direct coculture via CD11b-MACS depletion of M1-MΦ and used for qPCR analysis. The relative gene expression levels of IL-6 (A and B), IL-8 (C and D), TNF-α (E and F) and TGF-β1 (G and H) of both cell lines are depicted, normalised to the housekeeping gene GAPDH and presented as n-fold expression compared to the equivalent ctrl sample. Normally distributed data are presented as mean and standard error of mean, unpaired t-test was performed for statistical analysis. n=4

The blockade of IL-6 trans-signalling also led to an elevation of mRNA levels of TGF-β1 in the benign PDEC, irrespective of the glucose levels (2.32- and 2.11-fold increase compared to the equivalent control sample in normo- and hyperglycaemic conditions, respectively) (**Figure 43** G).

Interestingly, TGF-β1 mRNA levels were hardly influenced by blockade of trans-signalling in H6c7-kras cells (**Figure 43** H).

4.4.2.1.2 sgp130Fc increases the expression of EMT- and CSC-inducing transcription factors in PDEC

In H6c7-*pBp* cells, the EMT- and CSC-inducing transcription factors Snail, Slug and Zeb1 were all elevated through blockade of trans-signalling (**Figure 44** A, C and E).

A 3.01-fold increase in mRNA levels of Snail could be observed in the benign PDEC from normoglycaemic coculture upon treatment with sgp130Fc; cells arising from hyperglycaemic coculture showed a 1.92-fold elevation compared to the equivalent control (**Figure 44** A). Gene expression levels of Slug were more pronounced in cells from hyperglycaemic coculture, reaching a 1.83-fold increase compared to the equivalent control (**Figure 44** C). The effect of treatment with sgp130Fc on Zeb1 expression was glucose independent in the benign PDEC: a 2.83-fold and 2.69-fold increase was to be observed in normo- and hyperglycaemic coculture settings, respectively, compared to the control (**Figure 44** E).

In H6c7-*kras* cells, on the other hand, sgp130Fc treatment primarily showed effects in normoglycaemic coculture settings. A 1.77-, 1.26- and 1.55-fold increase was to be observed for mRNA levels of Snail, Slug and Zeb1 respectively (**Figure 44** B, D and F), whereas no changes could be stated upon treatment with sgp130Fc in cells arising from hyperglycaemic coculture settings. Once again, this stands in contrast to the effects observed upon treatment with Tocilizumab where Zeb1 mRNA levels had been significantly elevated in H6c7-*kras* cells arising from hyperglycaemic coculture (**Figure 38** F).

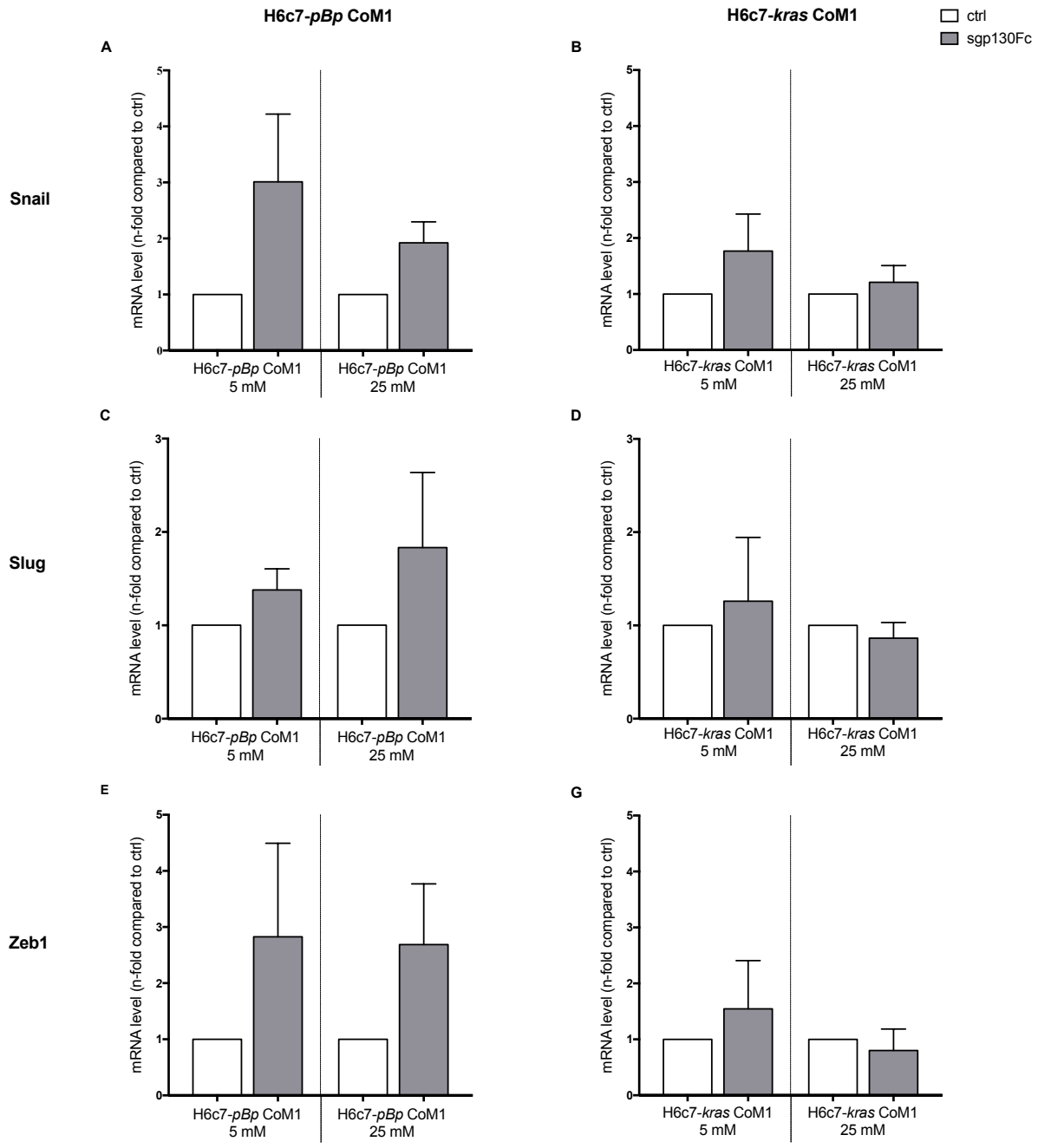

Figure 44: Blockade of IL-6-trans-signalling via sgp130Fc promotes the expression of Snail, Slug and Zeb1 in PDEC. H6c7-*pBp* or H6c7-*kras* cells were cocultured with M1-polarised macrophages (MΦ) for 5 days in normo- or hyperglycaemic settings (5 or 25 mM of glucose) and treated with 10 µg/ml of sgp130Fc or ctrlFc (ctrl). The epithelial cells were separated from direct coculture via CD11b-MACS depletion of M1-MΦ and used for qPCR analysis. The relative gene expression levels of Snail (A and B), Slug (C and D) and Zeb1 (E and F) of both cell lines are depicted, normalised to the housekeeping gene GAPDH and presented as n-fold expression compared to the equivalent ctrl sample. Normally distributed data are presented as mean and standard error of mean, unpaired t-test was performed for statistical analysis. n=4

4.4.2.1.3 Treatment with sgp130Fc increases the expression of both epithelial and mesenchymal markers in PDEC

Whereas the treatment with Tocilizumab had not influenced the gene expression level of epithelial or mesenchymal markers in the benign PDEC, treatment with sgp130Fc led to elevated mRNA levels of E-Cadherin (**Figure 45** A), Vimentin (**Figure 45** C) and L1CAM (**Figure 45** E). Except for L1CAM, this elevation was irrespective of the glucose levels at which the cells were cocultured. Interestingly, treatment with sgp130Fc did not show any impact at all on the gene expression level of L1CAM of benign PDEC in hyperglycaemic conditions, whereas a 2.87-fold increase was to be observed in normoglycaemic conditions. In the premalignant PDEC, treatment with sgp130Fc also led to increased gene expression levels of E-Cadherin (**Figure 45** B). However, this effect was less pronounced than in the benign PDEC, and more pronounced in the normoglycaemic than in the hyperglycaemic setting.

Intriguingly, the mRNA level of the mesenchymal marker Vimentin was reduced by 50% in H6c7-*kras* cells arising from normoglycaemic conditions treated with sgp130Fc, while no effect was observed upon sgp130Fc treatment of cells from hyperglycaemic coculture (**Figure 45** D).

L1CAM gene expression levels were elevated through the blockade of IL-6 trans-signalling in H6c7-kras cells arising from normo- (2.08-fold) and hyperglycaemic (2.79-fold) coculture (**Figure 45** F).

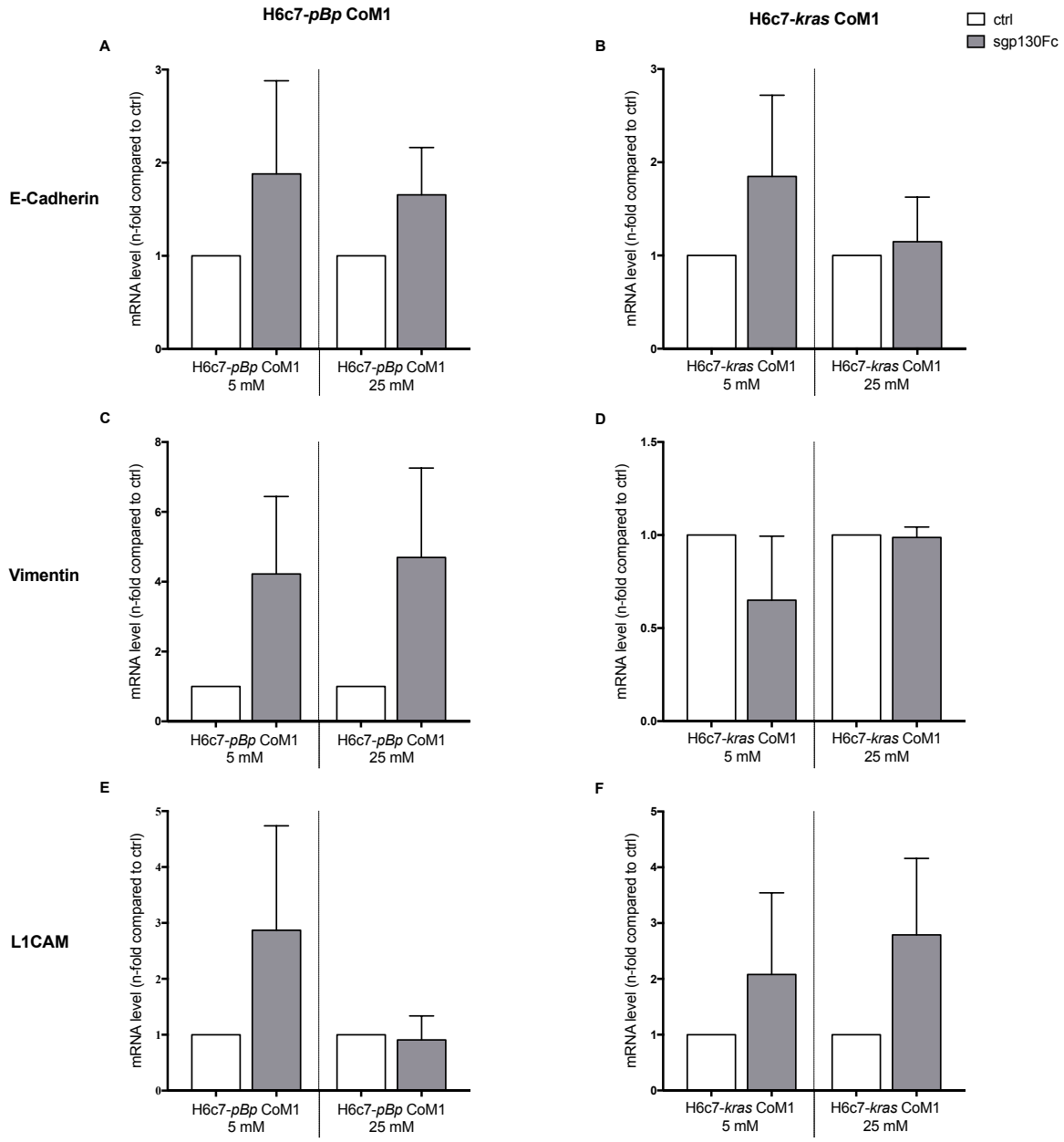

Figure 45: Blockade of IL-6 trans-signalling via sgp130Fc promotes the expression of epithelial and mesenchymal markers in PDEC. H6c7-*pBp* or H6c7-*kras* cells were cocultured with M1-polarised macrophages (MΦ) for 5 days in normo- or hyperglycaemic settings (5 or 25 mM of glucose) and treated with 10 µg/ml of sgp130Fc or ctrlFc (ctrl). The epithelial cells were separated from direct coculture via CD11b-MACS depletion of M1-MΦ and used for qPCR analysis. The relative gene expression levels of E-Cadherin (A and B), Vimentin (C and E) and L1CAM (E and F) of both cell lines are depicted, normalised to the housekeeping gene GAPDH and presented as n-fold expression compared to the equivalent ctrl sample. Normally distributed data are presented as mean and standard error of mean, unpaired t-test was performed for statistical analysis. n=4

4.4.2.1.4 Treatment with sgp130Fc impacts heterogeneously on gene expression levels of CSC markers in PDEC

The blockade of IL-6 trans-signalling led to a significant increase in gene expression levels of Nestin in H6c7-*pBp* cells arising from hyperglycaemic coculture (4.90-fold increase compared to the control) (**Figure 46** A). Interestingly, H6c7-*pBp* cells arising from normoglycaemic coculture were not impacted at all by treatment with sgp130Fc, whereas the treatment with Tocilizumab had caused an elevation of mRNA

levels of Nestin irrespective of the glucose level. In H6c7-*kras* cells, on the other hand, sgp130Fc treatment led to increased Nestin expression levels irrespective of the glucose level in coculture settings (**Figure 46** B). While Tocilizumab did not show any impact on the gene expression level of Nanog in the benign PDEC, sgp130Fc led to an 8.03-fold increase in cells arising from normoglycaemic and to a 2.80-fold increase in cells from hyperglycaemic coculture (**Figure 46** C).

Nanog showed weak tendencies of decrease in H6c7-*kras* cells upon treatment with sgp130Fc irrespective of the glucose level (**Figure 46** D). These results stand in contrast to those obtained by treatment with Tocilizumab: both CSC-markers had been elevated in H6c7-*kras* arising from hyperglycaemic coculture (**Figure 40** B and D).

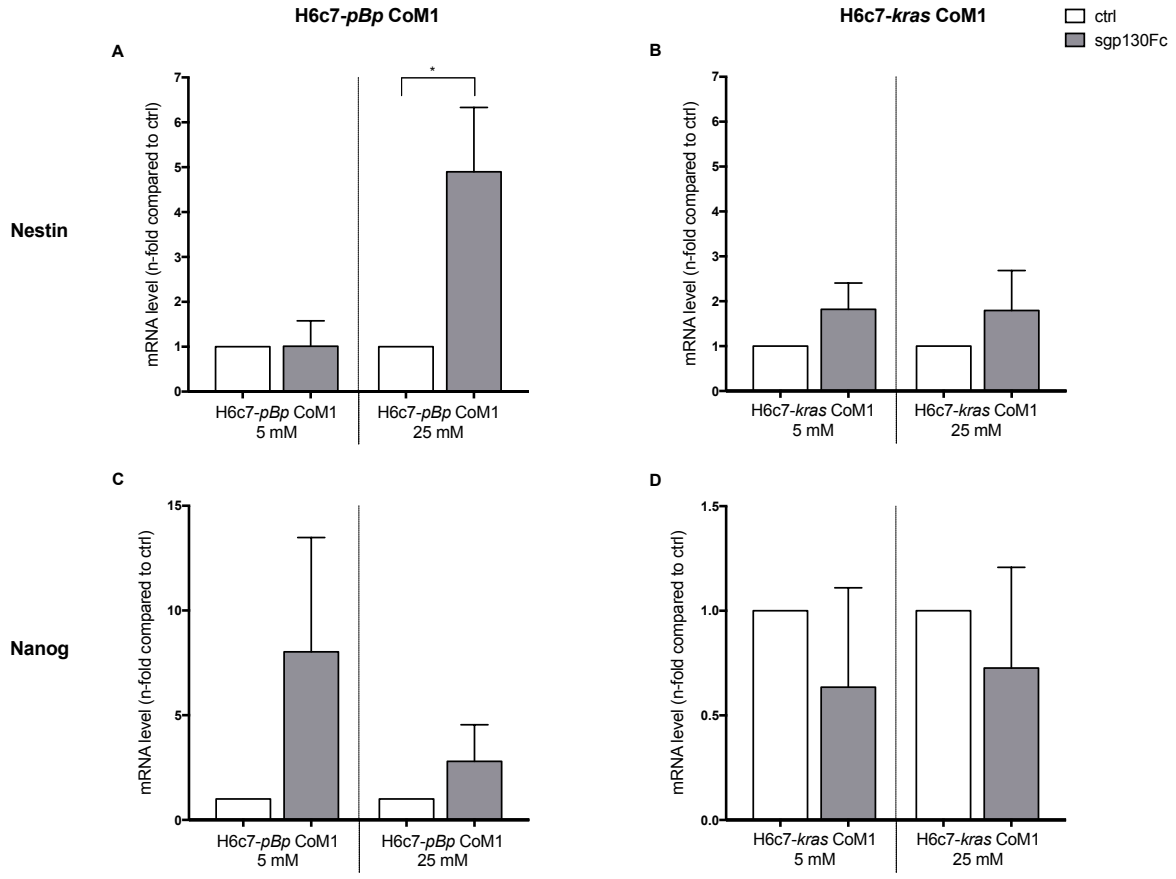

Figure 46: Blockade of IL-6-trans-signalling via gp130Fc promotes gene expression level of Nestin in PDEC. H6c7-*pBp* or H6c7-*kras* cells were cocultured with M1-polarised macrophage (MΦ) for 5 days in normo- or hyperglycaemic settings (5 or 25 mM of glucose) and treated with 10 µg/ml of sgp130Fc or ctrlFc (ctrl). The epithelial cells were separated from direct coculture via CD11b-MACS depletion of M1-MΦ and used for qPCR analysis. The relative gene expression levels of Nestin (A and E) and Nanog (C and F) of both cell lines are depicted, normalised to the housekeeping gene GAPDH and presented as n-fold expression compared to the equivalent ctrl sample. Normally distributed data are presented as mean and standard error of mean, unpaired t-test was performed for statistical analysis. *: 0,05>p>0,0332; n=4

To sum up, sgp130Fc treatment promotes gene expression of EMT- and CSC-inducing mediators and transcription factors, especially IL-8, TGF-β1, Slug and Zeb1. These effects were observed in both cell lines, however, they were more pronounced in benign than in premalignant PDEC. Furthermore, blocking IL-6 trans-signalling led to elevated mRNA level of both epithelial and mesenchymal markers in H6c7-*pBp* cells. In H6c7-*kras* cells, however, the epithelial marker E-Cadherin was also elevated, but the mesenchymal marker Vimentin decreased, suggesting a reversion of EMT.

4.4.2.2 Treatment with sgp130Fc impacts on the colony formation ability of PDEC

Finally, the impact of sgp130Fc on the colony formation ability of PDEC from normo- and hyperglycaemic coculture with M1-polarised macrophages was analysed via colony formation assays. For this, the quantity and quality of colonies formed by PDEC treated with either sgp130Fc or with the controlFc were analysed.

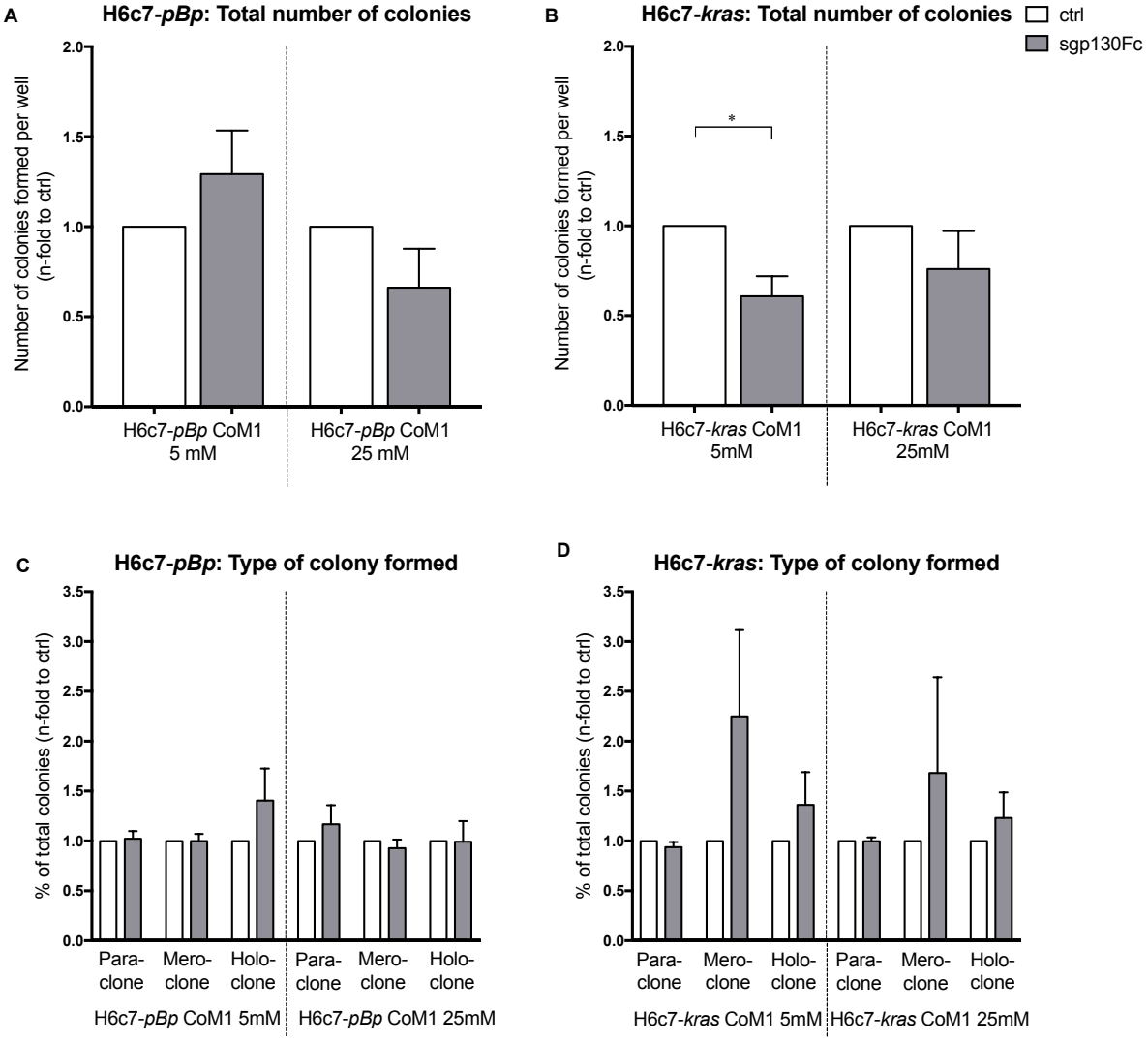

Figure 47: Impact of sgp130Fc on the colony formation ability of PDEC arising from normo- or hyperglycaemic coculture with M1-polarised macrophages (MΦ). H6c7-*pBp* or H6c7-*kras* cells were cocultured with M1-polarised MΦ for 5 days in normo- or hyperglycaemic settings (5 or 25 mM of glucose) and treated with 10 µg/ml of sgp130Fc or ctrlFc (ctrl). The epithelial cells were separated from direct coculture via CD11b-MACS depletion of M1-MΦ and used for colony formation assays. For this, 800 cells/well were seeded in duplicates and cultivated for 8 to 14 days. After fixation and staining, colonies of more than 50 cells were analysed. The total number of colonies per well (A and B) and the quality of colonies (C and D) formed under the differing treatments are shown. Data are depicted as n-fold compared to the equivalent ctrl sample. Normally distributed data are presented as mean and standard error of mean, unpaired t-test was performed for statistical analysis. *: 0,05>p>0,0332; n=6

H6c7-*pBp* cells arising from normoglycaemic settings showed a 1.29-fold increase in the total number of colonies formed upon treatment with sgp130Fc (**Figure 47** A). Cells from hyperglycaemic settings, however, formed less colonies after treatment with sgp130Fc. A 0.66-fold reduction was to be observed compared to the equivalent cells treated with ctrlFc.

Normoglycaemic premalignant PDEC treated with sgp130Fc showed a significant 0.61-fold reduction in the number of colonies formed compared to their control (**Figure 47** B). Hyperglycaemic H6c7-*kras* cells also showed a decrease in colonies formed upon treatment with gp130Fc, but this decrease was less pronounced than under normoglycaemic conditions.

Similar to the effects observed after treatment with Tocilizumab (**Figure 41** C), normoglycaemic H6c7-*pBp* cells treated with sgp130Fc showed a 1.4-fold increase in the percentage of holoclones (**Figure 47** C). In hyperglycaemic H6c7-*pBp* cells, sgp130Fc did almost not alter the percentage of para-, mero- or holoclones.

In the premalignant PDEC, on the other hand, sgp130Fc treatment in normoglycaemic setting evoked an increase of meroclones (2.25-fold elevation compared to the control) and a slight increase in holoclones (1.36-fold increase compared to the control) (**Figure 47** D). In hyperglycaemic settings, the effect of sgp130Fc was similar to the normoglycaemic settings, albeit less pronounced (1.61-fold increase in mero-, and 1.23-fold increase in holoclones compared to the equivalent control).

To sum up, colony formation abilities of PDEC were slightly altered by treatment with sgp130Fc. The decrease in the total number of colonies formed by H6c7-*kras* cells upon blockade is to be emphasized, as is the shift towards more meroclones. In H6c7-*pBp* cells arising from normoglycaemic coculture, an increase in holoclones is to note, which is similar to the results observed upon treatment with Tocilizumab.

Altogether, the blockade of IL-6 signalling pathways shows an impact on both EMT- and CSC-properties in PDEC.

Interestingly, the complete blockade of IL-6 signalling via Tocilizumab primarily has an EMT- and CSC-inducing effect in H6c7-*kras* arising from hyperglycaemic culture.

CSC-properties were also impacted in H6c7-*pBp* cells, especially elevated mRNA levels of Nestin and Nanog are to note in this context. Closely linked to this, the elevated capacity of H6c7-*pBp* cells to form holoclones is also important as an indicator for the acquisition of CSC-properties.

The exclusive blockade of trans-signalling via sgp130Fc, on the other hand, predominantly influenced the benign PDEC. A shift towards a more pro-inflammatory, mesenchymal phenotype was to be observed here. However, also the epithelial marker E-Cadherin, whose reduction is known to be the milestone in EMT induction, showed elevated gene expression levels upon treatment with sgp130Fc.

In H6c7-*kras* cells, sgp130Fc also provoked a shift towards a more pro-inflammatory phenotype, however, no gain in mesenchymal markers was to be observed. One may therefore suppose that EMT induction is reduced through the blockade of IL-6 trans-signalling. Furthermore, H6c7-*kras*' colony formation ability is reduced. Together with the finding that sgp130Fc decreases mRNA levels of Nanog in the premalignant PDEC this suggests a loss in CSC-properties.

5 Discussion

PDAC is among the few tumour entities with increasing incidence and mortality. 80 % of all PDAC patients are first diagnosed in late stages of tumourigenesis, leaving palliative treatment as the only option. In the last years, a special focus has been laid on the role of the local microenvironment in progression and initiation of PDAC as it is generally acknowledged that the high extent to which desmoplasia is present in PDAC tissue is characteristic and may be one potential point of attack for screening and treatment methods. In this context, an inflammatory stroma – which represents up to 90% of the entire tumour mass (Erkan et al., 2012) and comprises macrophages as one important immune cell population – and hyperglycaemia seem to play a pivotal role. In line with this, chronic inflammation, obesity and T2DM are considered prominent risk factors contributing to the initiation and progression of PDAC (Calle et al., 2003; Liao et al., 2015).

Infiltration of tumour tissue with macrophages is acknowledged to be associated with poorer prognosis in various tumour entities including PDAC (Bingle et al., 2002; Kurahara et al., 2013). The same also applies to high blood glucose levels: there are many studies showing that T2DM patients are subject to an increased risk to develop one of several cancer entities, e.g. PDAC (Huxley et al., 2005), but also breast cancer (Larsson et al., 2007), endometrium cancer (Friberg et al., 2007), colorectal cancer (Larsson et al., 2005) and others. Furthermore, Wang *et al.* could show that pancreatic tumour cell proliferation is promoted in diabetic mice (Wang et al., 2016).

Therefore, the aim of this study was to assess the interplay of macrophages and PDEC in the context of high glucose levels and to evaluate whether a T2DM-related inflammatory and hyperglycaemic microenvironment further promotes malignancy-associated alterations in PDEC. To assess this question, a direct coculture system was chosen to mimic this inflammatory microenvironment of benign or premalignant PDEC with macrophages under normo- or hyperglycaemic conditions. In a first step, focus was laid on alterations in macrophages themselves; in a second step, the glucose- and inflammation-induced impact on EMT and CSC induction in PDEC was evaluated.

5.1 Impact of hyperglycaemia and PDEC on macrophages

To examine macrophages' potential contribution to PDAC initiation, a direct coculture system of macrophages and PDEC was chosen, mimicking an obesity and T2DM-associated microenvironment. First findings of our group suggested that elevated TNF-α levels expressed by macrophages upon exposure to high glucose levels may influence EMT progression within PDAC development (Plundrich, 2017). This interplay between macrophages and PDEC in T2DM-associated hyperglycaemic conditions on macrophages themselves was now to be further elucidated. For this purpose, M1-polarised macrophages were chosen, as Castoldi *et al.* could show that macrophages adopt a pro-inflammatory phenotype in the state of metabolic disorder (Castoldi et al., 2016).

We could show highly elevated expression levels of pro- and anti-inflammatory cytokines and growth factors in macrophages exposed to PDEC and high glucose levels simultaneously. Especially IL-6 levels were highly upregulated, but also IL-8 levels and – in line with previous findings of Plundrich *et al.* – also TNF-α levels were increased. Furthermore, the mRNA levels of VEGF and anti-inflammatory IL-10 were upregulated in

macrophages arising from coculture with benign PDEC (**Figure 14**). Together, these findings highlight the role of macrophages as an important source for abundant cytokine expression in inflammatory tissue in metabolic disorders (Mantovani et al., 2008; Grivennikov et al., 2011) and also underline the plasticity of macrophages: even though macrophages had been polarised towards M1-macrophages according to a well-established protocol, they showed high levels of cytokines linked to both M1- and M2-associated expression profiles after coculture with PDEC and exposure to hyperglycaemia. This, once again, indicates that macrophages cannot clearly be categorised into the one or the other extreme. Rather, the polarisation of macrophages is influenced by their respective microenvironment (Helm et al., 2014a).

When further analysed, it turned out that changes in gene expression levels of these cytokines were mainly due to the presence of PDEC and only to a lesser extent due to the presence of high glucose levels (**Figure 15** and **Figure 16**). Apart from a glucose-dependent elevation of VEGF expression levels in macrophages cocultured with premalignant PDEC, hyperglycaemia alone did not show any relevant effect on the gene expression levels of the other cytokines analysed. This partly stands in contrast to findings of Cheng *et al.*, who could show elevated levels of especially pro-inflammatory cytokines in monocytes upon exposure to high glucose levels (Cheng et al., 2015). One possible explanation for this divergence is that human monocytes were isolated from blood samples and then differentiated to M1-polarised macrophages *in vitro* in the current study, whereas the group of Cheng *et al.* examined gene expression levels in monocytes prior to specific macrophage differentiation. In line with this, Moganti *et al.* could show that high glucose levels induce TNF-α gene expression in monocytes, but that this effect is no longer to be observed once the differentiation from monocytes towards macrophages starts (Moganti et al., 2017). Morey *et al.* also asserted glucose-dependent increases in expression levels of pro-inflammatory cytokines in macrophages (Morey et al., 2019). However, already the differentiation from monocytes to macrophages was performed under hyperglycaemic conditions in their experimental setup, whereas in our study exposure to hyperglycaemia started once macrophages were fully differentiated, attributing a particular importance to the glucose level throughout the differentiation process. Supporting this thesis are findings from Pavlou *et al.:* their experimental set up included macrophages differentiated from both monocytes in normoglycaemic and monocytes in hyperglycaemic conditions. In the latter, macrophages showed elevated gene expression levels of TNF-α and IL-6; gene expression levels of macrophages which had been differentiated under normoglycaemic conditions comparable to our study, however, did not respond to high glucose levels (Pavlou et al., 2018). In this context, it would be of interest to evaluate the cytokine profile of macrophages arising from the pancreata of e.g. diabetic mice, as these are constantly exposed to high glucose levels.

Furthermore, it is important to keep in mind that the human derived monocytes in our study arise from different blood donors. The expression patterns of cells originating from different blood donors were shown to vary largely depending on the marker analysed (Moganti et al., 2017). This helps to explain the wide range of expression levels obtained throughout the five experiments (and blood donors) and points out one limitation of the current study.

Nevertheless, the current results clearly underline the importance of macrophages in the acquisition of malignancy-associated properties in PDAC and with tumour initiation. Soluble mediators of EMT- and CSC-properties were highly elevated in macrophages in the concomitant presence of PDEC and high

glucose; IL-6, IL-10, TNF-α and VEGF are all known to be pro-tumourigenic factors (Mantovani et al., 2006; Solinas et al., 2009; Hermano et al., 2014). Furthermore, an immunosuppressive microenvironment is fostered by amplified secretion of IL-8, IL-10, and regulation of angiogenesis via VEGF (Kleeff et al., 2007; Pandol et al., 2009; Kurahara et al., 2013). Apart from IL-10 levels, all of the above effects were slightly more pronounced in macrophages in coculture with premalignant than with benign PDEC, suggesting a dependency on *kras* mutation. In this context, Lesina *et al.* and Gukovsky *et al.* report of *kras*-dependent self-amplifying signalling cascades (**Figure 3**), which attract macrophages and other immune cells and support their secretion of especially IL-6 and TNF-α, promoting invasiveness of PDEC (Lesina et al., 2011; Gukovsky et al., 2013). Furthermore, several studies promote the idea that a mutation in the oncogene *ras* is crucial for direct cross-talk between epithelial cells and macrophages (Guerra et al., 2011; Liou et al., 2015; Storz, 2015), which could also explain the more pronounced reaction of macrophages towards premalignant PDEC in this study.

Special attention needs to be paid to the highly elevated IL-6 levels in macrophages upon coculture with PDEC (838-fold and 1550-fold elevation in macrophages arising from hyperglycaemic coculture with H6c7-*pBp* and H6c7-*kras* cells, respectively) (**Figure 14**). High serum levels of IL-6 in PDAC patients have been associated with poorer prognosis in several studies (Okada et al., 1998; Scholz et al., 2003; Ebrahimi et al., 2004) and in line with our findings, Lesina *et al.* could identify macrophages as main source of IL-6 in pancreatic tumourigenesis (Lesina et al., 2011). The interplay of IL-6, macrophages and PDEC will be discussed in more detail in chapter 5.5 in the context of the IL-6 blockade experiments.

Altogether, this current study underlines that macrophages show abundant alterations in expression of cytokines known to play a pivotal role in pancreatic tumourigenesis upon interaction with PDEC, which can be further amplified in the presence of glucose. To further elucidate which mediators trigger these alterations, analysis of cytokines and soluble mediators in the equivalent supernatants are planned in future experiments.

5.2 Exposure to hyperglycaemia and/or high glucose levels induces EMT in PDEC

Further experiments investigated the impact of a T2DM-associated microenvironment on PDEC. H6c7-*pBp* and H6c7-*kras* cells were exposed to M1-polarised macrophages and/or hyperglycaemia in a direct coculture system.

Upon coculture in hyperglycaemic conditions, an induction of the mesenchymal markers Vimentin and L1CAM and a loss of the epithelial marker E-Cadherin was visible in both PDEC lines (**Figure 19** (mRNA level) and **Figure 29** (protein level)), indicating an EMT-promotion. Additionally, mRNA levels of the EMT-inducing transcription factors Zeb1, Snail and Slug were increased in H6c7-*kras* and H6c7-*pBp* cells (**Figure 18**). However, some of these EMT-associated alterations were more prominent in the premalignant cells than in their benign counterpart and vice versa; and when further analysed, it turned out that some changes were rather triggered by exposure to high glucose levels, others by exposure to macrophages and for some, synergistic effects of macrophages and hyperglycaemia were to be observed. Previous studies have

revealed that EMT in PDAC is promoted by the presence of macrophages (Helm et al., 2014a) or by exposure to hyperglycaemia (Wang et al., 2016), but there are only few studies analysing the combined effect. However, these phenomena are closely linked since both are crucial mediators of an inflammatory milieu. Last but not least it is known that glucose can also promote a pro-inflammatory phenotype in macrophages as described in chapter 5.1 and thereby reinforces their effect.

Loss in E-Cadherin levels – commonly referred to as the milestone in EMT – was most pronounced in H6c7-*kras* cells exposed to macrophages and hyperglycaemia, underlining a synergistic effect. The transcription factor Snail is known to repress E-Cadherin and other epithelial molecules (Batlle et al., 2000); in line with this, Snail levels showed a stronger increase in the premalignant than in the benign PDEC upon exposure to a T2DM-associated microenvironment. Congruent with our findings, several other studies could show that the expression of Zeb1, Slug and Snail is closely intertwined with the repression of E-Cadherin levels, and enhanced levels thus promote EMT (Peinado et al., 2007; Nieto et al., 2016). That these effects were more pronounced in the premalignant PDEC again implies a dependency on *kras* mutation. Coinciding with this hypothesis, several mice models demonstrated that caerulin-induced pancreatic inflammation leads to tumour progression exclusively in mice harbouring *kras*-mutation (Guerra et al., 2007; Carrière et al., 2009). Daniluk *et al.* suggest the idea of an inflammation-induced positive feedback loop via NF-κB which is strictly dependent on oncogenic *kras* causing an amplification of *kras* levels up to pathological levels, thereby promoting tumourigenesis. The group suggests it as a possible target for therapy via COX-2-inhibtor or inhibition of the inhibitor of NF-κB kinase 2 (Daniluk et al., 2012). As already mentioned in chapter 5.1, Storz *et al.* identified *kras* mutation as a mediator of ICAM-1 upregulation which attracts M1-polarised macrophages and promotes secretion of pro-inflammatory cytokines and proteases leading to tumour progression (Storz, 2015). Altogether, this might explain the pronounced effect in H6c7-*kras* cells in e.g. the loss in E-cadherin levels, where an additional *kras*-dependent direct crosstalk between macrophages and epithelial cells is possible, whereas this additional interaction is missing in the benign H6c7-*pBp* cells.

However, the upregulation of Vimentin and Zeb1 expression was more prominent in H6c7-*pBp* than in H6c7-*kras* cells upon exposure to macrophages and hyperglycaemia. Therefore, other mechanisms by which EMT is promoted by inflammatory processes also seem to be important and need further investigation.

TGF-β1 is referred to as one of the most potent EMT inducers in various cancer entities (Jing et al., 2011). In previous studies, our group could already identify TGF-β1 as a key player in glucose-dependent EMT induction in H6c7-*kras* and Panc1 cells (Rahn et al., 2018). In the current study, a predominantly glucose-dependent increase in TGF-β1 level in both PDEC lines could be observed (**Figure 21**). This points to the importance of TGF-β1 as a mediator of EMT initiation in a diabetes-associated microenvironment not only in (pre)malignant stages of PDAC but also in benign epithelial cells. The basal expression level of TGF-β1 was higher in H6c7-*kras* than in H6c7-*pBp* cells (data not shown). This is one further possible explanation for the more pronounced EMT induction in the premalignant than in the benign PDEC as several studies could show autocrine amplification of TGF-β1 signalling in epithelial cells thereby encouraging EMT progression (Derynck et al., 2001; Kalluri and Weinberg, 2009; Wu and Derynck, 2009). Furthermore, Oft

et al. point out a direct link between EMT induction via activation of autocrine TGF-β signalling loops and *ras* mutation in a human mammary epithelial cells (Oft et al., 1998). Moreover, elevated TGF-β1 expression through *ERK*-activation in dependency on a mutation in the oncogene *kras* is also reported for some other tumour entities (Tsubaki et al., 2011).

A further important mechanism by which TGF-β1 is linked to EMT in PDAC is described by Geismann *et al.*: upon exposure to myofibroblasts, L1CAM expression is upregulated in a TGF-β-dependent manner in PDEC, leading to a more mesenchymal and motile phenotype (Geismann et al., 2009). In the current study, we could also observe a coculture-dependent increase on the mRNA level of L1CAM in both PDEC lines (**Figure 27**), however, hyperglycaemia decreased gene expression levels in both cell lines (**Figure 23**). This challenges the hypothesis of its TGF-β1-dependency in our study, as TGF-β1 was upregulated in a glucose-dependent manner as described above; and points out the context-dependency of the effects caused by TGF-β1. Similar to our findings, Mrazkova *et al.* observed a reduction in L1CAM levels in cancer cells cultured in hyperglycaemic conditions (which could be reversed by interfering in the glycolytic metabolism) and suggested a link between L1CAM expression and glycolytic energy metabolism of tumour cells (Mrazkova et al., 2018).

Intriguingly, L1CAM was inversely affected on protein compared to mRNA level: coculture and hyperglycaemia synergistically increased L1CAM expression in H6c7-*pBp* cells; in H6c7-*kras* cells a coculture- dependent decrease and glucose-dependent increase were to be observed (**Figure 29**).

IL-8 is also described as an initiator of EMT in various cancer entities and IL-8 serum levels have been shown to be of prognostic value (Millar et al., 2008; Fernando et al., 2011; Chen et al., 2012; Wen et al., 2020). In this study, however, decreased levels of IL-8 were observed in H6c7-*pBp* cells when cocultured with macrophages, whereas no relevant changes at all were to be detected in H6c7-*kras* cells upon exposure to macrophages (**Figure 17**). One possible explanation for the divergence in IL-8 levels in the two cell lines might be found in gene expression levels of TNF-α, as IL-8 and TNF-α levels were shown to be directly correlated in other tumour entities (Ma et al., 2017). In the current study, TNF-α levels were decreased in a coculture-dependent manner in the benign cells, whereas contrary effects were seen in the premalignant cells. Furthermore, macrophages showed highly elevated levels of the anti-inflammatory IL-10 when exposed to the benign, but not the premalignant PDEC (**Figure 16**), which can be considered as one possible mediator of the coculture-dependent loss in in the expression of pro-inflammatory IL-8 and TNF-α in H6c7-*pBp* cells. However, to further support this hypothesis, supernatants should be analysed to verify the contribution of potential mediators to the observed alterations in the expression of EMT markers of PDEC upon exposure to a T2DM-associated microenvironment.

Collectively, the current study reveals that an enhanced inflammatory microenvironment not only leads to induction and promotion of EMT in premalignant PDEC already harbouring a *kras* mutation, but also in benign cells even though to a slightly lesser extent.

5.3 The acquisition of CSC-properties in PDEC is promoted by a T2DM-associated microenvironment

It is uncontroversial that the microenvironment also influences the CSC-properties of tumour cells (Ye et al., 2014; Plaks et al., 2015). In the current study, a gain in stemness-properties in PDEC could be observed upon exposure to a T2DM-typical microenvironment by evaluating expression levels of the CSC markers Nestin and Nanog and by analysis of colony formation.

Nestin is known to be involved in the regulation of cell proliferation and to play a crucial role in tumour growth, invasiveness and migratory potential of pancreatic cancer cells (Matsuda et al., 2011, 2012; Su et al., 2013). In our study, Nestin was highly upregulated through combined hyperglycaemia and coculture in the premalignant H6c7-*kras* cells, but only to a much lesser extent and in an exclusively glucose-dependent manner in the benign H6c7-*pBp* cells (**Figure 20** and **Figure 24**). Matsuda *et al.* were able to link enhanced Nestin levels with EMT progression (Matsuda et al., 2014) which coincides with our findings that H6c7-*kras* cells showed a greater shift towards a more mesenchymal phenotype upon exposure to T2DM-associated microenvironment than H6c7-*pBp* cells.

Intriguingly, Nanog levels were increased in H6c7-*pBp* cells through normoglycaemic, but decreased through hyperglycaemic coculture with macrophages, whereas in H6c7-*kras* cells Nanog expression was decreased upon both exposure to hyperglycaemia and/or macrophages (**Figure 20**). This partly stands in contrast to observations of Yang *et al.* who could identify a TAM-dependent increase in Nanog expression levels in breast cancer cells promoting their tumourigenicity (Yang et al., 2013). Furthermore, knockdown of Nanog and Oct-4 was shown to diminish CSC-properties in pancreatic cancer cells *in vitro* and *in vivo*, attributing to Nanog an important role in the acquisition of CSC-properties such as proliferation, migration, chemoresistance and tumourigenesis in PDAC (Lu et al., 2013). Moreover, there are also studies classifying the increase in Nanog expression levels as an early event in tumourigenesis. Wen *et al.* revealed elevated expression of Nanog and Oct-4 (which are co-expressed as Oct-4 is intertwined in the expression of Nanog) in non-cancerous pancreatic tissue and in precancerous lesions preceding *kras*-mutation (Wen et al., 2010). This is one possible explanation for the differing impact we observed in benign and premalignant PDEC; our findings might therefore attribute a significant role to Nanog in early inflammation-related acquisition of malignancy-associated alterations. However, further analysis is necessary here to fully understand the underlying mechanisms.

The pro-inflammatory cytokine TNF-α has been associated with the acquisition of both EMT- and CSC-characteristics in various tumour entities, including PDAC (Egberts et al., 2008; Storci et al., 2010; C. Li et al., 2012; Wang et al., 2013; Zhang et al., 2014). In the current study, TNF-α expression levels were highly elevated in a coculture-dependent manner in H6c7-*kras* cells, whereas they were decreased in the benign cells (**Figure 25**). In macrophages exposed to PDEC, TNF-α levels were also strongly elevated (**Figure 16**) – in a slightly more pronounced manner in macrophages arising from coculture with H6c7-*kras* cells implying a *kras*-dependency. Bates *et al.* suggest a link between macrophages' TNF-α expression and a thereby induced autocrine TNF-α production of epithelial cells which is dependent on *ERK*-activation (Bates and Mercurio, 2003). This could explain the higher gene expression level of TNF-α in premalignant

than in benign PDEC and further corroborates our findings of a complex crosstalk between macrophages and epithelial cells promoting and self-amplifying a favourable inflammatory microenvironment for the acquisition of EMT- and CSC-associated properties in PDEC. Storci *et al.* were able to link the acquisition of an aggressive stem cell like phenotype in breast cancer cells to the activation of EMT-associated transcription factor Slug via signalling cascades of TNF-α and its downstream target NF-κB (Storci et al., 2010). In our study, p-p65, the activated subunit of NF-κB, was clearly enhanced on protein level in both PDEC lines upon exposure to macrophages (**Figure 29**), with the basal expression level being substantially higher in the premalignant than in the benign PDEC. It is known that NF-κB can be activated in several ways, amongst others by pro-inflammatory cytokines secreted by TAMs or cancer cells themselves, or through oncogenic activation of *kras*. This explains the higher expression level of p-p65 in monocultured H6c7-*kras* cells compared to H6c7-*pBp* cells and leads to the assumption that the coculture-dependent induction in these cells is associated with the TNF-α elevation detected on mRNA level, which can in turn contribute to an autocrine activation of NF-κB (Gukovsky et al., 2013) and induce stemness features in the epithelial cells. In H6c7-*pBp* cells, however, other mechanisms seem to be responsible for the observed acquisition of CSC-properties, as TNF-α levels were contrarily influenced to NF-κB levels upon exposure to macrophages and hyperglycaemia.

Diabetic culture conditions were shown to promote proliferation and invasiveness of pancreatic cancer cells via elevated TNF-α and NF-κB levels (Wang et al., 2016). Inhibition of this signalling cascade decreased tumour size and ameliorated survival rates in diabetic mice bearing pancreatic tumours. In our study, however, glucose alone only marginally impacted on the gene expression level of TNF-α (**Figure 21**), they were predominantly influenced by the presence of macrophages (**Figure 25**).

Moreover, enhanced stemness features could be shown in PDEC upon exposure to glucose in colony formation assays. We refrained from evaluating the impact of coculture, as preliminary experiments had shown that the magnetic cell separation counterfeits an increased gain in CSC-associated properties (data not shown). However, hyperglycaemia led to a shift towards more mero- and holoclones at the expense of paraclones in both H6c7-*pBp* and H6c7-*kras* cells (**Figure 30**). Whereas the glucose-induced acquisition of CSC-associated properties was more pronounced in monocultured benign PDEC than in cocultured ones, the premalignant PDEC are similarly impacted under both cultivation conditions. This effect was congruent with the glucose-dependent increase of Nestin on mRNA level of PDEC, suggesting a direct link here. This is supported by a previous study of our group, in which a knockdown of Nestin in Panc1-Holoclones did not only decrease the total number of colonies formed but also induced a loss in the proportion of holoclones and a gain in mero- and paraclones (Knaack, 2018).

Together these findings again point to the importance of an enhanced inflammatory microenvironment and elevated glucose levels in the acquisition of malignancy-associated alterations with special regard to stemness features.

However, the experimental setting deserves some discussion. Even though the chosen direct-coculture system allows direct interaction between the respective cell populations, it evidently has some limitations. For one, it has to be kept in mind, that H6c7-*pBp* and H6c7-*kras* cells chosen as an *in vitro* model for benign

and premalignant PDEC were both retrovirally transduced. The possibility cannot be excluded that this causes genomic alterations not to be found *in vivo*. Finally, the chosen experimental setup cannot sufficiently represent the complexity of *in vivo* conditions as other cellular populations are not present in the culture system but *in vivo*. It serves as a simplified model of an inflammatory milieu in precursor lesions of PDAC. It is therefore necessary to transfer this into an *in vivo*, e.g. mouse model.

5.4 Impairment of TGF-β1 signalling partly abrogates the induction of hyperglycaemia and macrophage mediated EMT- and CSC-characteristics in PDEC

Further experiments analysed whether enhanced TGF-β1-expression contributed to the glucose- and coculture-dependent acquisition of malignancy-associated properties of PDEC. TGF-β1 is described as a mediator of PDAC promotion (Otsuru et al., 2019) and impaired TGF-β1 signalling was already shown to inhibit EMT in skin and colorectal cancer (Han et al., 2005; Pino et al., 2011). Indeed, the glucose- and macrophage-mediated acquisition of EMT- and CSC-properties was lost after knockdown of TGF-βRII in H6c7-*pBp* cells. This was demonstrated through reduction in gene expression levels of TNF-α and IL-6 (**Figure 31**), a gain in E-Cadherin and loss of Vimentin levels (**Figure 33**) and a decreased proportion of holoclones in CFAs (**Figure 35**). Furthermore, previous experiments of our group had revealed an increase in the migratory potential of PDEC arising from a hyperglycaemic and inflammatory surrounding (Plundrich, 2017), which we could now show to be reduced upon inhibition of TGF-β1-signalling (**Figure 36**).

In the premalignant cells, TGF-βRII knockdown also reversed some of the alterations that had been observed upon exposure to a T2DM-associated microenvironment. However, EMT was only partially reversed, as E-Cadherin levels were elevated, but so were Vimentin levels. Nevertheless, the migratory capacity was reduced, suggesting TGF-β as one potential contributor to the acquisition of malignancy-associated alterations in premalignant PDEC as well. Unexpectedly, Nestin expression was elevated upon TGF-βRII knockdown (**Figure 34**), which partly stands in contrast to previous findings of our group which revealed a decrease in Nestin levels when TGF-β signalling was impaired (Rahn et al., 2018). However, cells had only been monocultured in the previous study, suggesting that in the current study the presence of macrophages promotes the expression of stemness features by activating alternative signalling pathways. One possible mediator of this is TNF-α, which showed elevated gene expression levels upon knockdown of TGF-βRII in normoglycaemic conditions (**Figure 31**). In line with this, Slug levels were elevated and also the proportion of holoclones formed was higher (**Figure 32** and **Figure 35**). In hyperglycaemic conditions, on the other hand, all these markers showed reduced expression levels upon knockdown of TGF-βRII, pointing to a loss in CSC-properties.

Whereas the efficiency and stability of the TGF-βRII knockdown was verified to guarantee a stable gene suppression throughout the duration of the experiments, it still remains to analyse whether down-stream signalling is also effectively blocked.

In summary, we could show that TGF-β1 is at least partly responsible for the alterations in EMT- and CSC-properties in PDEC in a hyperglycaemic and inflammatory milieu. Especially in benign cells knockdown of TGF-βRII could undermine the acquisition of malignancy-associated features. In the presence of the oncogene *kras*, the cells seem to be able to activate alternative pathways to keep up at least some EMT- and CSC-characteristics. Further experiments, e.g. analysis of gene expression in macrophages after blockade of TGF-β signalling and assessment of secreted cytokines in the supernatants of all culture settings, are necessary to fully understand the underlying mechanisms. Nevertheless, these first experiments suggest TGF-β1 to be closely intertwined in the complex crosstalk between macrophages, hyperglycaemia and PDEC promoting acquisition of malignancy-associated alterations of the latter.

5.5 Induction of EMT- and CSC-characteristics in premalignant PDEC can partially be attributed to IL-6 trans-signalling

IL-6 is a pro-inflammatory cytokine known to be elevated in T2DM-patients and it is even attributed a prognostic value concerning the risk of T2DM onset (Spranger et al., 2003; Kristiansen and Mandrup-Poulsen, 2005). Similarly, elevated IL-6 serum levels were shown to be associated with a poorer prognosis in various cancer entities (Ebrahimi et al., 2004; Gao et al., 2007; Storci et al., 2010). As IL-6 gene expression was strongly modulated in macrophages upon exposure to PDEC and glucose, IL-6 signalling was blocked to determine whether this cytokine is a mediator of the EMT- and CSC-associated alterations in PDEC.

The complete blockade of IL-6 signalling via Tocilizumab (classic and trans-signalling impaired) predominantly induced EMT- and CSC-characteristics in H6c7-*kras* cells arising from hyperglycaemic conditions. Besides elevated levels of IL-8, TGF-β1 and IL-6 (**Figure 37**), the mesenchymal markers Vimentin and L1CAM were increased. However, the epithelial E-Cadherin was also upregulated, and the migratory capacity reduced upon Tocilizumab treatment, implying a partial EMT reversion. The acquisition of stemness features was reflected by elevated expression levels of Zeb1, Nestin and Nanog (**Figure 38** and **Figure 40**), as well as by an increase in the share in holoclones (**Figure 41**).

H6c7-*pBp* cells were hardly impacted through Tocilizumab treatment; only slight induction tendencies of CSC-features mirrored by an increase in Nestin expression level and, in line with this, an increase in holoclones were to be noted (**Figure 40**). Furthermore, the migratory potential of H6c7-*pBp* cells was elevated upon Tocilizumab treatment (**Figure 42**). However, these results need to be regarded with care as scratch assays were performed in cocultured PDEC, and it can thus not completely be guaranteed that migration of exclusively epithelial cells was evaluated and macrophages were not mistaken for epithelial cells. Moreover, cytokeratin stainings, which were performed in cocultured PDEC 24 hours after the scratch (and with this after termination of scratch assay analysis), revealed that the spatial distribution of the equivalent epithelial cells was not as dense as would be ideal for a scratch assay (data not shown), pointing out a further limitation of our current experimental setup.

The impact of Tocilizumab treatment observed on PDEC partly stands in contrast to findings of Wan *et al.* Their group attributed a great importance to elevated TAM-derived IL-6 levels in the context of invasiveness and acquisition of stemness features of hepatocellular carcinoma cell lines. They could show a reversion of these effects *in vitro* and reduced tumour growth in a xenograft mouse model upon Tocilizumab treatment (Wan et al., 2015). However, Wunderlich *et al.* revealed that the complete impairment of IL-6 signalling in hepatocytes can cause systemic inflammation. Levels of TNF-α and other pro-inflammatory cytokines were elevated upon blockade of IL-6 signalling in their study (Wunderlich et al., 2010), which is in line to the results we obtained in the hyperglycaemic premalignant cells (**Figure 37**). There are several other studies attributing IL-6 an important role not only in pro-inflammatory activities but also in the regulation of metabolic homeostasis. Haemostatic activities are attributed to classic signalling, whereas trans-signalling is responsible for the promotion of a pro-inflammatory environment. They show that a simultaneous blockade of classic and trans-signalling predominantly negatively impacts on the metabolic equilibrium (Matthews et al., 2010; Rose-John, 2012; Mauer et al., 2014; Kraakman et al., 2015). These studies are consistent with the shown findings in the premalignant cells treated with Tocilizumab. However, it remains to be elucidated why the benign PDEC are hardly impacted through Tocilizumab. Possibly, IL-6 classic signalling is of lesser importance for haemostatic activities in benign PDEC, thus its blockade is of lesser consequence. Possibly, the interplay of benign PDEC and macrophages counterbalances the Tocilizumab-dependent promotion of inflammation through anti-inflammatory mediators whose effect become more pronounced in the absence of IL-6 (which is not possible anymore in the premalignant cells harbouring a *kras*-mutation). Future experiments will have to further elucidate this issue.

The exclusive blockade of trans-signalling via sgp130Fc, on the other hand, predominantly influenced the benign PDEC. A shift towards a more pro-inflammatory, mesenchymal phenotype was observed. In H6c7-*kras* cells, sgp130Fc also provoked a shift towards a more pro-inflammatory phenotype, however, no gain in mesenchymal markers was to be observed (**Figure 43** and **Figure 45**). In normoglycaemic conditions, blockade of IL-6 trans-signalling even resulted in a reduced EMT induction. Furthermore, H6c7-*kras* cells' colony formation ability and mRNA levels of Nanog were decreased (**Figure 46** and **Figure 47**), suggesting a sgp130Fc-dependent loss in CSC-properties. Consistent with this are findings of Lesina *et al.* who could show that PanIN progression is promoted via IL-6 signalling in a *kras*-dependent manner. The group also demonstrated that IL-6 trans-signalling leads to an activation of STAT3 (whereas classic signalling does not) and that impaired STAT3 signalling stops PanIN progression but not its initiation (Lesina et al., 2011). This might explain why we could observe a loss in EMT- and CSC-characteristics through treatment with sgp130Fc in H6c7-*kras* cells but not in H6c7-*pBp* cells. Similarly, Brooks *et al.* report *kras*-driven lung carcinogenesis to be dependent on IL-6 trans-signalling and reversible through equivalent blockade in both *in vitro* and *in vivo* experiments (Brooks et al., 2016). The group of Grivennikov describes TNF-α levels to be directly linked to IL-6 trans-signalling, as blockade led to reduced, and treatment with Hyper-IL-6 to elevated TNF-α levels in mice bearing colitis-associated cancer (Grivennikov et al., 2009). The group promotes the idea of a cross-regulation between IL-6 and TNF-α which is reliant on trans-signalling pathways and causes enhanced chronic inflammation and tumourigenesis. As TNF-α was not reduced upon blockade of trans-signalling in our current study, the importance of glucose and macrophages, promoting

the expression of pro-inflammatory cytokines also in absence of IL-6 is underlined. Future experiments should therefore also tend to the analysis of gene expression levels in macrophages upon blockade of IL-6 signalling and to the analysis of supernatants from the equivalent coculture conditions to assess the secreted cytokines.

Overall, the results of this study reveal that IL-6 is indeed closely intertwined with the progression of EMT and the acquisition of CSC features in PDEC. Blockade of IL-6 trans-signalling which has been reported to be effective as anti-tumour therapy in other cancer entities (Selander et al., 2004; Grivennikov et al., 2009; Brooks et al., 2016), might be one possible point of attack to undermine malignant progression, although, not to prevent tumour onset in PDAC patients. In very early precancerous stages, it might be of greater importance to target the inflammatory milieu which hyperglycaemia and obesity promote via recruitment of macrophages and self-amplifying pro-inflammatory signalling cascades.

5.6 Outlook

Overall, the current study corroborates the complex interplay of macrophages and hyperglycaemia as an important contributor to the acquisition of malignancy-associated alterations in PDEC. A T2DM- and obesity-associated hyperglycaemic and inflammatory microenvironment promotes a gain in EMT- and CSC-features in PDEC. Partially, these alterations were more evident in the premalignant PDEC already harbouring a *kras* mutation, but benign H6c7-*pBp* cells acquired malignancy-associated properties through the presence of macrophages and/or hyperglycaemia, underlining the relevance of early prevention options. The observed alterations could partially be attributed to TGF-β signalling and partially to IL-6 signalling. Based on these findings, further experiments should be undertaken to reveal whether these cytokines and signalling cascades represent suitable target structures for the prevention of PDAC. Furthermore, the *in vitro* findings should be validated in an *in vivo* study, e.g., a diabetic mouse model, as coculture experiments are only a rough approximation and cannot fully mimic the complex *in vivo* microenvironment. Especially in high-risk patients, such as patients suffering from obesity or T2DM, an anti-inflammatory therapy might be a promising early therapeutic prevention option.

6 Summary

With less than 4 %, pancreatic ductal adenocarcinoma (PDAC) represents a small share in newly detected cancers but is among the few tumour entities with increasing incidence and mortality. By the year of 2030, PDAC is predicted to be the second most lethal neoplasia in western countries. Due to the lack of specific early symptoms, 80% of the patients are diagnosed in late tumour stages, leaving palliative treatment as the only therapeutic option.

Besides chronic inflammation, obesity and type 2 diabetes mellitus (T2DM) - both associated with hyperglycaemia - are risk factors contributing to the initiation and progression of PDAC. However, underlying mechanisms are not yet fully understood. It is known that already precursor lesions are characterised by an inflammatory stroma. Macrophages, representing one of the largest immune cell populations within this stroma, impact on pancreatic ductal epithelial cells (PDEC) by promoting their malignant progression. Previous studies showed that high glucose levels influence the phenotype of macrophages, leading to the question whether these changes in macrophages' phenotype in a T2DM-related inflammatory and hyperglycaemic microenvironment further facilitate malignancy-associated alterations in PDEC. In order to address this question, both, macrophages differentiated from human monocytes and H6c7-*pBp* and H6c7-*kras* cells mimicking benign and premalignant PDEC, were analysed after direct coculture under hyperglycaemia and compared to normoglycemic conditions.

In macrophages, IL-6 levels were most strongly elevated, along with other pro-inflammatory cytokines such as IL-8 and of TNF-α. In PDEC, the pro-inflammatory hyperglycaemic microenvironment enhanced the acquisition of tumourigenesis-associated alterations: Epithelial-Mesenchymal-Transition (EMT) and the acquisition of cancer stemness properties were promoted; and common soluble mediators of these two phenomena were increased in their expression levels as well. Many of these alterations were slightly more pronounced in H6c7-*kras* cells, however, also benign PDEC cells were shown to be driven into malignant progression through the complex interplay of an inflammatory hyperglycaemic surrounding. This underlines the importance of early intervention options in high-risk patients. Blockade of TGF-β signalling partially reversed the above-mentioned changes in PDEC, as did the blockade of IL-6 trans-signalling via sgp130Fc, suggesting a partial involvement of these factors in inflammation and hyperglycaemia driven acquisition of malignancy-associated alterations and pointing to possible therapeutic points of attack.

Overall, the current study corroborates the importance of the interplay of macrophages and hyperglycaemia as a leading contributor to the acquisition of malignancy-associated alterations in PDEC. It gives a new understanding of how metabolic disorders such as T2DM and obesity might initiate and promote PDAC. A better understanding of this is essential to foster ideas for potential early therapeutic intervention in high-risk patients - the current study pointing out an early anti-inflammatory therapy as one promising option in PDAC prevention.

7 References

Al-Hajj, M., Wicha, M., Benito-Hernandez, A., Morrison, S., Clakre, M. (2003): Prospective identification of tumorigenic breast cancer cells. Proc. Natl. Acad. Sci. U. S. A., 100, 3983–3988

Alison, M., Poulsom, R., Forbes, S., Wright, N. (2002): An introduction to stem cells. J. Pathol., 197, 419–423

Aponte, P. M., Caicedo, A. (2017): Stemness in cancer : Stem cells , cancer stem cells , and their microenvironment. Stem Cells Int., 5619472

Atreya, R., Mudter, J., Finotto, S., Müllberg, J., Jostock, T., Wirtz, S., Schütz, M., Bartsch, B., Holtmann, M., Becker, C., Strand, D., Czaja, J., Schlaak, J. F., Lehr, H. A., Autschbach, F., Schürmann, G., Nishimoto, N., Yoshizaki, K., Ito, H., Kishimoto, T., Galle, P. R., Rose-John, S., Neurath, M. F. (2000): Blockade of interleukin 6 trans signaling suppresses T-cell resistance against apoptosis in chronic intestinal inflammation: Evidence in Crohn disease and experimental colitis in vivo. Nat. Med., 6, 583–588

Barkhausen, T., Tschernig, T., Rosenstiel, P., Van Griensven, M., Vonberg, R. P., Dorsch, M., Mueller-Heine, A., Chalaris, A., Scheller, J., Rose-John, S., Seegert, D., Krettek, C., Waetzig, G. H. (2011): Selective blockade of interleukin-6 trans-signaling improves survival in a murine polymicrobial sepsis model. Crit. Care Med., 39, 1407–1413

Basturk, O., Hong, S.-M., Wood, L. D., Adsay, N. V., Albores-Saavedra, J., Biankin, A. V, Brosens, L. A. A., Fukushima, N., Goggins, M., Hruban, R.H., et al. (2015): A revised classification system and recommendations from the baltimore consensus meeting for neoplastic precursor lesions in the pancreas. Am. J. Surg. Pathol., 39, 1730–1741

Bates, R. C., Mercurio, A. M. (2003): Tumor Necrosis Factor-alpha Stimulates the Epithelial-to-Mesenchymal Transition of Human Colonic Organoids. Mol. Biol. Cell, 14, 1790–1800

Batlle, E., Clevers, H. (2017): Cancer stem cells revisited. Nat. Med., 23, 1124–1134

Batlle, E., Sancho, E., Francí, C., Domínguez, D., Monfar, M., Baulida, J., De Herreros, A. G. (2000): The transcription factor Snail is a repressor of E-cadherin gene expression in epithelial tumour cells. Nat. Cell Biol., 2, 84–89

Beaver, C. M., Ahmed, A., Masters, J. R. (2014): Clonogenicity : Holoclones and meroclones contain stem cells. PLoS One, 9, e89834

Becker, A. E., Hernandez, Y. G., Frucht, H., Lucas, A. L. (2014): Pancreatic ductal adenocarcinoma: Risk factors, screening, and early detection. World J. Gastroenterol., 20, 11182–11198

Benz, C., Dondelinger, F., McKean, P. G., Urbaniak, M. D. (2017): Cell cycle synchronisation of Trypanosoma brucei by centrifugal counter-flow elutriation reveals the timing of nuclear and kinetoplast DNA replication. Sci. Rep., 7, 1–10

Bergers, G., Brekken, R., Mcmahon, G., Vu, T. H., Itoh, T., Tamaki, K., Tanzawa, K., Thorpe, P., Itohara, S., Hanahan, D. (2000): Matrix metalloproteinase-9 triggers the angiogenic switch during carcinogenesis. Nat. Cell Biol., 2, 737–744

Bingle, L., Brown, N. J., Lewis, C. E. (2002): The role of tumour-associated macrophages in tumour progression: Implications for new anticancer therapies. J. Pathol., 196, 254–265

Blagih, J., Jones, R. G. (2012): Polarizing macrophages through reprogramming of glucose metabolism. Cell Metab., 15, 793–795

Bonnet, D., Dick, J. E. (1997): Human acute myeloid leukemia is organized as a hierarchy that originates from a primitive hematopoietic cell. Nat. Med., 3, 730–737

Braune, J., Weyer, U., Hobusch, C., Mauer, J., Brüning, J. C., Bechmann, I., Gericke, M. (2017): IL-6 Regulates M2 polarization and local proliferation of adipose tissue macrophages in obesity. J. Immunol.,

Brooks, G. D., McLeod, L., Alhayyani, S., Miller, A., Russell, P. A., Ferlin, W., Rose-John, S., Ruwanpura, S., Jenkins, B. J. (2016): IL6 trans-signaling promotes KRAS-driven lung carcinogenesis. Cancer Res., 76, 866–876

Burk, U., Schubert, J., Wellner, U., Schmalhofer, O., Vincan, E., Spaderna, S., Brabletz, T. (2008): A reciprocal repression between ZEB1 and members of the miR-200 family promotes EMT and invasion in cancer cells. EMBO Rep., 9, 582–589

Calle, E., Rodriguez, C., Walker-Thurmond, K., Thun, M. (2003): Overweight, obesity, and mortality from cancer in a prospectively studied cohort of U.S. adults. N. Engl. J. Med., 348, 1625–1638

Carrière, C., Young, A., Gunn, J., Longnecker, D., Korc, M. (2009): Acute pancreatitis markedly accelerates pancreatic cancer progression in mice expressing oncogenic Kras. Biochem. Biophys. Res. Commun., 382, 561–565

Castoldi, A., De Souza, C. N., Saraiva Câmara, N. O., Moraes-Vieira, P. M. (2016): The macrophage switch in obesity development. Front. Immunol., 6, 1–11

Chang, S. C., Yang, W. C. V. (2016): Hyperglycemia, tumorigenesis, and chronic inflammation. Crit. Rev. Oncol. Hematol., 108, 146–153

Chen, Y., Shi, M., Yu, G. Z., Qin, X. R., Jin, G., Chen, P., Zhu, M. H. (2012): Interleukin-8, a promising predictor for prognosis of pancreatic cancer. World J. Gastroenterol., 18, 1123–1129

Cheng, C. I., Chen, P. H., Lin, Y. C., Kao, Y. H. (2015): High glucose activates Raw264.7 macrophages through RhoA kinase-mediated signaling pathway. Cell Signal, 27, 283–292

Daniluk, J., Liu, Y., Deng, D., Chu, J., Huang, H., Gaiser, S., Cruz-Monserrate, Z., Wang, H., Ji, B., Logsdon, C. D. (2012): An NF-κB pathway–mediated positive feedback loop amplifies Ras activity to pathological levels in mice. J. Clin. Invest., 122, 1519–1528

Daousi, C., Casson, I. F., Gill, G. V., MacFarlane, I. A., Wilding, J. P. H., Pinkney, J. H. (2006): Prevalence of obesity in type 2 diabetes in secondary care: Association with cardiovascular risk factors. Postgr. Med J, 82, 280–284

Dawson, D. W., Hertzer, K., Moro, A., Donald, G., Chang, H., Go, V. L., Pandol, S., Lugea, A., Gukovskaya, A., Li, G., Hines, O., Rozengurt, E., Eibl, G. (2014): High Fat , High Calorie Diet Promotes Early Pancreatic Neoplasia in the Conditional Kras G12D Mouse Model. Cancer Prev. Res., 6, 1064–1063

Derynck, R., Akhurst, R. J., Balmain, A. (2001): TGF-β family signaling in tumor suppression and cancer progression. Nat. Genet., 29, 117–129

Distler, M., Aust, D., Weitz, J., Pilarsky, C., Grützmann, R. (2014): Precursor lesions for sporadic pancreatic cancer: PanIN, IPMN, and MCN. Biomed Res. Int., 2014

Donovan, P. J., Gearhart, J. (2001): The end of the beginning for pluripotent stem cells. Nature, 414, 92–96

Duan, W., Chen, K., Jiang, Z., Chen, X., Sun, L., Li, J., Lei, J., Xu, Q., Ma, J., Li, X., Han, L., Wang, Z., Wu, Z., Wang, F., Wu, E., Ma, Q., Ma, Z. (2017): Desmoplasia suppression by metformin-mediated AMPK activation inhibits pancreatic cancer progression. Cancer Lett., 385, 225–233

Ebrahimi, B., Tucker, S. L., Li, D., Abbruzzese, J. L., Kurzrock, R. (2004): Cytokines in pancreatic carcinoma: Correlation with phenotypic characteristics and prognosis. Cancer, 101, 2727–2736

Egberts, J. H., Cloosters, V., Noack, A., Schniewind, B., Thon, L., Klose, S., Kettler, B., Von Forstner, C., Kneitz, C., Tepel, J., Adam, D., Wajant, H., Kalthoff, H., Trauzold, A. (2008): Anti-tumor necrosis factor therapy inhibits pancreatic tumor growth and metastasis. Cancer Res., 68, 1443–1450

Epelman, S., Lavine, K. J., Randolph, G. J. (2015): Origin and functions of tissue macrophages. Immunity, 41, 21–35

Erkan, M., Hausmann, S., Michalski, C. W., Fingerle, A. A., Dobritz, M., Kleeff, J., Friess, H. (2012): The role of stroma in pancreatic cancer: Diagnostic and therapeutic implications. Nat. Rev. Gastroenterol. Hepatol., 9, 454–467

Erkan, M., Michalski, C. W., Rieder, S., Reiser-Erkan, C., Abiatari, I., Kolb, A., Giese, N. A., Esposito, I., Friess, H., Kleeff, J. (2008): The activated stroma index is a novel and independent prognostic marker in pancreatic ductal adenocarcinoma. Clin. Gastroenterol. Hepatol., 6, 1155–1161

Feng, X. H., Derynck, R. (2005): Specificity and versatility in TGF-β signaling through smads. Annu. Rev. Cell Dev. Biol., 21, 659–693

Fernando, R. I., Castillo, M. D., Litzinger, M., Hamilton, D. H., Palena, C. (2011): IL-8 signaling plays a critical role in the epithelial-mesenchymal transition of human carcinoma cells. Cancer Res., 71, 5296–5306

Ferrone, C. R., Pieretti-Vanmarcke, R., Bloom, J. P., Zheng, H., Szymonifka, J., Wargo, J. A., Thayer, S. P., Lauwers, G. Y., Deshpande, V., Mino-Kenudson, M., Fernández-del Castillo, C., Lillemoe, K. D., Warshaw, A. L. (2013): Pancreatic ductal adenocarcinoma: Long-term survival does not equal cure. Surgery, 152, S43–S49

Fesinmeyer, M. D., Austin, M. A., Li, C. I., De Roos, A. J., Bowen, D. J. (2005): Differences in survival by histologic type of pancreatic cancer. Cancer Epidemiol. Biomarkers Prev., 14, 1766–1773

Franken, N. A. P., Rodermond, H. M., Stap, J., Haveman, J., Van Bree, C. (2006): Clonogenic assay of cells in vitro. Nat. Protoc, 1, 2315–2319

Freemerman, A. J., Johnson, A. R., Sacks, G. N., Milner, J. J., Kirk, E. L., Troester, M. A., Macintyre, A. N., Goraksha-Hicks, P., Rathmell, J. C., Makowski, L. (2014): Metabolic reprogramming of macrophages: Glucose transporter 1 (GLUT1)-mediated glucose metabolism drives a proinflammatory phenotype. J. Biol. Chem., 289, 7884–7896

Friberg, E., Orsini, N., Mantzoros, C. S., Wolk, A. (2007): Diabetes mellitus and risk of endometrial cancer: A meta-analysis. Diabetologia, 50, 1365–1374

Fujisaka, S., Usui, I., Ikutani, M., Aminuddin, A., Takikawa, A., Tsuneyama, K., Mahmood, A., Goda, N., Nagai, Y., Takatsu, K., Tobe, K. (2013): Adipose tissue hypoxia induces inflammatory M1 polarity of macrophages in an HIF-1α-dependent and HIF-1α-independent manner in obese mice. Diabetologia, 56, 1403–1412

Fulawka, L., Donizy, P., Halon, A. (2014): Cancer stem cells - the current status of an old concept: Literature review and clinical approaches. Biol. Res., 47, 2–8

Furukawa, T., Duguid, W. P., Rosenberg, L., Viallet, J., Galloway, D. A., Tsao, M. S. (1996): Long-term culture and immortalization of epithelial cells from normal adult human pancreatic ducts transfected by the E6E7 gene of human papilloma virus 16. Am. J. Pathol., 148, 1763–70

Gaianigo, N., Melisi, D., Carbone, C. (2017): EMT and treatment resistance in pancreatic cancer. Cancers (Basel)., 9, 122

Gao, S. P., Mark, K. G., Leslie, K., Pao, W., Motoi, N., Gerald, W. L., Travis, W. D., Bornmann, W., Veach, D., Clarkson, B., Bromberg, J. F. (2007): Mutations in the EGFR kinase domain mediate STAT3 activation via IL-6 production in human lung adenocarcinomas. J. Clin. Invest., 117, 3846–3856

Geismann, C., Morscheck, M., Koch, D., Bergmann, F., Ungefroren, H., Arlt, A., Tsao, M. S., Bachem, M. G., Altevogt, P., Sipos, B., Fölsch, U. R., Schäfer, H., Müerköster, S. S. (2009): Up-regulation of L1CAM in pancreatic duct cells is transforming growth factor β1- and slug-dependent: Role in malignant transformation of pancreatic cancer. Cancer Res., 69, 4517–4526

Geissmann, F., Manz, M. G., Jung, S., Sieweke, M. H., Ley, K. (2010): Development of monocytes, macrophages and dendritic cells. Science., 327, 656–661

Grivennikov, S. I., Greten, F. R., Karin, M. (2011): Immunity, inflammation, and cancer. Cancer, 140, 883–899

Grivennikov, S., Karin, E., Terzic, J., Mucida, D., Yu, G. Y., Vallabhapurapu, S., Scheller, J., Rose-John, S., Cheroutre, H., Eckmann, L., Karin, M. (2009): IL-6 and STAT3 are required for survival of intestinal epithelial cells and development of colitis associated cancer. Cancer Cell, 15, 103–113

Groot, V. P., Rezaee, N., Wu, W., Cameron, J. L., Fishman, E. K., Hruban, R. H., Weiss, M. J., Zheng, L., Wolfgang, C. L., He, J. (2018): Patterns, timing, and predictors of recurrence following pancreatectomy for pancreatic ductal adenocarcinoma. Ann Surg., 267, 936–945

Guaita, S., Puig, I., Francí, C., Garrido, M., Domínguez, D., Batlle, E., Sancho, E., Dedhar, S., De Herreros, A. G., Baulida, J. (2002): Snail induction of epithelial to mesenchymal transition in tumor cells is accompanied by MUC1 repression and ZEB1 expression. J. Biol. Chem., 277, 39209–39216

Guerra, C., Collado, M., Navas, C., Schuhmacher, A. J., Hernández-Porras, I., Cañamero, M., Rodriguez-Justo, M., Serrano, M., Barbacid, M. (2011): Pancreatitis-induced inflammation contributes to pancreatic cancer by inhibiting oncogene-induced senescence. Cancer Cell, 19, 728–739

Guerra, C., Schuhmacher, A. J., Cañamero, M., Grippo, P. J., Verdaguer, L., Pérez-Gallego, L., Dubus, P., Sandgren, E. P., Barbacid, M. (2007): Chronic Pancreatitis Is Essential for Induction of Pancreatic Ductal Adenocarcinoma by K-Ras Oncogenes in Adult Mice. Cancer Cell, 11, 291–302

Gukovsky, I., Li, N., Todoric, J., Gukovskaya, A., Karin, M. (2013): Inflammation, autophagy, and obesity: Common features in the pathogenesis of pancreatitis and pancreatic cancer. Gastroenterology, 144

Gupta, G. P., Massagué, J. (2006): Cancer metastasis: Building a framework. Cell, 127, 679–695

Haidet, J., Cifarelli, V., Trucco, M., Luppi, P. (2012): C-peptide reduces pro-inflammatory cytokine secretion in LPS-stimulated U937 monocytes in condition of hyperglycemia. Inflamm Res, 61, 27–35

Halfdanarson, T. R., Rubin, J., Farnell, M. B., Clive, S., Petersen, G. M. (2009): Pancreatic endocrine neoplasms: Epidemiology and prognosis of pancreatic endocrine tumours 15, 409–427

Han, G., Lu, S. L., Li, A. G., He, W., Corless, C. L., Kulesz-Martin, M., Wang, X. J. (2005): Distinct mechanisms of TGF-β1-mediated epithelial-to- mesenchymal transition and metastasis during skin carcinogenesis. J. Clin. Invest., 115, 1714–1723

Han, H., von Hoff, D. (2014): SnapShot: Pancreatic cancer. Cancer Cell, 23, 424–424

Han, L., Shi, S., Gong, T., Zhang, Z., Sun, X. (2014): Cancer stem cells: therapeutic implications and perspectives in cancer therapy. Acta Pharm. Sin. B, 3, 65–75

Hanahan, D., Weinberg, R. A. (2011): Hallmarks of cancer: The next generation. Cell, 144, 646–674

Haschemi, A., Kosma, P., Gille, L., Evans, C. R., Burant, C. F., Starkl, P., Knapp, B., Haas, R., Schmid, J. A., Jandl, C., Amir, S., Lubec, G., Park, J., Esterbauer, H., Bilban, M., Brizuela, L., Pospisilik, J. A., Otterbein, L. E., Wagner, O. (2012): The sedoheptulose kinase CARKL directs macrophage polarization through control of glucose metabolism. Cell Metab., 15, 813–826

Hassan, M. M., Bondy, M. L., Wolff, R. A., Abbruzzese, J. L., Vauthey, J.-N., Pisters, P. W., Evans, D. B., Khan, R., Chou, T.-H., Lenzi, R., Jiao, L., Li, D. (2007): Risk factors for pancreatic cancer: case-control study. Am. J. Gastroenterol., 102, 2696–2707

Hayden, M., Ghosh, S. (2004): Signaling to NF-kappaB. Genes Dev., 18, 2195–2224

Helm, O., Held-Feindt, J., Grage-Griebenow, E., Reiling, N., Ungefroren, H., Vogel, I., Krüger, U., Becker, T., Ebsen, M., Röcken, C., Kabelitz, D., Schäfer, H., Sebens, S. (2014a): Tumor-associated macrophages exhibit pro- and anti-inflammatory properties by which they impact on pancreatic tumorigenesis. Int. J. Cancer, 135, 843–861

Helm, O., Held-Feindt, J., Schäfer, H., Sebens, S. (2014b): M1 and M2: There is no "good" and "bad"-How macrophages promote malignancy-associated features in tumorigenesis. Oncoimmunology, 3, 6–8

Hermann, P. C., Huber, S. L., Herrler, T., Aicher, A., Ellwart, J. W., Guba, M., Bruns, C. J., Heeschen, C. (2007): Distinct populations of cancer stem cells determine tumor growth and metastatic activity in human pancreatic cancer. Cell Stem Cell, 1, 313–323

Hermano, E., Meirovitz, A., Meir, K., Nussbaum, G., Appelbaum, L., Peretz, T., Elkin, M. (2014): Macrophage polarization in pancreatic carcinoma: Role of heparanase enzyme. J. Natl. Cancer Inst., 106

Herreros-Villanueva, M., Bujanda, L., Billadeau, D. D., Zhang, J. S. (2014): Embryonic stem cell factors and pancreatic cancer. World J. Gastroenterol., 20, 2247–2254

Hezel, A., Kimmelman, A., Stanger, B., N., B., DePinho, R. (2006): Genetics and biology of pancreatic ductal adenocarcinoma. Genes Dev., 20, 1218–1249

Hruban, R. H., Goggins, M., Parsons, J., Kern, S. E. (2000): Progression model for pancreatic cancer. Clin. Cancer Res., 6, 2969–2972

Hruban, R. H., Maitra, A., Goggins, M. (2008): Update on pancreatic intraepithelial neoplasia. Int. J. Clin. Exp. Pathol., 1, 306–16

Huxley, R., Ansary-Moghaddam, A., Berrington De González, A., Barzi, F., Woodward, M. (2005): Type-II diabetes and pancreatic cancer: A meta-analysis of 36 studies. Br. J. Cancer, 92, 2076–2083

Iacobuzio-Donahue, C. A. (2012): Pancreatic cancer genome sequencing project. Gut, 61, 1085–1094

Ino, Y., Yamazaki-Itoh, R., Shimada, K., Iwasaki, M., Kosuge, T., Kanai, Y., Hiraoka, N. (2013): Immune cell infiltration as an indicator of the immune microenvironment of pancreatic cancer. Br J Cancer, 108, 914–923

Jakowlew, S. B. (2006): Transforming growth factor-β in cancer and metastasis. Cancer Metastasis Rev., 25, 435–457

Jing, Y., Han, Z., Zhang, S., Liu, Y., Wei, L. (2011): Epithelial-Mesenchymal Transition in tumor microenvironment. Cell Biosci., 1

Johnson, A. R., Milner, J. J., Makowski, L. (2012): The inflammation highway: metabolism accelerates inflammatory traffic in obesity. Immunol. Rev., 249, 218–238

Jones, S., Zhang, X., Parsons, D. W., Lin, J. C., Leary, R. J., Angenendt, P., Mankoo, P., Carter, H., Jimeno, A., Hong, S., Fu, B., Lin, M., Eric, S., Kamiyama, M., Walter, K., Nikolskaya, T., Nikolsky, Y., Hartigan, J., Smith, D. R., Hidalgo, M., Leach, S. D., Alison, P., Jaffee, E. M., Goggins, M., Maitra, A., Iacobuzio-, C., Eshleman, J. R., Kern, S. E., Hruban, R. H., Papadopoulos, N., Parmigiani, G., Vogelstein, B., Victor, E., Kinzler, K. W. (2008): Core signaling pathways in human pancreatic cancers revealed by global genomic analyses. Science., 321, 1801–1806

Kaatsch, P., Spix, C. (2019): Krebs in Deutschland für 2015 / 2016. Robert Koch Inst.,

Kaatsch, P., Spix, C., Katalinic, A., Hentschel, S., Luttmann, S., Stegmaier, C., Waldeyer-Sauerland, M., Waldmann, A., Caspritz, S., Christ, M., Ernst, A., Folkerts, J., Hansmann, J., Klein, S., Kranzhöfer, K., Kunz, B., Manegold, K., Penzkofer, A., Treml, K., Weg-Remers, S., Wittenberg, K., Barnes, B., Bertz, J., Buttmann-Schweiger, N., Dahm, S., Fiebig, J., Haberland, J., Kraywinkel, K., Wienecke, A., Wolf, U. (2017): Krebs in Deutschland für 2013/2014

Kalluri, R., Weinberg, R. A. (2009): The basics of epithelial-mesenchymal transition. J. Clin. Invest., 119, 1420–1428

Kanda, M., Matthaei, H., Wu, J., Hong, S., Yu, J., Borges, M., Hruban, R., Maitra, A., Kinzler, K., Vogelstein, B., Goggins, M. (2012): Presence of somatic mutations in most early-stage pancreatic intraepithelial neoplasia. Gastroenterology, 142, 730–733

Kaneda, M. M., Cappello, P., Nguyen, A. V., Ralainirina, N., Hardamon, R., Foubert, P. (2016a): Macrophage PI3Kγ drives pancreatic ductal adenocarcinoma progression. Cancer Discov., 6, 870–885

Kaneda, M. M., Messer, K. S., Ralainirina, N., Li, H., Leem, C. J., Gorjestani, S., Woo, G., Nguyen, A. V., Figueiredo, C. C., Foubert, P., Schmid, M. C., Pink, M., Winkler, D. G., Rausch, M., Palombella, V. J., Kutok, J., McGovern, K., Frazer, K. A., Wu, X., Karin, M., Sasik, R., Cohen, E. E. W., Varner, J. A. (2016b): PI3Kγ 3 is a molecular switch that controls immune suppression. Nature, 539, 437–442

Karin, M. (2006): Nuclear factor-κB in cancer development and progression. Nature, 441, 431–436

Kisfalvi, K., Moro, A., Sinnett-Smith, J., Eibl, G., Rozengurt, E. (2013): Metformin inhibits the growth of human pancreatic cancer xenografts. Pancreas, 42, 781–785

Kleeff, J., Beckhove, P., Esposito, I., Herzig, S., Huber, P. E., Löhr, J. M., Friess, H. (2007): Pancreatic cancer microenvironment. Int. J. Cancer, 121, 699–705

Knaack, H. (2018): Metastasierung des Pankreaskarzinoms : Einfluss der hepatischen Mikroumgebung auf Stammzelleigenschaften und Differenzierung von Pankreasgangepithelzellen. Diss., Kiel

Koorstra, J.-B. M., Feldmann, G., Habbe, N., Maitra, A. (2008): Morphogenesis of pancreatic cancer: role of pancreatic intraepithelial neoplasia (PanINs). Langenbeck's Arch. Surg., 393, 561–570

Korc, M. (2010): Driver mutations: A roadmap for getting close and personal in pancreatic cancer. Cancer Biol. Ther. Ther, 10, 588–591

Korpal, M., Lee, E. S., Hu, G., Kang, Y. (2008): The miR-200 family inhibits epithelial-mesenchymal transition and cancer cell migration by direct targeting of E-cadherin transcriptional repressors ZEB1 and ZEB2. J. Biol. Chem., 283, 14910–14914

Kraakman, M. J., Kammoun, H. L., Allen, T. L., Deswaerte, V., Henstridge, D. C., Estevez, E., Matthews, V. B., Neill, B., White, D. A., Murphy, A. J., Peijs, L., Yang, C., Risis, S., Bruce, C. R., Du, X. J., Bobik, A., Lee-Young, R. S., Kingwell, B. A., Vasanthakumar, A., Shi, W., Kallies, A., Lancaster, G. I., Rose-John, S., Febbraio, M. A. (2015): Blocking IL-6 trans-signaling prevents high-fat diet-induced adipose tissue macrophage recruitment but does not improve insulin resistance. Cell Metab., 21, 403–416

Krieg, A., Riemer, J. C., Telan, L. A., Gabbert, H. E., Knoefel, W. T. (2015): CXCR4-a prognostic and clinicopathological biomarker for pancreatic ductal adenocarcinoma: A meta-analysis. PLoS One, 10, 1–17

Kristiansen, O., Mandrup-Poulsen, T. (2005): Interleukin-6 and diabetes - The good, the bad,or the indifferent? Diabetes, 54, S114–S124

Kurahara, H., Shinchi, H., Mataki, Y., Maemura, K., Noma, H., Kubo, F., Sakoda, M., Ueno, S., Natsugoe, S., Takao, S. (2011): Significance of M2-polarized tumor-associated macrophage in pancreatic cancer. J. Surg. Res., 167, e211–e219

Kurahara, H., Takao, S., Maemura, K., Mataki, Y., Kuwahata, T., Maeda, K., Sakoda, M., Iino, S., Ishigami, S., Ueno, S., Shinchi, H., Natsugoe, S. (2013): M2-Polarized tumor-associated macrophage infiltration of regional lymph nodes is associated with nodal lymphangiogenesis and occult nodal involvement in pn0 pancreatic cancer. Pancreas, 42, 155–159

Lanza-Jacoby, S., Yan, G., Radice, G., LePhong, C., Baliff, J., Hess, R. (2013): Calorie restriction delays the progression of lesions to pancreatic cancer in the LSL-KrasG12D; Pdx-1/Cre mouse model of pancreatic cancer. Exp. Biol. Med., 238, 787–797

Larsson, S. C., Mantzoros, C. S., Wolk, A. (2007): Diabetes mellitus and risk of breast cancer: A meta-analysis. Int. J. Cancer, 121, 856–862

Larsson, S. C., Orsini, N., Wolk, A. (2005): Diabetes mellitus and risk of colorectal cancer: A meta-analysis. J. Natl. Cancer Inst., 97, 1679–1687

Leibovich-Rivkin, T., Liubomirski, Y., Bernstein, B., Meshel, T., Ben-Baruch, A. (2013): Inflammatory factors of the tumor microenvironment induce plasticity in nontransformed breast epithelial cells:

EMT, invasion, and collapse of normally organized breast textures. Neoplasia an Int. J. Oncol. Res., 15, 1330–1346

Lenk, L. (2017): Metastasis of Pancreatic Cancer: Influence of the hepatic microenvironment on the growth behavior of pancreatic ductal epithelial cells Diss., Kiel

Lesina, M., Kurkowski, M. U., Ludes, K., Rose-John, S., Treiber, M., Klöppel, G., Yoshimura, A., Reindl, W., Sipos, B., Akira, S., Schmid, R. M., Algül, H. (2011): Stat3/Socs3 activation by IL-6 transsignaling promotes progression of pancreatic intraepithelial neoplasia and development of pancreatic cancer. Cancer Cell, 19, 456–469

Li, C., Heidt, D. G., Dalerba, P., Burant, C. F., Zhang, L., Adsay, V., Wicha, M., Clarke, M. F., Simeone, D. M. (2007): Identification of pancreatic cancer stem cells. Cancer Res., 67, 1030–1038

Li, C., Xia, W., Huo, L., Lim, S.-O., Wu, Y., Hsu, J., Chao, H., Yamaguchi, H., Yang, N., Ding, Q., Wang, Y., Hortobagyi, G., Hung, M. (2012): Epithelial-mesenchyme transition induced by TNF-α requires NF-κB-mediated transcriptional upregulation of Twist1. Cancer Res., 72, 1290–1300

Li, D. (2012): Diabetes and pancreatic cancer. Mol. Carcinog., 51, 64–74

Li, D., Mao, Y. (2015): Diabetes as a risk factor of pancreatic cancer. Pancreapedia Exocrine Pancreas Knowl. Base,

Li, W., Zhang, L., Chen, X., Jiang, Z., Zong, L., Ma, Q. (2016): Hyperglycemia promotes the Epithelial-Mesenchymal Transition of pancreatic cancer via hydrogen peroxide. Oxid. Med. Cell. Longev., 2016, 5190314

Li, Z., Yin, S., Zhang, L., Liu, W., Chen, B. (2017): Prognostic value of reduced E-cadherin expression in breast cancer: a meta-analysis. Oncotarget, 8, 16445–16455

Liao, W. C., Tu, Y. K., Wu, M. S., Lin, J. T., Wang, H. P., Chien, K. L. (2015): Blood glucose concentration and risk of pancreatic cancer: Systematic review and dose-response meta-analysis. Br. Med. J., 349

Liou, G., Döppler, H., Necela, B., Edenfield, B., Zhang, L., Dawson, D., Storz, P. (2015): Mutant Kras-induced expression of ICAM-1 in pancreatic acinar cells causes attraction of macrophages to expedite the formation of precancerous lesions. Cancer Discov., 5, 52–63

Liu, P. P., Liao, J., Tang, Z. J., Wu, W. J., Yang, J., Zeng, Z. L., Hu, Y., Wang, P., Ju, H. Q., Xu, R. H., Huang, P. (2014): Metabolic regulation of cancer cell side population by glucose through activation of the Akt pathway. Cell Death Differ., 21, 124–135

Löhr, M., Klöppel, G., Maisonneuve, P., Lowenfels, A. B., Lüttges, J. (2005): Frequency of K-ras mutations in pancreatic intraductal neoplasias associated with pancreatic ductal adenocarcinoma and chronic pancreatitis: a meta-analysis. Neoplasia an Int. J. Oncol. Res., 7, 17–23

Lu, Y., Zhu, H., Shan, H., Lu, J., Chang, X., Li, X., Lu, J., Fan, X., Zhu, S., Wang, Y., Guo, Q., Wang, L., Huang, Y., Zhu, M., Wang, Z. (2013): Knockdown of Oct4 and Nanog expression inhibits the stemness of pancreatic cancer cells. Cancer Lett., 340, 113–123

Luo, J., Guo, P., Matsuda, K., Truong, N., Lee, A., Chun, C., Cheng, S., Korc, M. (2001): Pancreatic cancer cell-derived vascular endothelial growth factor is biologically active in vitro and enhances tumorigenicity in vivo. Int. J. Cancer, 92, 361–369

Ma, Y., Ren, Y., Dai, Z. J., Wu, C. J., Ji, Y. H., Xu, J. (2017): IL-6, IL-8 and TNF-α levels correlate with disease stage in breast cancer patients. Adv. Clin. Exp. Med., 26, 421–426

Maier, H. J., Schmidt-Straßburger, U., Huber, M. A., Wiedemann, E. M., Beug, H., Wirth, T. (2010): NF-κB promotes epithelial-mesenchymal transition, migration and invasion of pancreatic carcinoma cells. Cancer Lett., 295, 214–228

Maitra, A., Kern, S., Hruban, R. (2006): Molecular pathogenesis of pancreatic cancer. Best Pract. Res. Clin. Gastroenterol., 20, 211–226

Malik, V., Popkin, B., Bray, G., Després, J., Hu, F. (2010): Sugar sweetened beverages, obesity, type 2 diabetes and cardiovascular disease risk. Circulation, 121, 1356–1364

Malvezzi, M., Carioli, G., Bertuccio, P., Boffetta, P., Levi, F., Vecchia, C. La, Negri, E. (2018): European cancer mortality predictions for the year 2018 with focus on colorectal cancer. Ann. Oncol., 29, 1016–1022

Mani, S. a, Guo, W., Liao, M., Eaton, E. N., Zhou, A. Y., Brooks, M., Reinhard, F., Zhang, C. C., Campbell, L. L., Polyak, K., Brisken, C., Yang, J., Weinberg, R. a. (2009): The epithelial-mesenchymal transition generates cells with properties of stem cells. Cell, 133, 704–715

Mantovani, A., Allavena, P., Sica, A., Balkwill, F. (2008): Cancer-related inflammation. Nature, 454, 436–444

Mantovani, A., Schioppa, T., Porta, C., Allavena, P., Sica, A. (2006): Role of tumor-associated macrophages in tumor progression and invasion. Cancer Metastasis Rev., 25, 315–322

Martinez, F. O., Gordon, S. (2014): The M1 and M2 paradigm of macrophage activation: time for reassessment. F1000Prime Rep., 6, 1–13

Masamune, A., Shimosegawa, T. (2009): Signal transduction in pancreatic stellate cells. J. Gastroenterol., 44, 249–260

Matrisian, L. M., Aizenberg, R., Rosenzweig, A. (2012): The alarming rise of pancreatic cancer deaths in the United states : Why we need to stem the tide today. Newsl. Pancreat. Cancer Action Netw., 1–12

Matsuda, Y., Kure, S., Ishiwata, T. (2012): Nestin and other putative cancer stem cell markers in pancreatic cancer. Med. Mol. Morphol., 45, 59–65

Matsuda, Y., Naito, Z., Kawahara, K., Nakazawa, N., Korc, M., Ishiwata, T. (2011): Nestin is a novel target for suppressing pancreatic cancer cell migration, invasion and metastasis. Cancer Biol. Ther. Ther, 11, 512–523

Matsuda, Y., Yoshimura, H., Ueda, J., Naito, Z., Korc, M., Ishiwata, T. (2014): Nestin delineates pancreatic cancer stem cells in metastatic foci of NOD/Shi-scid IL2Rγnull(NOG) mice. Am. J. Pathol., 184, 674–685

Matthews, V. B., Allen, T. L., Risis, S., Chan, M. H. S., Henstridge, D. C., Watson, N., Zaffino, L. A., Babb, J. R., Boon, J., Meikle, P. J., Jowett, J. B., Watt, M. J., Jansson, J. O., Bruce, C. R., Febbraio, M. A. (2010): Interleukin-6-deficient mice develop hepatic inflammation and systemic insulin resistance. Diabetologia, 53, 2431–2441

Mauer, J., Chaurasia, B., Goldau, J., Vogt, M. C., Ruud, J., Nguyen, K. D., Theurich, S., Hausen, A. C., Schmitz, J., Brönneke, H. S., Estevez, E., Allen, T. L., Mesaros, A., Partridge, L., Febbraio, M. A.,

Chawla, A., Wunderlich, F. T., Brüning, J. C. (2014): Signaling by IL-6 promotes alternative activation of macrophages to limit endotoxemia and obesity-associated resistance to insulin. Nat. Immunol., 15, 423–430

Meng, F., Li, W., Li, C., Gao, Z., Guo, K., Song, S. (2015): CCL18 promotes epithelial-mesenchymal transition, invasion and migration of pancreatic cancer cells in pancreatic ductal adenocarcinoma. Int. J. Oncol. J Oncol, 46, 1109–1120

Merika, E. E., Syrigos, K. N., Saif, M. W. (2012): Desmoplasia in pancreatic cancer. Can we fight it? Gastroenterol. Res. Pract., 2012, 781765

Millar, H. J., Nemeth, J. A., McCabe, F. L., Pikounis, B., Wickstrom, E. (2008): Circulating human interleukin-8 as an indicator of cancer progression in a nude rat orthotopic human non-small cell lung carcinoma model. Cancer Epidemiol. Biomarkers Prev., 17, 2180–2187

Mills, E. L., Kelly, B., Logan, A., Costa, A. S. H., Varma, M., Bryant, C. E. (2016): Repurposing mitochondria from ATP production to ROS generation drives a pro-inflammatory phenotype in macrophages that depends on succinate oxidation by complex II. Cell, 167, 457–470

Mitchem, J. B., Brennan, D. J., Knolhoff, B. L., Belt, B. A., Zhu, Y., Sanford, D. E., Belaygorod, L., Carpenter, D., Collins, L., Hewitt, S., Udupi, G. M., Gallagher, W. M., West, B. L., Wang-gillam, A., Goedegebuure, S. P., David, C. (2014): Targeting tumor-infiltrating macrophages decreases tumor-initiating cells, relieves immunosuppression and improves chemotherapeutic responses. Cancer Res., 73, 1128–1141

Moganti, K., Li, F., Schmuttermaier, C., Riemann, S., Klüter, H., Gratchev, A., Harmsen, M. C., Kzhyshkowska, J. (2017): Hyperglycemia induces mixed M1/M2 cytokine profile in primary human monocyte-derived macrophages. Immunobiology, 222, 952–959

Mohapatra, S., Majumder, S., Smyrk, T., Zhang, L., Matveyenko, A., Kudva, Y., Chari, S. (2015): Diabetes mellitus is associated with an exocrine pancreatopathy. Pancreas, 44, 1395

Morey, M., O'Gaora, P., Pandit, A., Hélary, C. (2019): Hyperglycemia acts in synergy with hypoxia to maintain the pro-inflammatory phenotype of macrophages. PLoS One, 14, 1–17

Morrison, S. J., Kimble, J. (2006): Asymmetric and symmetric stem-cell divisions in development and cancer. Nature, 441, 1068–1074

Mrazkova, B., Dzijak, R., Imrichova, T., Kyjacova, L., Barath, P., Dzubak, P., Holub, D., Hajduch, M., Nahacka, Z., Andera, L., Holicek, P., Vasicova, P., Sapega, O., Bartek, J., Hodny, Z. (2018): Induction, regulation and roles of neural adhesion molecule L1CAM in cellular senescence. J. Aging, 10, 434–462

Müerköster, S. S., Werbing, V., Koch, D., Sipos, B., Ammerpohl, O., Kalthoff, H., Tsao, M. S., Fölsch, U. R., Schäfer, H. (2008): Role of myofibroblasts in innate chemoresistance of pancreatic carcinoma - Epigenetic downregulation of caspases. Int. J. CancerJ C, 123, 1751–1760

Müerköster, S., Wegehenkel, K., Arlt, A., Witt, M., Sipos, B., Kruse, M. L., Sebens, T., Klöppel, G., Kalthoff, H., Fölsch, U. R., Schäfer, H. (2004): Tumor stroma interactions induce chemoresistance in pancreatic ductal carcinoma cells involving increased secretion and paracrine effects of nitirc oxide and interleukin-1β. Cancer Res., 64, 1331–1337

Nielsen, M. F. B., Mortensen, M. B., Detlefsen, S. (2016): Key players in pancreatic cancer-stroma

interaction: Cancer-associated fibroblasts, endothelial and inflammatory cells. World J. Gastroenterol., 22, 2678–2700

Nieto, M. A., Huang, R. Y. Y. J., Jackson, R. A. A., Thiery, J. P. P. (2016): Emt: 2016. Cell, 166, 21–45

Nowell, P. C. (1976): The clonal evolution of tumor cell populations. Science., 194, 23–28

Noy, R., Pollard, J. W. (2014): Tumor-associated macrophages: from mechanisms to therapy. Immunity, 41, 49–61

Oft, M., Heider, K. H., Beug, H. (1998): TGFβ signaling is necessary for carcinoma cell invasiveness and metastasis. Curr. Biol., 8, 1243–1252

Okada, S., Okusaka, T., Ishii, H., Kyogoku, A., Yoshimori, M., Kajimura, N., Yamaguchi, K., Kakizoe, T. (1998): Elevated serum Interleukin-6 levels in patients with pancreatic cancer. Jpn. J. Clin. Oncol., 28, 12–15

Otsuru, T., Kobayashi, S., Wada, H., Takahashi, T., Gotoh, K., Iwagami, Y., Yamada, D., Noda, T., Asaoka, T., Serada, S., Fujimoto, M., Eguchi, H., Mori, M., Doki, Y., Naka, T. (2019): Epithelial-mesenchymal transition via transforming growth factor beta in pancreatic cancer is potentiated by the inflammatory glycoprotein leucine-rich alpha-2 glycoprotein. Cancer Sci., 110, 985–996

Pan, Y., Wang, Y., Cai, L., Cai, Y., Hu, J., Yu, C., Li, J., Feng, Z., Yang, S., Li, X., Liang, G. (2012): Inhibition of high glucose-induced inflammatory response and macrophage infiltration by a novel curcumin derivative prevents renal injury in diabetic rats. Br. J. Pharmacol., 166, 1169–1182

Pandol, S., Edderkaoui, M., Gukovsky, I., Lugea, A., Gukovskaya, A. (2009): Desmoplasia of pancreatic ductal adenocarcinoma. Clin Gastoenterol Hepatol, 7, 44–47

Pavlou, S., Lindsay, J., Ingram, R., Xu, H., Chen, M. (2018): Sustained high glucose exposure sensitizes macrophage responses to cytokine stimuli but reduces their phagocytic activity. BMC Immunol., 19, 1–13

Peinado, H., Olmeda, D., Cano, A. (2007): Snail, ZEB and bHLH factors in tumour progression: An alliance against the epithelial phenotype? Nat. Rev. Cancer, 7, 415–428

Pelosi, E., Castelli, G., Testa, U. (2017): Pancreatic cancer: molecular characterization, clonal evolution and cancer stem cells. Biomedicines, 5(4):65

Peri, A. K., Wilgenbus, P., Dahl, U., Semb, H., Christofori, G. (1998): A causal role for E-cadherin in the transition from adenoma to carcinoma. Nature, 392, 190–193

Philip, B., Roland, C., Daniluk, J., Liu, Y., Chatterjee, D., Gomez, S., Ji, B., Huang, H., Wang, H., Fleming, J., Logsdon, C., Cruz-Monserrate, Z. (2013): A high-fat diet activates oncogenic kras and COX2 to induce development of pancreatic ductal adenocarcinoma in mice. Gastroenterology, 145, 148–159

Phillips, P. A., McCarroll, J. A., Park, S., Wu, M. J., Pirola, R., Korsten, M., Wilson, J. S., Apte, M. V. (2003): Rat pancreatic stellate cells secrete matrix metalloproteinases: Implications for extracellular matrix turnover. Gut, 52, 275–282

Pino, M. S., Kikuchi, H., Zeng, M., Herraiz, M., Sperduti, I., Berger, D., Park, D., Iafrate, A. J., Zukerberg, L. R., Daniel, C. (2011): The epithelial to mesenchymal transition is impaired in colon cancer cells with microsatellite instability. Gastroenterology, 138, 1406–1417

Plaks, V., Kong, N., Werb, Z. (2015): The cancer stem cell niche: How essential is the niche in regulating stemness of tumor cells? Cell Stem Cell, 16, 225–238

Plundrich, D. (2017): Initiation of pancreatic cancer : Impact of glucose on macrophage differentiation and their interplay with pancreatic ductal epithelial cells. Master's thesis, Kiel

Pollak, M. (2009): Insulin and insulin-like growth factor signalling in neoplasia. Nat. Rev. Cancer, 9, 224–238

Pozza, E. D., Dando, I., Biondani, G., Brandi, J., Costanzo, C., Zoratti, E., Fassan, M., Boschi, F., Melisi, D., Cecconi, D., Scupoli, M. T., Scarpa, A., Palmieri, M. (2015): Pancreatic ductal adenocarcinoma cell lines display a plastic ability to bi-directionally convert into cancer stem cells. Int. J. Oncol., 46, 1099–1108

Protti, M. P., De Monte, L. (2013): Immune infiltrates as predictive markers of survival in pancreatic cancer patients. Front. Physiol., 1–6

Qian, J., Niu, J., Li, M., Chiao, P. J., Tsao, M.-S. (2005): n vitro modeling of human pancreatic duct epithelial cell transformation defines gene expression changes induced by K-ras oncogenic activation in pancreatic carcinogenesis. Cancer Res., 65, 5045–5053

Radulović, P., Krušlin, B. (2018): Immunohistochemical expression of NEDD9, E-cadherin and γ-catenin and their prognostic significance in pancreatic ductal adenocarcinoma (PDAC). Bosn. J. Basic Med. Sci., 18, 246–251

Rahib, L., Smith, B. D., Aizenberg, R., Rosenzweig, A. B., Fleshman, J. M., Matrisian, L. M. (2014): Projecting cancer incidence and deaths to 2030: the unexpected burden of thyroid, liver, and pancreas cancers in the united states. Cancer Res., 74, 2913–2921

Rahman, F., Cotterchio, M., Cleary, S. P., Gallinger, S. (2015): Association between alcohol consumption and pancreatic cancer risk: A case-control study. PLoS One, 10, 1–10

Rahn, S., Zimmermann, V., Viol, F., Knaack, H., Stemmer, K., Peters, L., Lenk, L., Ungefroren, H., Saur, D., Schäfer, H., Helm, O., Sebens, S. (2018): Diabetes as risk factor for pancreatic cancer: Hyperglycemia promotes epithelial-mesenchymal-transition and stem cell properties in pancreatic ductal epithelial cells. Cancer Lett., 415, 129–150

Raimondi, S., Maisonneuve, P., Lowenfels, A. B. (2009): Epidemiology of pancreatic cancer: An update. Nat. Rev. Gastroenterol. Hepatol., 6, 699–708

Rasheed, Z. A., Matsui, W., Maitra, A. (2012): Pathology of pancreatic stroma in PDAC. Vol. 14

Reya, T., Morrison, S., Clarke, M., Weissman, I. (2001): Stem cells, cancer, and cancer stem cells. Nature, 414, 105–111

Rhim, A. D., Mirek, E. T., Aiello, N. M., Maitra, A., Jennifer, M., Mccallister, F., Reichert, M., Beatty, G. L., Anil, K., Vonderheide, R. H., Leach, S. D., Stanger, B. Z. (2012): EMT and dissemination precede pancreatic tumor formation. Cell, 148, 349–361

Rhyu, D. Y., Yang, Y., Ha, H., Lee, G., Song, J., Uh, S., Lee, H. (2005): Role of reactive oxygen species in TGF- 1-induced mitogen-activated protein kinase activation and epithelial mesenchymal transition in renal tubular epithelial cells. J. Am. Soc. Nephrol., 16, 667–675

Ricci-Vitiani, L., Lombardi, D. G., Pilozzi, E., Biffoni, M., Todaro, M., Peschle, C., De Maria, R. (2007): Identification and expansion of human colon-cancer-initiating cells. Nature, 445, 111–115

Robak, T., Gladalska, A., Stepien, H., Robak, E. (1998): Serum levels of interleukin-6 type cytokines and soluble interleukin.6 receptor in patients with rheumatoid arthritis. Mediators Inflamm., 7, 347–353

Rose-John, S. (2012): Il-6 trans-signaling via the soluble IL-6 receptor: Importance for the proinflammatory activities of IL-6. Int. J. Biol. Sci., 8, 1237–1247

Rose-John, S., Scheller, J., Elson, G., Jones, S. A. (2006): Interleukin-6 biology is coordinated by membrane-bound and soluble receptors: role in inflammation and cancer. J. Leukoc. Biol., 80, 227–236

Rőszer, T. (2015): Understanding the mysterious M2 macrophage through activation markers and effector mechanisms. Mediators Inflamm., 2015, 1–16

Sainz, B., Martín, B., Tatari, M., Heeschen, C., Guerra, S. (2014): ISG15 is a critical microenvironmental factor for pancreatic cancer stem cells. Cancer Res., 74, 7309–7320

Samuel, S. M., Varghese, E., Varghese, S., Büsselberg, D. (2018): Challenges and perspectives in the treatment of diabetes associated breast cancer. Cancer Treat. Rev., 70, 98–111

Scheller, J., Garbers, C., Rose-John, S. (2014): Interleukin-6: From basic biology to selective blockade of pro-inflammatory activities. Semin. Immunol., 26, 2–12

Scholz, A., Heinze, S., Detjen, K. M., Peters, M., Welzel, M., Hauff, P., Schirner, M., Wiedenmann, B., Rosewicz, S. (2003): Activated signal transducer and activator of transcription 3 (STAT3) supports the malignant phenotype of human pancreatic cancer. Gastroenterology, 125, 891–905

Sciacca, L., Vigneri, R., Tumminia, A., Frasca, F., Squatrito, S., Frittitta, L., Vigneri, P. (2013): Clinical and molecular mechanisms favoring cancer initiation and progression in diabetic patients. Nutr. Metab. Cardiovasc. Dis., 23, 808–815

Selander, K. S., Li, L., Watson, L., Merrell, M., Dahmen, H., Heinrich, P. C., Müller-Newen, G., Harris, K. W. (2004): Inhibition of gp130 signaling in breast cancer blocks constitutive activation of Stat3 and inhibits in vivo malignancy. Cancer Res., 64, 6924–6933

Serbina, N., Jia, T., Hohl, T., Pamer, E. (2008): Monocyte-mediated defense against microbial pathogens. Annu. Rev. Immunol., 26, 421–452

Shackleton, M., Quintana, E., Fearon, E. R., Morrison, S. J. (2009): Heterogeneity in cancer: cancer stem cells versus clonal evolution. Cell, 138, 822–829

Shi, C., Pamer, E. G. (2009): Monocyte recruitment during infection and inflammation. Nat. Rev. Immunol., 11, 762–774

Shibuya, K., Okada, M., Suzuki, S., Seino, M., Seino, S., Takeda, H., Kitanaka, C. (2014): Targeting the facilitative glucose transporter GLUT1 inhibits the self-renewal and tumor-initiating capacity of cancer stem cells. Oncotarget, 6, 651–661

Sica, A., Erreni, M., Allavena, P., Porta, C. (2015): Macrophage polarization in pathology. Cell. Mol. Life Sci., 72, 4111–4126

Sica, A., Schioppa, T., Mantovani, A., Allavena, P. (2006): Tumour-associated macrophages are a distinct M2 polarised population promoting tumour progression: Potential targets of anti-cancer therapy. Eur. J. Cancer, 42, 717–727

Siegel, R. L., Miller, K. D., Jemal, A. (2018): Cancer statistics , 2018. CA. Cancer J. Clin., 68, 7–30

Silva, J., Nichols, J., Theunissen, T. W., Guo, G., van Oosten, A. L., Barrandon, O., Wray, J., Yamanaka, S., Chambers, I., Smith, A. (2009): Nanog is the gateway to the pluripotent ground state. Cell, 138, 722–737

Singh, S., Hawkins, C., Clarke, I., Squire, J., Bayani, J. (2004): Identification of human brain tumour initiating cells. Nature, 432, 396–401

Solinas, G., Germano, G., Mantovani, A., Allavena, P. (2009): Tumor-associated macrophages (TAM) as major players of the cancer-related inflammation. J. Leukoc. Biol., 86, 1065–1073

Spaargaren, M., Bischoff, J. R., McCormick, F. (1995): Signal transduction by Ras-like GTPases: A potential target for anticancer drugs. Gene Expr., 4, 345–356

Spranger, J., Kroke, A., Möhlig, M., Hoffmann, K., Bergmann, M. M., Ristow, M., Boeing, H., Pfeiffer, A. F. H. (2003): Inflammatory cytokines and the risk to develop type 2 diabetes: Results of the prospective population-based european prospective investigation into cancer and nutrition (EPIC)-potsdam study. Diabetes, 52, 812–817

Storci, G., Sansone, P., Mari, S., Uva, G. D., Tavolari, S., Guarnieri, T., Taffurelli, M., Ceccarelli, C., Santini, D., Marcu, K. B., Bonafè, M. (2010): TNFalpha up-regulates SLUG via the NF-kappaB/HIF1alpha axis, which imparts breast cancer cells with a stem cell-like phenotype. Cell Physiol., 225, 682–691

Storz, P. (2015): The crosstalk between acinar cells with Kras mutations and M1-polarized macrophages leads to initiation of pancreatic precancerous lesions. Oncoimmunology, 4, 10–12

Su, H.-T., Weng, C.-C., Hsiao, P.-J., Chen, L.-H., Kuo, T.-L., Chen, Y.-W., Kuo, K.-K., Cheng, K.-H. (2013): Stem cell marker nestin is critical for TGF-beta1-mediated tumor progression in pancreatic cancer. Mol. Cancer Res., 11, 768–779

Sugihara, E., Saya, H. (2013): Complexity of cancer stem cells. Int. J. Cancer J Cancer, 132, 1249–1259

Tan, H. Y., Wang, N., Li, S., Hong, M., Wang, X., Feng, Y. (2016): The reactive oxygen species in macrophage polarization: Reflecting its dual role in progression and treatment of human diseases. Oxid. Med. Cell. Longev., 2016, 1–16

Tan, L., Sui, X., Deng, H., Ding, M. (2011): Holoclone forming cells from pancreatic cancer cells enrich tumor initiating cells and represent a novel model for study of cancer stem cells. PLoS One, 6, e23383

Thiery, J. P., Huang, R. Y. J., Nieto, M. A. (2009): Epithelial-mesenchymal transitions in development and disease. Cell, 139, 1–13

Torres-Castro, I., Arroyo-Camarena, U., Martínez-Reyes, C., Gómez-Arauz, A., Duenas-Andrade, Hernández-Ruiz, J., Béjar, Y., Zaga-Clavwllina, V., Morales-Montor, J., Terrazas, L., Kzhyshkowska, J., Escobedo, G. (2016): Human monocytes and macrophages undergo M1-type inflammatory polarization in response to high levels of glucose. Immunol. Lett., 176, 81–89

Tsubaki, M., Yamazoe, Y., Yanae, M., Satou, T., Itoh, T., Kaneko, J., Kidera, Y., Moriyama, K., Nishida, S. (2011): Blockade of the Ras/MEK/ERK and Ras/PI3K/Akt pathways by statins reduces the expression of bFGF, HGF, and TGF-β as angiogenic factors in mouse osteosarcoma. Cytokine, 54, 100–107

Valastyan, S., Weinberg, R. A. (2011): Tumor metastasis : Molecular insights and evolving paradigms. Cell, 147, 275–292

Valle, S., Martin-Hijano, L., Alcalá, S., Alonso-Nocelo, M., Sainz, B. (2018): The ever-evolving concept of the cancer stem cell in pancreatic cancer. Cancers (Basel)., 10

van Heek, N., Meeker, A., Kern, S., Yeo, C., Lillemoe, K., Cameron, J., Offerhaus, G., Hicks, J., Wilenetz, R., Goggins, G., De Marzo, A., Hruban, R., Maitra, A. (2002): Telomere shortening is nearly universal in pancreatic intraepithelial neoplasia. Am. J. Pathol., 161, 1541–1547

Varol, C., Mildner, A., Jung, S. (2015): Macrophages: Development and tissue specialization. Annu. Rev. Immunol.,. Vol. 33

Vats, D., Mukundan, L., Odegaard, J. I., Zhang, L., Smith, K. L., Morel, C. R., Greaves, D. R., Murray, P. J., Chawla, A. (2006): Oxidative metabolism and PGC-1β attenuate macrophage-mediated inflammation. Cell Metab., 4, 13–24

Wan, S., Zhao, E., Kryczek, I., Vatan, L., Sadovskaya, A., Simeone, D. M., Zou, W., Welling, T. H. (2015): Tumor-associated macrophages produce interleukin 6 and signal via STAT3 to promote expansion of human hepatocellular carcinoma stem cells. Gastroenterology, 147, 1393–1404

Wang, H., Wang, H. S., Zhou, B. H., Li, C. L., Zhang, F., Wang, X. F., Zhang, G., Bu, X. Z., Cai, S. H., Du, J. (2013): Epithelial-Mesenchymal Transition (EMT) induced by TNF-α requires AKT/GSK-3β-mediated stabilization of snail in colorectal cancer. PLoS One, 8

Wang, L., Bai, Y.-Y., Yang, Y., Hu, F., Wang, Y., Yu, Z., Cheng, Z., Zhou, J. (2016): Diabetes mellitus stimulates pancreatic cancer growth and epithelial-mesenchymal transition-mediated metastasis via a p38 MAPK pathway. Oncotarget, 7, 38539–38550

Wehler, T., Wolfert, F., Schimanski, C. C., Gockel, I., Herr, W., Biesterfeld, S., Seifert, J. K., Adwan, H., Berger, M. R., Junginger, T., Galle, P. R., Moehler, M. (2006): Strong expression of chemokine receptor CXCR4 by pancreatic cancer correlates with advanced disease. Oncol. Rep., 16, 1159–1164

Weinberg, R. A. (2008): Mechanisms of malignant progression. Carcinogenesis, 29, 1092–1095

Weisberg, S., McCann, D., Desai, M., Rosenbaum, M., Leibel, R., Ferrante, A. (2003): Obesity is associated with macrophage accumulation in adipose tissue. Clin. Investig. (Lond)., 122, 1796–1808

Wellen, K., Hotamisligil, G. (2015): Inflammation , stress , and diabetes. J. Clin. Invest., 115, 1111–1119

Wellner, U., Schubert, J., Burk, U. C., Schmalhofer, O., Zhu, F., Sonntag, A., Waldvogel, B., Vannier, C., Darling, D., Hausen, A. Zur, Brunton, V. G., Morton, J., Sansom, O., Schüler, J., Stemmler, M. P., Herzberger, C., Hopt, U., Keck, T., Brabletz, S., Brabletz, T. (2009): The EMT-activator ZEB1 promotes tumorigenicity by repressing stemness-inhibiting microRNAs. Nat. Cell Biol., 11, 1487–1495

Wen, J., Park, J. Y., Park, K. H., Chung, H. W., Bang, S., Park, S. W., Song, S. Y. (2010): Oct4 and nanog expression is associated with early stages of pancreatic carcinogenesis. Pancreas, 39, 622–626

Wen, J., Zhao, Z., Huang, L., Wang, L., Miao, Y., Wu, J. (2020): IL-8 promotes cell migration through regulating EMT by activating the Wnt/β-catenin pathway in ovarian cancer. J. Cell. Mol. Med., 24, 1588–1598

Wheeler, K. C., Jena, M. K., Pradhan, B. S., Nayak, N., Das, S., Hsu, C. D., Wheeler, D. S., Chen, K., Nayak, N. R. (2018): VEGF may contribute to macrophage recruitment and M2 polarization in the decidua. PLoS One, 13, 1–18

Wu, J., Chen, J., Xi, Y., Wang, F., Sha, H., Luo, L., Zhu, Y., Hong, X., Bu, S. (2018): High glucose induces epithelial-mesenchymal transition and results in the migration and invasion of colorectal cancer cells. Exp. Ther. Med., 16, 222–230

Wu, L., Derynck, R. (2009): Essential role of TGF-β signaling in glucose-induced cell hypertrophy. Dev. Cell, 17, 35–48

Wunderlich, F. T., Ströhle, P., Könner, A. C., Gruber, S., Tovar, S., Brönneke, H. S., Juntti-Berggren, L., Li, L. S., Van Rooijen, N., Libert, C., Berggren, P. O., Brüning, J. C. (2010): Interleukin-6 signaling in liver-parenchymal cells suppresses hepatic inflammation and improves systemic insulin action. Cell Metab., 12, 237–249

Xia, P. (2014): Surface markers of cancer stem cells in solid tumors. Curr. Stem Cell Res. Ther., 9, 102–111

Xie, G., Yao, Q., Liu, Y., Du, S., Liu, A., Guo, Z., Sun, A., Ruan, J., Chen, L., Ye, C., Yuan, Y. (2012): IL-6-induced epithelial-mesenchymal transition promotes the generation of breast cancer stem-like cells analogous to mammosphere cultures. Int. J. Oncol., 40, 1171–1179

Xu, H., Barnes, H., Yang, Q., Tan, G., Yang, S., Chou, C., Sole, J., Nichols, A., Ross, J., Tartaglia, L., Chen, H. (2003): Chronic inflammation in fat plays a crucial role in the development of obesity-related insulin resistance. J. Clin. Invest., 112, 1821–1830

Xu, J., Lamouille, S., Derynck, R. (2009): TGF- β -induced epithelial to mesenchymal transition. Cell Res., 19, 156–172

Yang, J., Liao, D., Chen, C., Liu, Y., Chuang, T. H., Xiang, R., Markowitz, D., Reisfeld, R. A., Luo, Y. (2013): Tumor-associated macrophages regulate murine breast cancer stem cells through a novel paracrine egfr/stat3/sox-2 signaling pathway. Stem Cells, 31, 248–258

Yang, J., Waldron, R. T., Su, H.-Y., Moro, A., Chang, H.-H., Eibl, G., Ferreri, K., Kandeel, F. R., Lugea, A., Li, L., Pandol, S. J. (2016): Insulin promotes proliferation and fibrosing responses in activated pancreatic stellate cells. Am. J. Physiol. Gastrointest. Liver Physiol., 311, 675–687

Yang, Y. L., Chen, M. W., Xian, L. (2014): Prognostic and clinicopathological significance of downregulated E-cadherin expression in patients with non-small cell lung cancer (NSCLC): A meta-analysis. PLoS One, 9

Ye, H., Zhou, Q., Zheng, S., Li, G., Lin, Q., Wei, L., Fu, Z., Zhang, B., Liu, Y., Li, Z., Chen, R. (2018): Tumor-associated macrophages promote progression and the Warburg effect via CCL18/NF-kB/VCAM-1 pathway in pancreatic ductal adenocarcinoma. Cell Death Dis., 9, 1–19

Ye, J., Wu, D., Wu, P., Chen, Z., Huang, J. (2014): The cancer stemcell niche: Cross talk between cancer stemcells and their microenvironment. Tumor Biol., 35, 3945–3951

Yona, S., Kim, K., Wolf, Y., Mildner, A., Varol, D., Breker, M., Strauss-Ayali, D., Vikuov, S., Guillams, M., Misharin, A., Hume, D., Perlman, H., Malissen, B., Zelzer, E., Jung, S. (2013): Fate mapping reveals origins and dynamics of monocytes and tissue macrophages under homeostasis. Immunity, 38, 79–91

Zhang, J., Liu, C., Mo, X., Shi, H., Li, S. (2018): Mechanisms by which CXCR4/CXCL12 cause metastatic behavior in pancreatic cancer. Oncol. Lett., 15, 1771–1776

Zhang, L., Jiao, M., Wu, K., Li, L., Zhu, G., Wang, X., He, D., Wu, D. (2014): TNF-α induced epithelial mesenchymal transition increases stemness properties in renal cell carcinoma cells. Int. J. Clin. Exp. Med., 7, 4951–4958

Zhang, Q., Zeng, L., Chen, Y., Lian, G., Qian, C., Chen, S., Li, J., Huang, K. (2016): Pancreatic cancer epidemiology, detection, and management. Gastroenterol. Res. Pract., 2016, 1–10

Zhao, H., Duan, Q., Zhang, Z., Li, H., Wu, H., Shen, Q., Wang, C., Yin, T. (2017): Up-regulation of glycolysis promotes the stemness and EMT phenotypes in gemcitabine-resistant pancreatic cancer cells. J. Cell. Mol. Med., 21, 2055–2067

Zhou, L., Xue, H., Yuan, P., Ni, J., Yu, C., Huang, Y., Lu, L. M. (2010): Angiotensin AT1receptor activation mediates high glucose-induced epithelial-mesenchymal transition in renal proximal tubular cells. Clin. Exp. Pharmacol. Physiol., 37, 152–157

Zhu, Y., Herndon, J., Sojka, D., Kim, K., Knoldhoff, B., Zuo, C., Cullinan, D., Luo, J., Bearden, A. (2017): Tissue resident macrophages in pancreatic ductal adenocarcinoma originate from embryonic hematopoiesis and promote tumor progression. Immunity, 47, 323–338

Zhu, Z.-J., Yang, S., Li, Z. (2015): Transcriptome research on spermatogenic molecular drive in mammals. Asian J. Androl., 17, 961

8 Acknowledgements

First of all, I wish to express my gratitude to my supervisor Professor Dr. Susanne Sebens. I thank you for the opportunity to work on this fascinating project, for the excellent supervision and support and your continual availability for discussions, comments and exchange. I tremendously enjoyed the openness and the unique working atmosphere in the group. Your enthusiasm and commitment are inspiring, it was a pleasure working with you. Thank you!

I also want to thank the whole working group *Inflammatory Carcinogenesis*. Thank you to Elsa, Frederik, Lisa, Luisa and Sascha, I greatly enjoyed working with you. I wish to express special thanks to Ole, who introduced me into the topic, helped with new techniques and answered many questions with an untiring patience and kindness. Many thanks also to Dagmar, for your excellent, warm-hearted, never tiring technical assistance.

And last but not least, I want to thank my parents, sister and friends for always supporting and encouraging me. I count myself very fortunate to be surrounded by such great people. I am especially grateful to my parents who gave me the chance to take this direction, thank you for your unconditional support and patience.

9 Publications

Otto, L.; Rahn, S.; Daunke, T.; Walter, F.; Winter, E.; Möller, J.L.; Rose-John, S.; Wesch, D.; Schäfer, H.; Sebens, S. Initiation of Pancreatic Cancer: The Interplay of Hyperglycemia and Macrophages Promotes the Acquisition of Malignancy-Associated Properties in Pancreatic Ductal Epithelial Cells. Int. J. Mol. Sci. 2021, 22, 5086. https://doi.org/10.3390/ijms22105086

Walter, F., Winter, E., Rahn, S., Heidland, J., Meier, S., Struzek, A-M., Lettau, M., Phillip, L-M., Beckinger, S., Otto, L., Möller, J.L., Helm, O., Wesch, D., Scherließ, R., Sebens, S. (2020): Chitosan nanoparticles as antigen vehicles to induce effective tumor specific T cell responses. PlosOne., 15(9): e0239369

Otto, L., Rahn, S., Winter, E., Walter, F., Faltinek, L., Wesch, D., Helm, O., Sebens, S.: Diabetes as Risk Factor for Pancreatic Cancer: Hyperglycaemia and Macrophages impact Epithelial-Mesenchymal-Transition and Stemness Features in Pancreatic Ductal Epithelial Cells, 20th International AEK Cancer Congress, Heidelberg